

Craców University of Technology
Department of Mechanical Engineering

Tim Eichner M.Sc.

PhD Thesis

Finding of geometrical parameters as a base of
In-process metrology system in WPM gear forming

Promoter: **Dr hab. eng. M. Wieczorowski prof. PP**

Craków 2013



*I would like to thank
for their help, valuable advice and care*

*Prof. Dr. Michal Wieczorowski (Poznan University of Technology)
Prof. Dr. Jerzy A. Sladek (Craków University of Technology)
Dr. Adam Gaska and Dr. Marcin Krawczyk*

*Prof. Dr.-Ing. Ernst Hammerschmidt (University Darmstadt)
and his colleagues and employees*

Dipl.-Ing. Ingo Lindner M.Sc. (Hexagon Metrology, Leitz)

*All my family for their support and understanding
especially my wife Duygu and our little son Batu
who gave the right relief the last couple of months*

June 2013

A. Agenda

A. Agenda	1
B. List of Abbreviations	3
C. List of Tables	5
D. List of Appendix.....	6
E. List of Figures	7
1. Introduction.....	11
2. State of the art - Production toothed machine elements	15
2.1. Toothed Machine Elements	16
2.1.1. Spline Shafts	18
3. Metal Forming	22
3.1. Rolling Methods	24
3.1.1. Advantages of Rolling Methods	29
3.2. Rolling according to the WPM Method.....	31
4. Production of Test Parts.....	38
4.1. Preparing of Rolling Tests	38
4.2. Test Parameters / Measuring Equipment.....	41
4.3. Engineering Results and Assessment.....	50
4.4. Measurement Results and Evaluation	57
5. Geometry Measurements PMM 654.....	60
5.1. Technical Basis coordinate measuring technology	60
5.1.1. Construction of the Coordinate Measuring Device / Measurement Accuracy	62
5.2. Measurement of Blank Geometry	66
5.2.1. Determination of the Workpiece Coordinate System	66
5.3 Measurements Toothing Geometry (DIN 3960 ff)	77
5.3.1 Probe Configuration and Calibration	77

5.3.2	Determination Workpiece Coordinate System	78
5.3.3	Acquisition of the Tothing Geometry	79
5.4	Measurement Geometry Rolling Tools.....	91
5.4.1	Probe Configuration and Calibration	91
5.4.2	Coordinate System Rolling Tools.....	92
5.4.3	Acquisition Geometry Outer Contour of the Tools	94
5.4.4	Acquisition Gear Geometry Rolling Tools	95
5.5	Contour Measurements on Rolling Samples	101
5.5.1	Contour Measurements Rolling Samples	103
5.6	Contour Measurements of Tools	108
6.	Evaluation / Discussion Geometry Results	113
6.1	Evaluation / Discussion of Measurement DIN.....	113
6.2	Evaluation / Discussion of Contour Measurements.....	127
7.	In-Process Acquisition of the Geometrical Peculiarities	132
7.1	Acquisition of Geometrical Deviations.....	133
7.1.1	Acquisition of Tooth Profile.....	135
7.1.2	Acquisition of Axial Position.....	135
7.1.3	Acquisition of Angular Position.....	136
7.2	Application / Distance Sensors / WPM Work Cycles	137
7.3	Geometrical Deviations / Peculiarities.....	139
7.3.1	Eccentricity.....	139
7.3.2	Pitch (Angular, Fluctuation) / Tooth Thickness	142
7.3.3	Axial Position and Orientation.....	149
7.3.4	Tooth Trace	151
7.4	Sensor Requirements.....	153
7.4.1	Instrumentation	153
7.4.2	Conclusions of In-Process Measurement Requirements using Suitable Sensors	156
8.	Conclusion and Outlook	157
9.	Abstract/ Streszczenie.....	161

B. List of Abbreviations

2nd	second
3D	3-Dimensional
A	Amper
AXI	Axis
Acc.	according
CIR_M	Circle Mitte
CIR_O	Circle Oben
CIR_U	Circle Unten
CNC	Computerized Numerical Control
CSY	Coordinate System
CYL	Cylinder
Calc.	calculation
D	diameter
DDR	Double Data Rate
DIN	Deutsche Industrie Norm
Diff.	difference
e.g.	exempli gratia
FA	Total pitch/profile deviation
FB	Tooth trace total deviation
ff.	further following
ffA	Profile form deviation
ffB	Tooth trace form deviation

fHA	Profile angle deviation
fHB	Tooth trace angle deviation
fp	Individual pitch deviation
Fp	Total pitch deviation
fu	Pitch error
GB	Gigabyte
GHz	Gigahertz
HV	Vickers hardness
Hz	Hertz
ISO	International Organization of Standardization
kHz	Kilohertz
kW	Kilowatt
m	module
MB	Megabyte
min	minute
mm	milimeter
Nm	Newtonmeter
pcs.	pieces
PNT	Point
PRB	Probe
Rp	Pitch fluctuation
VDI	Verein Deutscher Ingenieure
vs.	versus
WPM	Polish Rolling Machine

C. List of Tables

Table 1:	Sensor Fabricate / Sony Magnescale	43
Table 2:	Sensors	44
Table 3:	Sensor Leuze Electronics	46
Table 4:	Sensor Hydrosens Löfflingen	47
Table 5:	Arrangement of the Tactile Pins.....	77
Table 6:	Evaluated Specific Criteria	82
Table 7:	Evaluated Specific Criteria	85
Table 8:	Tooth Trace	87
Table 9:	Principle of Operation.....	135

D. List of Appendix

Appendix 1: Blank Geometry	164
Appendix 2: Gear tooth quality (DIN 3960 ff.)	172
Appendix 3: Tool geometry (DIN 3960 ff)	189
Appendix 4: Statistical analysis of gear tooth quality (DIN 3960 ff)	203
Appendix 5: List of Literature.....	237
Appendix 6: List of Standards	241

E. List of Figures

Figure 1	Thesis Structure.....	14
Figure 2	Compilation of the various technologies and processes	16
Figure 3	Pair of Gears.....	17
Figure 4	Pair of Gears – Toothed Shaft / Internal Gear Hub	17
Figure 5	Shaft-Hub Connection	19
Figure 6	Shaft-Hub Connection	19
Figure 7	Shaft-Hub Connection / Flank Centered	20
Figure 8	Shaft-Hub Connection / Root Diameter Centered	21
Figure 9	Shaft-Hub Connection / Tip Diameter Centered.....	21
Figure 10	Ingression of a wedge-shaped tool.....	25
Figure 11	PeeWee / External Toothed Tools.....	26
Figure 12	RotoFlow / Rack Shaped Rolling Tools	27
Figure 13	WPM / two internally toothed tools.....	27
Figure 14	Cutting / Rolling	29
Figure 15	Preliminary Diameters.....	29
Figure 16	Material Structure after Rolling	30
Figure 17	Fragment of the Volume Rolled Spline	31
Figure 18	WPM - Motion Principle Rolling Tools / Workpiece.....	31
Figure 19	Machine WPM 120	32
Figure 20	Machines top view / Three Massive Columns / Feed Carriage .	33
Figure 21	Main Drive.....	33
Figure 22	Tool Movement / Four Eccentric Shafts/Left Auxiliary Drive ...	34
Figure 23	Left Side Hydraulic Tip	35
Figure 24	Right Side the Spring-Biased Tip	35
Figure 25	Feed Carriage / Feed Drive	36
Figure 26	Geometry Spline Shaft	38
Figure 27	Drawing Blank	39
Figure 28	Mounting Notch / Assembly Ruler	40

Figure 29	Clamping Tools	40
Figure 30	High-Resolution Position Measuring Sensors.....	42
Figure 31	Power Measurement	44
Figure 32	Stroke Frequency	45
Figure 33	Sensor / Pre-charged Pressure	46
Figure 34	Path – Feed Carriage	50
Figure 35	Enlarged Path / Time	52
Figure 36	Power Consumption – Main Drive.....	54
Figure 37	Power Consumption – Main Drive / Start after 10 sec.	56
Figure 38	Power Consumption – Feed Drive	58
Figure 39	Resulting Signals of an Inductive Sensor – Tool Movement....	59
Figure 40	Basic Principle of Coordinate Metrology.....	60
Figure 41	Principle of Tactile 3-D Metrology.....	61
Figure 42	Components of a Coordinate	63
Figure 43	Measuring Machine PMM 654.....	64
Figure 44	probe pin configuration	66
Figure 45	Machine and workpiece coordinate system	67
Figure 46	Blank Geometry	70
Figure 47	Measurement strategy / Geometry detection on the blank.....	71
Figure 48	Workpiece coordinate system.....	72
Figure 49	Clamping situation blank / measuring machine table	73
Figure 50	Scanning a circle / ROUNDNESS	74
Figure 51	Cylindrical Tothing Zone / FORM OF CYLINDERS.....	75
Figure 52	Probe Configuration, b = 60 mm	77
Figure 53	Clamping situation of a sample.....	78
Figure 54	Workpiece coordinate system rolling sample	79
Figure 55	probe configuration	80
Figure 56	Measurement Pitch / Concentricity	81
Figure 57	Situation in PMM Measurement Pitch	82
Figure 58	Pitch / Concentricity Deviation w/o and with Eccentricity	83
Figure 59	Probing / Profile Measurement.....	84

Figure 60	Situation in PMM	Scan line / Profile Measurement.....	84
Figure 61	Profile deviations of 4 gaps		85
Figure 62	Measurement / Probing / Tooth Direction / Flank Line		86
Figure 63	Scane Line / Flank Direction.....		87
Figure 64	Flank Line Deviations of 4 gaps		88
Figure 65	Detection Tip- / Root Circle Diameter		89
Figure 66	Probing Point Root Diameter	Probing Point Tip Diameter	89
Figure 67	Situation in PMM		90
Figure 68	Tip circle diameter	Root circle diameter	90
Figure 69	Probe Configuration		92
Figure 70	Detection of the Outer Cylinder	Coordinate System Tools	93
Figure 71	Situation in PMM Roundness Outer Cylinder		94
Figure 72	Frontal Flats	Alignment Groove.....	95
Figure 73	Measuring / Probing Strategy		95
Figure 74	Situation in PMM		96
Figure 75	Pitch / Concentricity Deviation of the Tools		97
Figure 76	Internal Tooth Profile Deviations Rolling Tools		98
Figure 77	Flank Trace Deviations Internally Toothed Rolling Tools		99
Figure 78	Roundness Root Circle Fk Internally Toothed Rolling Tools...		100
Figure 79	Contour Measurement Workpiece		104
Figure 80	Scan-Line Workpiece	Situation in PMM.....	104
Figure 81	Contour Sections Workpiece.....		105
Figure 82	Contour Cut.....		107
Figure 83	Contour Sections Tools.....		109
Figure 84	Situation in PMM		109
Figure 85	Contour Cuts		110
Figure 86	Side View of a Sample		111
Figure 87	Profile Deviation – Gap 1 – 4	$v = 100 \text{ mm / min}$	116
Figure 88	Profile Deviation – Gap 1 – 4	$v = 300 \text{ mm / min}$	117
Figure 89	Tooth Trace Deviations	$v = 100 \text{ mm / min}$	118
Figure 90	Tooth Trace Deviations	$v = 300 \text{ mm / min}$	118

Figure 91	Root Circle Diameter.....	119
Figure 92	Tip Circle Diameter.....	120
Figure 93	Development of tip- / root diameter dependence feed rate..	121
Figure 94	Axial Course of Tip Circle Diameter	123
Figure 95	Profile Lines in different axial Heights.....	124
Figure 96	Pitch / Concentricity different Heights.....	126
Figure 97	Axial Tooth Tip contour, Axial Scan Line in the ZX-Plane	127
Figure 98	Cross-Sectional Contour of the Tooth	128
Figure 99	Forms of Teeth / Different Feed Rates.....	129
Figure 100	Config. sensors / workpiece coord. system R, Z, φ	134
Figure 101	Principle sampling sequence / surface in forming phase n ..	137
Figure 102	Principle sampling sequence / surface in axial feed phase...	137
Figure 103	Principle sampling sequence / forming phase n+1	138
Figure 104	Sensor signals / forming / axial feed / rotational.....	138
Figure 105	Signal curves for forming cycle n+1 (schematical)	139
Figure 106	Specification Runout Tolerance / workpiece acc. ISO 1101 .	140
Figure 107	Sensor placement / determination eccentricity (Sensor 2)..	141
Figure 108	Principal sensor signal vs. time and calc. of eccentricity	141
Figure 109	Path of the sensor spot pitch variation / gap thickness.....	143
Figure 110	Signal process. pitch, pitch fluctuation, tooth, gap thickness	144
Figure 111	Tooth profile, (Chapter 5)	147
Figure 112	Analysis of form deviation / tip symmetry / asymmetric.....	148
Figure 113	Measuring Axial Position Orientation.....	150
Figure 114	Sensor signals Axial- Position Orientation.....	150
Figure 115	Axial Configuration 2 Sensors for the acquisition	151
Figure 116	2 distance sensors / axial angle diff. / tooth trace deviation	152
Figure 117	Calculation of tool trace deviation $h_{F\beta}$	153

1. Introduction

The elaboration describes a research which is based on a little-known rolling technology which was developed in Poland in the 70's. To better understand the facts today in connection therewith statements made by a witness of the former WPM activities should be prepended. It is important to know that at that time in Europe, the communist and the capitalist block faced. Correspondingly, it was especially difficult to design projects between politically different blocks at that time as part of economical-technological exchanges between states.

Theoretically, the WPM-Rolling-Technology was developed by Prof. Z. Marciniak. The WPM-Rolling is characterized by two internally toothed rolling tools which move on symmetrical eccentric courses around the workpiece. The aim is to produce a spline chipless. Back then, the machine and the rolling method WPM was highly suitable for chipless production of large face-gear machine elements in the range of module 2,5 and higher. Other methods on the market with a similar performance were known only partially. The Polish company Plasomat designed and produced in accordance with this tool-motion principle, rolling machines like the type WPM 120. Some machines were used in the Ursus tractor factory in Warsaw, others in the former Soviet Union.

The foreign trade company Metalexport, of the then communistic Poland cooperated with the West German firm German Industrial Society and other interested companies. End of the 70's one of those rolling machines WPM 120 reached to the Institute for Metal Forming of the Technical University of Darmstadt, Prof. Dr.-Ing. D. Schmoeckel. The machine has been tested and it was found that the achievable spline quality of this machine did not meet the quality standards required by the industry. The machine WPM 120 was

not scientifically examined because their structural design was quickly recognized as a fundamental cause of the insufficient quality of the rolling results. The principle of motion in itself is classified as extremely interesting, so that various prototype machines were developed in the following years. The political developments of the late 80-ies and other technological developments in the machinery market led to the machine WPM 120 fell into oblivion. The rolling on the WPM method of Prof. Z. Marciniak is now described in standard works of the literature of metal forming. About WPM only a few reports were published (Prof. Z. Marciniak, Z. Kopacz, Prof. Schmoeckel and employees). Other research papers that examine the issue of rolling with internally toothed tools in detail are not known worldwide. This is explained by the history of the rolling method WPM.

Prof. Dr.-Ing. Ernst Hammerschmidt, University of Darmstadt, Department of Mechanical Engineering, Head of Metrology Laboratory

Since 1994, probably the only still functioning rolling machine WPM 120 is located at the University of Applied Science Darmstadt in the laboratory for production technology. The machine serves there as a laboratory machine for student internships, bachelor's and master's theses.

Professor Hammerschmidt and his colleagues at the University of Darmstadt cooperate since about 1980 with the company Leitz in Wetzlar. At that time measurement software for measuring gears has been developed together. A former student of the University of Darmstadt Ingo Lindner got to know the rolling technology developed by Prof. Marciniak during his engineering studies. The later Master's degree in Industrial Engineering from Ingo Lindner and Tim Eichner led to the first joint studies of rolling technology WPM. At that time, Ingo Lindner was head of development of Leitz. In the course of his business, he realized in the market of production technology that the in-process monitoring in machine tools would become increasingly important. That's how the idea of using the rolling machine WPM 120 as a base for de-

veloping a process control for machine tools arose. Such a development could lead to a new and particularly interesting commercial business area of the company Leitz. Technical discussions with professors in Darmstadt and work-related contacts with Professor Sladek (Krakow) and Prof. Wieczorowski (Poznan) in the field of coordinate metrology led to the idea of developing a metrological policy framework for machine tools. The starting point for this research is the increasing economic importance of forming technology on the global market. In this connection, the chipless production of toothed machine elements has been standard practice for decades. However, the achievable geometric quality of the teeth and their magnitude set $m > 2$ are clearly limited. Besides the technical advantages, such as the solidification and the economic benefits, such as material savings and the shorter manufacturing time all relevant processes have in common that the so produced work pieces have specific geometric characteristics. These characteristics are typical for the respective forming technology. They are mainly caused by the tool movement of the forming principle and the resultant forces during forming. The geometric quality of such tothing is dependent on the quality of the tool guiding during the forming process and of the unwanted movement of the workpiece by the forces required for deformation. Both factors determine the manufactured geometric quality of the toothed machine elements without using a cutting method. The forming production of toothed components is only then economical when they are manufactured in large batches. A reliable statement about the resulting part quality after forming is nowadays fully possible only through the coordinate metrology in form of geometric POST-process measurements. A quality control of this kind takes time. The result is therefore a conflict of aims between the economic demands of mass production of tothing and the need for a comprehensive quality control of production [4]. The above described circumstances suggest monitoring the deformation process even during the transformation in order to react quickly to any unwanted change of events. The ideal situation would be a process monitoring for chipless production of toothed ma-

chine elements. In this sense, the basis for our own studies is the rolling machine WPM 120 located in Darmstadt. This machine is suitable for non-cutting production of toothed machine parts, for example shafts according to DIN 5480 [ST 10]. The rolling machine WPM 120 is ideal for the development of a monitoring process. This machine is ideal for the development of a monitoring process [30]. This statement is justified by the special qualities of guiding of the rolling tools, the relatively high forming forces and the typical geometrical features of the chipless manufactured components [17]. The geometrically investigated components of this work were produced on this machine [ST 10]. To make sure that all components and especially their teeth were produced under the same conditions, the key mechanical engineering parameters were determined by measuring during the forming. The aim of this work, reported in sequence, is to determine how far the geometric features can be detected on the components thru post-process measurements to create a basis for a future in-process control of the forming event.

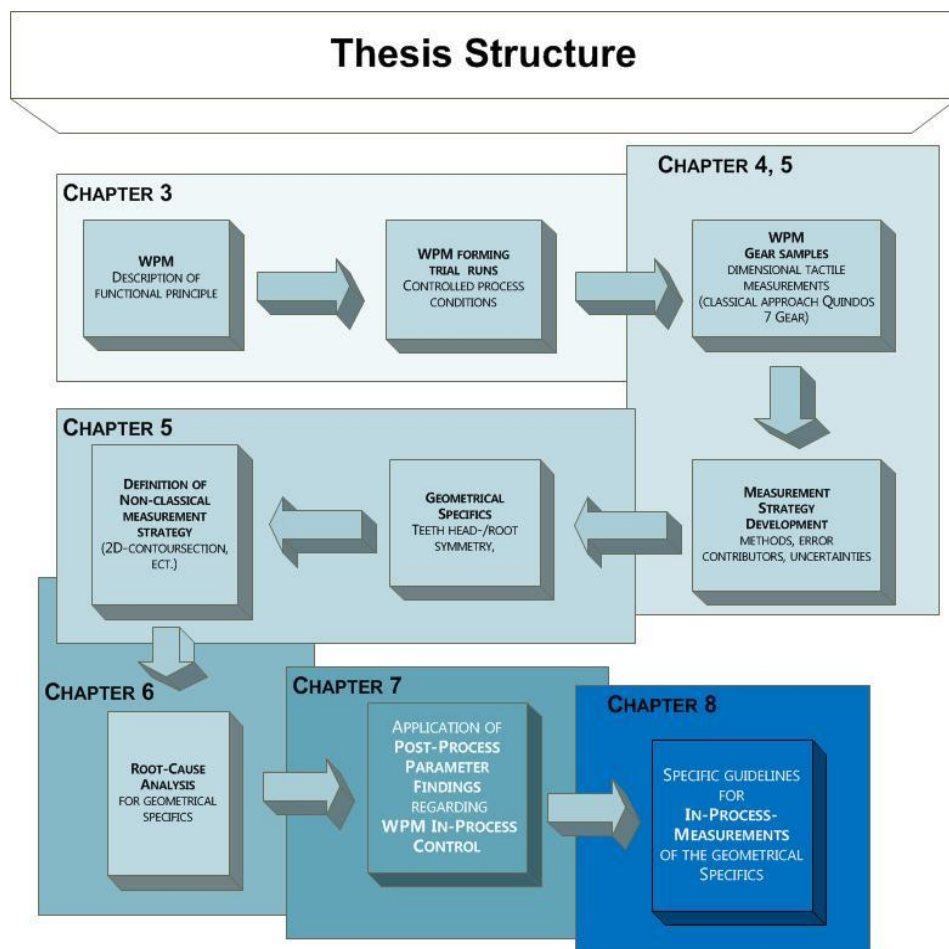


Figure 1 Thesis Structure

2. State of the art - Production toothed machine elements

The modern production technology for the manufacture of splined components is complex. All currently known production technologies are used here [3]. The production of toothed parts is in general distinguishable into the manufacturing of individual parts and mass production [57].

A single component or a small amount of splined components is manufactured usually by machining. In this case various metal cutting methods are used. In the context of series production large numbers are usually produced in a combination of different technologies [61]. Here at the beginning of the production chain is the primary forming or metal forming [65, 58]. This means that, for example, thru the primary forming or metal forming a preform is produced [66].

The final shape is then formed by subsequent metal cutting or other metal forming processes [94]. The structure of such production lines, for example, depends on the geometry of the toothed part, the material from which the part is made, and the quality requirements to the final geometry [54].

Each series production is dominated by questions of production efficiency. In this sense, individual parts or small quantities of toothed components cannot be made through a preform by primary forming or metal forming.

The arising high tool costs would affect the economics of such production negatively [37]. For individual parts in this sense the production line starts with, for example, semi-finished bars. The following figure shows a compilation of the various technologies and processes that are used in modern gear manufacturing. The figure 2 shows typical methods used in the large-scale production of gears in combination. Starting from a preform which has been produced e.g. by molding or forming, is made by rotating the output body [ST 9]. Then the toothing is realized by machining or forming. Onto the mention of various intermediate steps, in particular the metrological examination of the various production steps has been abdicated.

METHOD for manufacturing toothed machine elements

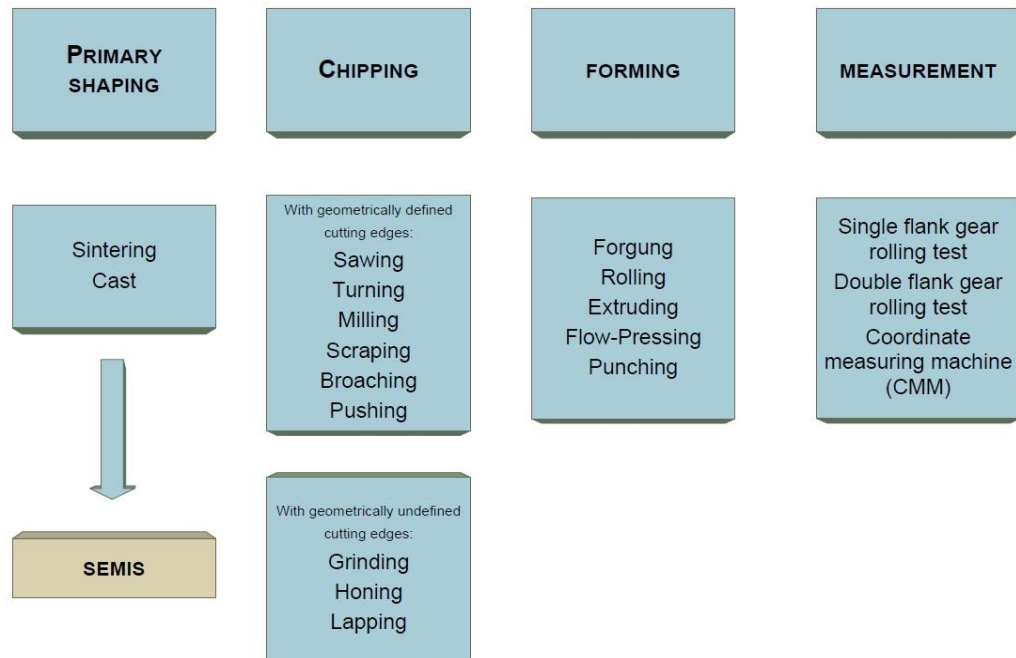


Figure 2 Compilation of the various technologies and processes

2.1. Toothed Machine Elements

Toothed machine elements are components with specific geometric functional elements. The functional elements are used for various purposes, such as the transmission of movements and / or torques [102, 103]. The geometric structure of a toothed part can be divided into primary and secondary functional elements. In this sense, in a toothed machine element the tothing by itself is in the center of attention. The teeth of such a component are thus main functional elements. Usually toothed components are paired with another toothed part, whereby the intended mechanical function arises [ST 1]. Geometric regions or areas on the main functional elements of a tothing, through which the mechanical function is realized, are called the main func-

tion areas. The following discussion refers only to face-geared machine elements as exemplified in the following pictures [ST 2, ST3].

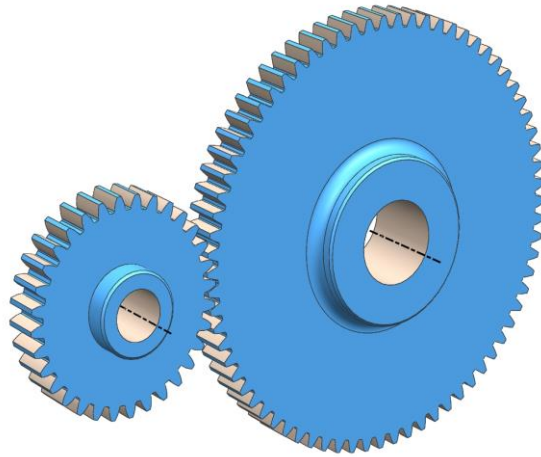


Figure 3 Pair of Gears

Figure 3 indicates a gear pair of two externally toothed components. The rotational movement of one gear wheel is transferred to the other. This leads to a ratio of the rotational movement, which corresponds to the ratio of the respective numbers of teeth. Thereby the transmitted torque is inversely proportional to the respective speeds. The main functional elements of the two components, the teeth, determine the mechanical function of the pairing. The mechanical function is realized in this example by the main function areas of the teeth, their flanks. Figure 4 shows another gear pair in which a toothed shaft is positioned in an internal gear hub [ST 10].

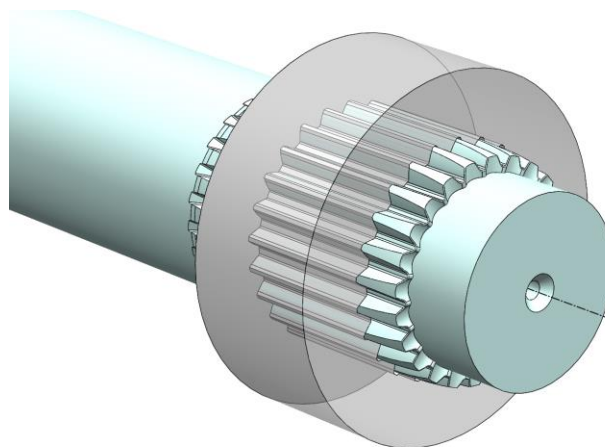


Figure 4 Pair of Gears – Toothed Shaft / Internal Gear

A relative movement between the two components in the circumferential direction is not possible. Such a combination of two toothed components serves to transmit torque while permitting axial displacement. It is a typical shaft-hub connection, as it is often used in the automotive industry in the large-scale production. For clarity the hub is shown transparent.

The examples shown above figures 2, 3 will serve to illustrate how different the functions of teeth can be in toothed machine elements. For the sake of good order, it should be noted that these two examples are only two of a vast number of other applications of toothed parts. Not always the tothing is placed on a rotationally symmetrical part. They are often a part of a rod-shaped machine element. A typical example of the linear arrangement of teeth is a rack. It should be emphasized that most toothed machine elements are combined in industrial use with another toothed component. Only by the interaction of a pair of gears arises then the intended mechanical function. As shown later, arise by the pairing of gears, special geometric quality requirements for the single toothed machine element [5].

2.1.1. Spline Shafts

Splines are mass parts that are required, for example in the automotive industry in very large numbers [ST 1, ST 10]. Spline shafts are usually paired with an internal gear hub. This component combination, they are called shaft-hub connection and are used for the transmission of torque allowing axial displacement of the shaft against the hub.

Figure 5 shows such a shaft-hub connection. The aspired geometric ideal of this pairing is that the center of the externally toothed shaft and the center of the internal gear hub in the assembled state are identical.

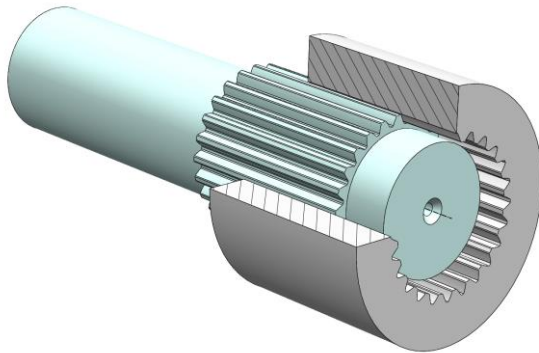


Figure 5 Shaft-Hub Connection

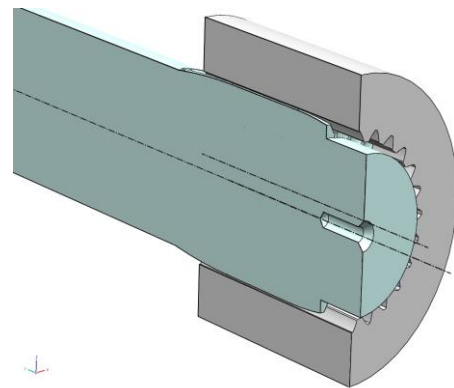


Figure 6 Shaft-Hub Connection
Cut-Open View

The figure 6 above, the center line of the short and the long hub of the shaft are shown offset. The deviation from the ideal pairing of hub and shaft would have in technical use significant negative consequences. The symmetry of the load distribution on both machine elements would be disturbed. The geometric points of contact or contact surfaces of both components should therefore be absolutely symmetrically regarding an identical center after fabrication. This receivable means technically that the functional elements (teeth) on the two components based on the same center in shape and position should be made absolutely identical. Only then the main functional surfaces of both teeth on the same geometric locations in the space have the ideal mechanical contact. This is the production-technical challenge that must be overcome in the mass production of such gear pairings [32, 33]. In the present work are splined shafts in accordance with DIN 5480 in

the center of attention [ST 10, 96]. In simple terms, a problem with such a gear pair results. This is the centering of the two machine elements against each other. Accordingly, DIN 5480 T1 defines the different types of mutual centering [ST 10].

To illustrate this geometric relationships in the sequence images are shown. In such a partial volume of the pair is shown broken.

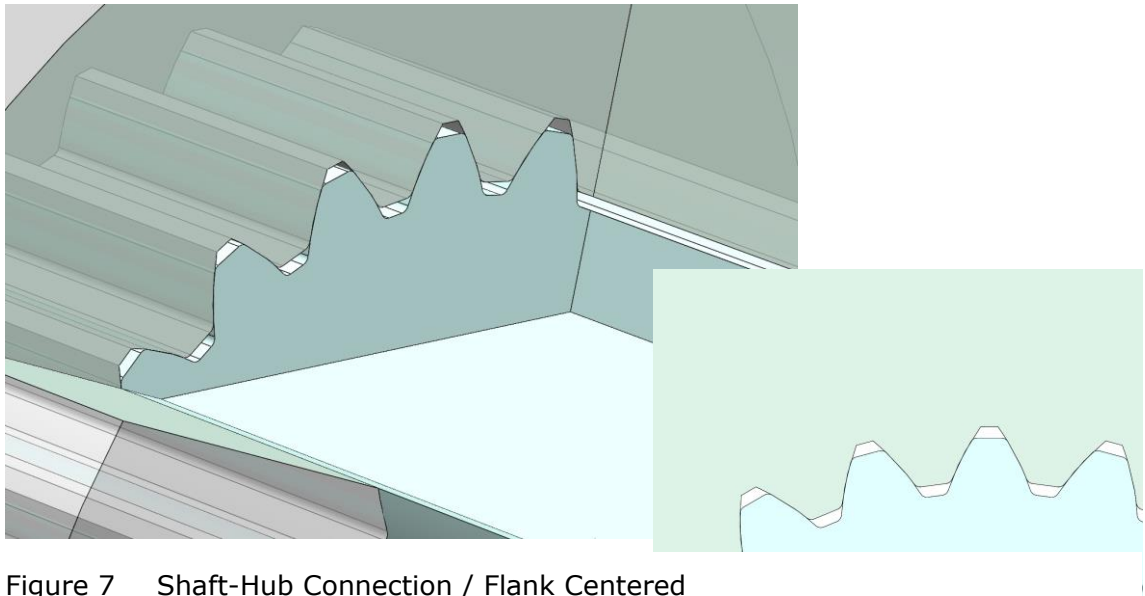


Figure 7 Shaft-Hub Connection / Flank Centered

Flank Centering At the flank-centered connection (Figure 7), the flank areas of each gearing are used for torque transmission, to guide in the axial movement and also for centering. The head circle and root circle diameter of the two elements should therefore be developed as they do not allow any mechanical contact between the components. Only the main functional areas of the two elements define the quality of the centering of the parts against each other. The manufacturing technology resulting clearance between the two components defines the quality of the fit.

Diameter Centering Diameter centered connections of hub and shaft are centered in the outer diameter of the hub root diameter and the spline tip diameter, if it is an external centering. Or they are centered on the hub-tip diameter and spline root diameter, if it is an internal centering.

In both cases (Figure 8, 9), this type of centering principle must sufficient backlash between the two elements are provided in order to avoid over-determination of the centering. By measuring centering means require a considerably larger production cost because of the resulting tolerances, so this type of shaft-hub connection is used in industrial applications are rare.

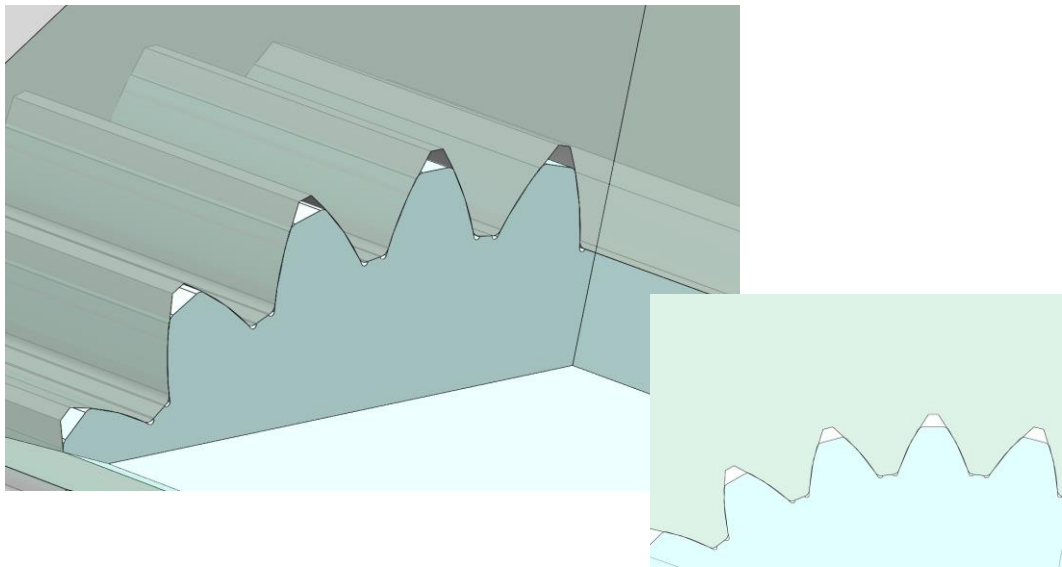


Figure 8 Shaft-Hub Connection / Root Diameter Centered

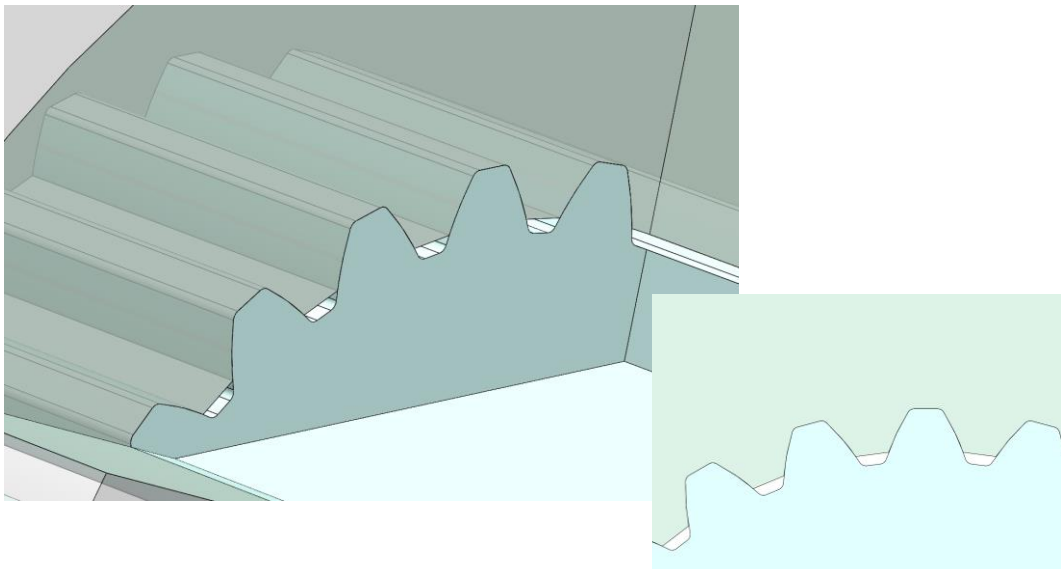


Figure 9 Shaft-Hub Connection / Tip Diameter Centered

3. Metal Forming

Metal forming is a very old technology for shaping components. One of the oldest methods of forming is the forging of metals [123]. Thereby, thru one or more tools the required energy for shaping is introduced into the material [60, 62, 115, 116]. At all methods of forming mechanical energy changes the shape of a material volume [45, 46, 80]. The volume of the processed material remains constant, regardless of whether it is solid or sheet-shaped material [68, 81]. At toothed machine elements mostly solid material is in the center of attention. A distinction is made into hot, warm and cold forging. During hot-or semi-hot forming, the volume is deformed dependent on the material at temperatures of approximately 600°C – 1200°C, while cold forming at room temperature [47]. Nowadays, toothed machine elements are produced chipless thru forging, extruding or rolling [117, 124]. The desired geometrical quality of the components determines the employed manufacturing process [120]. The advantages of all forming processes are inter alia the material savings and the associated solidification of the material structure thru metal forming. Today, for the production of toothed machine elements, all known methods of forming technology are used [123]. Forging is used primarily for the production of a preform [1]. The resulting geometric components quality after forging does not always match the required quality standard [7, 73, 74]. The required quality is usually achieved by subsequent cutting processes [63, 101]. Extrusion is used mostly by cylindrical components with a long axial toothing. And the rolling processes are always used wherever rotationally symmetric components are to be toothed. Often, the reshaping is followed by a carburizing and / or a hardening process, so that the surface or near-surface areas of the teeth have better abrasion behavior [93]. For the highest geometric requirements the reshaping can also be followed by a cutting process such as grinding. A clear statement which method or combination of methods is used for specific

types of gear components cannot be made [75]. The variety of different geometric shapes of such components and the desired quality characteristics are too different [64]. The goal of any production must be to work with the lowest expenses [54]. Consequently, the technical necessary production steps are also evaluated in terms of costs [55]. As long as, the required technical function of the toothed component is ensured, different combinations of manufacturing steps and used methods can result in success [59, 67]. The question of the success of a production is closely linked to the issue of quality control of production. Mass production and technical standards for the quality of manufactured components include various trade-offs. Mass production vs. part accuracy and part accuracy vs. material properties are particularly for cutting production, the key challenge [76, 77]. Besides many other factors the metal forming is determined thru the material properties of the deformed material and the unavoidable tool abrasion [79]. Unwanted variations of the composition of the formed material or changes of the tool shape thru abrasion can significantly affect the resulting quality. This statement concerns the geometry of the component after forming, as well as the then existing mechanical component properties.

At the forming production of toothed machine elements, this relationship is of particular importance. The proper function of teeth is directly dependent on the geometric quality of the teeth. By which the large need for control of forming production is explained. Mass production and quality control are another conflict, which takes a special importance while manufacturing toothed machine elements. Short production times that are required in connection with mass production, and great loss of time through quality control is a contradiction in terms. Thru this the economics of production is significantly influenced ultimately [69]. The large amount of time which has to be provided for the correct geometric control of a toothed element, allows just only random checks after the production of a component series. Therefore, the post-process control can only record individual components. Consequently, a comprehensive inspection of all parts is only possible within the manufactur-

ing process. The challenge for the future is to control the mass production of toothed machine elements completely by monitoring the forming process [132]. For the own research test samples were manufactured under controlled conditions. The sample material came from a batch of steel production and was examined metallurgical to its composition. Then the used sequence of manufacturing steps begins for example with rod-shaped carbon steel C15. Accordingly long pieces of this material were annealed ($HV \sim 130$) and shaped to predetermined dimensions by turning. The desired geometry of the blank is determined by the method which is used for the production of the toothed component. In this research, it was the rolling according to the Polish WPM method [92]. Here the teeth are formed without cutting through two internally toothed tools. The roll samples were rolled in the cold state (room temperature).

3.1. Rolling Methods

Rolling processes includes the area of the pressure forming processes, DIN 8583 T1/T2 [ST 11]. In these methods, mainly compressive stresses resulting in the forming zone [11, 12, 13]. The rolling processes for manufacturing toothed components are usually divided by the geometric shape of the used tools [6, 9, 94]. The method are differed into methods with rotationally symmetrical external toothed tools (PeeWee), with flat back shaped tools (RotoFlow), with internal toothed tools (WPM) and the so-called planetary rolling method (Grob), about which will not be further reported [72, 78, 123]. In consequence, the aforementioned rolling processes will only be explained briefly in principle. Specific process variants remain unmentioned. The two oldest methods, PeeWee and RotoFlow were developed for non-cutting thread production end of the 20-ies. A typical component is the screw, as it is produced worldwide for many decades [129]. The screw is a cylindrical toothed machine element, which includes inter alia an essential geometric functional element, the thread. The technological relationships

and sequence of manufacturing steps are very similar to the modern manufacturing sequence in modern manufacturing of toothed components [67, 69]. Starting from a cylindrical preform, the blank, portions of the preform are formed to the desired functional elements, threads or gears. The screw is a typical mass-part; the production is based almost exclusively on the metal forming. For screw production about 20 years ago different process monitoring systems have been developed. Without the monitoring a modern screw production is hard to imagine today. However, the qualitative requirements for the process monitoring of a screw-production are significantly lower than in the manufacturing of toothed machine elements. The process monitoring of screw production is based solely on the detection of technical machine data during the forming. At all the aforementioned rolling processes enters a wedge-shaped tool in the surface contour of the blank and displaces the material [123].

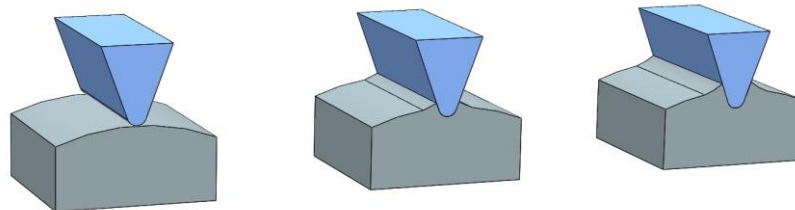


Figure 10 Ingression of a wedge-shaped tool

The impacted material reacts plastically and flows into the gaps next to the wedge-shaped tool. In the gap between two wedge-shaped tools, teeth of the forming tool, a tooth is formed on the workpiece. The shape of the thus formed tooth is dominantly depending on the tool shape and the tool movement during the rolling and the resulting rolling movement between the tools and the deformed material [106, 133]. Insofar tooth shapes arise in each of these rolling processes which are typical for the respective rolling

process [94, 107]. Each of the aforementioned rolling processes are based on a typical machine mechanics and typical drive kinematic which implements the tool movements.

PeeWee Rolling When rolling with the PeeWee method two rotationally symmetrical externally toothed rolling tools are included on two parallel drive shafts and rotated [14, 15]. The rotating tool shafts are either one sided or both sided moved towards the blank. Normally the blank is handled between tips [18, 20, 109]. In the mechanical contact with the blank the tool contours penetrate into the material on both sides and put the blank in rotation [19, 89]. After repeated overexpansion the circumference of the workpiece the tool teeth reach their machine side predetermined penetration depth [16, 88]. The transformation is complete. The rolling tools are moved back into their starting position. The finish-rolled component is removed from the machine.

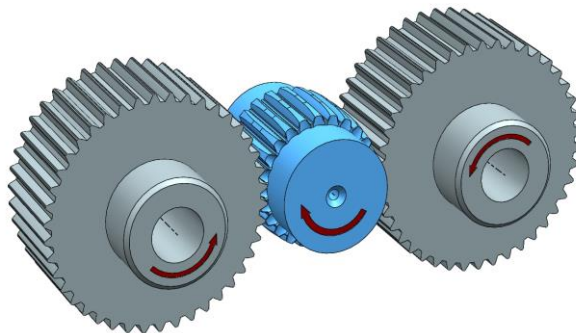


Figure 11 PeeWee / External Toothed Tools

RotoFlow Rolling When using the RotoFlow method rack shaped rolling tools (dies) are used. The two dies are moved in direction towards the blank which is located between two tips. After the first contact of the tools with the material the blank starts to rotate. The shape of the tool toothing has an ascending profile so that initially only a small depth of penetration results of the tool teeth [21]. As the stroke motion of the dies increases according to

the ascending profile of the tool teeth the material is penetrated deeper [22]. Only after a complete stroke movement and repeated rotation of the workpiece, the deforming is finished.

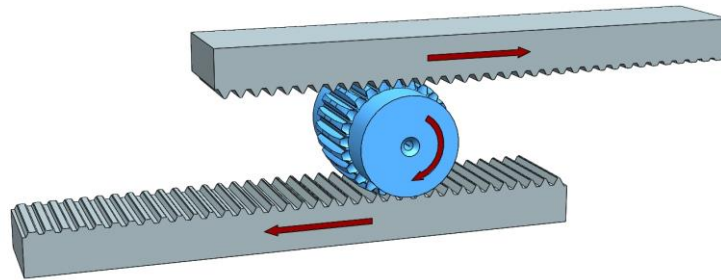


Figure 12 RotoFlow / Rack Shaped Rolling Tools

WPM Rolling Rolling according WPM method is based on two internally toothed rolling tools which move on symmetric eccentric courses [38, 92]. The blank is held between tips and turns driven by the machine. The rotating blank is fed between the rolling tools. The tool teeth grasp the material, make the blank rotate and forms teeth on the entire circumference of the workpiece. The resulting tothing on the blank per feed step is formed completely. After every stroke the tools open and release the workpiece for the next feed step. The magnitude of the axial extension of the developing serration per stroke is dependent upon the feed rate at which the blank is inserted between the tools [44]. Since this process is in the center of this work, this method is explained detailed in the next chapter.

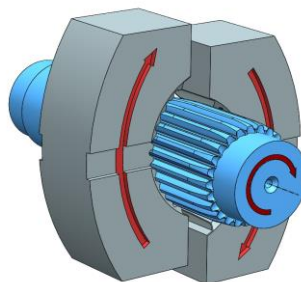


Figure 13 WPM / two internally toothed

The above briefly described rolling methods cover the entire area of the geometric possibilities to use just a solid tool contour and only a linear or rotary motion to stress a cylindrical blank surface so that a set of teeth is formed by forming [39, 44, 118, 119]. Industrial practice in dealing with these rolling process shows that not each of these methods is suitable for every type of toothed components [2, 108, 119]. Assuming appropriate performance of the machine technology and stability of the rolling tools arise nevertheless significant differences [25, 110, 111]. The size of the teeth and producible quality of the achievable teeth are set process-specific limits. Responsible for this are the resulting forces of the deformation. These are dependent on the strength of the metallic material and the contact surfaces between the tool and the workpiece material during forming [37, 40, 41, 48, 112]. The reaction forces as a result of metal forming act on the workpiece. The workpiece attempts to evade these forces and thereby loses its ideal location between the tools. Whereby, a loss in quality of the resulting gear quality must be accompanied. In this respect, the guiding characteristics of the tools referring to the stressed workpiece are of dominant importance [113]. Comparing the three methods described above in this regard, it should be noted that the externally toothed tools (PeeWee) overlap the workpiece toothing the least, the rack-shaped tools (RotoFlow) a little more and the internally toothed tool (WPM) the largest [38, 39, 114]. The internal gear tools of the WPM process guide the work piece during the forming the best. This is inter alia the reason that, with this method, spline shafts on the order module ≥ 2.5 can be rolled, which is with the two other methods not possible.

3.1.1. Advantages of Rolling Methods

Material Savings According to DIN 5480 a splined shaft is defined with $m = 2.5$, $z = 24$ and tip diameter of 64.5 mm [ST 10]. This diameter must be at least present when the teeth of the shaft are produced by cutting [104].

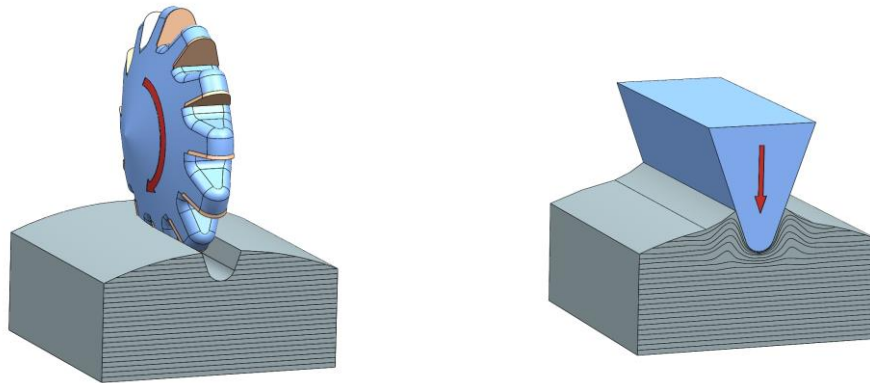


Figure 14 Cutting / Rolling

If the same gear is produced by rolling, then a preliminary diameter of 62.3 mm is enough. At a tothing length of 200 mm a material saving of 0.172 kg results per toothed component. Thru the rolling, consequently a considerable economic advantage occurs [54, 55]. This is especially true when these splines are mass produced. The figures 14, 15 are intended to illustrate this relationship. When cutting, a loss of material takes place, since the initial diameter must be larger than if a rolling process is used [105]. If a rolling process is used a smaller diameter is sufficient, because due to the penetration of the tool, the material moves into the tip diameter.

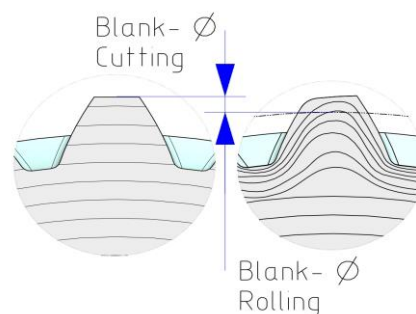


Figure 15 Preliminary Diameters

Solidification of the Material Structure In the following figure 16, the material structure is shown as formed by rolling.

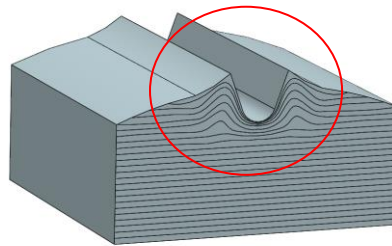


Figure 16 Material Structure after Rolling

Through previous processing steps, such as extrusion (semi-manufacturing), generated alignment of the crystalline structure of the steel runs almost linearly through the material. The penetrating tool displaces the material so that the structure adjusts to the wedge-shaped tool geometry. The structural changes which occur through the plastic deformation of the material lead to a hardening of the material where it got displaced the most [ST 13, 84]. The largest solidification is noted in the foot circle of the resulting tooth gap [71]. Depending on the material and, for example, carbon content of the steel, an increase of the material strength of up to about 20% is observed. The huge advantage is that where under stress the greatest reaction tensions of load may occur in the material, the largest material compression is present. The teeth are overall more suitable to greater loads than a tothing produced by cutting. When cutting, the originally existing structure of the semi-finished material is cut [70]. The figure 17 shows a fragment of the volume of a rolled spline. To recognize is a harmonious course of the structure contours, as previously described. The above described issues are not new. For decades, we know that rolled threads to e.g. steel screws can handle significantly higher loads, as threads produced by cutting [4, 91]. The material-

technical aspects and advantages of the material solidification at the notch root of a thread are similar to the rolling of gears.

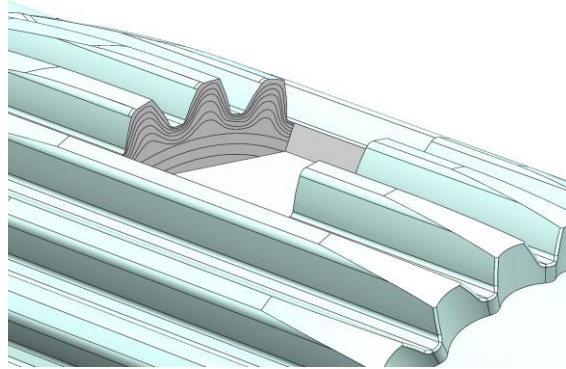


Figure 17 Fragment of the Volume Rolled Spline

3.2. Rolling according to the WPM Method

Motion principle rolling tools / workpiece The rolling according to the WPM method of Prof. Z. Marciniak is characterized by two internally toothed rolling tools [92]. The tools move in symmetrical and circular eccentric courses, as shown in the figure 18 below.

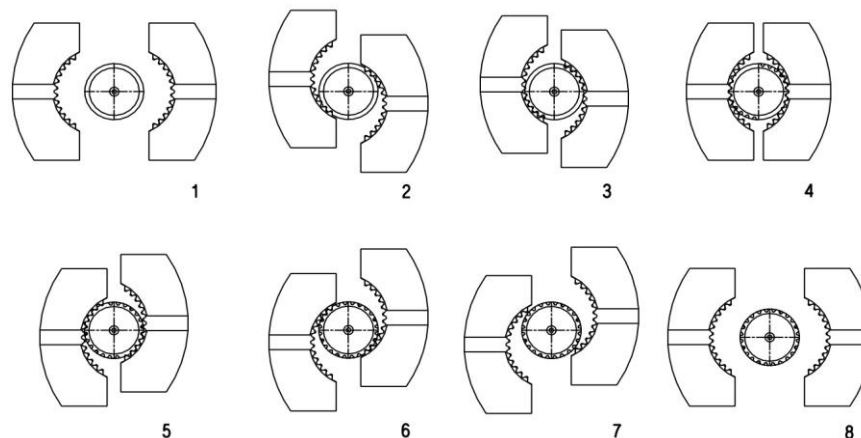


Figure 18 WPM - Motion Principle Rolling Tools / Workpiece

The rolling process starts with rotating rolling tools. In accordance with the machine set up of the eccentricity, the tools teeth approach (2) and remove at every stroke (7) from the center of a cylindrical blank. The blank rotates with the same peripheral speed as the tools and is inserted axially between

the rolling tools. The tool teeth engage the blank and penetrate into the material (2, 3, 4, 5, 6, 7), so that the tool teeth get reproduced in the material. At each tool stroke arise therefore a rolling phase and a phase in which the tools are opened (1, 8). In the open state of the tools the blank is axially advanced and the rolling process begins again. At each tool stroke the teeth penetrate into the material to their possible maximum depth so that the entire circumference of the roll sample a complete tothing is formed [42]. The axial extent of the resulting spline shaft is given by the number of tool strokes per time and the machine side set up of the feed rate with which the workpiece is advanced axially [43].

Machine technology WPM 120 The available rolling machine WPM 120 is about 35 years old and is in its original condition. Except for the replacement of the drive belt of the drive technology, lubrication of bearings and the replacement of some electrical components no repairs were carried out on this machine in the past.

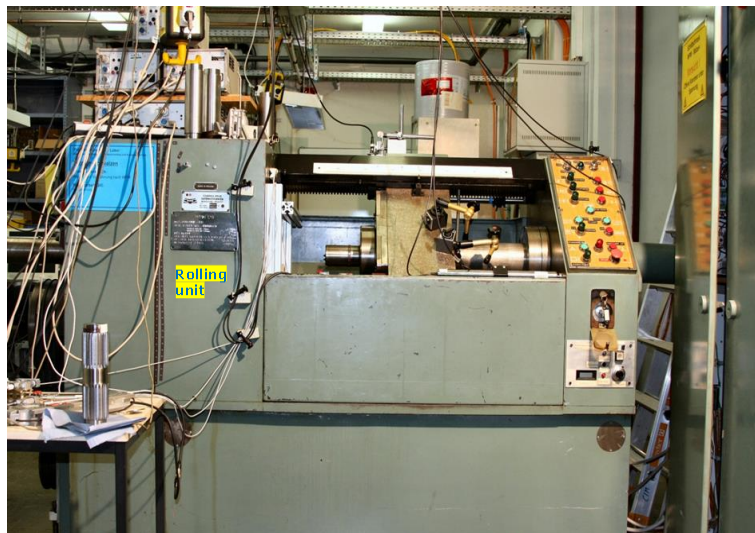


Figure 19 Machine WPM 120

The constructive relationships of the machine WPM 120 are complex. Detailed design drawings were not available. A disassembly of the machine was not possible. The following statements cannot reflect all the details of this machine design. The machine's mechanical drive technology and the cast

elements are added on a sturdy welded frame. The rolling unit is connected via three massive columns (1, 2, 3) with the transmission unit.

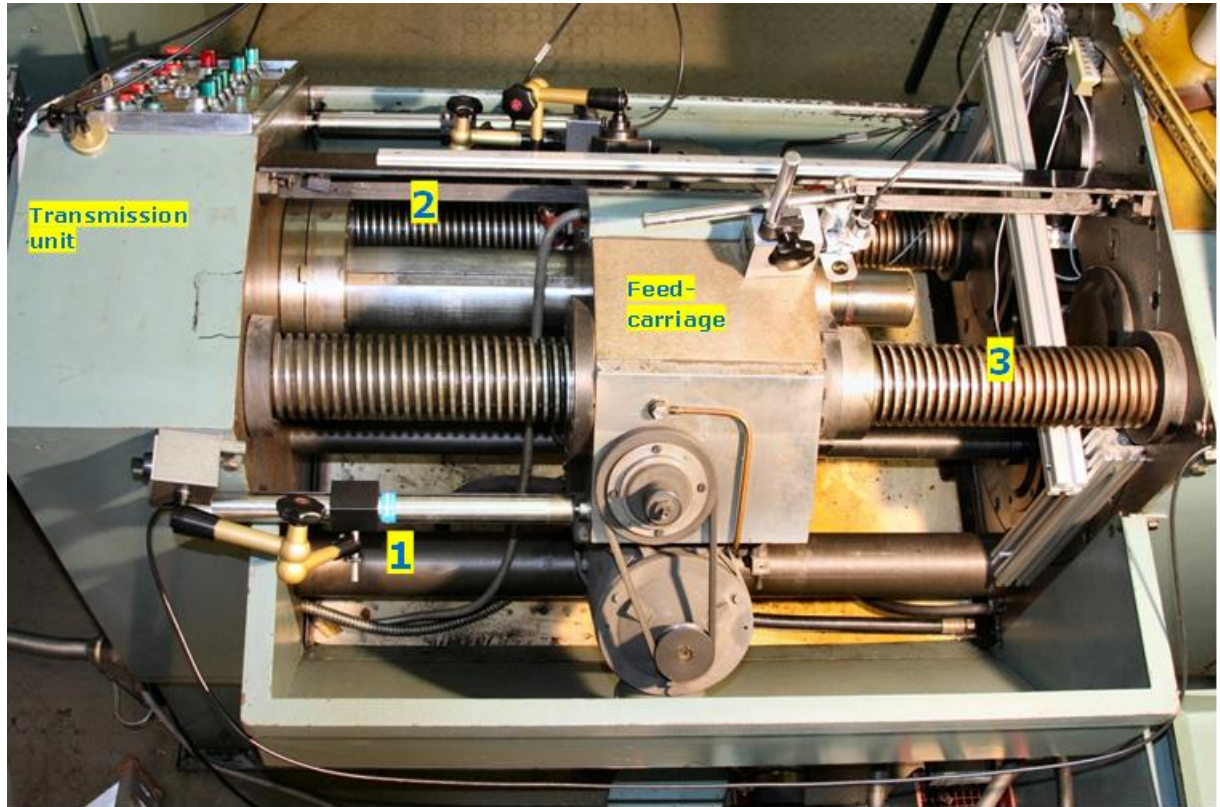


Figure 20 Machines top view / Three Massive Columns / Feed Carriage

A very robust asynchronous three - phase - cage motor with nominal power of 7.5 kW is the main drive. Via several drive belts an intermediate shaft with an integrated electromagnetic clutch is driven by the main drive.

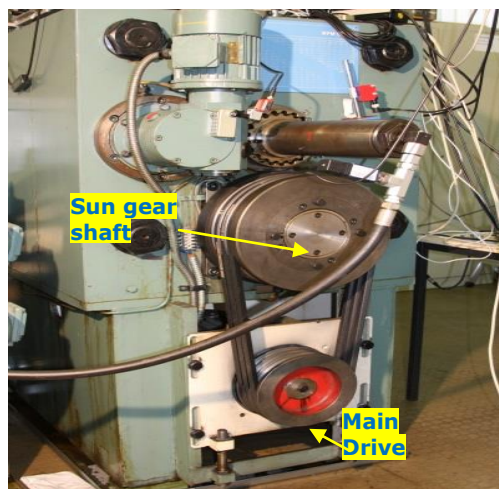


Figure 21 Main Drive

Tool Movement The intermediate shaft drives by gears 2 central sun gear shafts. The sun gear shafts are coaxial, driving over two planetary gears four eccentric shafts. By rotating the two coaxial sun gear shafts, the eccentricity of the four eccentric shafts can be set synchronously and identical for all four eccentric shafts in mechanically defined stages. Two opposite eccentric shafts lead flying mounted a respective cup-shaped tool carrier, which each receive an internally toothed tool segment.

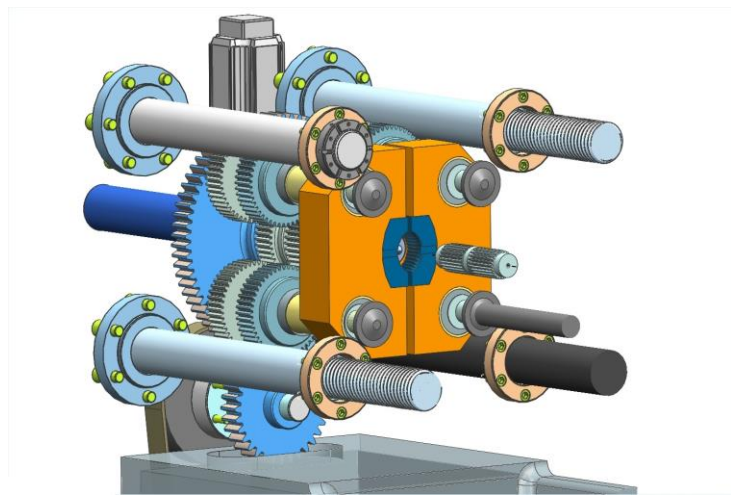


Figure 22 Tool Movement / Four Eccentric Shafts/Left Auxiliary Drive

The sun gear shaft can alternatively also be driven with a small auxiliary drive and a worm gear. Also this auxiliary drive is connected via an electromagnetic clutch.

The auxiliary drive only allows a slow stroke motion of the tools. It is used to move the tools defined before rolling, for example, when setting up the machine. After rolling a workpiece, the rolling tools are moved by this auxiliary drive to open completely. The rolled workpiece can then be taken out axially from the mold space, in order to remove the workpiece.

Workpiece Movement The workpiece is held between tips. Centrally between the tools shown in figure 23 one of the two tips is shown, which is pushed by a hydraulic cylinder against the workpiece.

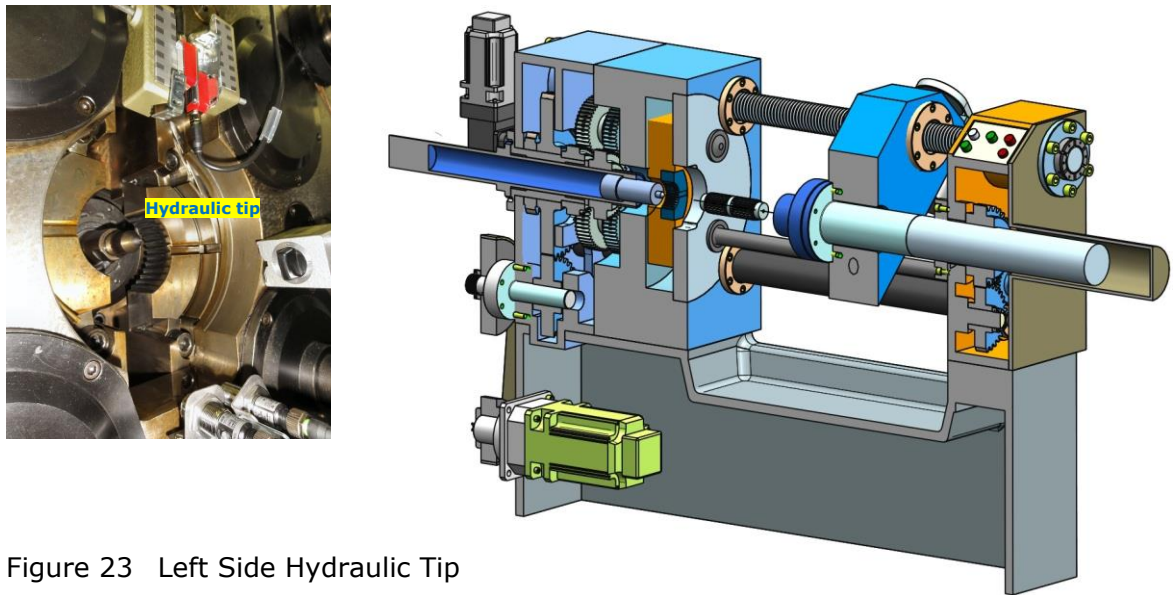


Figure 23 Left Side Hydraulic Tip

The other side of the rolling sample is held by a spring-biased tip (Figure 24), which is held in a sleeve. The installed state of a rolling sample is also shown in figure 24. The rolling sample is clamped between the spring biased tip and the hydraulic tip.

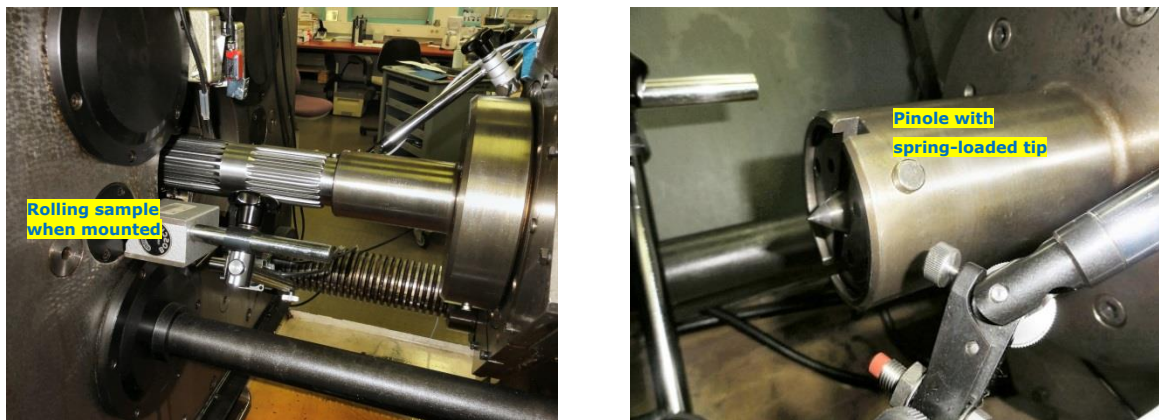


Figure 24 Right Side the Spring-Biased Tip

Figure 24 shows that the sleeve is rotatable mounted in a feed slide. The rotational movement of the sleeve is directly derived from one of the four eccentric shafts rigidly mechanically. The rotational movement of one eccentric shaft is a gear box fed behind the feed slide, and transferred to an axially displaceable splined shaft. The sleeve (Figure 25) is driven from the rear of this spline shaft for synchronizing the rotation of the workpiece movement to the rotational movement of the tool segments. The spline shaft allows the

feed motor can move the feed slide axially without the synchronization of the workpiece rotation is lost when axial feed between the tool segments.

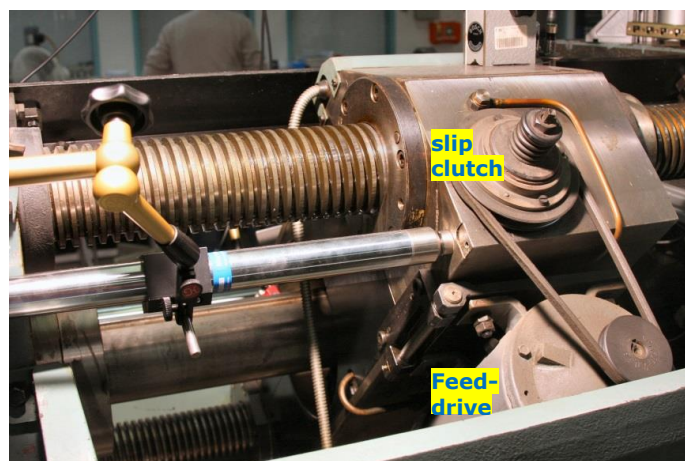
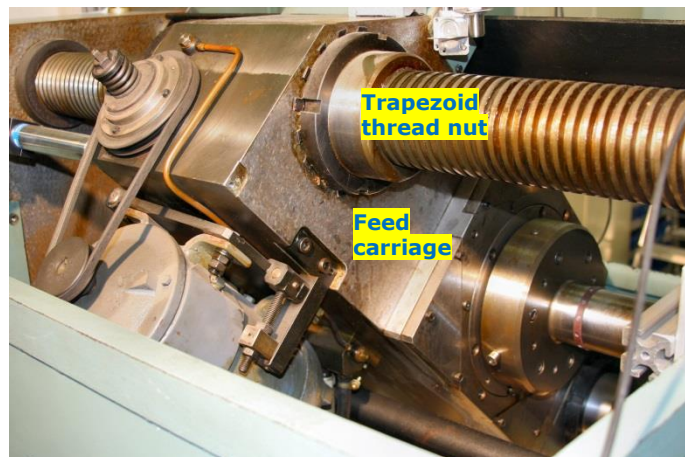
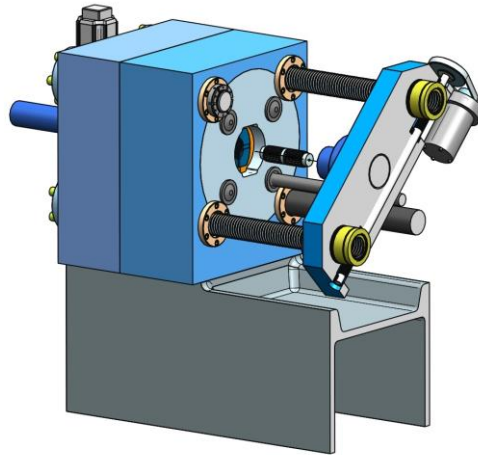


Figure 25 Feed Carriage / Feed Drive

The axial feed of the workpiece between the rolling tools is realized with a DC motor (power 0.8 kW). The feed drive is seated on the feed carriage, and is screwed to it. By means of a belt, and a slip clutch are driven, each with a screw top and the bottom of the feed slides each a worm. These worm wheels are simultaneously nuts that the feed slides on each of a large trapezoidal threaded rod drive up and down the machine bed or in the feed slide and lead. During the rolling operation the axial feed of the workpiece is blocked. The aforementioned clutch at the DC motor allows slippage. If then the rolling tools are in the open position, the next step of advance happens.

4. Production of Test Parts

For the geometric research spline shafts according to DIN 5480 were rolled on the WPM 120 [ST 10]. The choice of this form of geometry was not arbitrary. It resulted from the fact that for this component geometry corresponding tools were developed 35 years ago and were available at the Institute in Darmstadt for own researches. A new development of tools would be too costly. This is one of the main reasons why such a rolling process is only economical when mass products are manufactured. With mass production the high tooling costs become relative. The former tool costs were in the order of DM 25.000,- / set. The rolling tools cannot be used for any toothing part. They are calculated in relation to the tooth geometry, which is desired to be produced. The calculation is based on the number of teeth ratio between tools / component gearing and machine-set 12.92 mm eccentricity of the rolling tools. The required blank diameter results related to this.

4.1. Preparing of Rolling Tests

Geometry of the spline shafts Based on the existing rolling tools and the therefor machine set up of the eccentricity of the tools shows the drawing figure 26 of a spline shaft with toothing according to DIN 5480 [ST 10].

The specifications of these teeth are: module = 2,5, number of teeth = 24, pressure angle = 30°, helix angle = 0°. Rolled was a gearing of the length of 90 mm. Each blank was used for two test runs.

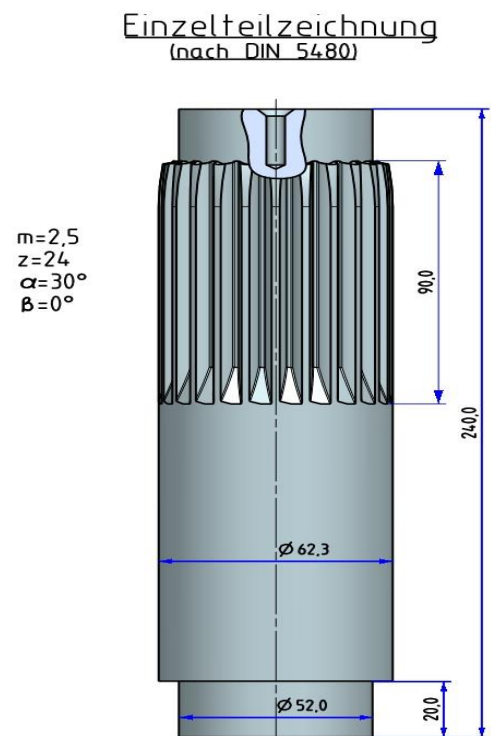


Figure 26 Geometry Spline Shaft

Blank Production Of decisive importance for the resulting quality of the teeth when rolling is the correct manufactured blank diameter. This diameter must be within very tight tolerances. If it is too large, then there is the risk that the rolling tools break. If it is too small, the tooth gaps of the tools are not filled up with material. Furthermore it is important that all blanks are made of the same material under the same processing conditions.

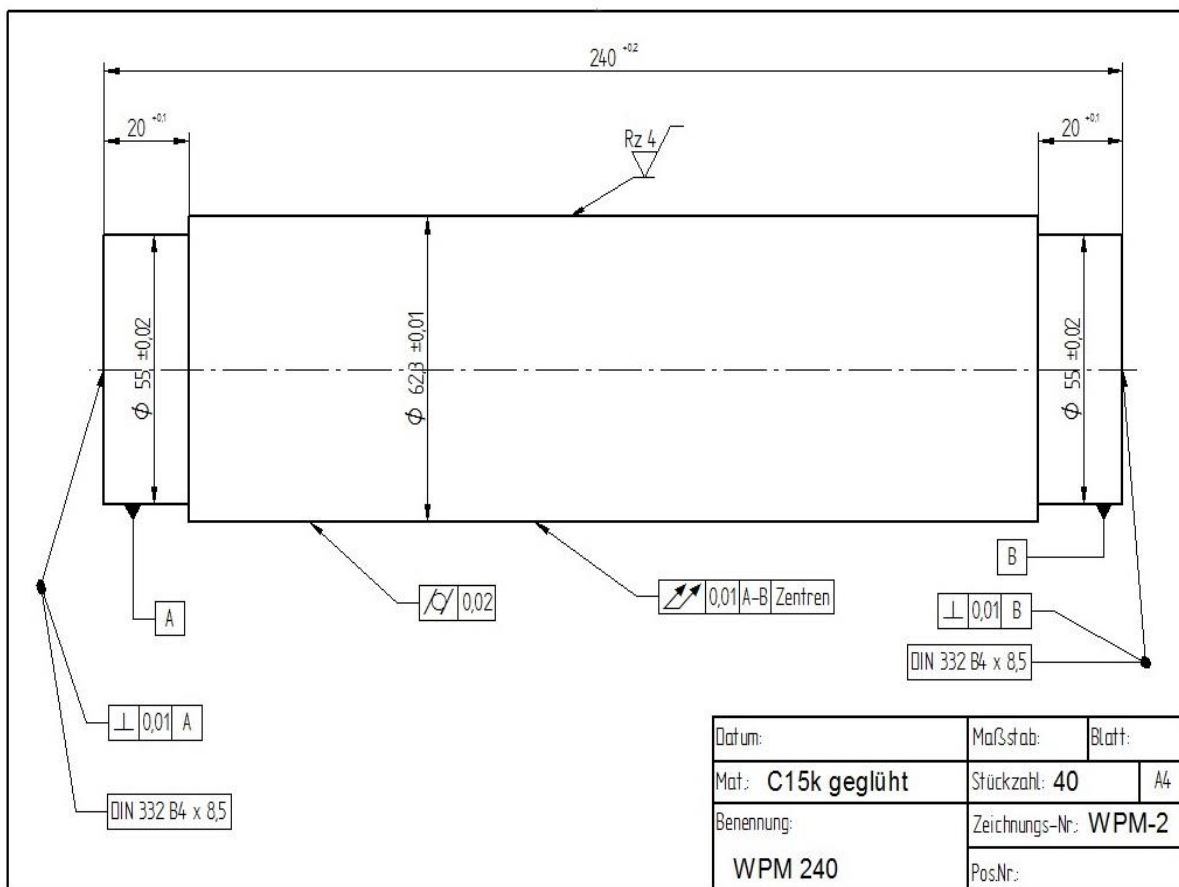


Figure 27 Drawing Blank

A total of 100 blanks from certified materials C 15k = 40 pcs., C 35k = 30 pcs. and C45K = 30 pcs were made. The material was delivered cold pulled and cut to lengths of 250 mm. All samples were annealed at 650°C for 5 hours. After this, centering holes according to DIN 332 B4x8, 5 were set [ST 12]. On a CNC turning machine the exact dimensions according to the drawing, figure 27, were made. All rolling samples were fabricated the same way and afterwards measured on the PMM 654 (Chapter 5).

Tools To assemble the tools the machine side eccentricity is set to zero. The tools carry a respectively mounting notch. They are aligned with an assembly ruler, as shown in the figure 28.

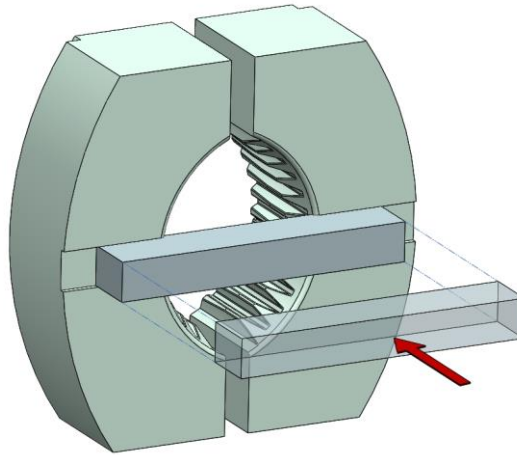


Figure 28 Mounting Notch / Assembly Ruler

In the then found symmetric position, both tool segments are clamped in the tool holders with screws via wedges (Figure 29).



Figure 29 Clamping Tools

The tool geometry and the blank diameter matching eccentricity of the rolling tools was set at 12.92 mm. In preliminary tests, it was found that only the above-mentioned eccentric setting leads to well-formed teeth on the rolling samples. The mechanically predetermined gradations other eccentric settings revealed no reasonable rolling results.

4.2. Test Parameters / Measuring Equipment

The in the following described measurements on the machine WPM 120 had the goal of verifying and ensuring the consistency of conditions during the sample realization. The reason is that the test machine is already about 35 years old. Possibly existing mechanical defects of the motion control or the control technology might affect the rolling result. To obtain and interpret meaningful results from the measurements of the resulting tooth geometry on the PMM 654, it must be ensured, that all rolling samples were rolled under the same mechanical conditions. Several preliminary tests are not reported here.

Test Parameters The following parameters are adjustable on the machine in general.

- a) Eccentricity of the rolling tools.
 - b) Hydraulic pressure to the axial tension of the rolling sample
 - c) Feed rate
- a) A variation of the eccentricity of the rolling tools did not make sense, because the existing tools do not allow the use of another eccentric setting.
- b) The unit for adjustment of the hydraulic pressure allows by adjusting a pressure control valve a change of the pressure. However, at higher pressures resulted a significant noise in the hydraulic system, so that only a slight increase in pressure seemed to make sense. The clamping pressure of the sample was varied between 1 to 2 bar. An influence on the rolling action could thus not be detected. The machine manufacturer specifies in its technical documents that with a bar clamping pressure of up to 2 should be worked.
- c) The feed rate was already recognized in the preliminary tests as the major influence of the machine set up with influence on the rolling action. The rolling was carried out at the main experiments with feed rate 100/200/300 mm / min.

d) The rolling machine WPM 120 operates with a stroke frequency of the rolling tools of 5 strokes / sec. The stroke rate is set fixed and unchangeable. In combination with the maximum feed rate (~ 400 mm / min) results a maximum length of toothed gearing of ~ 400 mm / min.

Measurement Parameters During the main tests for the production of rolled samples, the following measurement parameters were recorded:

- | | |
|--|-----------------|
| A) Path with respect to time | $s = f(t)$ |
| B) Power of main drive with respect to time | $P_{MD} = f(t)$ |
| C) Power feed drive with respect to time | $P_{FD} = f(t)$ |
| D) Stroke frequency tools with respect to time | $n = f(t)$ |

Position measuring at the feed slide To capture the current position of the slide precisely, 2 high-resolution position measuring sensors (1, 2) were used. The feed slide sits on two massive trapeze spindles and is moved axially in these two trapezoidal nuts. The movement of this feed carriage is important for the axial movement of the workpiece.

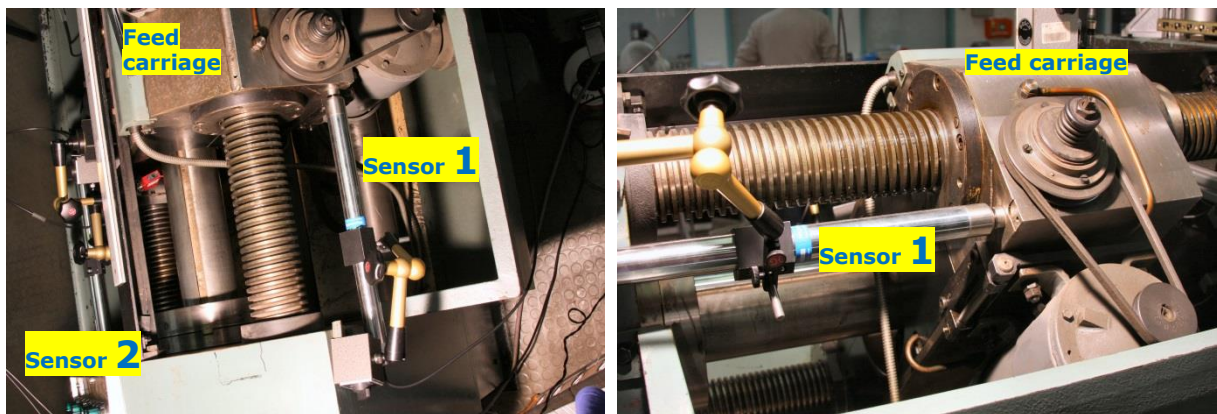


Figure 30 High-Resolution Position Measuring Sensors

In this respect, through the use of two identical positions measuring sensors next to the trapeze spindles it was supposed to ensure, that on both sides of the feed slide similar courses in similar times are made. A possible pitch or tilt of the slide would be transferred to the roll geometric sample and thus affect the geometry of the tothing after the rolling results negative.

Position measuring Sensor The feed path over the time was measured. The signal acquisition was implemented with the following described two identical sensors.

Table 1: Sensor Fabricate / Sony Magnescale

Typ	DK155 PR5 selection 2 μ m
Measuring stroke	max. 155 mm
Resolution	incremental system 0.5 micron resolution
Max deviation	guaranteed under 2 μ m
Design	cylindrical 32 mm
Mechanical coupling	clamped on the outside diameter Φ 32
Spindle Φ 8	magnet Φ 22 with very strong adhesive force
Outputinterface	2 shifted by 90°, and each also inverted square signals with TTL level
Signal processing	Beckhoff
Typ	32-bit incremental BeckhoffEL5101
Max frequency	over 4 million increments / s
Max interpolation	1/256 bit mircoincrements
Interface	Ether CAT
Counter over/underflow	CNC axis software Beckhoff Twin CAT NC

From the current position of the slide the particular feed rate can also be identified with the software TwinCAT2. Once the carriage moved back to the starting position (part exchange), then both sensors are set back to an identical start value according to the following start of the next test rolling.

Because of the bearing clearance in the trapezoidal screw spindles, tilts the directional reversal carriage movement at the start of rolling. It results probably always a small path offset, but this makes the uniformity of the carriage movement very clearly visible.

Accuracy of the position measuring A significant measurement uncertainty could result from the installation position of sensors. At a non-parallel mounting position of the two sensors, differences could be measured which do not correspond to reality. These differences, however, would be negligibly small compared to the slope errors of the trapeze spindles and the partially uncontrolled slippage of the clutch on the feed drive.

Power Measurement For measuring the power consumption of the 7.5 kW main drive motor for the eccentric tappet of the rolling mill a very fast analyzing three-phase active power measuring system of the latest state of

the art is used. The same measurement set-up with an identical but suitably configured for the smaller power rating meter APM380 is also used for the axial advance of the workpiece, with the DC motor (power 0.8 kW).

Since there is no intermediate circuit and no significant energy storage, it also was measured very close to the engine, and thus measured on the process.

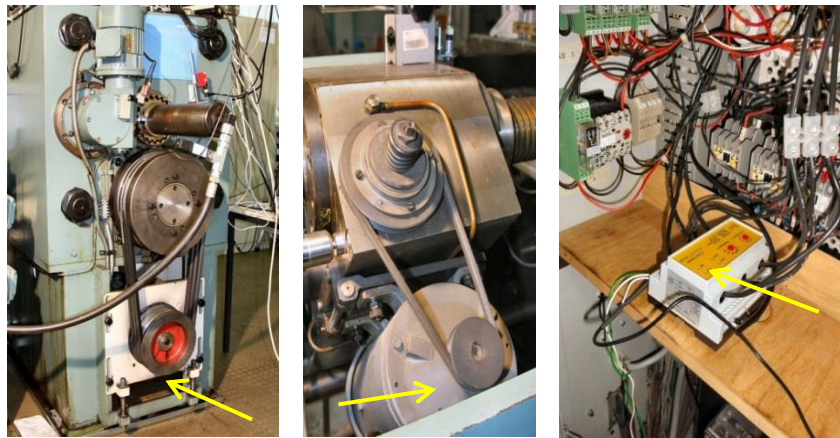


Figure 31 Power Measurement

Table 2: Sensors

Manufacturer	Ulrich Buhr Industrial Soltau (Sales D) Hydria Electronics ApS
Type	Unipower APM 380
Voltage	230 - 575V switchable
Current range	1-80A (max. 140A), switchable
Measurement	Hall sensors without phase shift
Accuracy	Class2
Frequency range	10Hz - 1kHz
Pulse and analog outouts	programmable
digital filter	programmable

The analog measurement output is programmed to 0 ... 10V for each scale value and then again with a 16-bit differential input to a Beckhoff - analog / digital converter EL3104 on EtherCAT bus digitally recorded (Input filter limit frequency: 5 kHz sampling rate 1 kHz, no oversampling).

Uncertainty of power measurements Regarding the selection of the measuring range a compromise between the resolution and the full scale had to be entered. When starting the machine, very high power peaks occur. These power peaks of the main drive were previously reported separately just for the documentation of them. For the main experiments the full deflection of the measuring range has been adjusted to the resulting rolling power curves appropriate. The drive train of the movement mechanics of the rolling tools is associated with high friction parts and very high inertial masses. The friction components were found to be highly temperature dependent. The lubrication system of the machine always required a long duration until stable constant conditions were set. In consequence, the main tests were always carried out only after an operating time of the machine of at least 3 hours. Regarding the feed drive, it was found that the influence of the slipping clutch is speed-dependent. Without prejudging the later discussed outcome, it was noticed, that the clutch of the feed drive rarely slips, but hardly comprehensible. Whereby, the results of the feed drive performance measurement are of course influenced.

Stroke frequency of the rolling tools To ensure that the manufacturer information of strokes is 5 / sec actually comply, the time interval of the cycle of movement of the receiving cups of the tools has been captured.

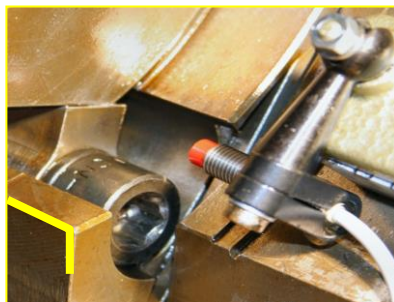


Figure 32 Stroke Frequency

As shown in the figure 32, with an inductive sensor the front edge of the right cradle was raised. This edge moves through the magnetic field of this sensor, then a high resolution signal is generated. The time interval between multiple strokes or during the rolling phase has been so detected.

The sensor is an inductive probe of the company Leuze electronics with the following specifications:

Table 3: Sensor Leuze Electronics

Manufacturer	Leuze Electronics
Typ	IS 208 N5
Operating range	0-2.0 mm
Operating frequency	5 kHz
Installation position	not flush, stainless steel

The output signal is detected with an input terminal at the Beckhoff EL1018 EtherCAT bus.

Measuring pressure of the hydraulic preload The inside of the hydraulic cylinder mechanism mounted tip is, as already mentioned above, hydraulically pre-stressed. Although already recognized in the preliminary tests, the pre-charge pressure has no visible impact on the metal forming. Nevertheless, the pressure profile was measured to make sure that actually no influence of the metal forming is happening.

Directly on the rotary joint at the shaft end (Figure 33), was measured with a T-piece with large diameter and the maximum pressure to avoid throttle effects and additional dead volumes.



Figure 33 Sensor / Pre-charged Pressure

Table 4: Sensor Hydrosens Löfflingen

Manufacturer	Hydrosens Löfflingen
Type	DRTR-AL-10V-R6B
Connection	1/4" female with a large opening
Nominal pressure	6 bar
Overload protection	15 bar
Analog output	10V = 6 bar fixed
Measuring frequency	2 kHz
Accuracy	0.2% of the max error relative to full scale is 6 bar

Data acquisition / analysis Data were collected with a Beckhoff system. It is a system (Intel Pentium M 1.8 GHz, 1 GB DDR Ram, 64 MB Compact Flash card) with an EtherCAT fieldbus interface. The measurement system and the installed software TwinCAT allow continuous recording of measured data in real time. The system structure is modular, optimized to the Ethernet bus integrate specifically for data collection designed slots per channel. Possible, therefore, the acquisition of digital and analogue input channels with a sampling rate of more than 100 kHz at 16 bit resolution. Special digital inputs for recording period and / or event measurements can be marked with time stamps in the processor clock. Thus a precise synchronization of the measurement signals, for example, to determine the time sequence of signals is possible. By problem-oriented software developed the measurement period, the number of channels and the respective resolution of a measuring channel is freely scalable. The recorded data files were transferred over a local network to a Windows PC and evaluated using the DIADEM software 2012.

Expected statements of the mechanical measurements:

Position measuring In the position measuring it was expected that the intermittent rolling process leads to clearly identifiable stages in path-time processes. Possibly asymmetries in the movement of the slide on the two trapezoidal spindles can be detected.

Main drive power measurement It was expected that the power of the main drive is dependent on the feed rate. The larger the individual feed step of the blank between the rolling dies, the greater is the per stroke tools deformed material volume per time. Thereby, the energy demand of the main drive should increase.

Furthermore, it was expected that the power consumption of the main drive changes when different materials are rolled. Since the rolling experiments, various carbon steels have been used the main drive power should increase with increasing carbon content of the raw material.

The carbon content characterizes the strength of the material and is of critical importance for its solidification during forming [ST 13]. With increasing yield stress of the material, thus increasing its resistance to deformation. This necessarily results in higher energy consumption.

Performance measurement feed drive: Regarding the power consumption of the feed drive it was expected a clear dependence on the adjusted feed rate. To accelerate masses of the feed mechanism higher power consumption with increasing feed rate is required. A dependence of the power consumption of the feed drive regarding the different materials should not be detected.

Stroke frequency of the rolling tools An influence of the stroke frequency of the rolling tools by the set feed rate or the used blank material cannot be expected. The existing inertial masses of the drive mechanism of the WPM 120 are so large that here a more consistent stroke rate can be expected.

Pressure measurement of the hydraulic preload Even at the preliminary tests, it was found that a clean measurement of the pressure profile of the hydraulic preload of the blanks is difficult. The hydraulic unit is for an operating time of approx. 35 years, apparently no longer fully functional. This results in fluctuating pressure curves for each parameter combination of the performed preliminary tests. Nevertheless, the measurement of the

pressure profile is maintained in the main experiments. Meaningful and purposeful statements about these pressure measurements were not expected.

Experimental design For the main experiments 100 rolling samples were prepared (40 pcs. material C15, 30 pcs. C35, 30 pcs. C45). Considering previous experiments, the feed speed and the blank material were defined as the two important experimental parameters. In consequence 9 series were designed with 10 parts with the parameter combinations of the three feed rates and the three materials. Parallel to the rolling tests, after the completion of a series of experiments, the measurement work in the PMM was started. It could be checked to what extent changes in the test procedure may be useful. The background to this approach was that even at the preliminary tests no significant differences between the materials C 35 and C 45 were found. For both materials approximately the same geometry deviations resulted.

So a total of 90 samples was planned to roll. At the beginning of the study the series with the material C 15 were fully rolled. In the series with the materials C 35 and C 45 confirmed the findings from the preliminary tests. Of crucial importance for the further course of action was that even after 11 rolling samples C35 considerable engine noises occurred. After 9 rolling experiments with the material C45, this engine noise increased significantly. It was assumed that the drive mechanism of the machine had reached its limit. To avoid damage, all until then rolled samples were measured geometrically. It should be noted, how far additional rolling tests would increase the knowledge. In all until then available rolling samples (C35, C45), no effect on the resulting geometry results was found. Further insights were not expected, more rolling tests were not necessary. The results presented in later chapters geometric are based therefore on rolling sample 30 x C15, 11 x C35 and 9 x C 45. The further statements (Chapter 5, 6) made are based on the complete C15 series.

4.3. Engineering Results and Assessment

A detailed graphical representation of all results has been omitted. The aim of the mechanical tests was not a systematic analysis of the machinery in detail. Here, only the uniformity of the respective roll attempts should be ensured as a basis for the subsequent geometric investigations. The results shown in the following charts are thus to be understood as examples to explain the technical aspects.

Distance / Time of feed-slide These measurements had the goal to determine in how far for all rolling samples and each set of feed rates, identical path-time processes occurred. This is, as already mentioned, of importance for the per path step reshaped volume of the blank material. The following figure 34 shows the resulting path-time processes at three speeds 100/200/300 mm / min.

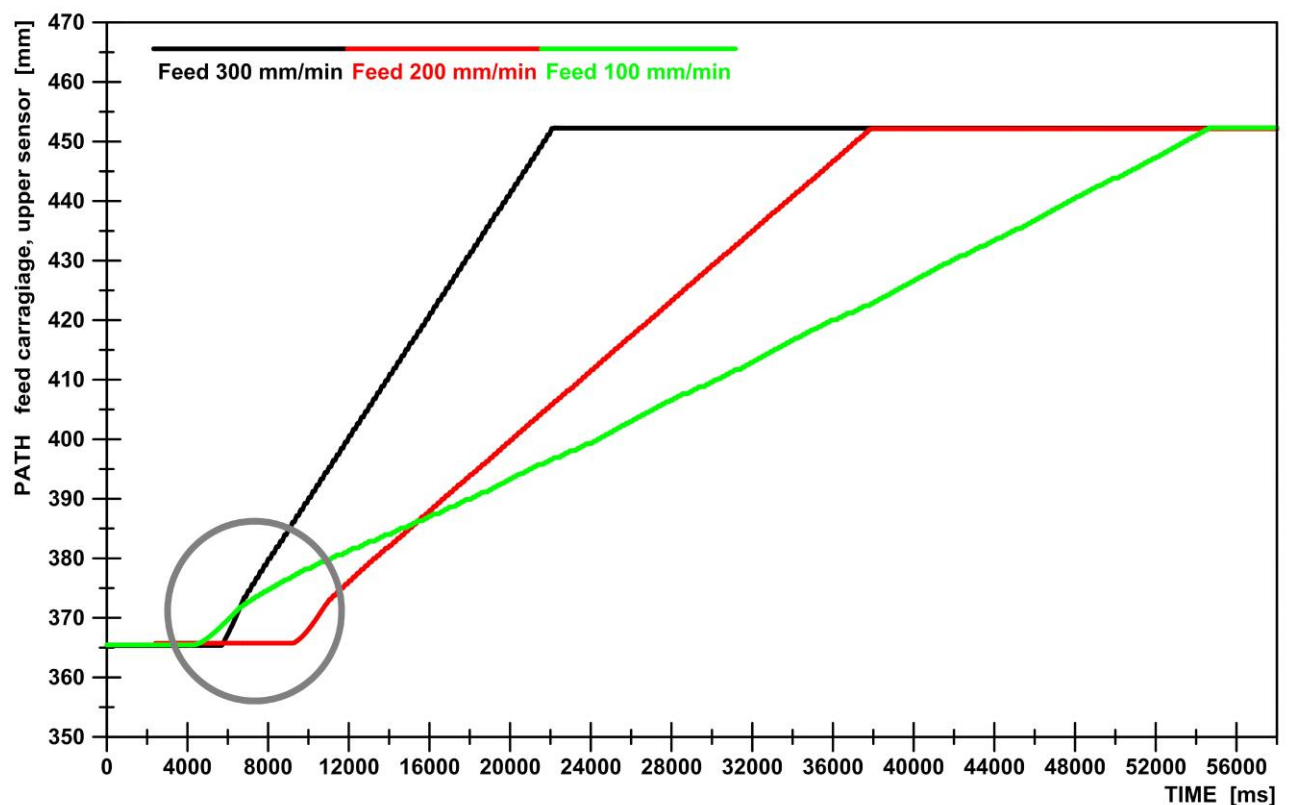


Figure 34 Path – Feed Carriage

The shown graphs, figure 34, represent the upper sensor on the upper part of the feed geometry. The graphs shown are original data without any data manipulation. They show an example of the resulting path-time process which resulted for all combinations of parameters almost identical. In figure 34 is shown the initial region of the feed movement characterized by a circle. The shown starting points are not identical because the start of the movement and the start of the measurement recording data were triggered by hand. An identical start time could thus not be realized. It shows the beginning of the slide movement through the first bend in the curves. The adjusted feed rates give different ascending paths in the initial region. Within short distances of the initial region (circle) the tools contact the blank and are decelerated, so that a second sharp bend results in the graphs. Later the graph shows rising lines according to the current feed rates. After 450 mm horizontal curves result. The carriage is then in its final position. The time period within the end position is optional, as the return stroke of the carriage movement is also triggered by hand. In all experiments, there were always identical path-time processes with just minimal deviations. As far as the feed movement of the respectively set feed velocities, all the rolling samples were produced under the same conditions.

Position / Time of feed-slide (upper + lower Sensor 1 + 2)

The measurements of the paths with two sensors on the feed carriage had to determine how far the slide moves symmetrically on the two trapezoidal spindles. A tilting of the carriage would affect the middle position of the rolling part negative. It should also be determined whether the intermittent rolling process can be found in stages of the carriage movement. The following figure 35 shows a period of one second process time whereby path-time processes appear enlarged.

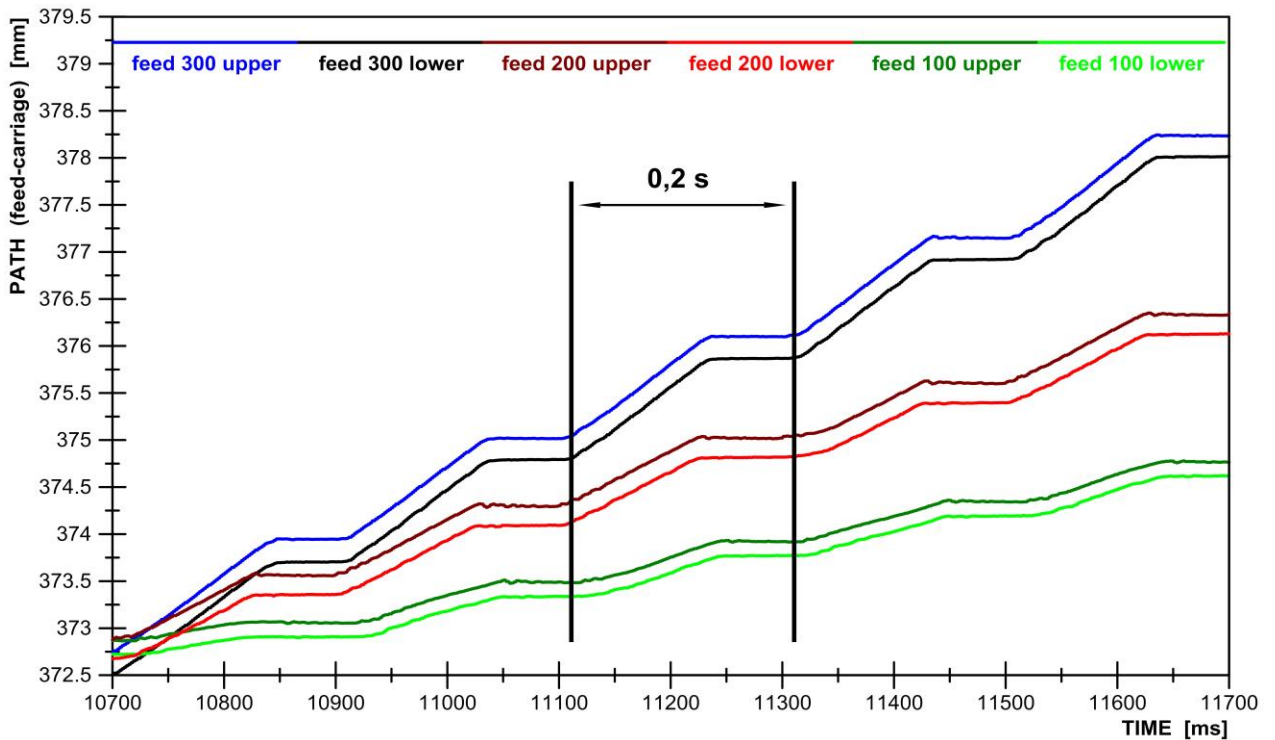


Figure 35 Enlarged Path / Time

Shown for each feed rate are two signals of the sensors (1 and 2) on the carriage in the “y” direction slightly offset so that the single profile is clearly visible. Without this manipulation, both graphs were identical superimposed and be indistinguishable. This data shown in the figure 35 is presented without any further manipulation. It can be seen that the two sensors provide approximately identical values. A tilting of the feed carriage during movement can therefore be ruled out. The machine side predetermined stroke frequency of the rolling tools of 5 strokes per second is clearly visible. Starting from a bend in the curve follows a rising line according to the set feed rate. Then followed by a further bend, the curve enters into a horizontal course. This is the period in which the tools are in contact with the blank, and therefore the blank cannot be displaced axially. Then the next bend occurs, from which the tools release the blank and a further advance happens. The intermittent rolling process can be detected unambiguously. As indicated by vertical lines in the figure 35, results in accordance the above-described timing of the tool movement a period of time per cycle of 0.2 seconds.

This corresponds to the manufacturer's specification of the WPM 120 of five strokes per second of the rolling tools. Furthermore, shown in figure 35, the largest feed rate shows a sharp bend (transition of the rolling phase to position tools open). With decreasing feed rates result rather smooth transitions between these phases of a motion cycle of the rolling tools. One explanation for this is that the forward movement of the carriage is stopped by the contact of the rolling part with the rolling tools. The feed drive works however continues at this stage. Namely against a slipping clutch, which slips when the tools and the blank are in mechanical contact. The smaller the feed steps between the tools (small feed rate), the smaller the formed volume and thus the contact area of the tool with the material. The contact area between the rolling tools and the blank material increases with increasing feed rate. This results in a better guiding of the tools relative to the rolling part. At smaller steps of feed rate a lower guide of the material is given by the tools. This will obviously allow axial movement of the blank, even though the tools are still in the rolling phase. The graphs shown above were obtained for all the experiments carried out independently of the rolling parameter combination nearly identical. The expected results of the measurements of the paths of the feed carriage were confirmed.

Power measurement main drive

The graphs in the following figure 36 show the power consumption of the main drive of the rolling tools.

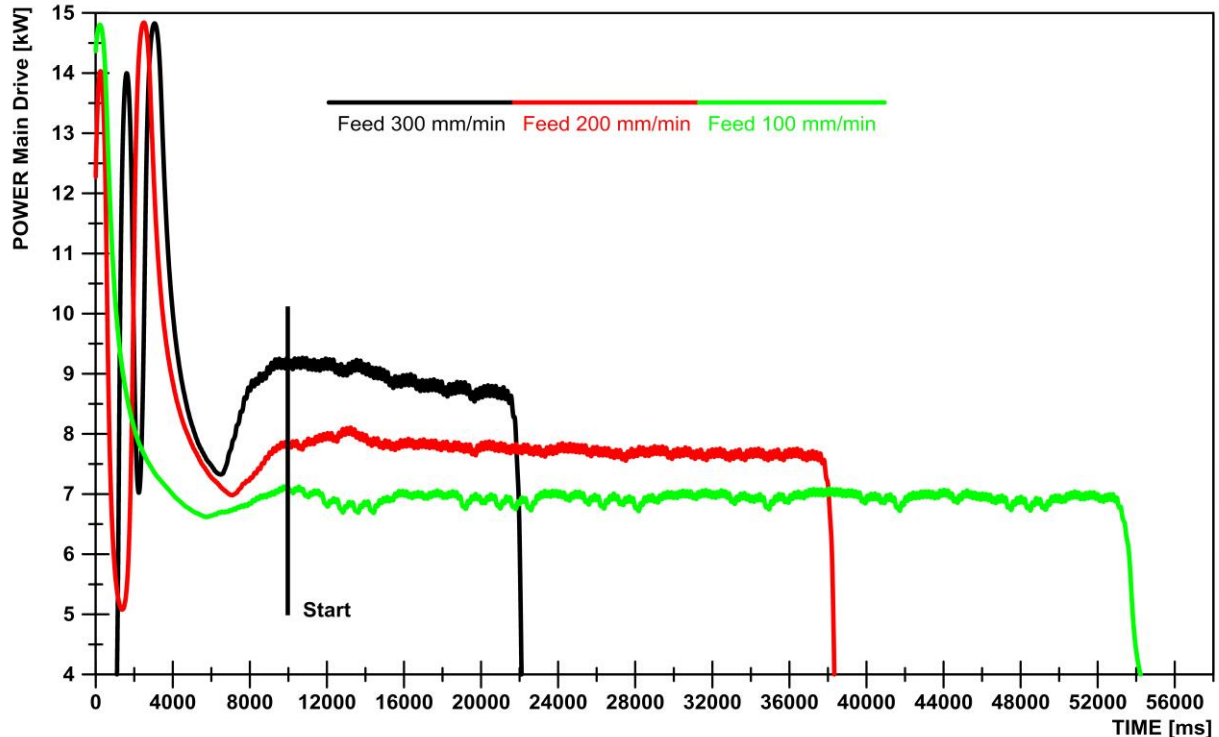


Figure 36 Power Consumption – Main Drive

When turning on the main drive, high peaks of power of up to ~ 15 kW results. The curves do not start at the same time. The reason for this is as well as previously mentioned at the path measurements that the start of the engine and the start of the measurement data acquisition were triggered manually. Thus, no identities of the temporal starting points are to expect. This does not affect the desired statement of the research. A manipulation of the data in terms of a temporal shift was not deemed necessary. The advantage is that the measurement graphs are to differ so visually.

After the graphs drop in in the direction of the idle power follows a steep rise. At this time the tools have the first contact with the blank, which is inserted by the feed drive between the tools. This increase results differently depending on the set on the machine feed rate. This can be explained by the then reshaped respective material volume. The greater the feed rate, the greater is the volume per unit of time to be formed. The larger the volume

to be formed, the greater the power requirement for the metal forming is. At this time interval starts the rolling process. In almost all attempts resulted at the start of the rolling process different graphs within this time interval. The differences were not significant, but still clearly visible. This can be explained by the difference in volume to be formed as a function of the local position of the blank with respect to the geometric position of the rolling tools to their 360° movement. Once this position is reached (a complete feed step occurs between the tools) the maximum volume relative to the adjusted feed rate is formed. In all other positions smaller volumes are deformed. To guarantee always equal volumes at the beginning of the rolling phase, the first working cycle has to match exactly with the temporally position of the respective tool-stroke movement. This cannot be the case, at the existing purely mechanically controlled rolling machine WPM 120 (1978). But in order to make room for all the rolling tests an identical basis in the graphs, all initial points of view were obtained and set to the time of 10 seconds after the start of the main drive. This shows the vertical line labeled "Start". Furthermore, all of the performance curves have been smoothed (2nd order filters Tschebyscheff 5 Hz), as completely irregularly power peaks occurred once in a while. These occurred extremely irregular at all parameter combinations and could not be assigned to the respective rolling process in any way. The made smoothing affects the tendency of the course of the graph only slightly. In all experiments gently sloping curves with increasing duration of rolling at the individual rolling test resulted. The greater the feed rate, the greater the tendency for the drop in performance was observed. In average of all tests with the same combination of parameters with the feeding rate 300 mm / at the beginning of the rolling process about 9.3 kW was captured by the main drive. At the end of each rolling test in average ~ 8.9 kW. In the higher-strength materials such as C45 resulted in the beginning with the high feed rate (300 mm / min) on average ~ 12.2 kW and at the end of each rolling experiment ~ 11.5 kW. One possible explanation for this is the increase of the temperature rise of the machine during each rolling. As much

work was carried out from the mechanical system as much higher was their warming. In addition a potentially warming improving lubrication of the moving machine parts results.

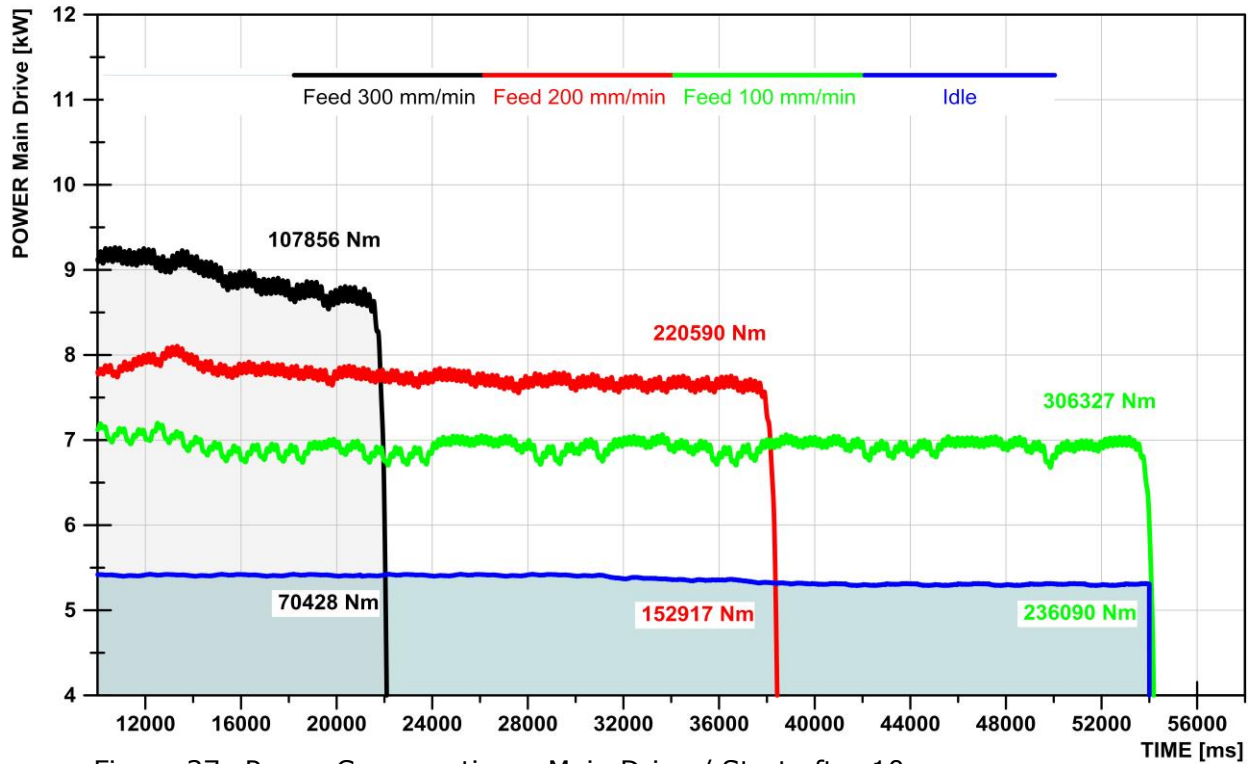


Figure 37 Power Consumption – Main Drive / Start after 10 sec.

The figure 37 shows an example in another scaling the power of the main drive for the three feed rates and the associated idle performance. The idle performance was determined in separate experiments, and always matching to the required feed rates by processing times. It is noticeable that in the idle power for the slowest feed rate (100mm/min) a total of ~52 seconds duration of the process, a slight, but significant decrease in performance of the idle power is evident. This can be seen, even though the engine was before each test series at least 3 hours switched in idle mode. In connection with the above discussed slight performance degradation in all these experiments could be explained by the already in idle mode occurring degraded performance. That would rather point to the possibly improving lubrication of machine elements with increasing process time.

The registered numbers in the figure 37 result from the calculation of the work as $W = P dt$ within the time limits of the respective rolling experiment. In the above example result for the feed rate 300 mm / min and for the material C15 a value of applied work $W = 107856$ Nm minus the idle labor of $W_0 = 70428$ Nm. The power required for the pure forming operation of this rolling test was thus 37428 Nm. For each rolling experiment of all parameter combinations work content was determined. In a series of tests with the same parameter combination the deviations between the individual tests were below 3%. The determination of the required work content for each rolled piece served as a criterion for the uniformity of the process. The material C15 was particularly useful for metal forming, while the material C45 yield problems. Even a feed rate of 200 mm / min caused considerable engine noises. At the feed rate of 300 mm / min and the material C 45 the noise increased. With this combination of parameters power peaks of up to 12.6 kW resulted. Perhaps the components of the drive systems are overloaded due to age. Anyhow, because no significant difference between the roll-results was observed within a combination of parameters, not all the planned blanks were toothed. The machine WPM 120 could have been damaged. For all combinations of parameters approximately the same results were obtained. The expected measurement results of the main drive power results were confirmed.

4.4. Measurement Results and Evaluation

Power measurement feed drive The following figure 38 exemplifies a diagram in which the power absorbed of the feed drive is shown over time. Shown are the profiles of the three feed rates and the respective associated idle power. It is apparent that a greater feed rate increases the associated idle power.

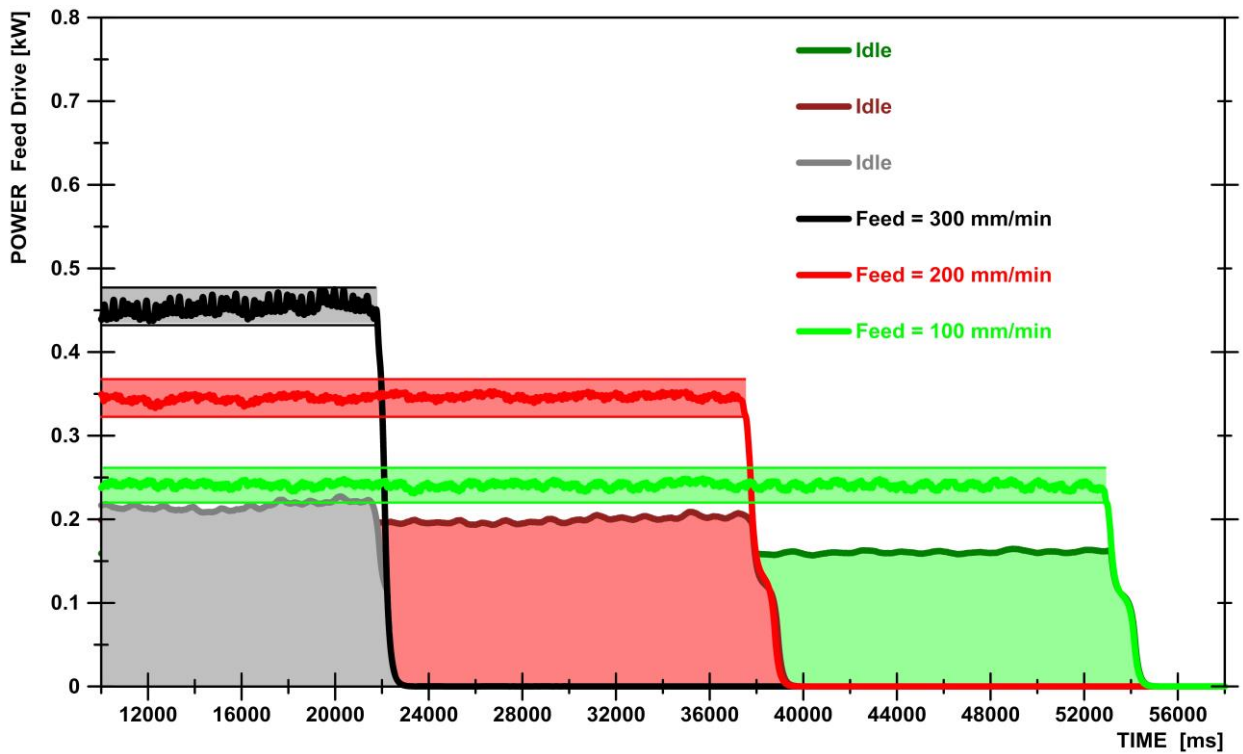


Figure 38 Power Consumption – Feed Drive

Furthermore shows figure 38 in the form of horizontal colored bands the maximum and minimum deviations of the recorded powers in a test series. Onto the representations of other curves was dispensed because it would not increase knowledge. An influence of the firmness of the rolled material on the feed power could not be determined. For all combinations of parameters approximately the same results were obtained. The expected results of the measurements of feed power were confirmed.

Stroke frequency of the rolling tools

resulting signals of an inductive sensor.

The figure 39 shows the re-

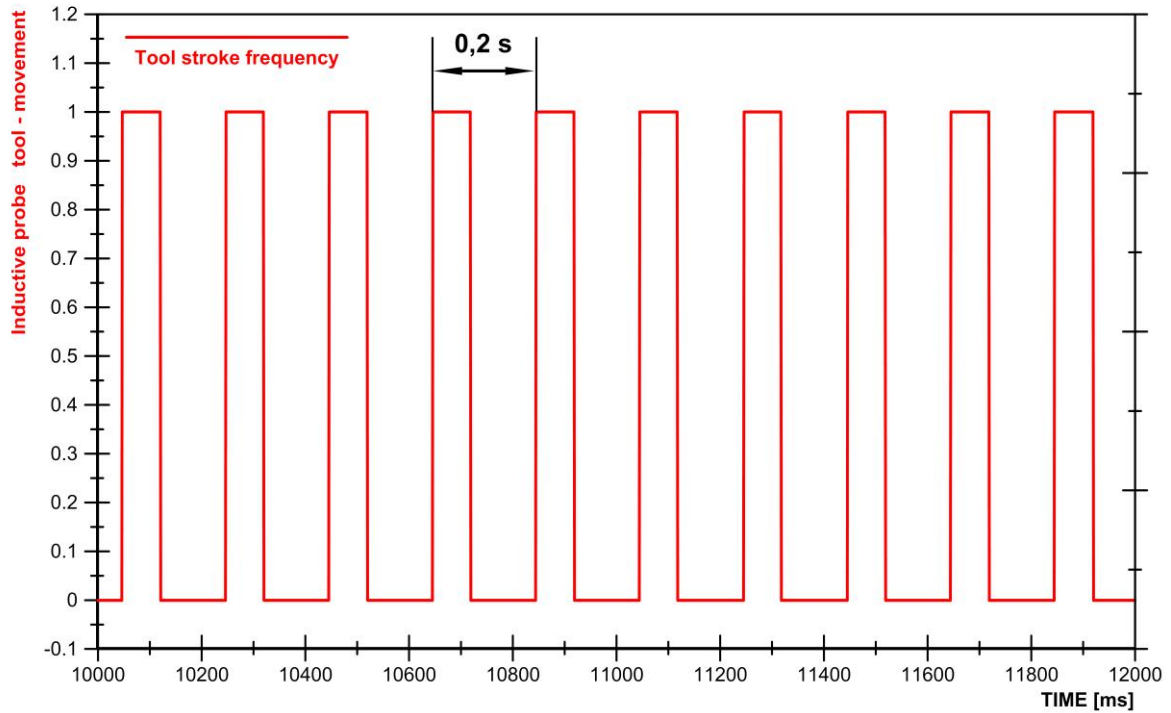


Figure 39 Resulting Signals of an Inductive Sensor – Tool Movement

At each pass of the front edge of the tool holder results in a signal. For each tool stroke result signals, the distance to each other is the same and is always 0.2 seconds. This is the same time interval that has been found already in the position measurements on the feed carriage. The machine operates with 5 strokes per second.

In all serial- / parameter combinations and measured variables almost identical outcomes and curves resulted. The calculated work contents of the main drive power differed only slightly from one another. It can therefore be basically assumed that the toothed samples were produced under approximately the same mechanical and technical conditions.

5. Geometry Measurements PMM 654

5.1. Technical Basis coordinate measuring technology

The principle of coordinate measuring technique is based on the fundamental relationship that each workpiece realized by manufacturing technology, can be described by points in space geometrically (Figure 40) [27, 31, ST 4].

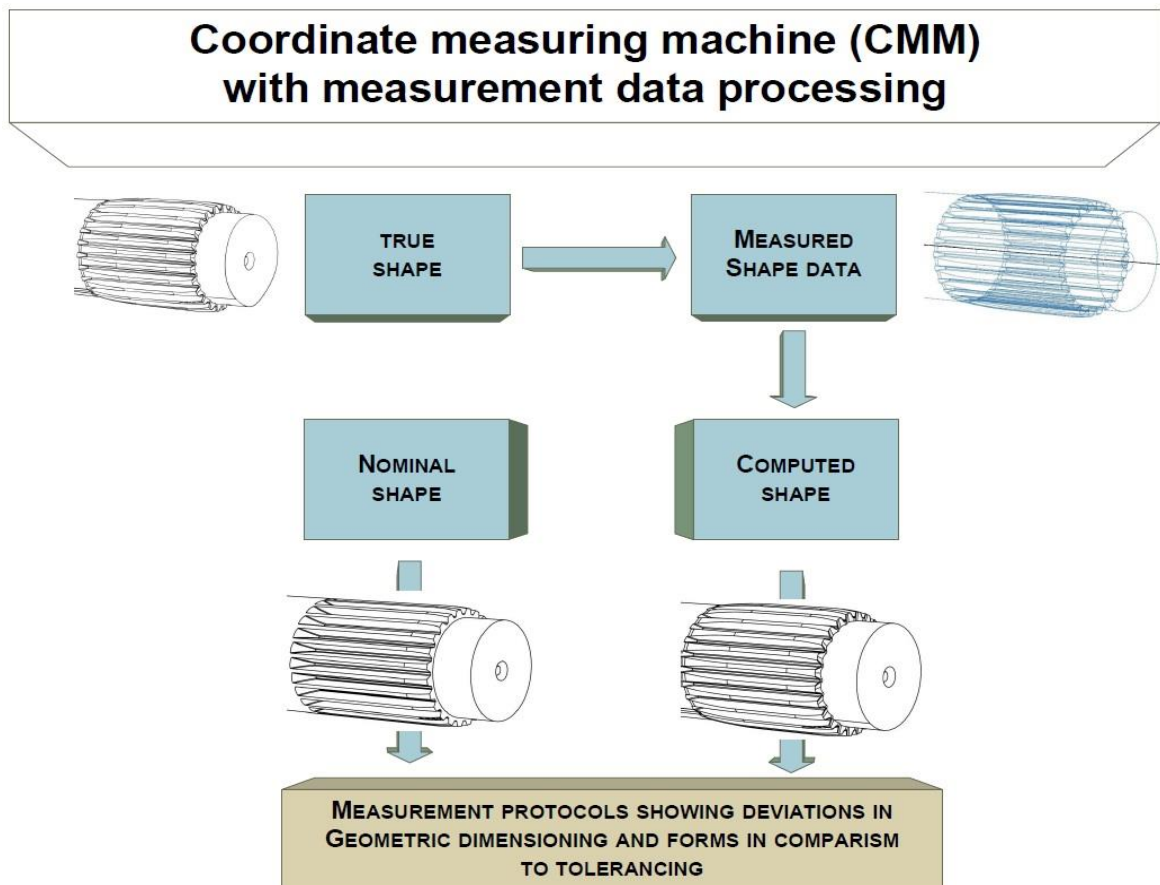


Figure 40 Basic Principle of Coordinate Metrology

Each point in space is described geometrically by three coordinates. These are the geometric lengths (distances) of the point in space relative to the origin of the corresponding coordinate axes. The principle of tactile three-coordinate measuring technique (Figure 41) contains the probing of the spa-

tial points by tactile pins of a sensing head. The sensing head realizes the probing and the acquisition of values. A connected computer system takes over and stores the measured values of the probed points in space, links them to geometric elements, determines the actual geometry, conducts a target/actual performance comparison if necessary and calculates / rates and documents the resulting deviations.

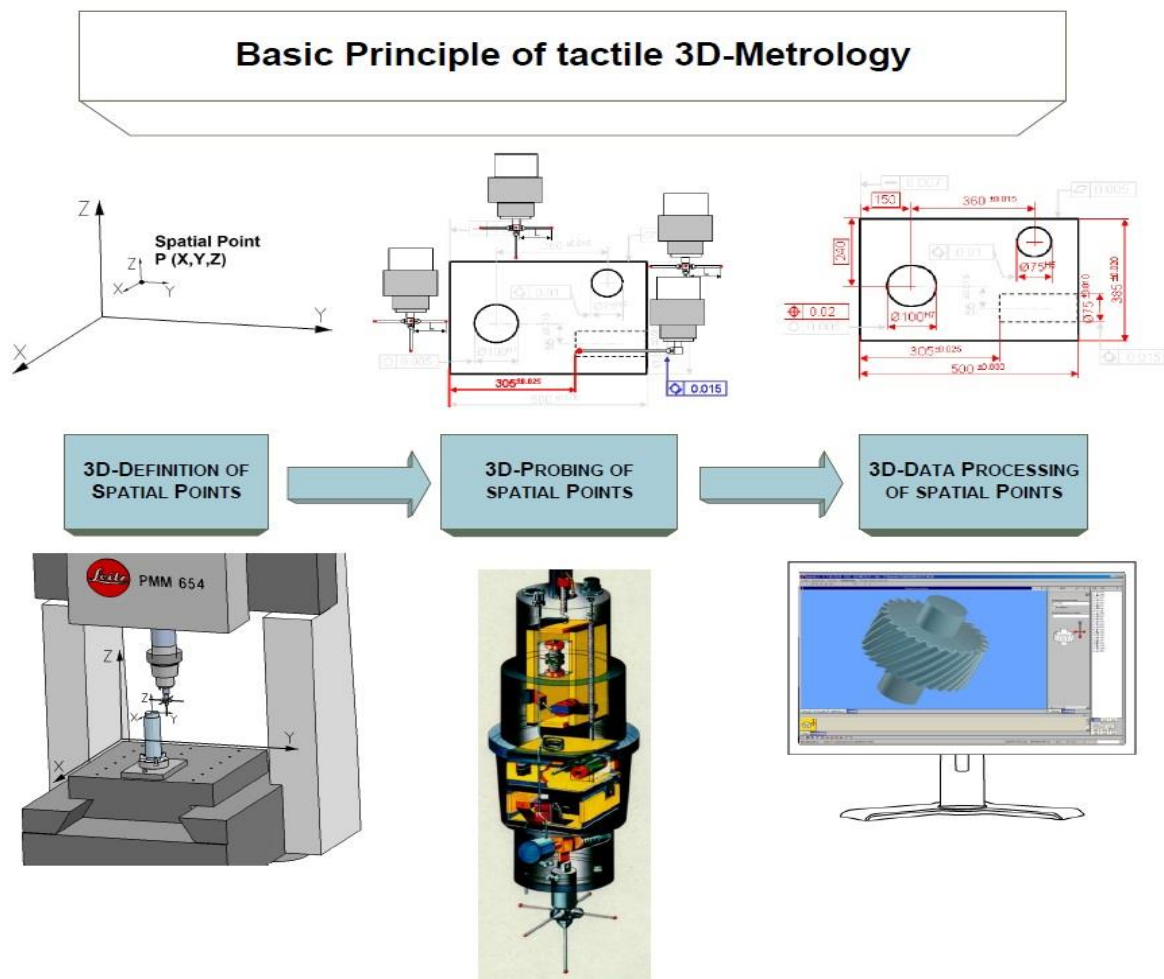


Figure 41 Principle of Tactile 3-D Metrology

Modern tactile coordinate measuring instruments have a wide variety of hardware and software components. The interaction of these modules is essential to ensure that test results can be determined with accuracy characteristics in the order of 1 to 2 microns. One of these modules is, for example, the "caliper calibration." This is used to determine the geometric posi-

tions of the probe center points in space and to determine the spatial curvature of the probe pins under the action of the contact force.

Before starting a measurement, the probe pins that are to be used in the upcoming measurement must be calibrated by a certain sequence of probing points on a highly precise ceramic calibration sphere. Another important module in this context is the "probe radius compensation". It determines the geometric position of the touching point on the tactile pin sphere and corrects this probing value to the center of the ball of the probe pin. All measured values of the probing are then related to the center of the probe sphere. In the following chapters of the required use of such software modules will be discussed in more detail.

5.1.1. Construction of the Coordinate Measuring Device / Measurement Accuracy

For the own work, a Leitz PMM 654 of the company Hexagon Metrology GmbH in Wetzlar has been used. The measurement machine is in the metrological laboratory of Professor Hammerschmidt at the University of Applied Science in Darmstadt. The figure combination 654 defines the possible travel distances or ranges of the machine axes in the X, Y, and Z directions, ie, $X = 600$, $Y = 500$ mm, and $Z = 400$. On the control computer of this measuring machine is the measurement software QUINDOS, version 7 installed. The machine is located in an air conditioned room at a constant temperature of 20° Celsius. The structural design and the most important components of a coordinate-measuring instrument are shown in figures 42, 43.

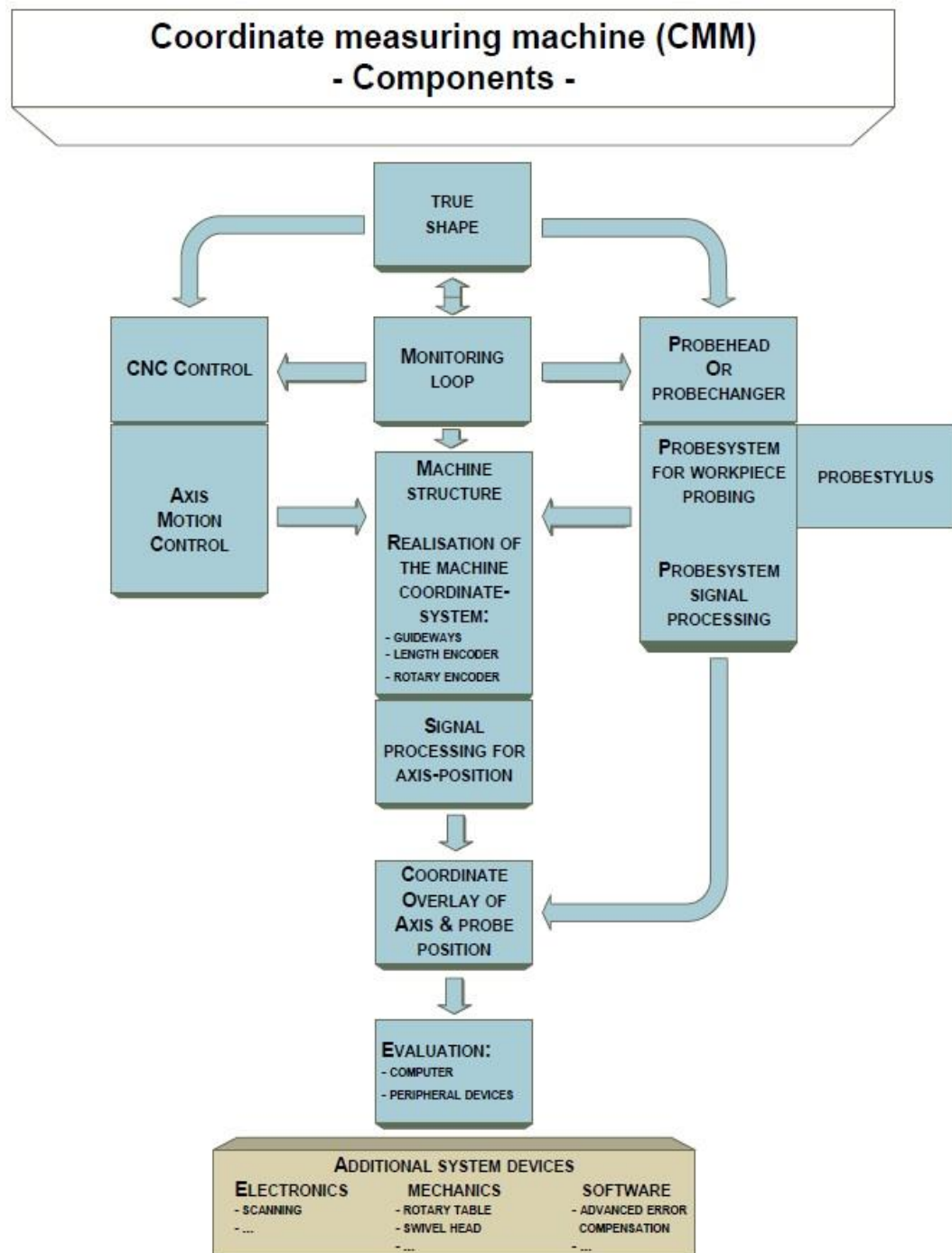


Figure 42 Components of a Coordinate Measuring Machine

For the measurements described below, no round table was basically used. Although, by using a round table the probe pin arrangement would be greatly simplified, the rotary table could lead to additional measurement uncertainties.

In this respect the own measurements were performed with appropriate probe combinations.

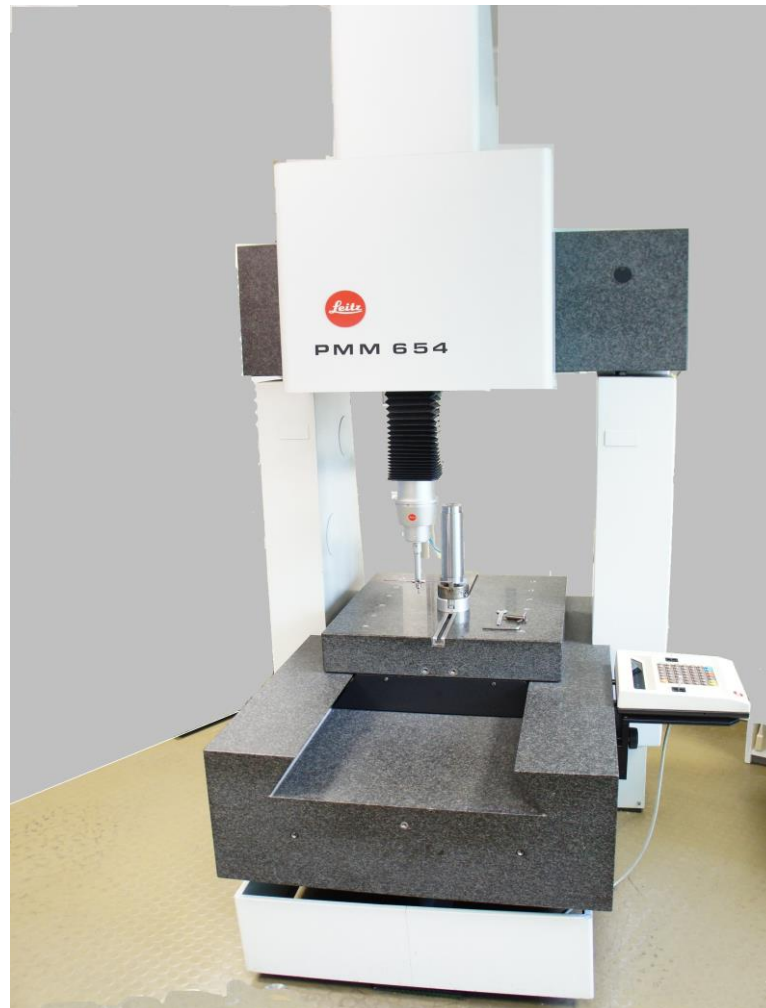


Figure 43 Measuring Machine PMM 654

The measurement uncertainty (in accordance with VDI 2617) diagonally in space with $U = 1.2 + L / 300$ [microns] and the reproducibility of the probe system when probing with $R < 0.7$ [microns] are specified by the manufacturer [121, 122, ST 14]. The measurement uncertainty and the reproducibility of probing points of the probe system are detected by measurements and protocol of the manufacturer.

Measurement uncertainty (according to VDI 2617) The diagonal measurement uncertainty in space is given by $U = 1.2 + L / 300$ [μm], the reproducibility of the probe system in probing with $R < 0.7$ [μm] by the manufac-

turer. The measurement uncertainty and the reproducibility of probing of the probe are detected by measurement and protocol of the manufacturer. The test suitability of the PMM 654 for gear measurement, derived from the expected accuracy class, may be evaluated according to VDI 2612 [ST 15].

The expected geometric qualities of the examined involute toothing are IT 5-11 for concentricity and pitch and IT 8-12 for flank- and profile line variations. According to VDI 2612, arise therefrom as a requirement for the profile measuring device (PMM 654), within the allowable measurement uncertainty based on profile and flank line measurement:

- | | | |
|--------------------------------|-----|-------------------------|
| 1. Profile angle deviation | fHA | 2,5-4,5 μm , |
| 2. Total pitch deviation | FA | 3,0-6,0 μm , |
| 3. Tooth trace angle deviation | fHB | 2,5-4,5 μm , |
| 4. Tooth trace total deviation | FB | 3,5-7,0 μm , |

The repeatability of the individual line measurements should be at 0.5 to 1.0 microns. The manufacturer documented actual measurement uncertainties of the used PMM 654 (VDI 2617) leads to the following classification in terms of gear measurement [ST 14]:

- | | | |
|--------------------------------|-----|-----------------------|
| 1. Profile angle deviation | fHA | < 1,2 μm , |
| 2. Total pitch deviation | FA | < 1,7 μm , |
| 3. Tooth trace angle deviation | fHb | < 1,7 μm , |
| 4. Tooth trace total deviation | FB | < 2,0 μm , |

According to above statements may in principle be assumed that the available coordinate measuring machine PMM 654 satisfies the demands made. The qualitative performance of the measuring machine is significantly better than required [121].

5.2. Measurement of Blank Geometry

5.2.1. Determination of the Workpiece Coordinate System

Reference driving The first step of any measurement program is the reference driving of the incremental linear scales of the machine. In this way, the zero points of the glass scales in the machine coordinate system are defined.

Probe calibration As already stated above, the second step of each measurement program is the calibration of the selected tactile pins of the sensing head on the machine.



Figure 44 probe pin configuration

For this, a program-specified procedure is called and the data (diameter, length and location) of the employed tactile pins is entered. Through pre-programmed probing points the spheres of the probe pins on a highly accurate calibration sphere made of ceramic material (Figure 44) the probe pins center points and the bending of the probe pins will be determined in all directions with contact force acting. All data of the measuring pins are stored for further use (calculation of probing points and analysis of test results) in a database of the measurement software QUINDOS.

The vertical probe PRB (1) has a sphere diameter of 5 mm, a length of 30 mm and is located in the Z-direction. The PRB probe (1) is the reference probe, to which the positions of all the other probes refer. The horizontal probe PRB (2) and PRB (3) have a spherical diameter of 5 mm, a length of 80 mm and are located in -Y and + Y direction. This probe configuration is required to capture all geometric criteria on the blank correctly.

Determination of the workpiece coordinate system The next step is to determine the workpiece coordinate system on the blank. In any coordinate measuring device the machine coordinate system is defined by the position and the origin of coordinates, the zero points of the scales. In the present case the position of the axes of the machine coordinate system is defined as shown in figure 45. The workpiece coordinate system is of dominant importance to the informational value of the resulting measurements, i.e., the geometric quality of the workpiece coordinate system ultimately determines the quality of the measurement result [ST 4].

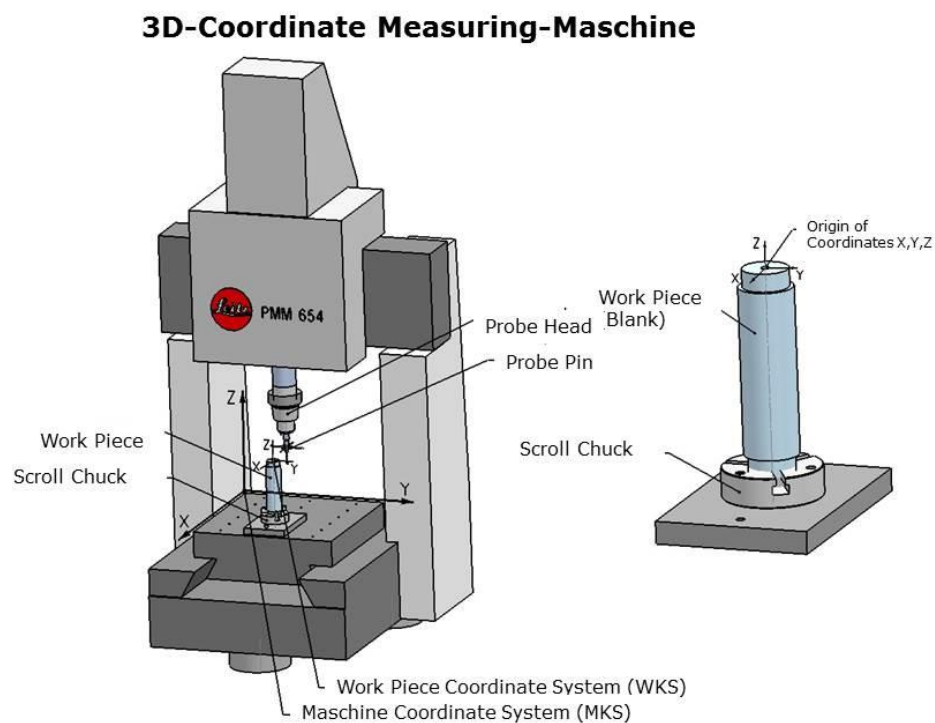


Figure 45 Machine and workpiece coordinate system

The reasons for the mandatory provision of a workpiece coordinate system are discussed briefly below.

1. The workpiece coordinate system is the reference coordinate system for each measurement of a geometric criterion in the following program and their subsequent evaluation. A reference that is located outside of the component, for example, the machine coordinate system, is useful neither for the programming of the measurements nor for the subsequent evaluation of the component geometry.
2. The workpiece coordinate system must be on or in the component to be tested, since the geometry of the component is described thru dimensions in a drawing corresponding to the component. A dimensioning with an external reference system does not make sense from the perspective of production or from the perspective of testing.
3. The workpiece coordinate system defines geometrically the position of the component in the machine coordinate system. Without a workpiece coordinate system, calibrated to the component, location and clamping errors of the component with respect to the machine coordinate system would occur in the test results and lead to erroneous analysis results. A negative example would be in this context, an angular position deviation in the central axis of the workpiece. This is geometrically defined by the clamping on the measuring table based on the defined Z-axis of the machine coordinate system. Such an angular position deviation would lead to significant errors and thus massive misinterpretation of the actual geometry of the work pieces to be tested.
4. In the case of the present work it is about blanks, as well as sample parts after rolling, whose geometry is essentially rotationally symmetrical. The main reference axis of rotationally symmetric components is the central axis of the components. The position of the central axis with respect to the overall geometry must be determined by suitable probe points of the component connected to suitable geometric elements. The result is therefore a reference axis for the component. All other geometric determinants of the

component relates to this reference axis. The resulting toothed machine elements after rolling are partially cylindrically shaped and partially externally toothed. The external toothing is the essential functional element of these machine elements. For those, the same reference axis is of importance.

5. The reference system for the detection of the blank geometry and toothed rolling sample must be identical and after the same probing pattern. Only then the geometry of the blanks and the rolling samples can be comparatively analyzed and weighted. In both cases is the main reference axis, the central axis of the blank and toothed sample.

6. In the case of the PMM it is a CNC-controlled machine with a program control. Thus, is the control once programmed it is able to measure programs to drain automatically and particularly identical. Without a workpiece coordinate system on / in the part, the usefulness of a CNC control is no longer guaranteed, since even small positional deviations of the position of the components on the measuring table cause that the coordinates of probing points need to be re-programmed or learned. With a workpiece coordinate system, only the probing points of the geometric elements of the workpiece coordinate system have to be learned or programmed.

Definition of the workpiece coordinate system According to the production drawing (Figure 46) the blank consists of three cylindrical zones, an upper and lower collar and a central cylinder. The upper and bottom collar are used to hold the part in the rolling machine. But also for holding the part in the measuring machine and for the determination of the workpiece coordinate system by corresponding probe points.

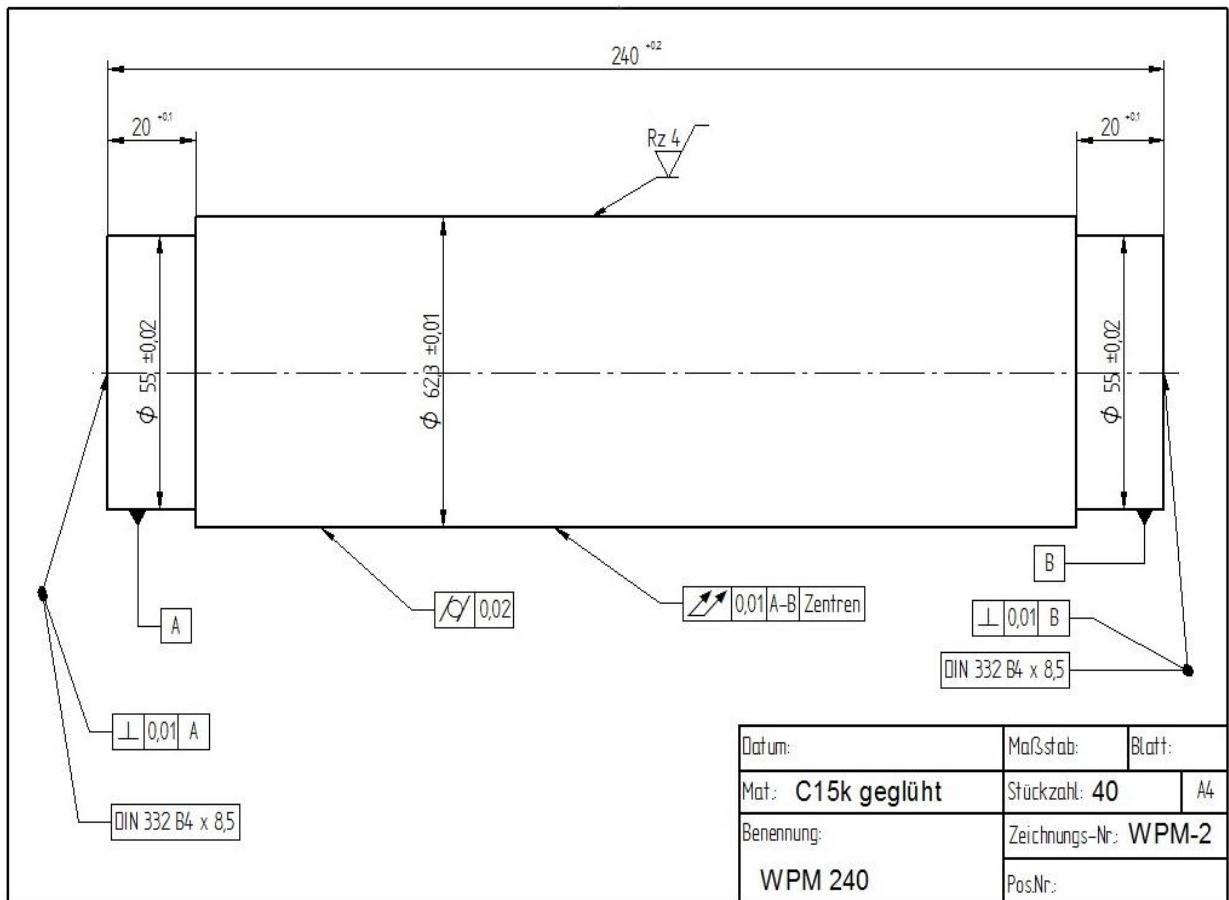


Figure 46 Blank Geometry

The central cylinder, which will be toothed during rolling, and the two collars were turned in one clamping between soft tips to minimize production-related geometric errors. This is also important for the center cylinder which is toothed during the rolling. The determination of the workpiece coordinate system by probing points of basic geometric elements starts in the machine coordinate system. The main axis of the workpiece coordinate system, the same as the central axis of the work piece, are determined by circular probe points at the top (CIRCLE (1)) and lower collar (CIRCLE (2)). The circular probe points (each 12 points on the circumference) can be realized by the horizontal probe PRB (2) and PRB (3). Linking the two circle center points of the lower and upper collars to an axis (AXI (1)) generates the Z-axis of the workpiece coordinate system. The positive direction is defined by the lower collar to the upper collar. Thus the position of the blank is defined in the

space. X-and Y-axis of the workpiece coordinate system generates the X-and Y-axis of the machine coordinate system. A probe point on the upper front face (PNT (1)) is required to define the origin of coordinates, the zero points of the coordinate system completely. The origin of coordinates in the X-and Y-direction component defines the central axis (Z-axis), the zero point in the Z direction is given by the upper front face.

The procedure is shown in figures 47, 48 in detail. All following measurements on the blank are executed in the coordinate system (CSY (1)) and the determined deviations are based on this coordinate system.

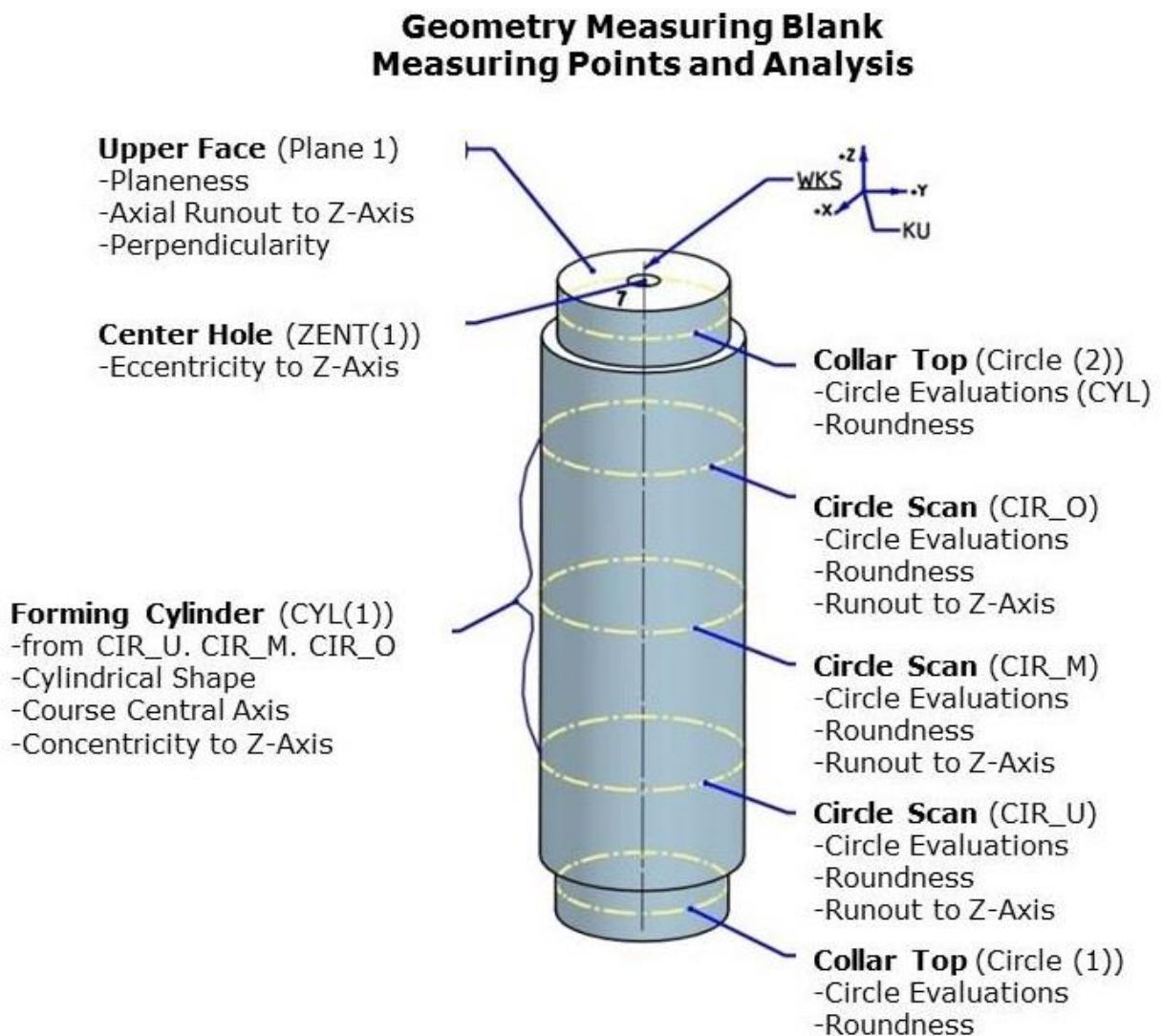


Figure 47 Measurement strategy / Geometry detection on the blank

Work Piece Coordinate System (WKS)

Z-Axis = Connecting of the centers of the circles
Collar Top / Collar Bottom

X-Axis = X-Axis Machine-CS

Origin of Coordinates (KU) = X,Y=0 on Z-Axis
Z=0 on Top end face

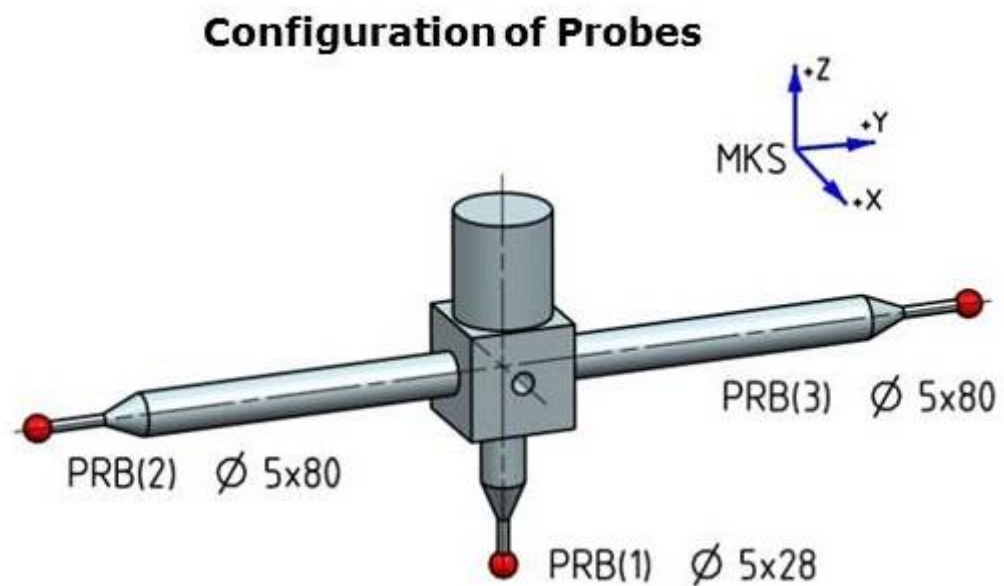


Figure 48 Workpiece coordinate system

Acquisition of the actual geometry of the blank

The clamping situation of the blank on the table of the measuring machine can be seen in figure 49.

The blank is clamped in a three jaw chuck, which is anchored on the table of the measuring machine. Location and arrangement of probes is also indicated in figure 49.



Figure 49 Clamping situation blank /
measuring machine table

As part of the own studies, the accurate recording of the blank geometry is mandatory for the following reasons. Defective blanks, that do not meet the strict geometrical requirements must be identified and sorted out for further series of experiments. The influence of the blank geometry on the resulting toothing geometry is significant. The blank geometry affects dominant the position of the blank in the rolling machine. An assessment of the geometry results on the toothed samples is only possible within a series, when almost identical manufactured blanks were produced. The criteria of geometry listed in the following were collected and analyzed at each blank. The way of measuring / probing and their evaluation is discussed for the respective case. Standardized graphical representations of the actual geometry or the deviations are exemplified attached. All measurements and test results are related to the above-mentioned workpiece coordinate system. The individual geometry criteria and the corresponding probing strategy can be found in the figure 47.

Shape, diameter and concentricity of the tothing zone

In the tothing zone, three circles in different Z-heights (CIR_O, CIR_M, CIR_U) are measured by scanning. That means that the respective probe moves in contact with the workpiece and records and stores during the measuring run 2 points per mm path way. For a scanned probing of a two-dimensional contour the computer has to be specified regarding the start point, direction point and stop point. The two horizontal probes can detect only half a circumference on the blank. By collecting the actual probing points the two semi-circles are summarized into an overall circuit in the evaluation. Diameter and roundness are analyzed according to DIN ISO 1101 [ST 16].

Figure 50 shows an example of the circularity of such scanned circle. The red line represents the actual shape of the circle. In the lower part of the image, the analysis in the form of numerical values is shown.

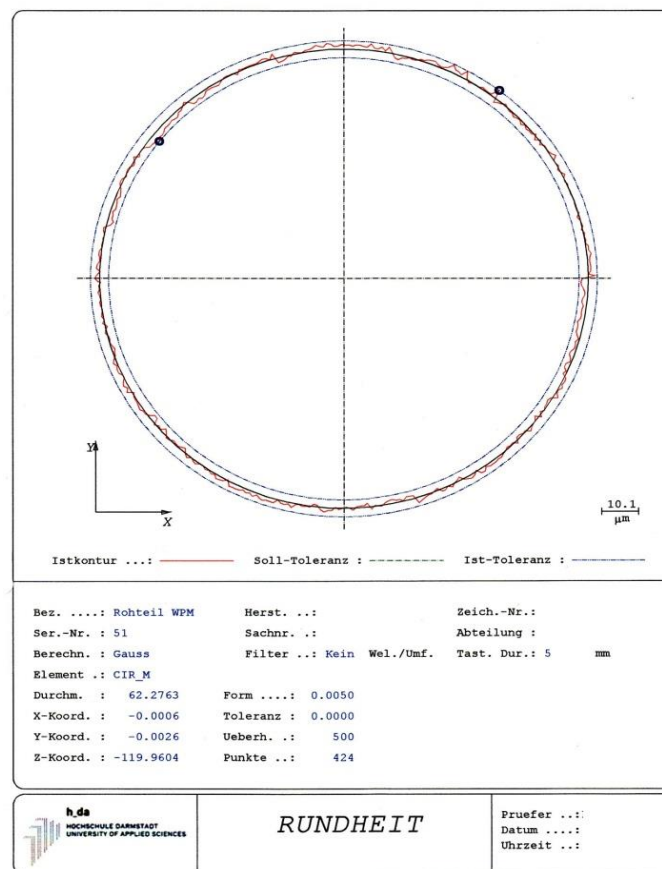


Figure 50 Scanning a circle / ROUNDNESS

As part of the further evaluation, these circuits are summarized by collecting the actual probing points to a cylinder (CYL) (1). Figure 51 shows an example of the cylindrical shape of deviation according to DIN ISO 1101 [ST 16].

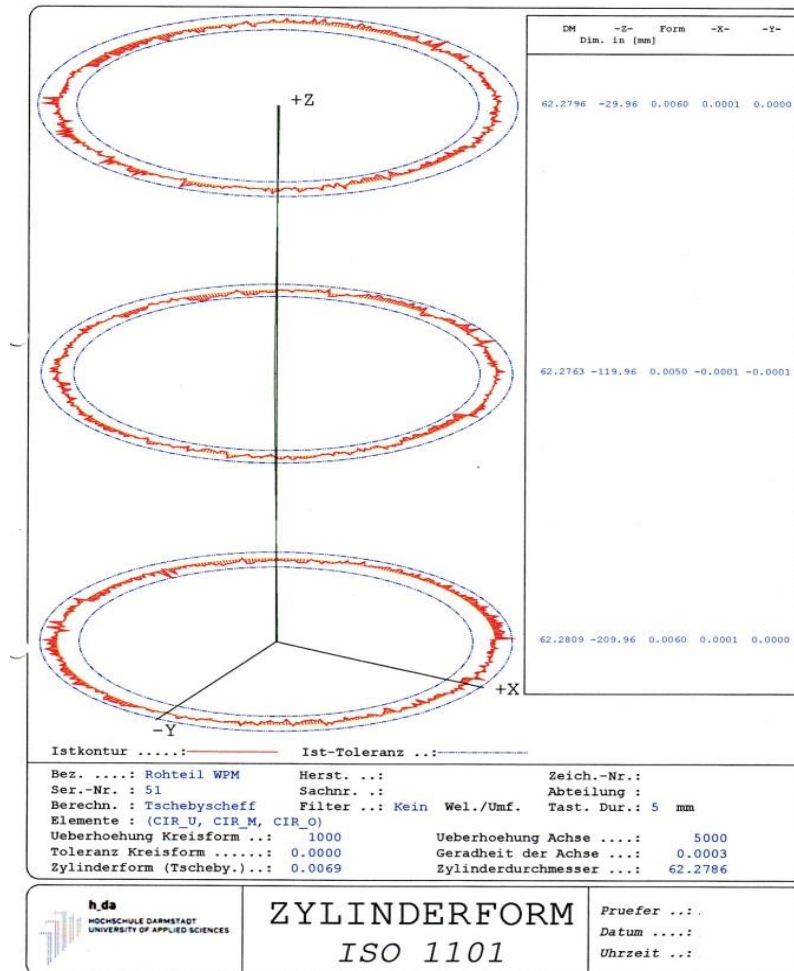


Figure 51 Cylindrical Toothing Zone / FORM OF CYLINDERS

Three circles in different Z-heights show the course of roundness and the location of cylinder centerline. The concentricity of the three circles and the overall run of the cylinder to ISO 1101 are evaluated [ST 16]. Reference in both cases is the Z-axis of the workpiece coordinate system. Subsequently the angular position of the center axis of the toothed zone to the central axis zone of the collars is checked (Z-axis of the workpiece coordinate system). This angle must correspond to the manufacturing process for forming the

raw material. In the present case it was the rotation of the overall geometry in one clamping. The workpiece was clamped between tips. A very small angle error was detected by a correctly turned sample, ($\sim 0.001^\circ$).

Shape, runout and perpendicularity of the forehead levels

The position of the end faces of the blank influences the position of the blank in the forming machine. This effect must be considered in the final geometry. Therefore, the location of these front faces was measured. The top face has been probed with single points (LEVEL (1)) with the vertical probe pin. Flatness, runout and perpendicularity were evaluated according to DIN ISO 1101 [ST 16].

Eccentricity of the center holes The blanks to create the splined shaft are clamped between tips in the rolling machine. The two center holes on the face of the blank are the basis of the concentricity of the component in the rolling machine before and partly during the rolling operation. In preliminary tests it was shown that the positions of the center holes have a decisive influence (eccentricity relative to the cylinder axis) on the resulting pitch and concentricity deviations [28]. The center hole on the front surface was thus probed self-centered by the vertical probe pin. The distance in the XY plane of the probe-tip center to the central axis of the component (Z-axis of the workpiece coordinate system) has been evaluated as eccentricity. For rolling samples to be used in the investigation, only blanks with minimal eccentricities (less than 0.01 mm) were allowed. All results describing the measured blank geometry (circles outer cylinder, roundness, cylinder form deviation) are shown in appendix 1, exemplary for part 32.

5.3 Measurements Toothing Geometry (DIN 3960 ff)

5.3.1 Probe Configuration and Calibration

For the capturing of the tothing geometry, a Probe configuration is selected as figure 52 shows. This arrangement is obtained as a result of necessarily demands that all the teeth on the circumference of the sample have to be measured.

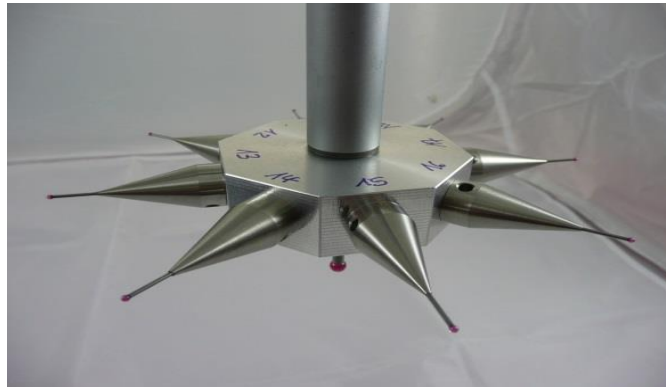


Figure 52 Probe Configuration, $b = 60$ mm

All teeth had to be measured without a Roundtable. The reasons for the avoidance of the use of a rotary table have already been explained above briefly. The arrangement of the tactile pins is selected as follows:

Table 5: Arrangement of the Tactile Pins

Vertical Pins PRB(10)	$d = 5,0$ mm	$l = 30$ mm	(-) Z-Richtung
Horizontal Pins PRB(11)	$d = 1,5$ mm	$l = 40$ mm	(-) X-Richtung
Horizontal Pins PRB(12)	$d = 1,5$ mm	$l = 40$ mm	
Horizontal Pins PRB(13)	$d = 1,5$ mm	$l = 40$ mm	(+) Y-Richtung
Horizontal Pins PRB(14)	$d = 1,5$ mm	$l = 40$ mm	
Horizontal Pins PRB(15)	$d = 1,5$ mm	$l = 40$ mm	(+) X-Richtung
Horizontal Pins PRB(16)	$d = 1,5$ mm	$l = 40$ mm	
Horizontal Pins PRB(17)	$d = 1,5$ mm	$l = 40$ mm	(+) Y-Richtung
Horizontal Pins PRB(18)	$d = 1,5$ mm	$l = 40$ mm	

The vertical Probe PRB (10) is the reference probe. The probes have been adjusted in succession by probing points at the calibration sphere.

5.3.2 Determination Workpiece Coordinate System

The clamping situation of the toothed workpiece on the measuring machine table is shown in figure 53. The toothed part is positioned in a three jaw chuck in the center of the table.



Figure 53 Clamping situation of a sample

To evaluate the influence of the blank geometry on the resulting tothing geometry after rolling the workpiece coordinate system of the gear measurement must necessarily be the same as the coordinate system for the blank measurement (see chapter 5.2.1 Workpiece coordinate system blank) [ST 5, 82]. Accordingly, the workpiece central axis (Z-axis) in the gear measurement was also formed from the midpoints of the probed circles at the lower and upper collars. X-and Y-axes represent the axes of the machine coordinate system. The origin is located on the upper end surface ($Z = 0$) and on the central axis ($X, Y = 0$), (Figure 54).

Work Piece Coordinate System Measurement of the Tothing

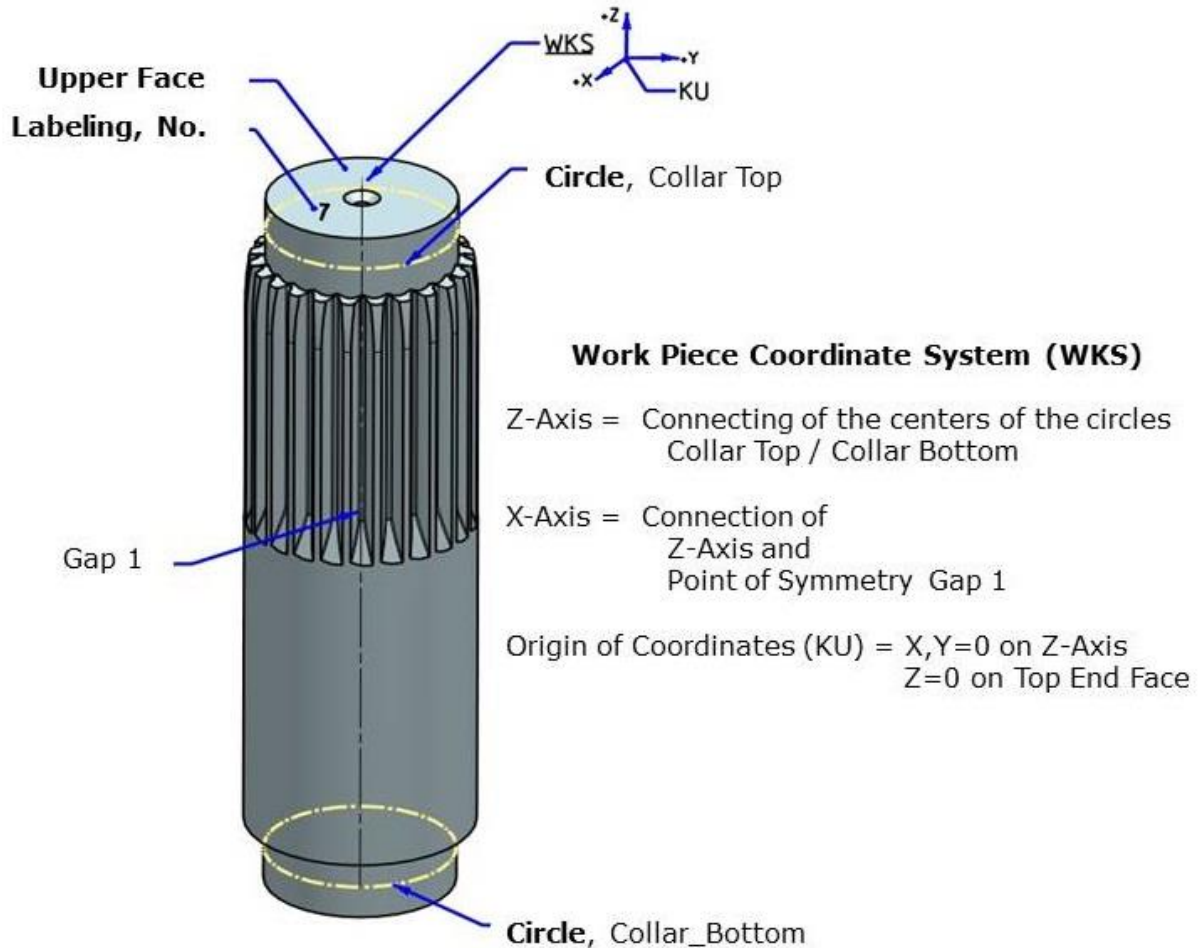


Figure 54 Workpiece coordinate system rolling sample

5.3.3 Acquisition of the Tothing Geometry

The detection of the tothing geometry and the analysis of gearing-deviations were made in accordance with the requirements of DIN 3960 and of the following standards [ST 5].

The basis for all designations relating to tothing geometry is the DIN 3960 ff. The tothing is a splined shaft with involute flanks to DIN 5480 [ST 10]. Workpiece geometry, Probe configuration and orientation of the rolling sam-

ple are presented in Figure 55. Gap 1 of the tothing has been defined in the + X direction of the workpiece coordinate system. It should be noted that the tothing is viewed with regard to the generated and measured gaps, and not in terms of resulting teeth. To DIN the definition of right and left flank of a gap is as follows. Direction of view is the top view of the front side of the toothed sample. In this perspective RIGHT is the right flank of the gap. LEFT is the left edge of the gap (see figures 54, 55). Furthermore also should be noted that the symbols of the geometrical deviations of the teeth are identical in the symbols, as specified by the measurement software. This does not correspond to the requirements for these symbols according to DIN [ST 5]. However, to ensure compatibility between designations in the text and in the diagrams of Quindos, the designations of Quindos were retained.

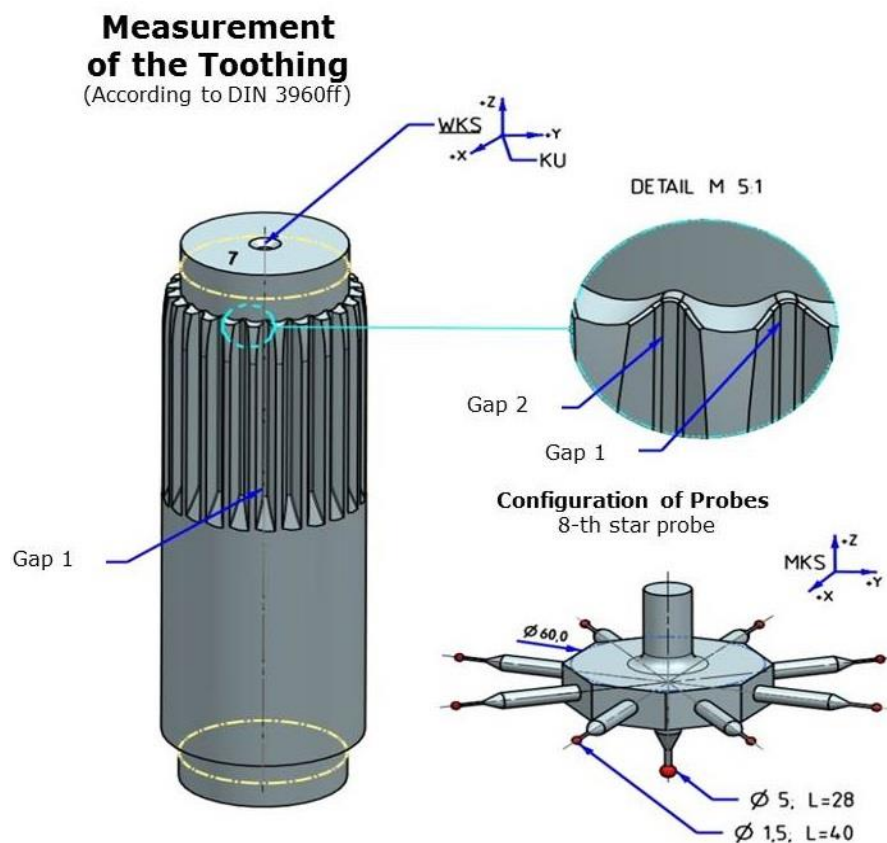


Figure 55 probe configuration

According to the standards DIN 3960 ff the following listed geometry criteria of the toothed parts were recorded and evaluated [ST 5, 82]:

- Pitch, concentricity deviation
- Total profile-, profile angel-, profile form-deviation
- Tooth trace-, trace angel-, and trace form deviation
- Tip -, root circle diameter deviation

Acquisition of pitch and concentricity deviations Pitch and concentricity deviations on the toothing were recorded using single-point probing at each tooth flank in the middle of the profile height of the tooth flank. Here are used the 8 probes $d = 1.5$ mm of the probe-star application, whereby a probing of each 48 tooth flanks at the periphery is guaranteed. The Probing is illustrated in figure 56, 57.

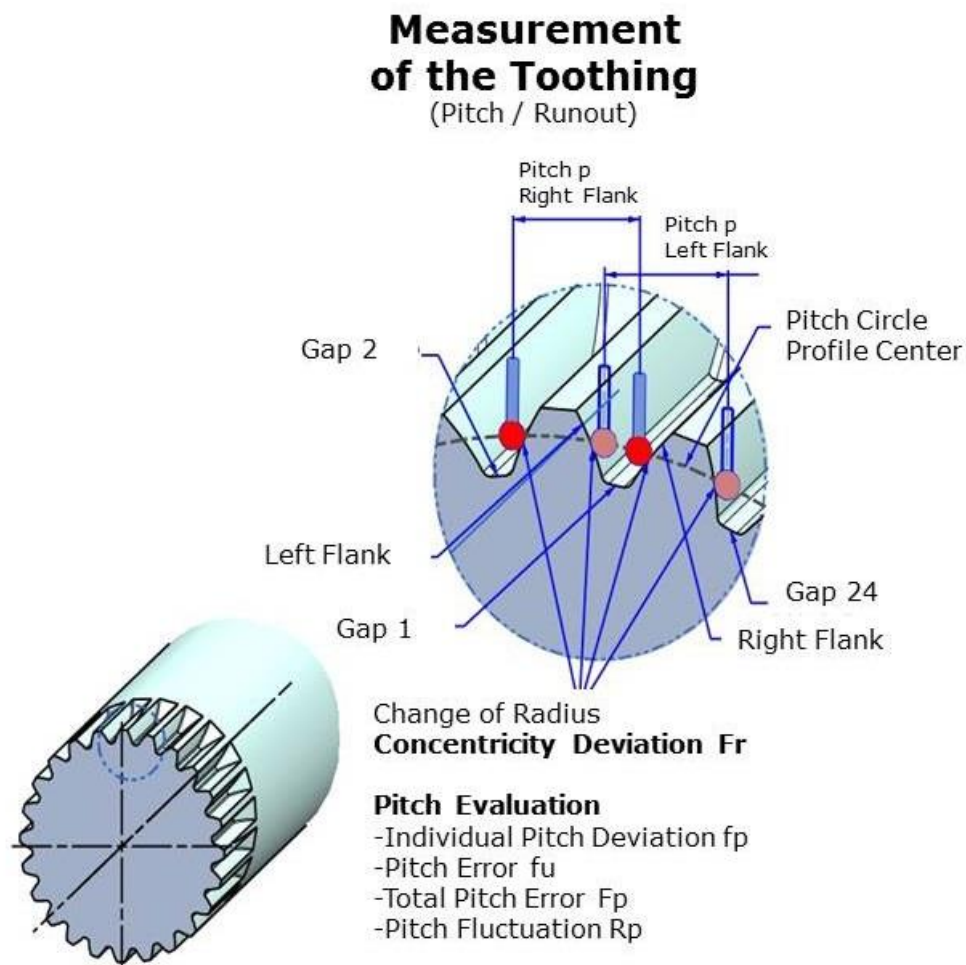
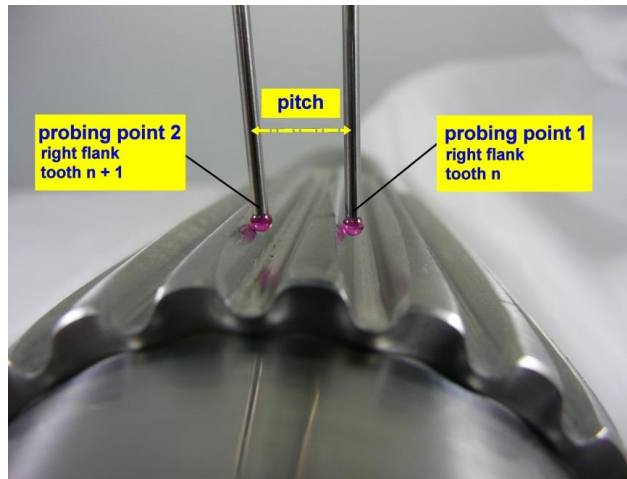


Figure 56 Measurement Pitch / Concentricity



Figure 57 Situation in PMM



Measurement Pitch

In order to analyze the impact of changing tooth profile over the height of the tothing on pitch and concentricity deviations were on the roll-sample pitch and concentricity measurements in 13 different Z-heights along the tooth flanks performed. From probing the pitch as per standard the following specific criteria were evaluated. The analysis is performed separately for left and right flank.

Table 6: Evaluated Specific Criteria

Individual pitch deviation	f_p
Total pitch deviation	F_p
Pitch error	f_u
Pitch fluctuation	R_p

The concentricity deviation, defined as the change in radius over the circumference, has been calculated from the probed pitch points. For analysis of the pitch and concentricity deviations of the teeth the eccentricity of the center teeth to the central axis of the component is very important [ST 6, ST 7, ST 8]. For this reason, a separate evaluation of pitch and eccentricity deviation was made. Even with the determined eccentricity deviation included in the result and once without the eccentricity included in the result.

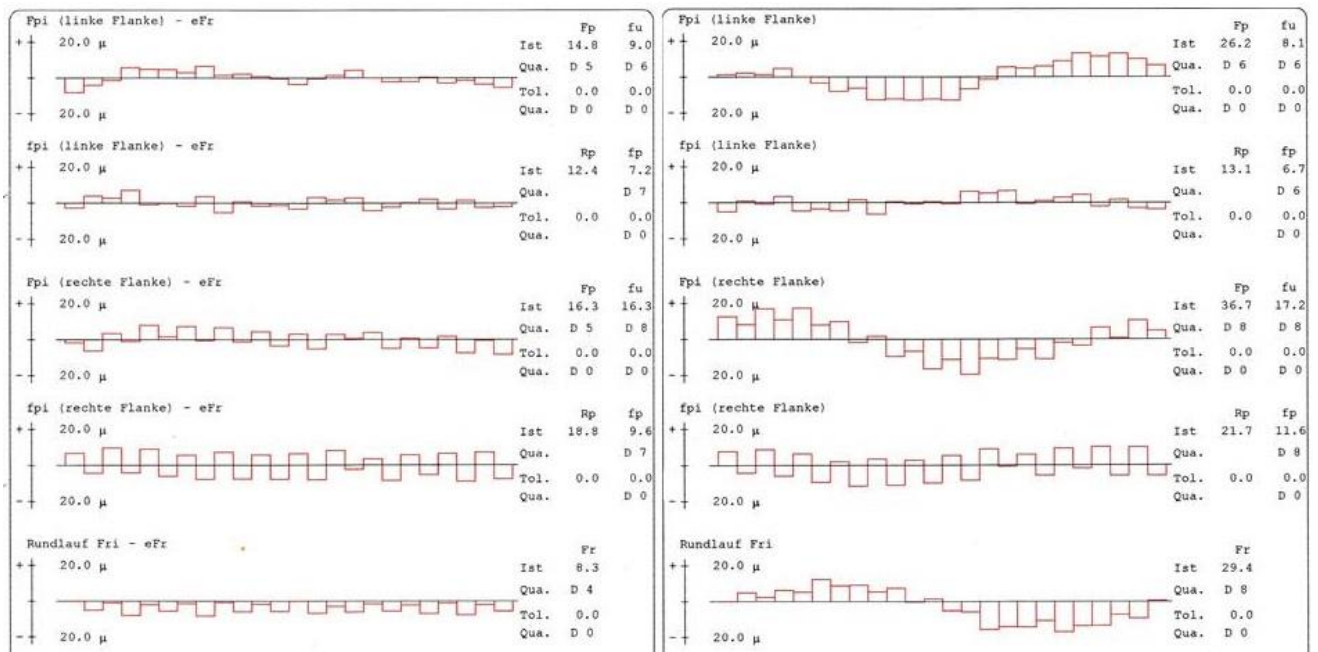


Figure 58 Pitch / Concentricity Deviation w/o and with Eccentricity

This means that in this case, the eccentricity subtracted numerically from the pitch and concentricity deviation.

In figure 58 an example of the graphics pitch and concentricity deviations of teeth with and without eccentricity are shown. This form of graphical representation is determined by the gearing norm. Clearly visible are the difference between the two resulting graphs and therefore the significant influence of the eccentricity of the blank on pitch and concentricity deviations.

Acquisition of the tooth profile deviations Each tooth flank profile (involute) on the circumference was probed (scan line) by one of the 8 calipers $d = 1.5$ mm.

The scan line runs from the root radius to the tip radius of the tooth flank. The density of points is 25 points per millimeter of the traversing. Measurement and evaluation limits are specified in relation to the diameter result diagrams. Also these profile measurements were performed in different Z-heights of the teeth to illustrate the change of the tooth geometry [128]. The measurement and probing for the profile measurement is shown in figures 59, 60.

Measurement of the Tothing (Profile / Evolute)

Profile Evaluation

- Total Profile Deviation FA
- Profile Angle Deviation fHA
- Profile Form fFA

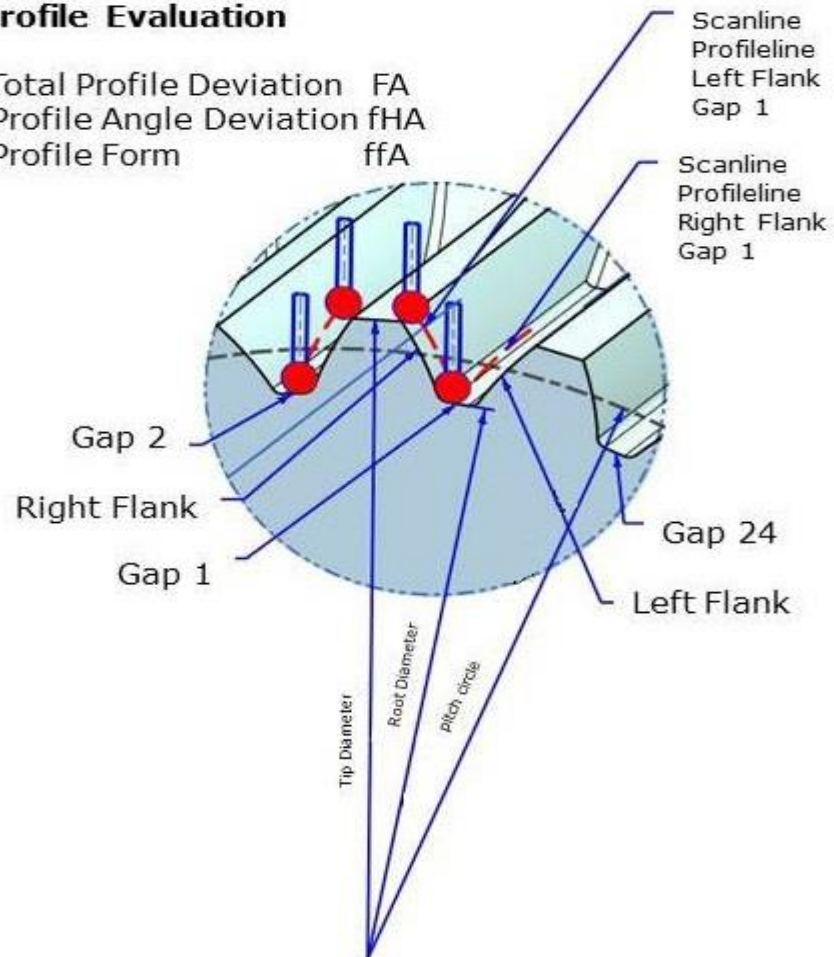
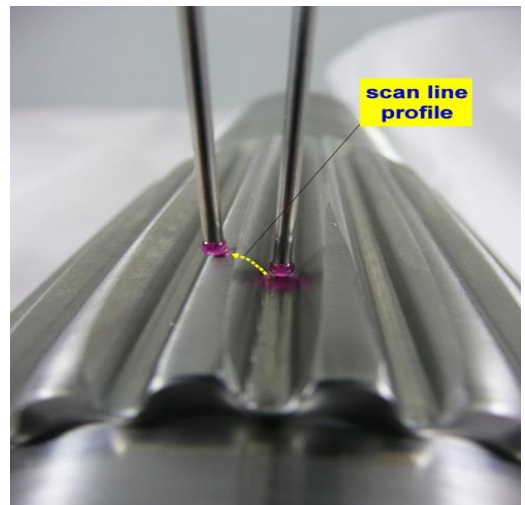


Figure 59 Probing / Profile Measurement



Figure 60 Situation in PMM



Scan line / Profile Measurement

The probing points of the scan lines and the calculated data of the desired involutes a desired-actual comparison in the computer is carried out. That leads to the result to the following profile deviations. Analyzed were the following variables.

Table 7: Evaluated Specific Criteria

Profile angel deviation	fHA
Total profile deviation	FA
Profile form deviation	ffa

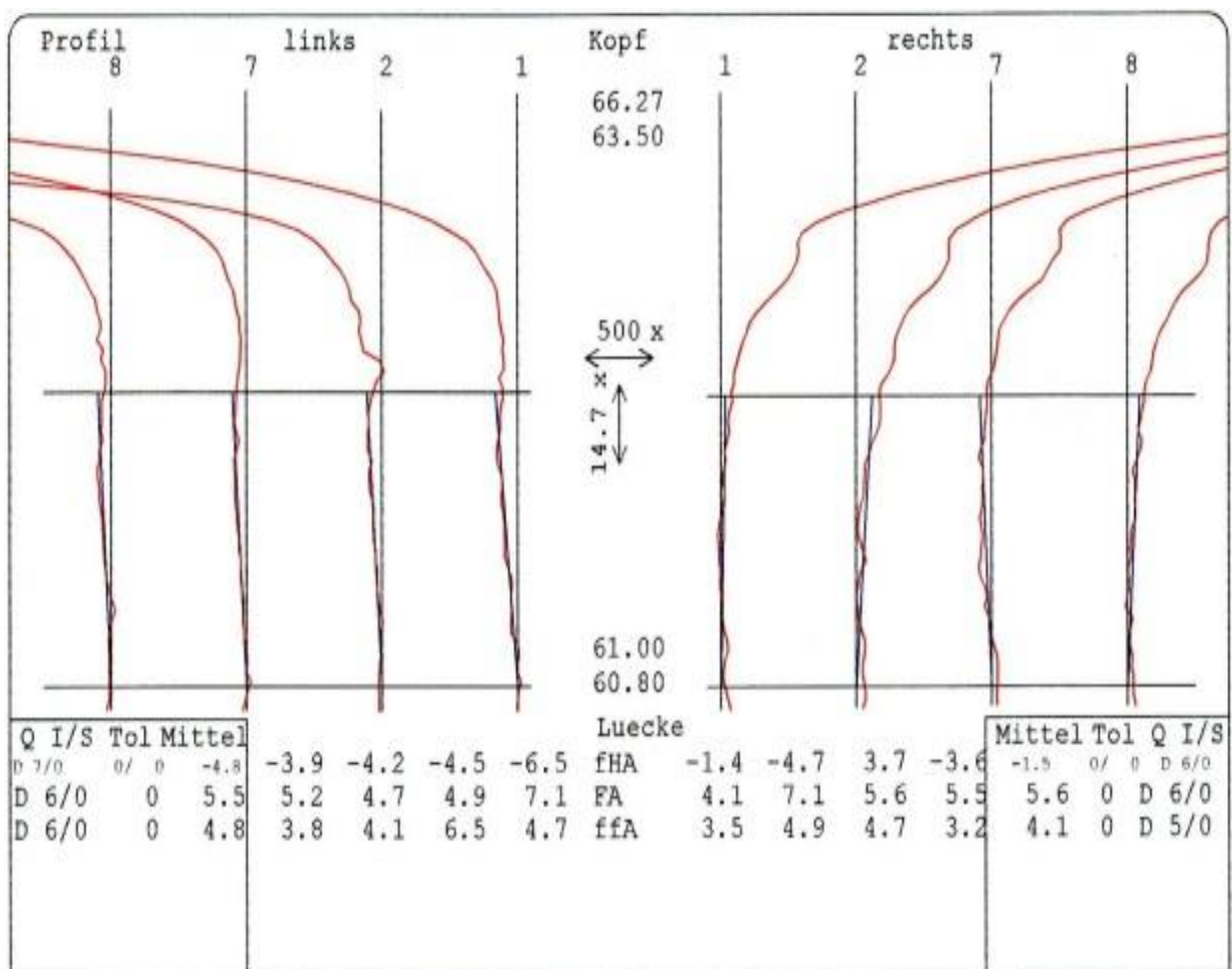


Figure 61 Profile deviations of 4 gaps

The analysis and documentation of the resulting profile deviations are prescribed by the DIN standard [ST 6, ST 7, ST 8]. Figure 61 shows an example of the graph of 4 left and right profiles of a set of teeth. The black vertical line represents in principle the desired involute.

The red line represents the actual deviations from the desired involute. The blue line shows the average actual deviations to evaluate the angular deviation [128]. Among the graphs respectively, the deviations are reproduced numerically. These values are the basis for the subsequent statistical analysis of gearing qualities DIN [ST 6, ST 7, ST 8].

Acquisition tooth trace deviations The course of the flank line (tooth direction) in the axial direction of the tooth was detected by scanning lines parallel to the central axis at the height of the profile center. The probes 11 to 18 ($d = 1.5$ mm) are used. The scan line is in the + Z direction from the bottom upwards.

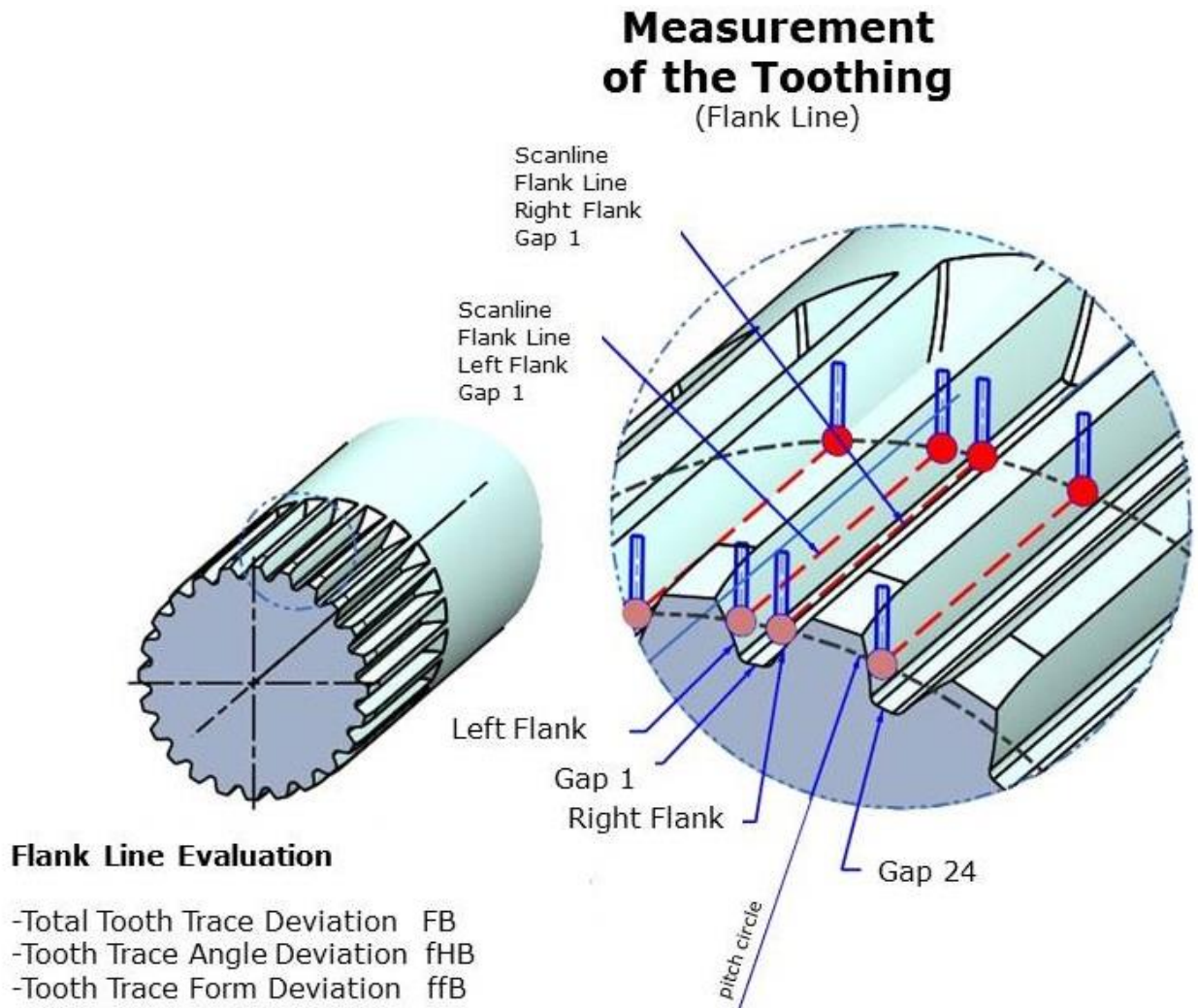


Figure 62 Measurement / Probing / Tooth Direction / Flank Line

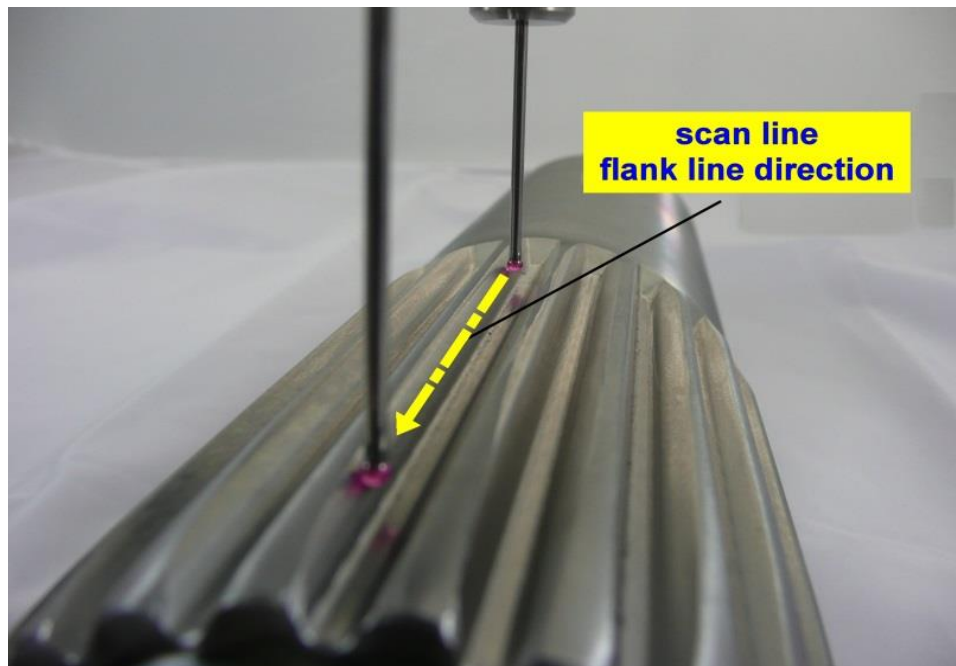


Figure 63 Scane Line / Flank Direction

The density of points was 2 points per millimeter the traversing path. Selected samples measurements were performed on different heights, i.e. the profile of the edge direction was in 3 different heights (1 mm above the middle profile, mid-profile, 1 mm below middle of the profile) of the involute recorded and analyzed. Measuring and probing for the tooth direction are shown in Figure 62, 63, 64. The following specific criteria were evaluated:

Table 8: Tooth Trace

Total trace deviation	FB
Tooth trace angle deviation	fHB
Tooth trace form deviation	ffB

The evaluation and documentation of the resulting edge line deviations are prescribed by the DIN standard [ST 6, ST 7, ST 8]. Figure 64 shows an example of the graph of 4 left and right edge lines on a toothed sample. The black vertical lines represent the principle target edge line. The red lines represent the actual deviations from the desired tooth direction.

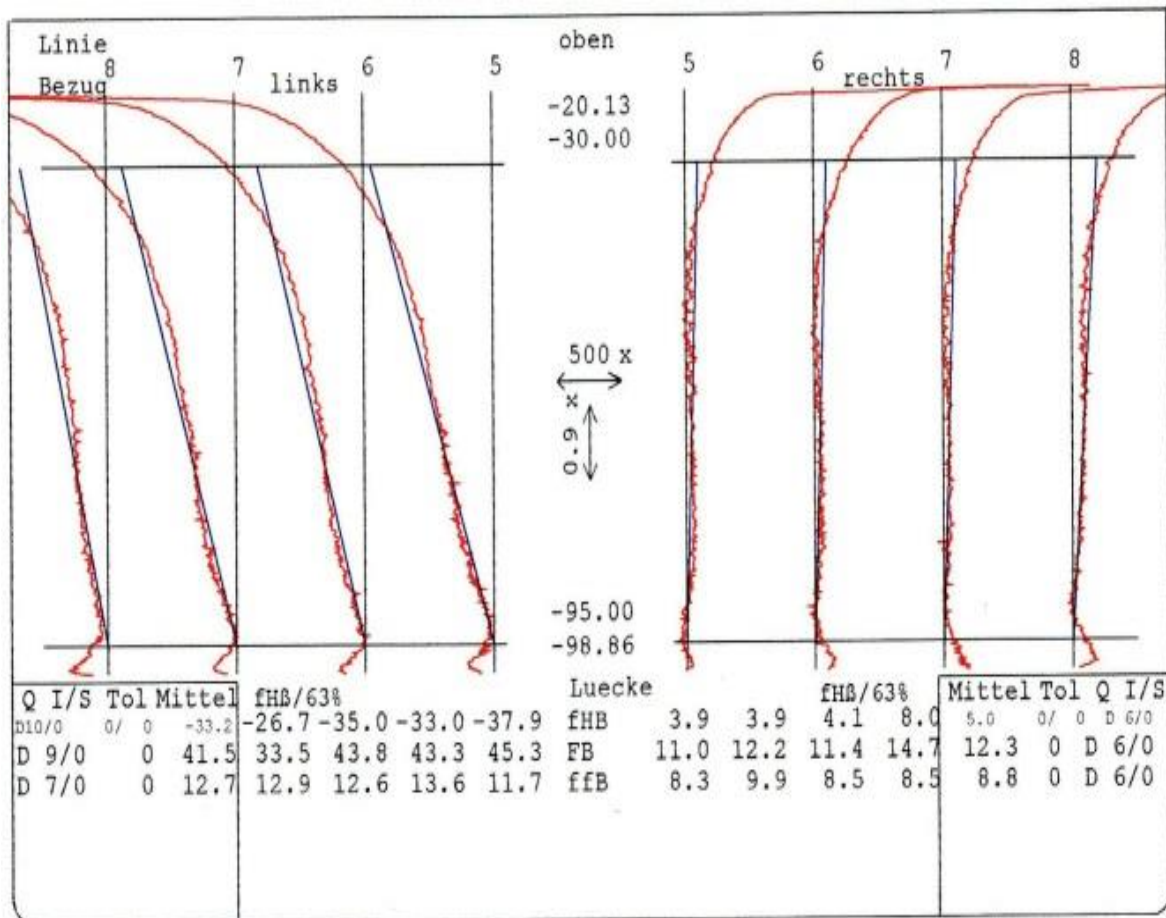


Figure 64 Flank Line Deviations of 4 gaps

The blue lines show the average actual deviations to evaluate the angular deviation. Among the graphs respectively, the deviations are shown numerically. These values are the basis for the subsequent statistical analysis of gearing qualities DIN [ST 6, ST 7, ST 8].

Acquisition tip- / root circle diameter The tip and root circle diameter of the tooth were detected by single-point probing on all 24 teeth in the center of the tooth tip and the center gap in the tooth root. As can be seen on the outer contour of the teeth is visually, the tooth heights vary along the length of the teeth. To document this course, head and root circle diameter in different Z-heights are recorded. Measuring and probing strategy for the measurement of the tip and root circle diameter show figures 65, 66, 67.

Measurement of the Tothing (Tip-/Root Diameter)

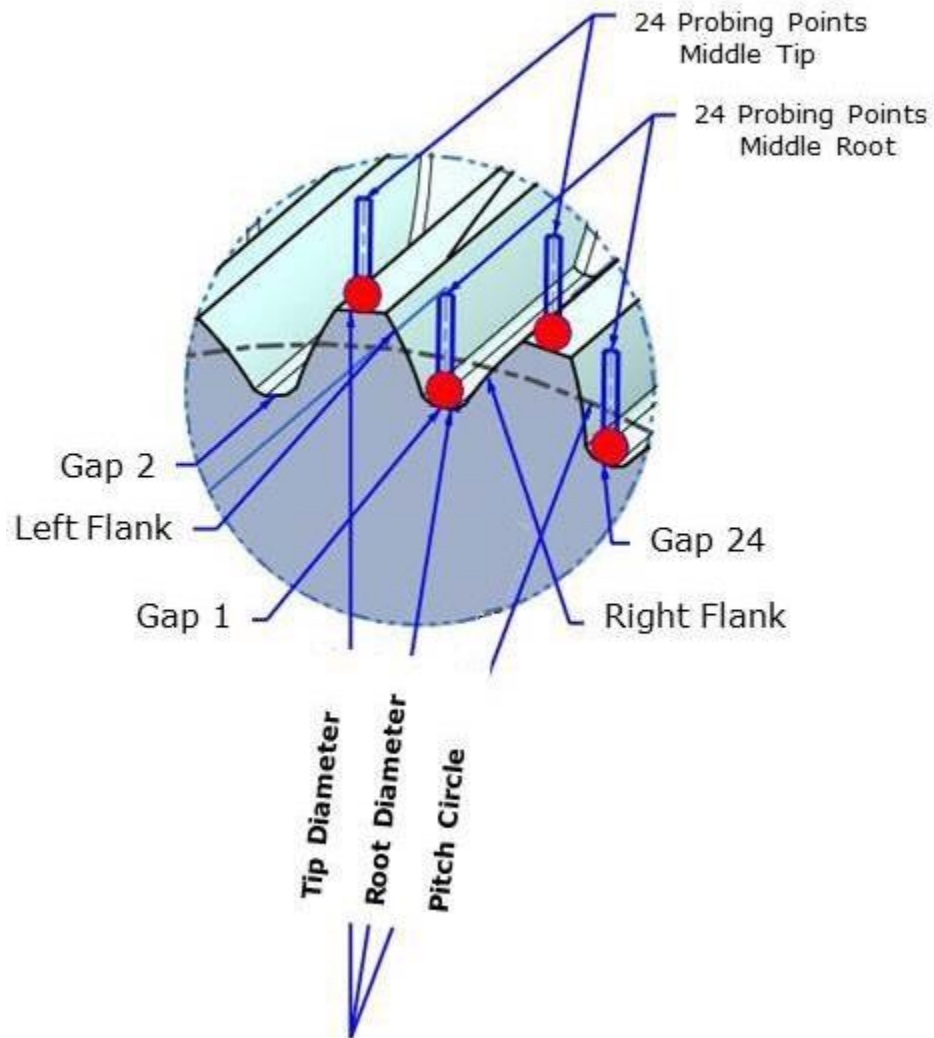


Figure 65 Detection Tip- / Root Circle Diameter

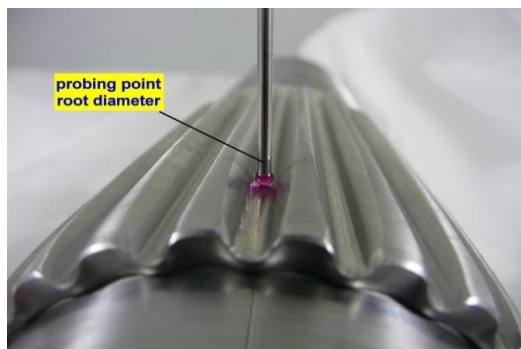
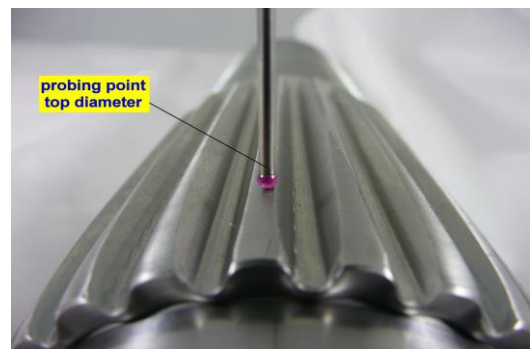


Figure 66 Probing Point Root Diameter



Probing Point Tip Diameter



Figure 67 Situation in PMM

The 24 probing points were grouped to form a circle and its roundness is evaluated and documented according to DIN and ISO 1101 [ST 16]. The results of tip and root circle diameter represent the diagrams in figure 68.

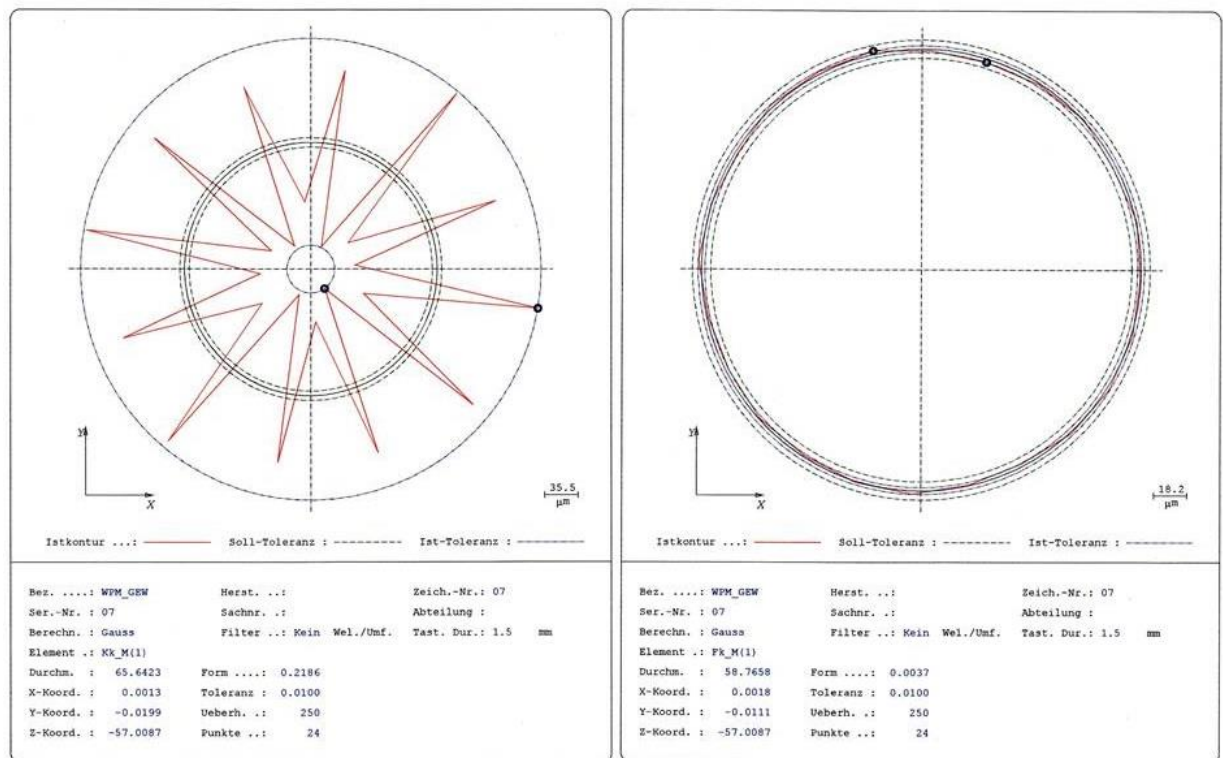


Figure 68 Tip circle diameter

Root circle diameter

All above mentioned quality features of tothing, pitch/concentricity deviation, root diameter/roundness, tip diameter/roundness, tooth trace deviation and profile deviation are shown in appendix 2 for all 24 teeth, exemplary for the sample 07. There was no specific reason to choose sample 07. The results of all other samples look more or less identical.

5.4 Measurement Geometry Rolling Tools

As the drawing shows, the rolling tools are half-shells with 12 teeth arranged on the inner contour, according to DIN 5480 for each half [ST 10]. The contour of the teeth in the vertical direction is divided into several conical zones, which is required for the intended course of the forming process. The detection of the tool geometry is important for two reasons. The geometry of elements of the outer shape of the rolling tools, as the outer cylinder and the front sides, determine the position of the tools in the rolling machine.

The precise measurement of the tooth geometry of the rolling tools is of such great importance. Since otherwise the analysis of the deviations of teeth of the toothed sample are not possible. Especially for the reasoning of the causes of errors and deviations of the teeth on the work pieces, the knowledge of the generating tool geometry is mandatory. If significant errors of tool geometry can be found, they must affect the resulting geometry of the toothed sample significantly. However, this should then be found almost identical at all rolling samples.

5.4.1 Probe Configuration and Calibration

For the acquisition of the geometry of the rolling tools a probe-star could not be used. The reason is the curvature of the inner toothing. Therefore, for the measurements only a vertical probe in Z-direction (sphere diameter $d = 2$ or 3 mm, length $l = 60$ mm) was used. Another probe ($d = 3$ mm) is required in the X direction only for the detection of the outer shape of the rolling tools. Position and bending of these probes have been identified as described above. A snapshot of the work tool measurements configuration is shown in figure 69.



Figure 69 Probe Configuration

5.4.2 Coordinate System Rolling Tools

The tool half was on a magnetic prism, which is anchored to the measuring machine table, as fixed that all the specifics of geometry of the half shell elements can be achieved by the two probes (Figure 69). The coordinate system of the rolling tool is defined by the end faces and the outer cylinder, as these determine the position of the geometric elements and the tool in the rolling machine (Figure 70).

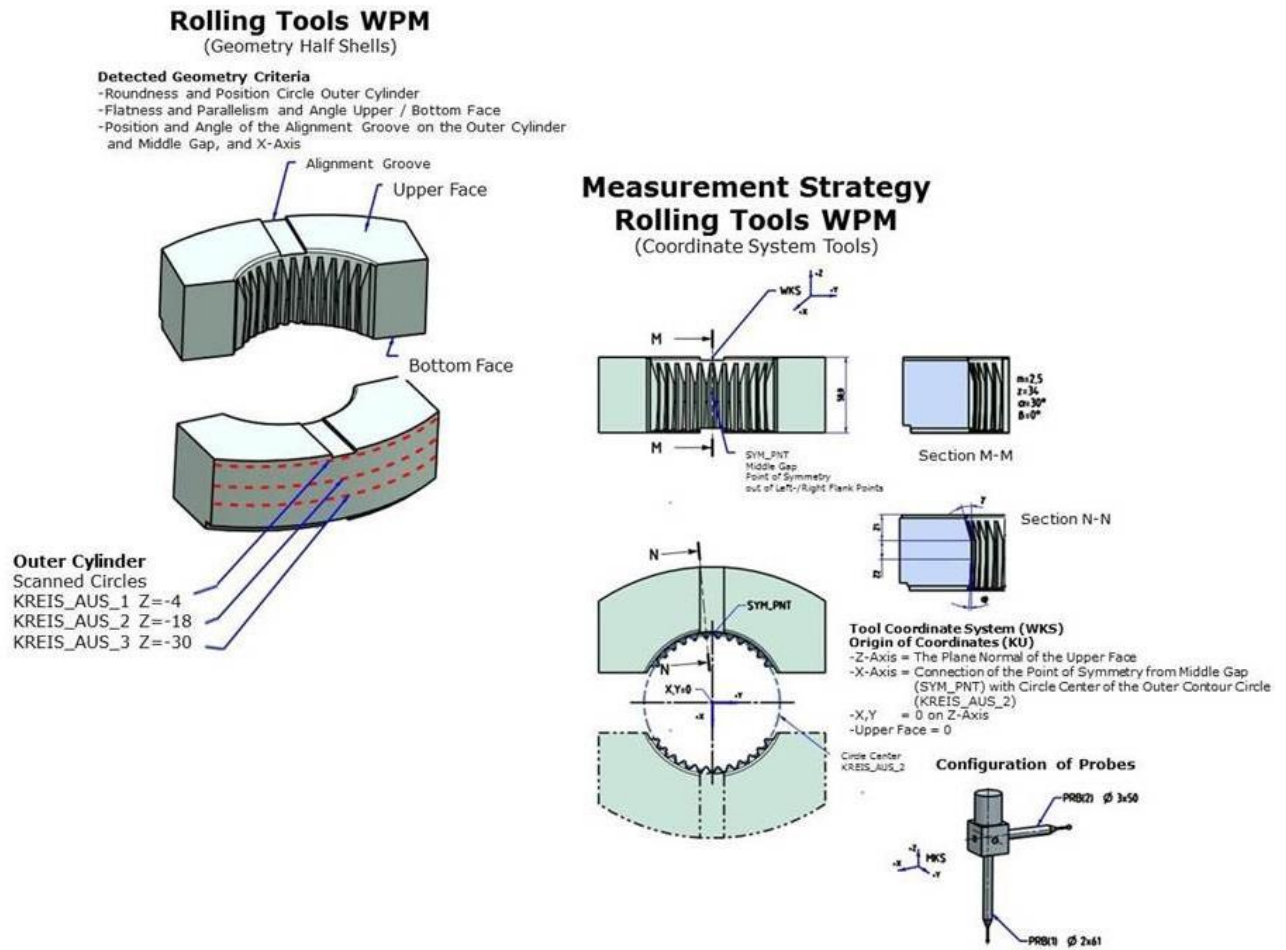


Figure 70 Detection of the Outer Cylinder Coordinate System Tools

First the upper end face of the tool was probed as a plane. The normal plane of the end face is the end of the Z-axis of the workpiece coordinate system. On the outer cylinder of the half shell, three circles (KREIS_AUS_1, 2, 3) are scanned in different Z-heights. In the central tooth gap a symmetry point was determined, which is produced from two-point probing on the right and the left gap edge. The connection between these symmetric points with the symmetry center of the circle of the average outer circle (X_AXIS) forms the X-axis of the workpiece coordinate system.

The coordinate origin is derived from the zero points in the X-and Y-direction defined by the center of the outer circle center and the zero point in the Z direction by the upper end face.

5.4.3 Acquisition Geometry Outer Contour of the Tools

The outer contour of the rolling tools determines the position of the tool halves in the rolling machine. For this reason it is necessary to capture the following geometry elements on the outer contour of the half-shells of the rolling tools (Figure 71, left side) to evaluate them.

Outer cylinder On the outer cylinder of the shells were 3 circles in different Z-heights ($Z = -4$, $z = -18$, $z = -30$) scanned. On the right side of figure 71 an example of a diagram of the roundness of a circle of the outer cylinder of the rolling tool is illustrated.

Frontal flats Upper and lower end flats were probed with the two described probes. Flatness, parallelism and angular position of the two tool faces are evaluated to each other.

Alignment groove For aligning the position of the tools in the machine on the upper end face, a groove is produced by machining. This groove defines the mounting position inside the machine and is therefore very important. This groove was probed at the two side surfaces. The position of the groove to the X-axis of the coordinate system, and to the middle of the tooth gap is evaluated. The probing of the alignment groove during the measurement process is shown in figure 72.

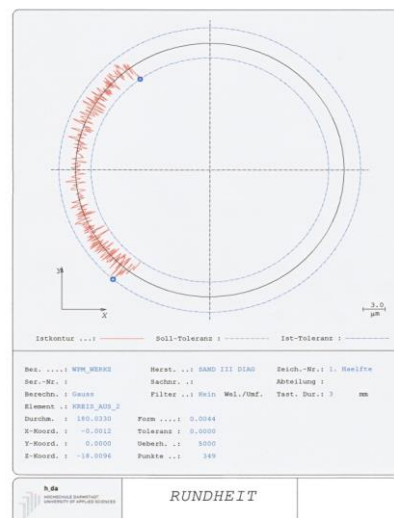
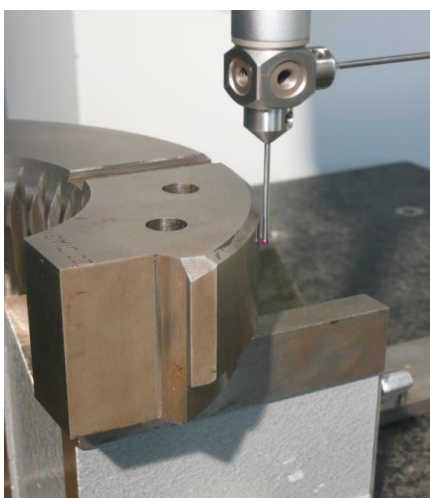


Figure 71 Situation in PMMRoundness Outer Cylinder

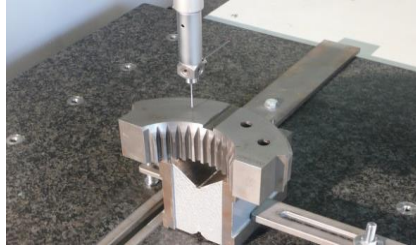
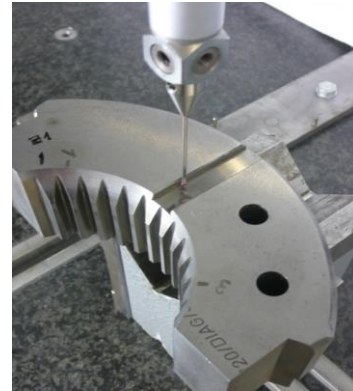


Figure 72 Frontal Flats



Alignment Groove

5.4.4 Acquisition Gear Geometry Rolling Tools

It should be noted that the teeth of the tools have been considered and measured with regard to the teeth and not to the tooth gaps (just the same as with the toothed samples). The reason for this is that the teeth of the tools produce the gaps in the samples.

Measurement Strategy Rolling Tools WPM

(Gear Measurement according to DIN 3960ff)

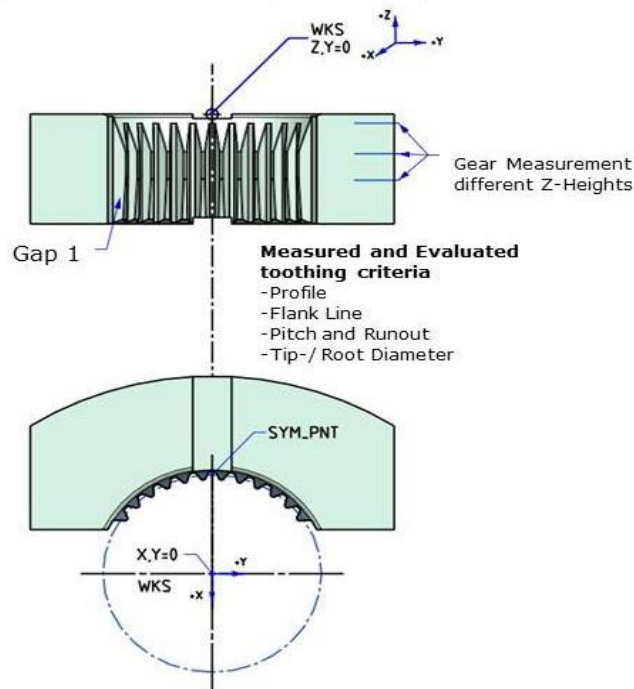


Figure 73 Measuring / Probing Strategy

In the half-shells are in each case 12 teeth of the mentioned geometry according to DIN 5480 [ST 10]. The length extension of the teeth in the Z-direction is divided into three different conical and cylindrical zones (see Figures 73, 74). This categorization is established by the expiry of the rolling process. To capture the toothed geometry of these zones the pitch, concentricity and profile was measured several times in different Z-heights.



Figure 74 Situation in PMM

Specifically, according to the standard, the following teeth criteria were measured and evaluated. The evaluation is based on the above-mentioned workpiece coordinate system. Starting point of the measurements is the left outer tooth. All criteria were measured in different heights. Pitch and concentricity, profile of all flanks, flank trace of all flanks, tip- and root-diameter.

Pitch and concentricity Pitch and concentricity were evaluated from probing points on the tooth flanks in the middle of the profiles. These probing's were performed using the vertical probe with a sphere diameter $d = 2$ mm. Pitch and concentricity were evaluated with and without considering the eccentricity of the gear/workpiece centerline, just as with the rolled samples. Figure 75 shows an example of a pitch and concentricity evaluation of the internal gear with recognized eccentricity. Clear differences in pitch and eccentricities in different Z-heights of the tools are not detectable.

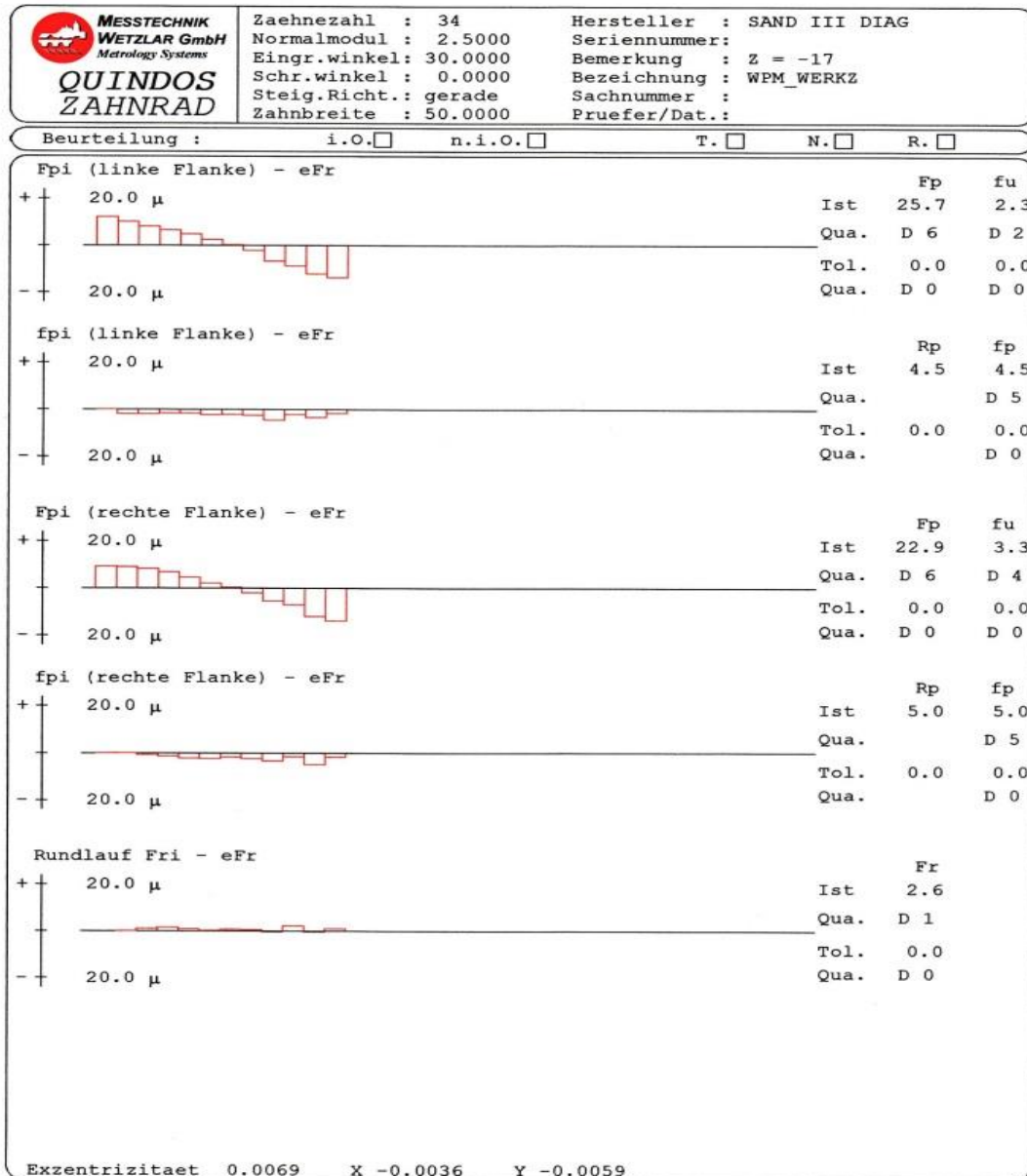


Figure 75 Pitch / Concentricity Deviation of the Tools

Profile of the tooth flanks (involute)

The profile of the tooth flanks was recorded by scanning with a point density of 25 points per mm traversing path. Here, the flank geometry was determined from root radius to tip radius. By the conical regions of the tool half the tooth heights change and therefore the possible measuring length. Probing points, measuring and reporting limits are shown in figure 76.

Figure 76 shows alternatively for the entire tooth profile, deviations on four teeth. Differences of the profile deviations in different Z-heights of the tools are classified as very low.

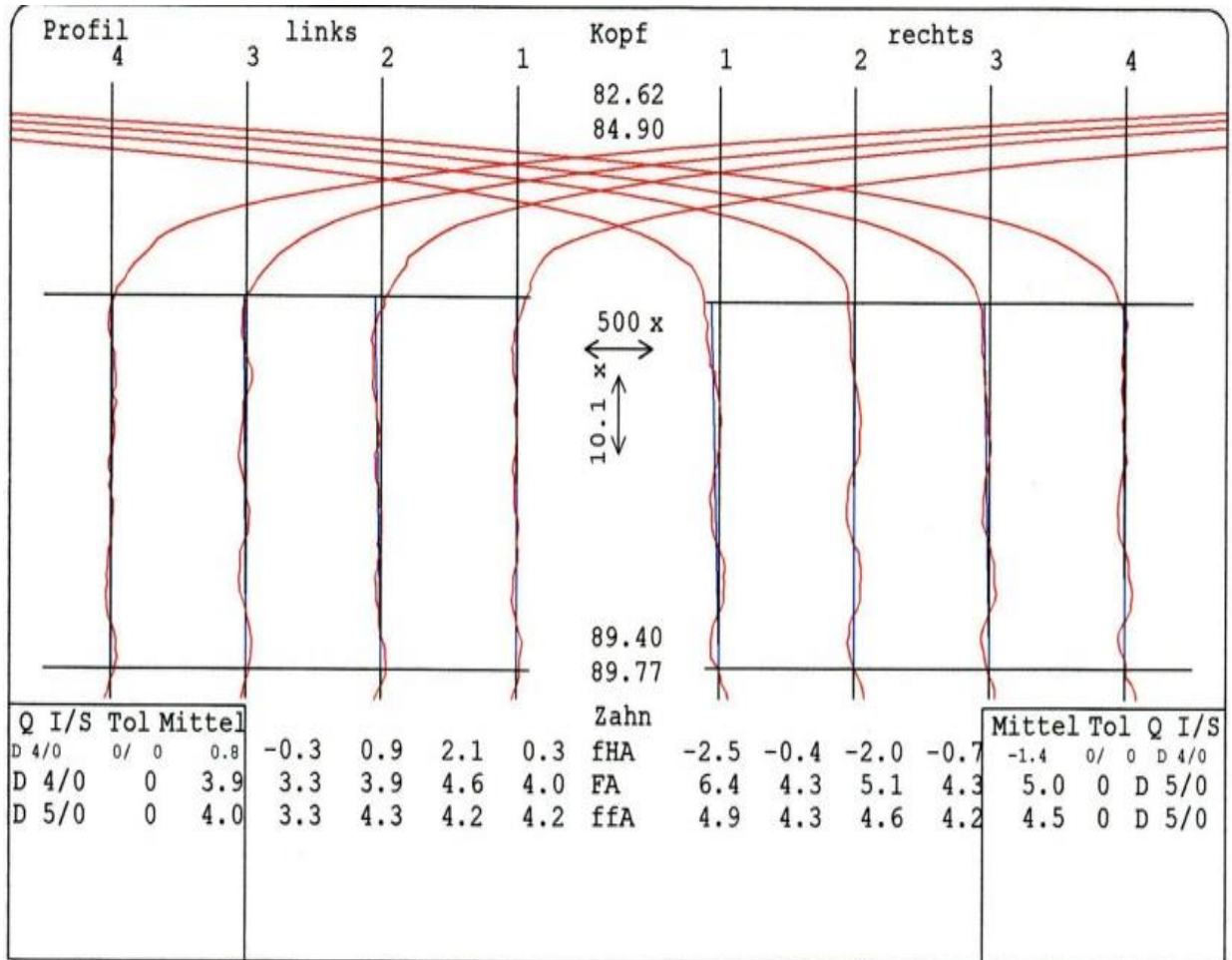


Figure 76 Internal Tooth Profile Deviations Rolling Tools

Tooth trace The tooth trace measurements had to be performed with a vertical probe with sphere diameter $d = 3$ mm, due to the great bend of the probe $d = 2$ mm. The tooth trace deviations were also recorded in scanning parallel to the tooth axis at the level of the middle of the profile with a density of 2 points per mm traversing path. Caused by the concentricity of the teeth, the possible measurement range of the edge lines on the tool is limited, so that not the entire tooth length can be scanned.

Measurement and evaluation-lengths are indicated in each image. Figure 77 shows an example of such a diagram with the tooth trace deviations of 4 teeth of a rolling tool-half.

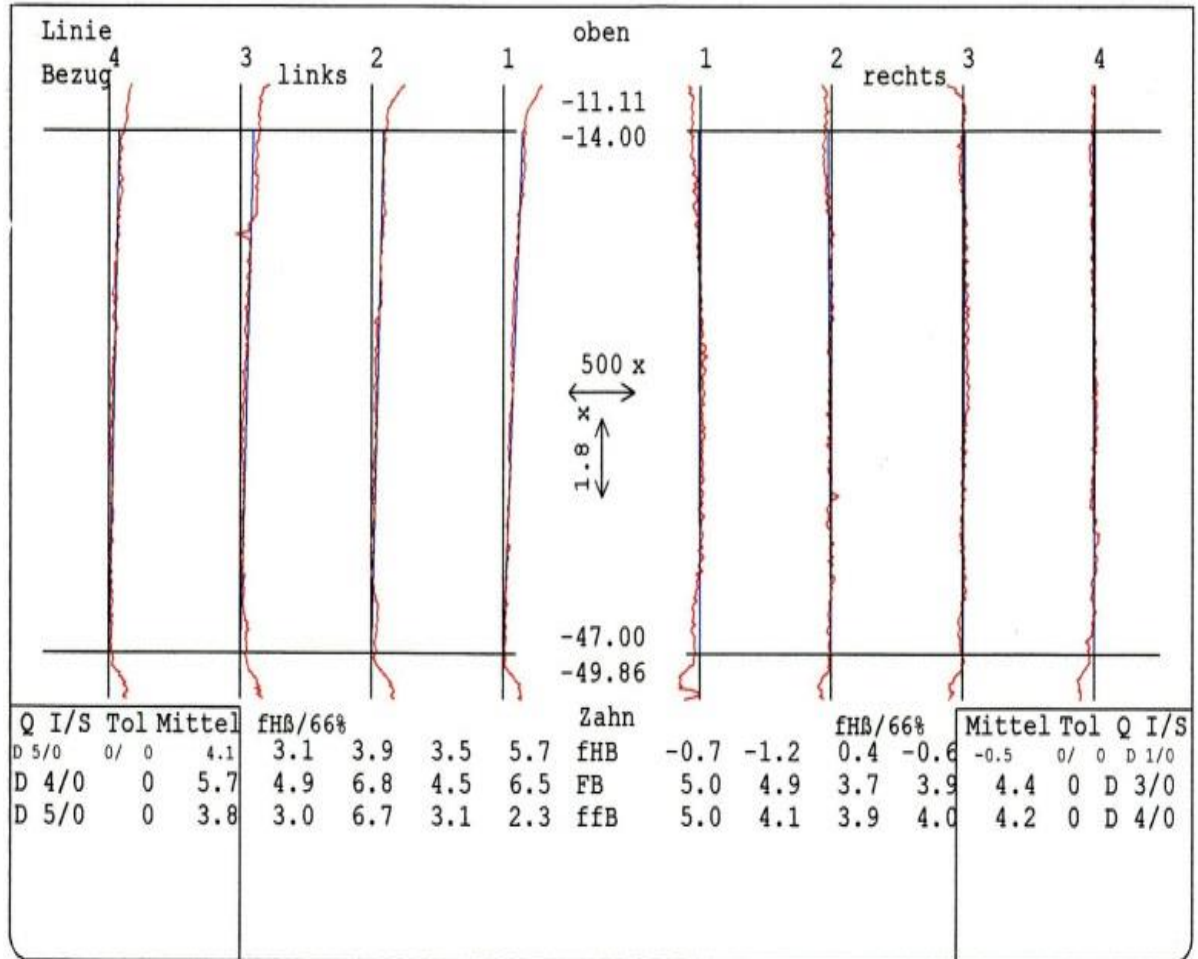


Figure 77 Flank Trace Deviations Internally Toothed Rolling Tools

Tip and root circle diameter Tip and root diameter were determined by single-point probing respectively on the tooth tip and the middle of the gaps of the internal toothing. In figure 78 the roundness of the head and the root circle diameter of a tool half is shown in a diagram. It can be seen in both cases, the slight deviations in shape. This applies also to the root diameter in different Z-heights of the internal toothing. The curve of the tip circle diameter is characterized by the conical shape of the internal toothed tool.

In Annex 2 to this work the full diagrams of all 12 teeth of a tool half according to DIN can be found [ST 3]. Specifically, these are pitch and concentricity with and without consideration of the eccentricity, the profile deviations, the tooth trace deviations and tip circle and root diameter. The evaluation of the deviations in accordance with DIN 3960 ff. leads to the following tooth- ing qualities of the internal toothed tools, pitch Q7, concentricity Q4, profile Q6 and tooth trace Q6 [ST 5]. This analysis includes all above mentioned single criteria deviations according to DIN. These relate according to DIN, only the teeth with the largest found discrepancies, all other teeth are of a better quality. For both tool halves result almost identical measuring results. Significant geometric errors on the roll-tools cannot be ascertained. The tools show a significantly better quality Q7, as the best samples Q9.

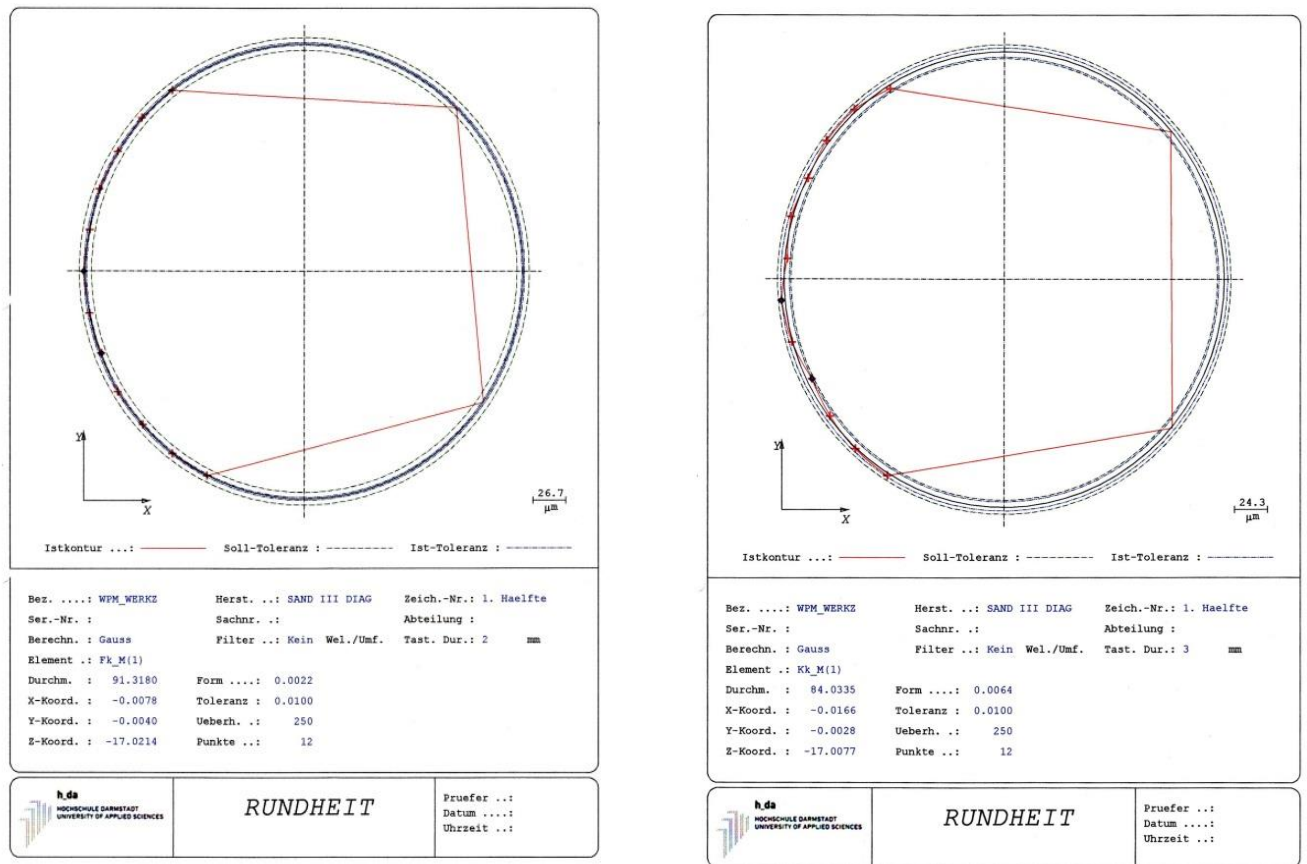


Figure 78 Roundness Root Circle Fk Internally Toothed Rolling Tools
Roundness Tip Circle Kk Internal Toothed Tool

Summary of all results measured in accordance with DIN

All samples were measured according to the procedure as described.

Due to the enormous amounts of data all the above images and graphs only show examples of the generated results. Because all correlations found invariably repeated, this approach was adopted. Appendix 3 shows all geometry results concerning the tool.

A) Rolling tools The conical shape of the internal toothed tools defines the ratio of per stroke radially and axially displaced material volume.

This results in a significant influence on the resulting geometry of the displaced material. Both tool halves are identical, because they are made of a complete internal toothed ring. After separation of this ring emerged two identical halves. They show no significant geometry errors that could be associated in any way with geometric results of the rolling sample measured.

B) Material of the blanks An influence on the results of the geometry using several forming materials could not be determined. All materials yielded almost identical results. Material related trends could not be determined.

C) Feed rate As observed in the preliminary experiments, the feed rate determines the geometry of the rolling samples. The feed rate is the most important experimental parameter. Detailed observations of the individual geometric quality criteria follow in Chapter 6.

5.5 Contour Measurements on Rolling Samples

Justification for contour measurements The aforementioned measurements and evaluations of gear geometry according to DIN 3960 ff are used for decades in this form to assess the quality of gears of all types [ST 5]. This type of measurement is a selective or partial evaluation of the geometry of a toothed machine element. For example, pitch / concentricity, tip and root diameter of a toothed geometry is recognized only punctually and described. In the case of the profile, only the region of the involute is included in the analysis. This also applies to the flank line, which is defined as a

line of the tooth profile. The above-described method of collection and analysis of gear geometries meet the requirements for the assessment of precision and gear quality in modern industrial practice. It is assumed that only certain areas of the teeth are of importance for their function. In this view, the respective production process plays a significant role. If a tothing is produced by cutting methods, then the known measurement and analysis methods are quite sufficient. When machining the gap material is converted into chips. Therefore, it is assumed that the desired cutting geometry almost exactly results. It also assumes that the geometry of the flanks of the teeth is produced symmetrical and evenly distributed over the circumference of the gearing. All this is to be understood in the context of manufacturing precision and consideration of wear and positional stability of the component in the machine. When manufactured without cutting, the tothing will show other geometric structures with special geometric features. These characteristics are typical of the forming process which is used. It is important to detect and describe these characteristics geometrically. As already explained above, the production of toothed machine elements by metal forming, blank material is displaced by the action of the tool. Several gaps result by this action. The desired shapes of the gaps are such that a complete tothing results. What is required here is symmetry of the teeth with high geometric quality. The material of the gaps will be displaced, so that it constitutes a tothing. In consequence, this means that the assessment of the geometry of metal forming shaped teeth cannot be limited to parts of the teeth. The entire contour of the teeth must be included in the assessment. Only in this way the material flow or the volume distribution of the material is to describe and analyze. Consequently, results the requirement to capture the entire contour of the teeth in all three dimensions. To meet this requirement as described the following measurement methodology and strategy will be used.

5.5.1 Contour Measurements Rolling Samples

Probe configuration and calibration Central requirement for the contour detection was to detect the contour in all axial regions of the respective toothing. Therefore e.g. the narrow tooth root area was measured with small sphere radii. For this purpose, a probe-star with 8 horizontal star-shaped probes (sphere diameter $d = 1.5$ mm) and a vertical probe ($d = 5$ mm) had to be used. This probe-star was already used in the gear measurement on the rolling samples. This probe calibration has already been explained in section 5.3.1.

Workpiece coordinate system To compare the measurements in accordance to DIN, for the contour measurements an identical workpiece coordinate system had to be used [ST 6, ST 7, ST 8]. The workpiece center axis forms the z-axis of the coordinate system, X- and Y-axes correspond to the axes of the machine coordinate system, the zero points in the X and Y direction are located on the Z-axis, the zero point in the Z-direction lies on the upper end face of the roll sample. The determination of the workpiece coordinate system is described in detail in section 5.2.1.

Acquisition of the contour cuts rolling samples The clamping situation of the workpiece on the table of the PMM and the probe configuration is already shown in figure 49. This arrangement has been retained. The contour sections were scanned as two-dimensional contours in the XY plane (Figure 79, 80).

Contour Measurement Tothing (Work Piece)

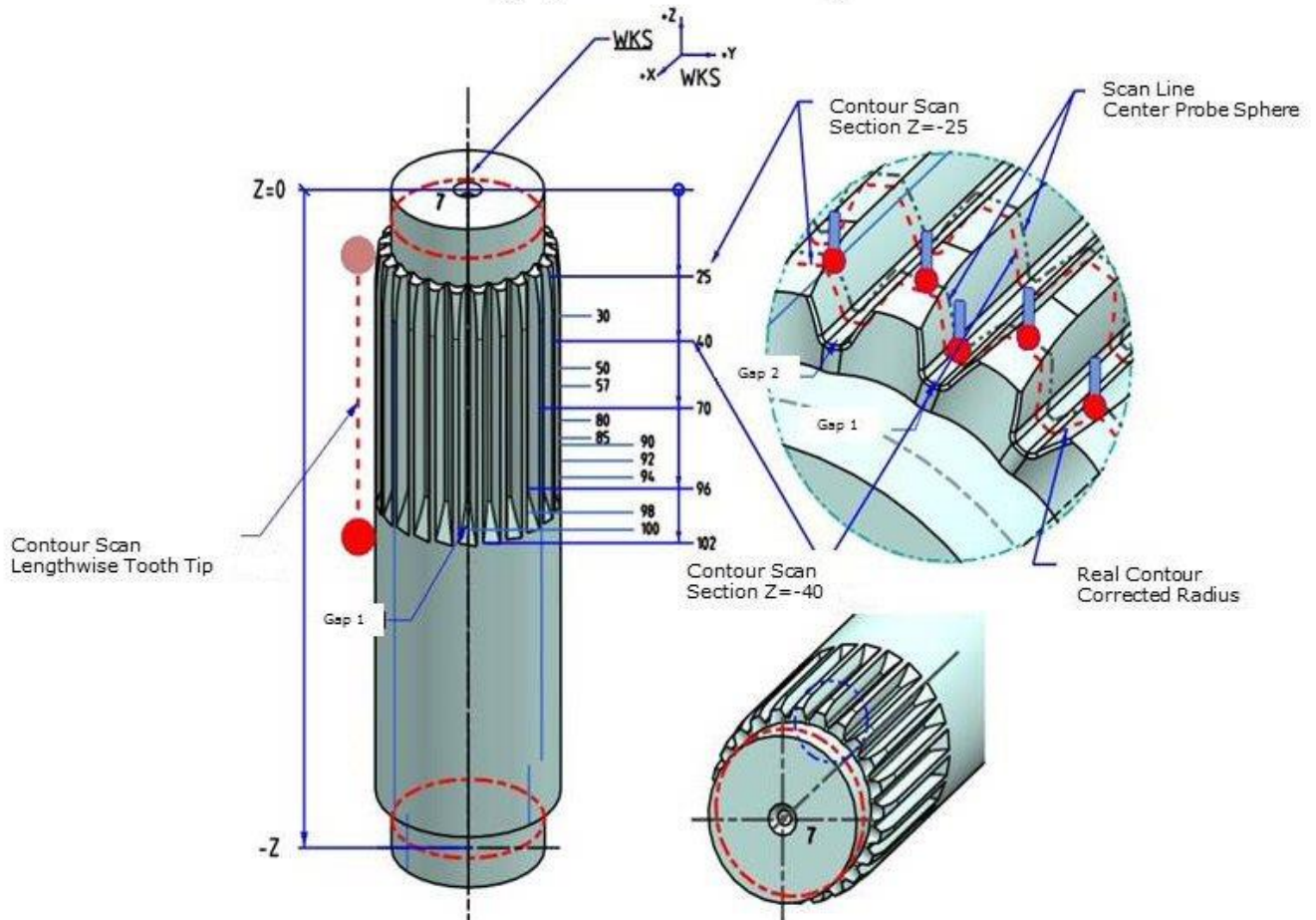


Figure 79 Contour Measurement Workpiece

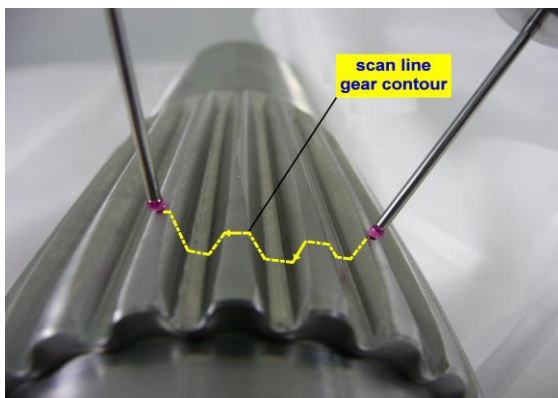


Figure 80 Scan-Line Workpiece



Situation in PMM

To measure the scan lines horizontal probe pins were used (sphere diameter $d = 1.5$ mm). With these little sphere diameters could be ensured that the entire contour could be scanned, including the smallest occurring radius in

the tooth root. To capture all of the teeth on the circumference, every three teeth the probe had to be changed and a new scan line was generated.

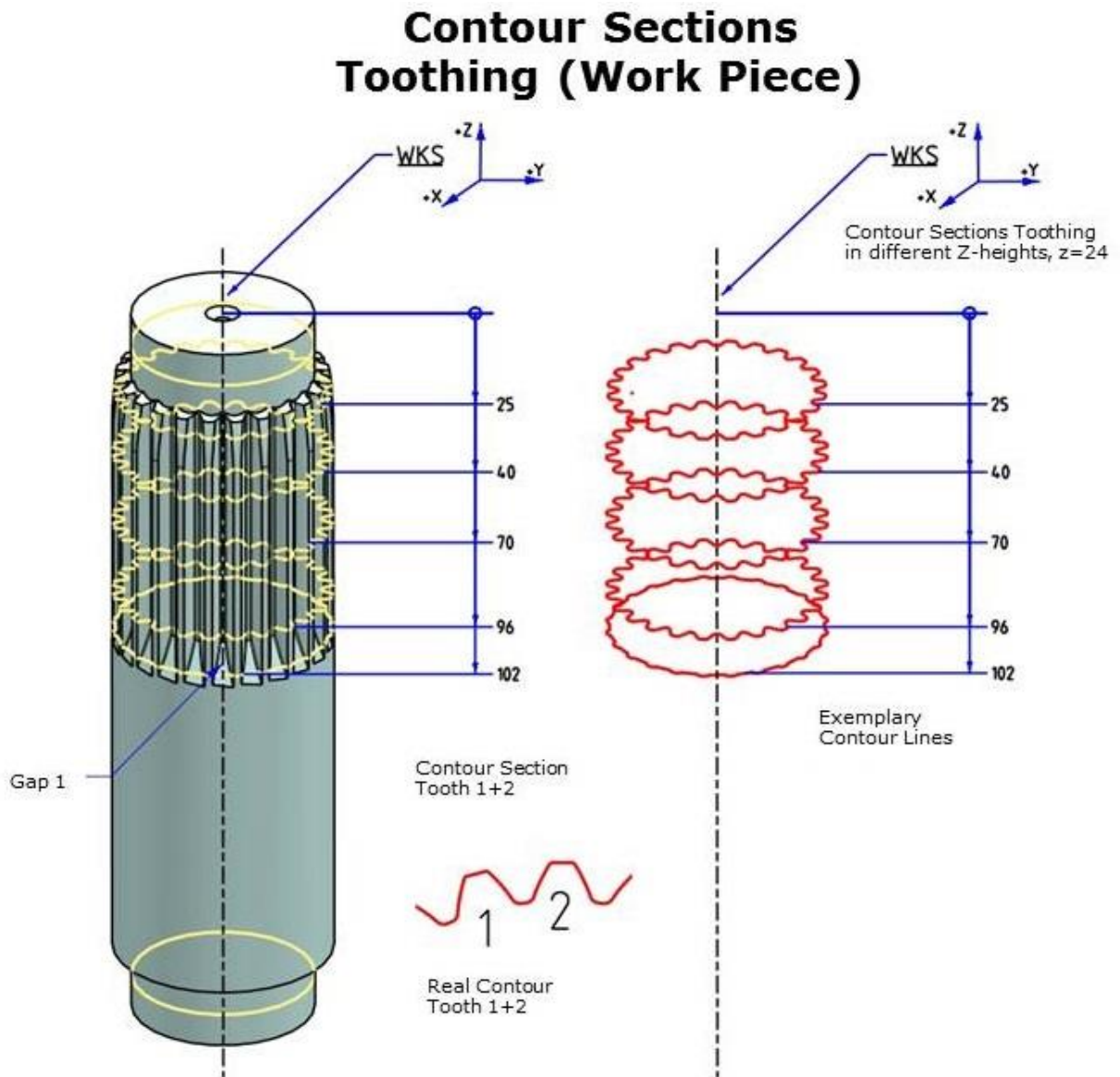


Figure 81 Contour Sections Workpiece

The resultant individual scan lines were subsequently combined on the entire circumference in the evaluation of the 24 teeth. It was measured with a scanning speed of 0.3 mm / sec and a density of 25 or 50 dots per mm trav-

erse path. Preliminary tests for the selection of point density had revealed that with 50 points per mm traverse path, compared to 25 points, no significant improvement of the informational value of the measurements was achieved (Figure 81).

The scan lines of the individual teeth were measured with a dot density of 50 dots per millimeter traversing path. The related time involved was taken into account, as only these specific geometric problems could be analyzed. Appropriate preliminary experiments led to this discovery.

Thus generated contour cuts of the tothing in the XY plane of the workpiece coordinate system are shown in figure 81. In all representations of the work pieces can be seen visually that the geometry of the gear changes in the longitudinal direction (Z-direction). This is caused by the flow of material during the rolling of the teeth. This geometric feature is also dependent on the rolling parameters. To capture these specific metrological, various sections were scanned on the length of the teeth in different Z-heights.

The axial position of these sections was unevenly distributed over the entire length. Cuts were performed in the following Z-heights $Z = -20, -25, -30, -40, -50, -57, -70, -80, -85, -90, -92, -94, -96, -98, -100, -102$.

Thereby the contour of the teeth over the entire axial extent is detected. Especially in the axial zones in which geometric features can be recognized visually, contour cuts were laid. The axial position of the cuts starts at -20, because starting from the end face $Z = 0$ at the tothing -20 starts in accordance with the position of the workpiece coordinate system. In the initial region of the sample at the upper collar cuts were set closely spaced, since the tooth geometry is subject to changes over the length. Largest contour changes over a short length can be seen visually in the forming area at the lower end of the tothing.

In the middle part of the tooth length the tooth geometry is over a greater length approximately constant.

In figure 82 an example of the contour cutting of tooth 1 to 5 of a tooth from the middle region ($Z = -57$) is mapped to the corresponding explanations.

Further on individual teeth of the tothing longitudinal scan lines have been recorded on the tooth head (tip) in the Z-direction.

Thereby the change in the head heights of the teeth over the length of the tothing is graphically evident. This is one of the reasons for the sense of contour cuts. More on this topic will be explained in the discussion of results in Chapter 6.

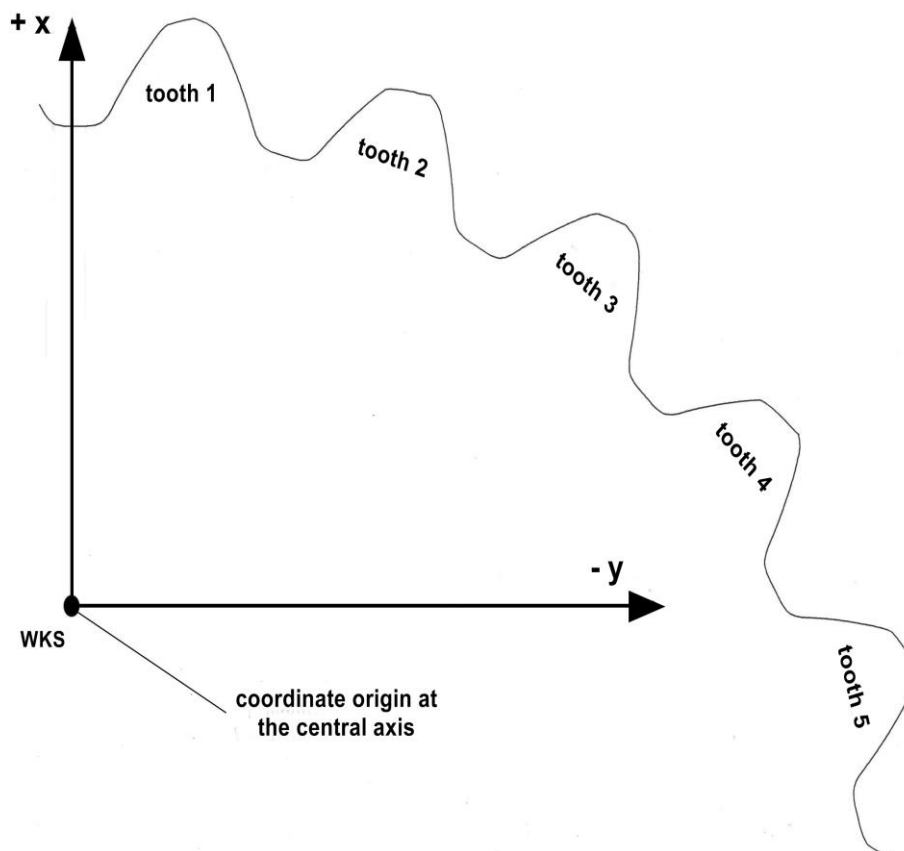


Figure 82 Contour Cut

5.6 Contour Measurements of Tools

Probe configuration and calibration For the acquisition of contour cuts to the rolling tools simply a vertical probe (sphere diameter $d = 2$ mm, length $l = 60$ mm) is required (see chapter 5.4.1).

Coordinate system rolling tool The clamping situation of the rolling tools on the table of the measuring machine is shown and explained in Chapter 5.4.2. For reasons of comparability, of course, the same coordinate system for the following contour measurements was used as for the gear measurement according to DIN. The description of the determination of the workpiece coordinate system is given in Chapter 5.4.2. The Z-axis is defined by the normal plane to the upper end face. The X-axis is determined by the center point of the outer cylinder and the point of symmetry of the right and left flank of the central gap. The zero points of the X and Y axes are located on the tool central axis, the zero point in the Z-direction lies on the upper end face.

Contour sections rolling tool To discuss the tooth geometry of the rolling samples, according to the contour workpiece measurement also contour cuts in various levels were recorded at the rolling tool. The procedure for the collection of these contours is explained graphically in figure 83, 84.

Measurement Strategy Rolling Tools WPM

(Contour Measurement XY-Plane, Cross Sections)

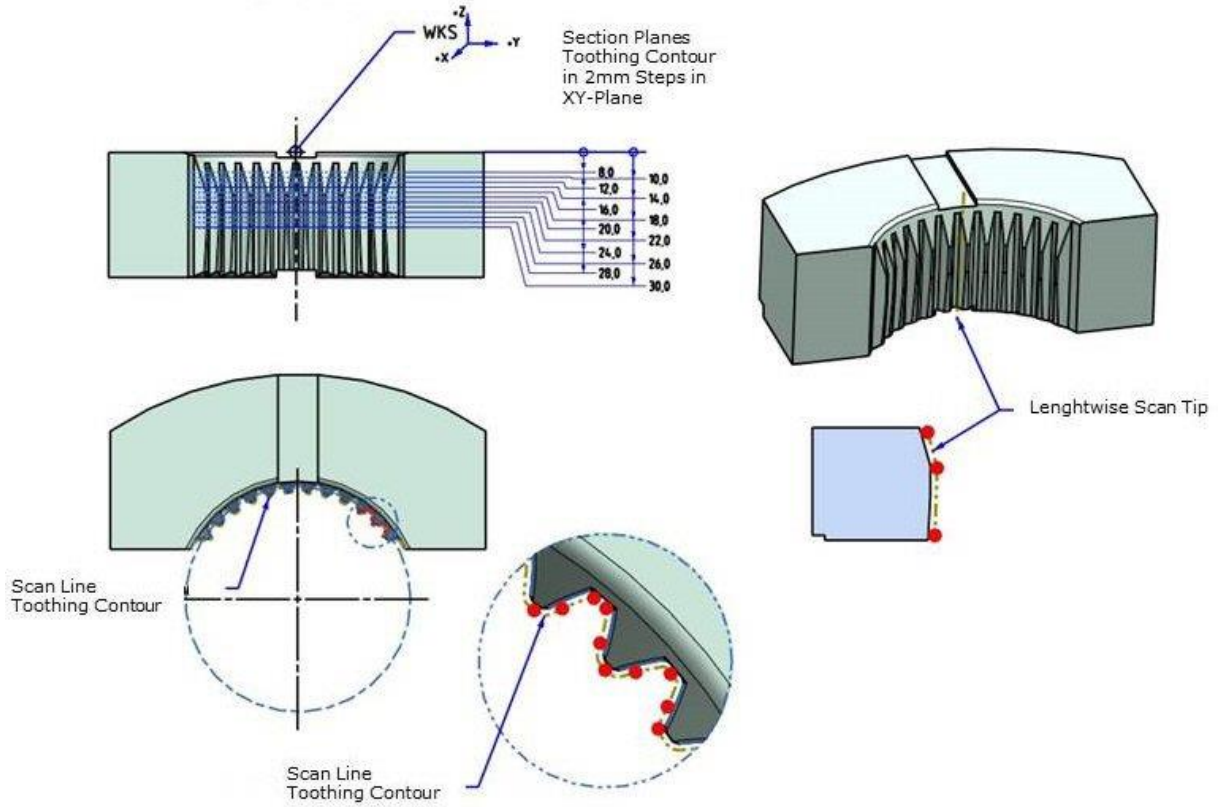


Figure 83 Contour Sections Tools

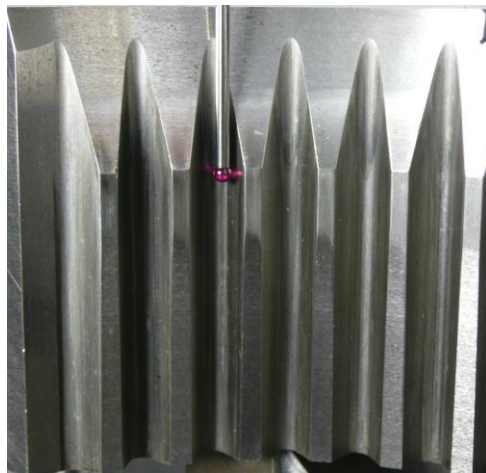


Figure 84 Situation in PMM

As with the toothed work pieces, contour cuts were measured on the tool on different Z-heights in the tooth area. This contour cuts show as axial snapshot the tooth geometry in a Z-height of the tools.

The scan lines have been measured with a dot density of 25 dots per millimeter traversing path in the XY plane of the coordinate system with a scanning speed of 0.3 mm / sec with a probe ball diameter $d = 2$ mm (Figure 84). The conical inlet zone can be seen in the upper tool section.

On the tooth head of some tool teeth longitudinal sections were scanned in the Z-X-plane. Point density and scan speed are the aforementioned scanning parameters. Figure 85 shows the different parts of the teeth in the Z-direction of the coordinate system.

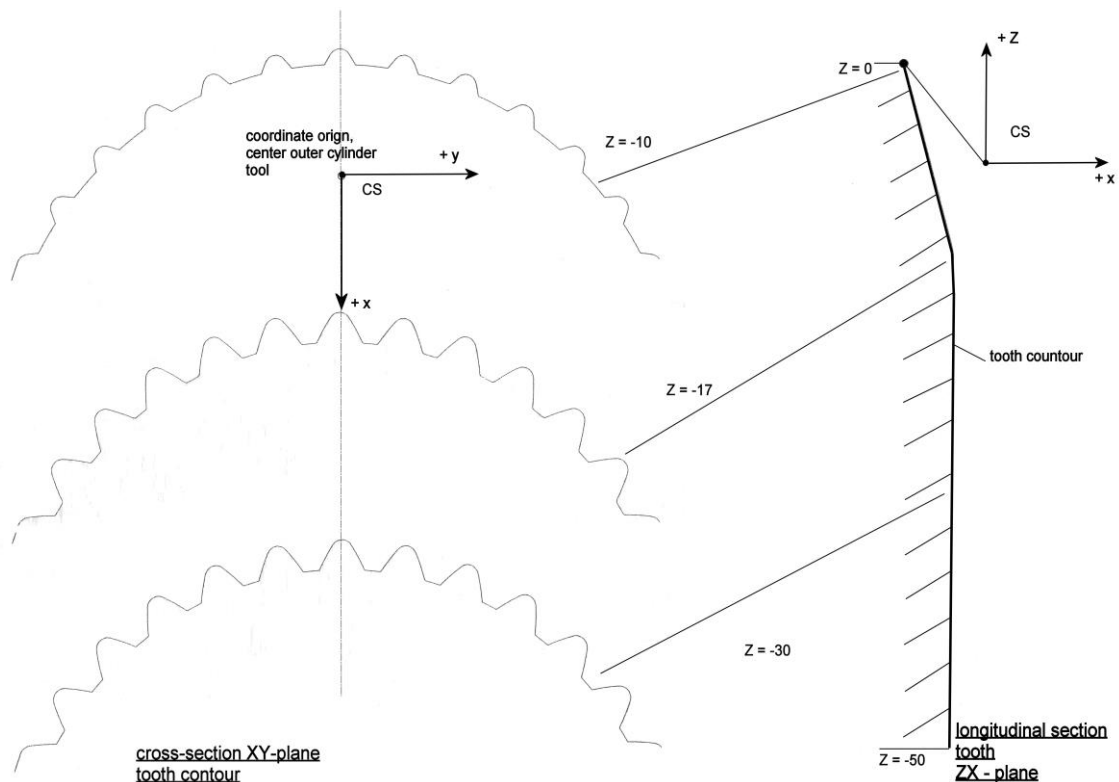


Figure 85 Contour Cuts

In figure 85 an example contour cut and a longitudinal cut are shown together to illustrate the progression of gear contour in space. Both in the contour-cuts of the XY plane and in the longitudinal contour of the tooth head, the ZX plane, the conical portions of the geometry of the tool teeth and the traces of which are visible. The tool geometry produces the particular shape of the resulting geometry of the rolled samples.

The following figure 86 shows this in a side view. It is shown the peculiarities of the axial gear progression.



Figure 86 Side View of a Sample

In figure 86 can be seen on the left (start of the metal forming) that the material flows axially. Therefore, result no properly shaped teeth at the beginning of the sample. In the central region, the teeth are formed completely. A head height falling results on the right side (the tools had contact with the material for the last time) again. Clearly is to recognize the footprints of the conical inlet zone of the tools in the material. For the course of the teeth of the rolled sample the timing of the forming and the axial shape of the tool teeth are responsible. Of particular importance is the conical entrance zone of the tools, the realized cone angle.

Summary of Results contour measurement

The previously repeatedly shown geometric characteristics in rolled sample geometry are the result after forming with the WPM method. These characteristics are not, or only partially be determined by the conventional tothing measurement according to DIN [ST 5]. For the evaluation of the process and the achievable geometric qualities contour measurements on the fabricated samples are necessary. The previously described contour measurements correspond and confirm overall the results of the measurements according to DIN [ST 6, ST 7, ST 8]. The following set of results cannot be ascertained with the traditional measurement methodology according to DIN. The entire tooth form is formed convex in the longitudinal Z-direction. Between the inlet at the beginning of the forming process, the central region and the end region of the metal forming results in considerable differences with respect to the height of head and the head-shape. It was found that between two low tooth tips is always a high tooth. The high gear is always fully formed than the two adjacent teeth of low head height. This statement corresponds to a further realization, which affects the respective tooth shape. The resulting tooth shapes are dependent on the tooth height, so that typical tooth shape characteristics can be noted. With regard to the statement regarding the significance of the feed rate on the resulting geometry results the contour measurement, confirm the results of the measurements according to DIN.

6. Evaluation / Discussion Geometry Results

All rolled samples were examined metrological. In terms of geometrical results all rolled samples show the same tendencies. Due to the resulting large amount of data, only the results are exemplified and discussed which are particularly meaningful. All measurement results are listed in appendix 1 - 4. The analysis and discussion of the results of the workpiece geometry measurements in detail is divided into two parts.

- A)** Evaluation / discussion of the measurements according DIN (standard)
- B)** Evaluation / discussion of the contour measurements (non-standard)

6.1 Evaluation / Discussion of Measurement DIN

A) The results of the tooth geometry according to DIN were separately statistically evaluated after the individual criteria of a tothing geometry and namely for the gearing qualities, which are defined in the DIN 3960 ff. [ST 5]. The quality of the gear geometry is divided into 12 classes (1 to 12) wherein these classes represent areas of permissible variations [95]. Quality 1 has the smallest range of permissible variations from the desired geometry while in grade 12 the maximum variations are permitted. These areas again are dependent on the relative size and dimensions of the considered tothing. So a tothing module $m = 3$ with the same quality class may have greater variability than a tothing module $m = 1$. This size-dependence of the permissible variations per quality-class course applies also for the diameter of the tothing as well as their axial extent. Diagrams, in which the percentage of the work pieces or rather the tooth flanks relative to the total number applied to the gearing quality, result from the statistical analysis. This analysis is performed separately for left and right sides for all major stated in the standard single geometry criteria.

The individual geometric criteria that describe the geometry of a tooth are shown in the sequence. The various sub-criteria of the tooth geometry are

explained in the following. The order of discussion of the results is done as follows:

- Pitch
- Concentricity
- Flank profile
- Tooth trace
- Root- / tip circle diameter

All graphs of statistical analysis can be found in Appendix 4, separated by geometric criteria and feed rates.

Pitch The pitch, as a single deviation criterion, the pitch error F_p and individual pitch deviation f_p separately for right and left edges are evaluated statistically. The pitch deviations are each represented by only one result value = maximum deviation of the workpiece, so that the percentage of work pieces is evaluated based on the total number of workpiece combinations of these parameters. Furthermore, the diagrams shown for the three different feed rates are applied separately. Each chart is shown in each case with eccentricity (F_p, f_p) and without eccentricity (F_{p-e}, f_{p-e}). This has to be understood as follows. At the pitch deviation in the measurement, the eccentricity of the tothing to the workpiece center axis of the workpiece coordinate system is calculated from the measured data. This eccentricity is found in the diagrams without eccentricity mathematically eliminated from the pitch deviations. This procedure is useful for splines according to DIN 5480. These splined shafts are centered in the internal tothing of the hollow counterparts [ST 10]. The diagrams of the total pitch deviation with and without eccentricity for the 3 feed rates are illustrated in Appendix 4.1. to 4.12. The diagrams of the individual pitch deviation can be found in Appendix 4.13 to 4.24. The study of these diagrams shows no significant effects of variable parameters on the resulting quality classes. This fact is not surprising, since this was already found in previous investigations. The magnitude

of the pitch deviations is dominated by the location of the workpiece in the rolling machine, the kinematics tool / workpiece and the blank geometry. This state of affairs will change nothing when using selected blanks with minimal geometric deviations. The investigation of other pitch criteria, such as pitch error f_u and pitch fluctuation showed a similar picture. Their detailed presentation has been omitted. Neither the variations in feed rate, nor the blank-material showed a significant effect on the resultant distribution of the determined pitch deviations.

Concentricity The concentricity deviations are defined as the maximum radius variation of the circumference of a tothing. The graphs of the percentage distribution of the concentricity deviations are shown in the graphs 4.25 to 4.30 Appendix 4. As with the pitch deviations, according to the standard only one value is evaluated for the entire tothing without flank distinction. Clearly the difference in the concentricity with and without eccentricity is evident. This is logical, since the observed eccentricity represents geometrically a part of the concentricity next to the circular deviation. This is the reason that the concentricity error without eccentricity results always significantly less than the concentricity error with eccentricity. A dependence of the observed eccentricities of the feed rate and the blank material is not visible. The reasons are already the same as those related to the pitch deviations mentioned above.

Profile deviations The profile variations of the tooth flanks (involute profile), the total deviation profile FA, the profile angle deviation FHA and the profile form deviation ffA were evaluated and documented graphically. The graphs of the percentage distribution of the flanks of these geometry criteria are separately presented for the right and left side in diagrams 4.31 to 4.48, Appendix 4.

Depending on the feed rate significant shifts to poorer qualities at the total profile deviation and the profile angle deviations, can be seen. The focus of the Gaussian distribution of the plots varies significantly towards poorer qualities. In the angular deviations, the entire curve deteriorates to a quality

class with the highest feed rate. The profile form deviations are not affected from this trend. Further the height of the profile is affected by the feed rate, which can be seen from the values of the measured heights of the tip (Figure 87, 88). That situation will be discussed in detail in the next chapter tip and root diameter. In figures 87, 88, the profile deviations of 4 teeth, depending on the feed rate can be seen.

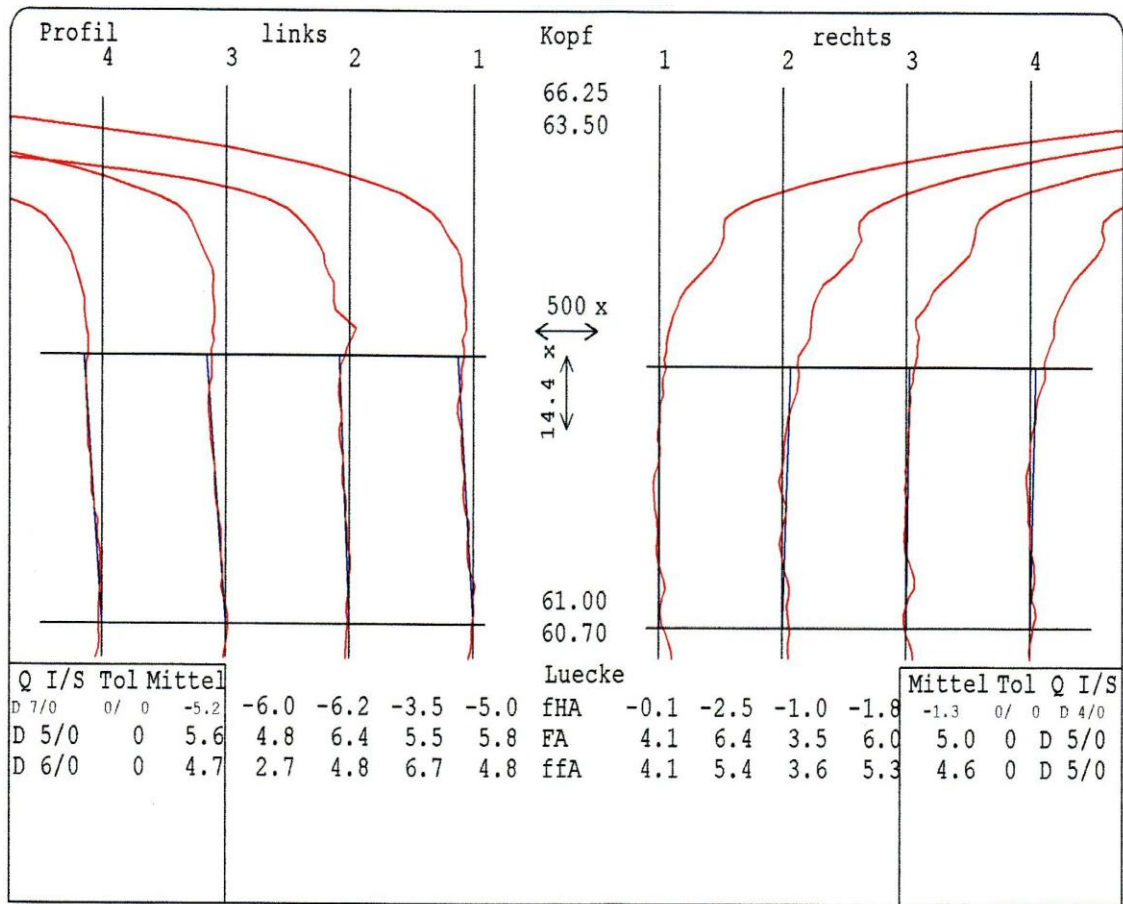


Figure 87 Profile Deviation - Gap 1 - 4 v = 100 mm / min

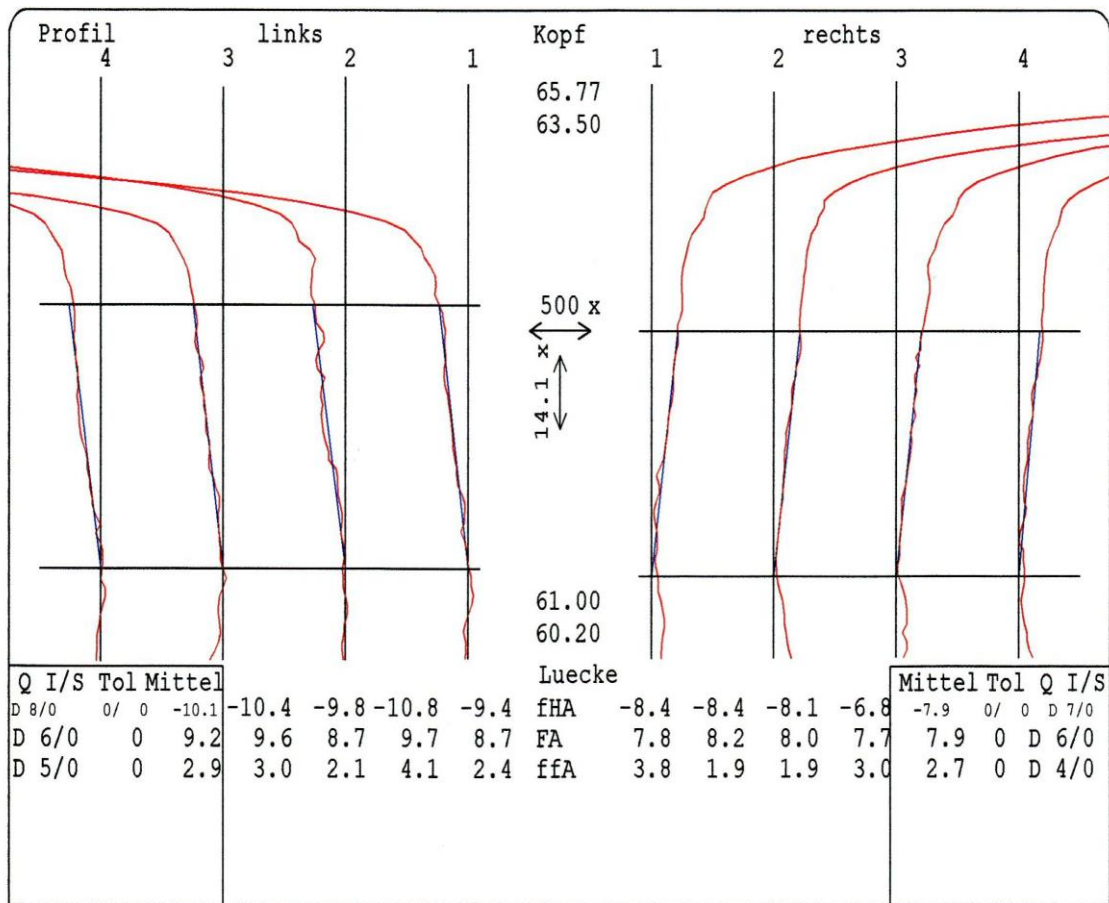


Figure 88 Profile Deviation - Gap 1 - 4 $v = 300 \text{ mm / min}$

Tooth trace deviations Regarding the tooth trace, 3 single criteria (total tooth trace deviation FB, the tooth trace angle deviation fHB and the tooth trace form deviation ffB) are described. Each case is evaluated and documented separately for the right and left flanks (Appendix 4, diagrams 4.49 to 4.66). A clearly dependence of the tooth trace deviations regarding the rolling parameters and workpiece material in any of the three individual criteria is not detectable. This is well founded by the fact that the variance of the deviations in the course of the circumference of a tothing varies greatly. This relationship has been found in the Appendix 2, where the deviations of a complete tothing are shown. Particularly striking are the variations around the circumference at the flank lines. These variations are so great that any other influence is dominated. The total tooth trace deviations are dominated in almost all teeth by tooth trace deviations, as figures 89, 90 show exemplary.

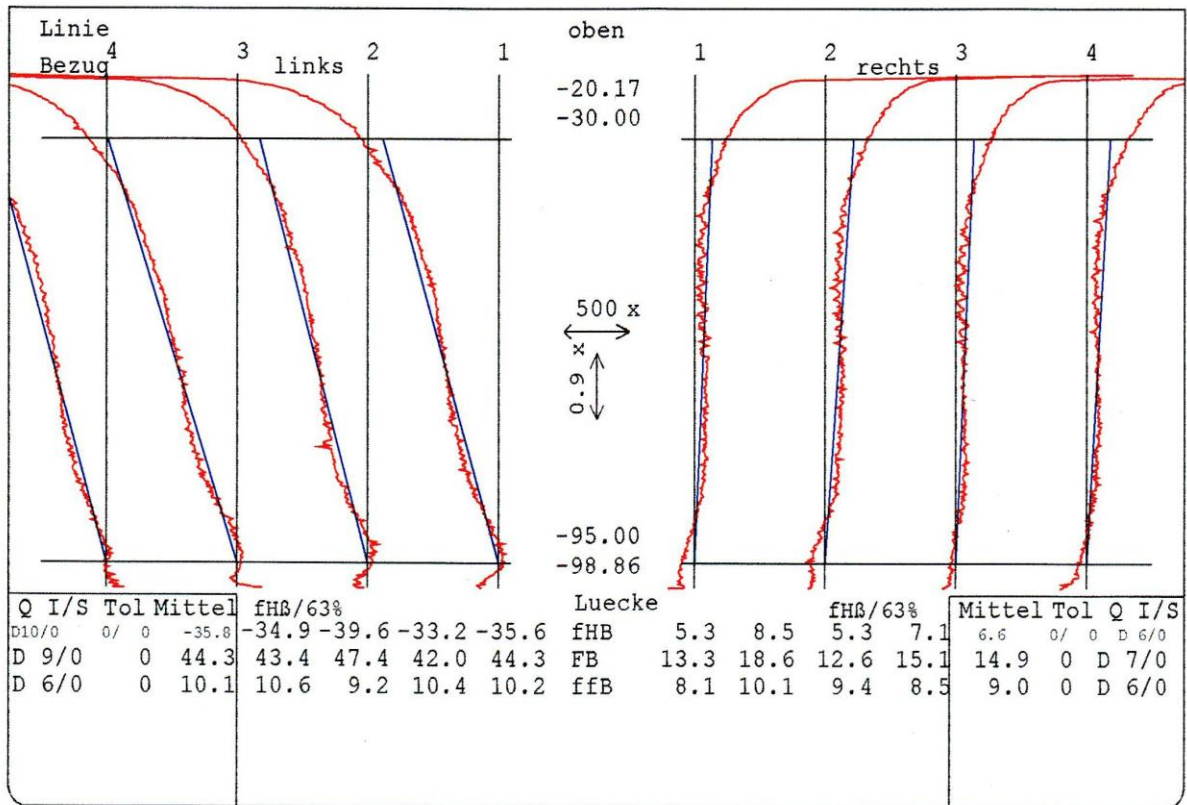


Figure 89 Tooth Trace Deviations

v = 100 mm / min

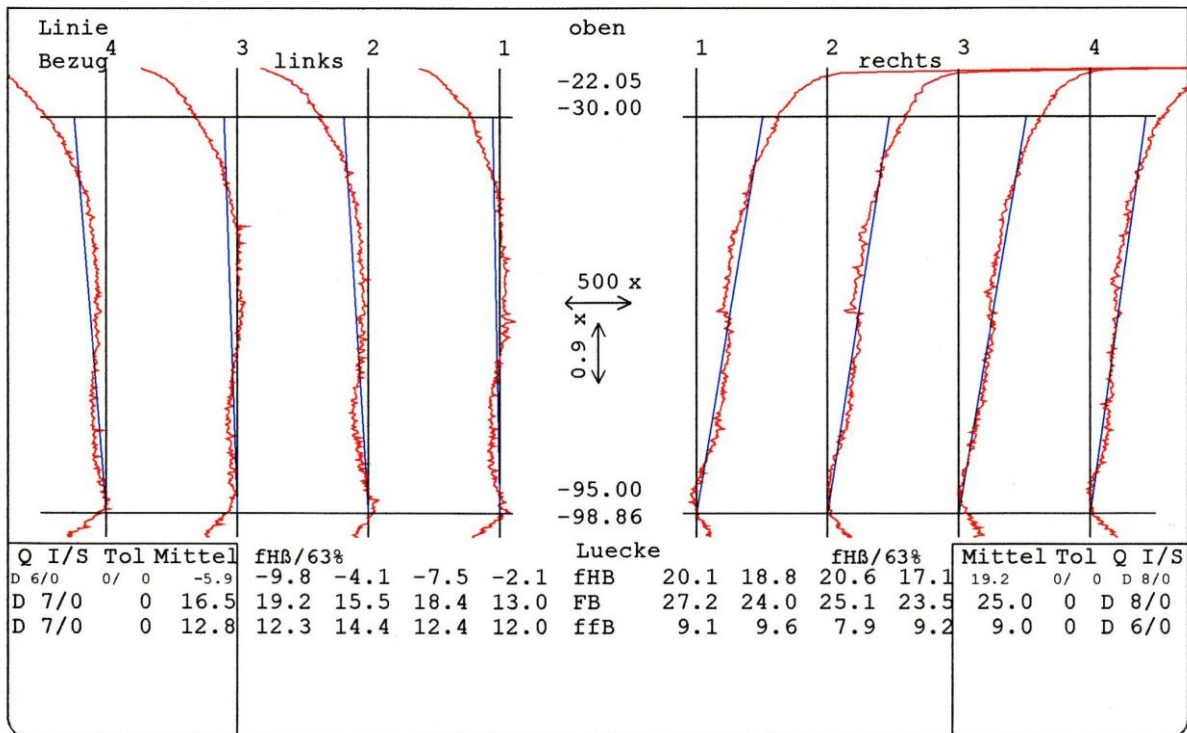


Figure 90 Tooth Trace Deviations

v = 300 mm / min

Root circle diameter The root diameter of all samples, detected in each of 24 teeth gaps, shows very low roundness deviations in the order of less than 0.01 mm. This statement applies to all combinations of parameters of feed rate and blank material. The figure 91 is an example of results of two resultant root circle diameter at different feed rates.

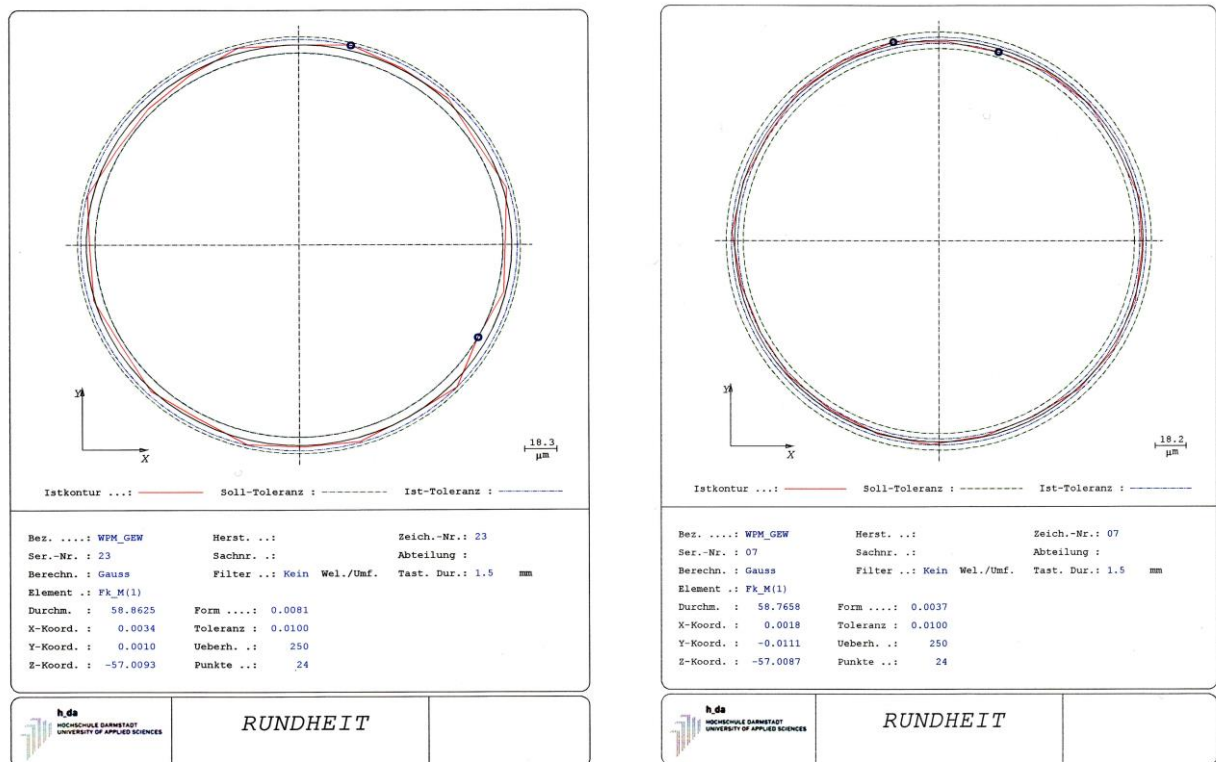


Figure 91 Root Circle Diameter
v = 100 mm / min

v = 300 mm / min

The absolute diameter of the root circle (calculation method according to Gauss) falls only slightly with increasing feed rate on average in the order of about 0.1 mm (Figure 91). The very good quality result of the root circle diameter shows that based on the existing tools an approximately correct combination of the tools set eccentricity and compatible blank diameter in the present experiments was rolled.

Tip Circle Diameter A very different result shows the tip circle diameter of all samples tested. The figure 92 shows two diagrams of the roundness of a tip circle according to feed speeds of $v = 100 \text{ mm / min}$, and $v = 300 \text{ mm / min}$. Significantly in comparison to the root circle, extreme roundness deviation of up to 0.25 mm can be seen. Furthermore noticeable is that each high tooth on the circumference on both sides is surrounded by a lower tooth. Each high tooth is surrounded by less high teeth. Obviously, there are asymmetries in the distribution of material on the circumference of the rolling samples. The feed rate defines the deformed volume of the material per tool-stroke. An asymmetry is created in the distribution of material on the circumference, since the movement of the tools from one stroke to the next stroke is identical and always in the same circumferential direction.

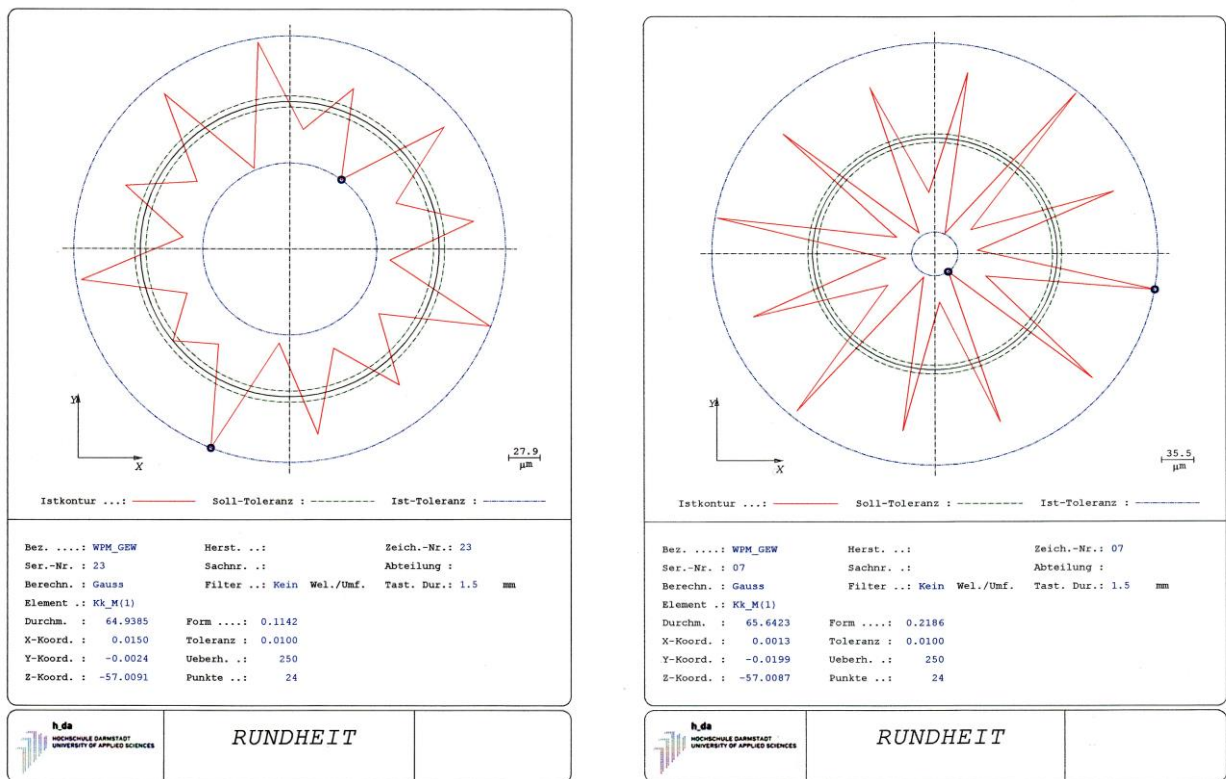


Figure 92 Tip Circle Diameter
 $v = 300 \text{ mm / min}$

$v = 100 \text{ mm / min}$

The roundness of the tip circle is defined as the average deviation between the largest and smallest radius distance of the tips with respect to the center. Consequently, the roundness of the tothing affects the asymmetry of the material distribution.

Figure 93 shows the effect of feed rate on the tip circle diameter. With increasing feed rate smaller tip diameters of up to 0.7 (!) mm result. One reason for these facts is the different flow behavior of the workpiece material at varying material volume per feed step. Different feed rates realize different volumes per step. The smaller the single steps of advance, the more often comparable volume sections are radially loaded. The material movement happens mainly radially, but also in the axial direction.

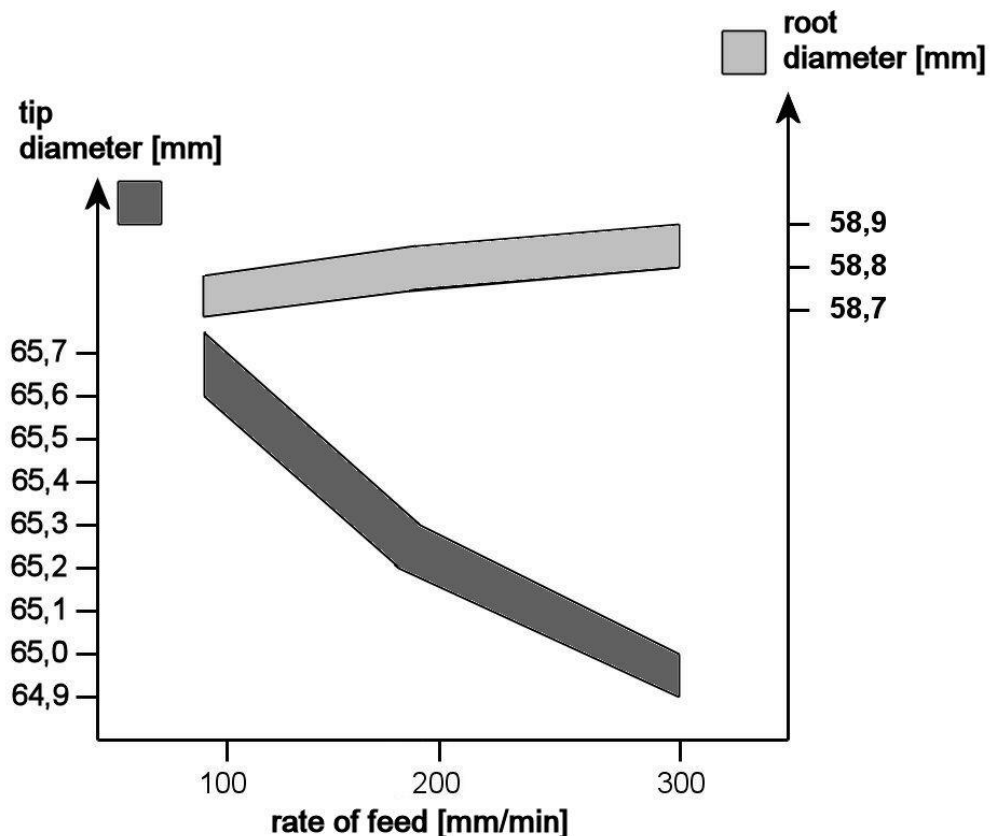


Figure 93 Development of tip- / root diameter dependence feed rate

The axial proportion of material movement is very small compared to the radial component. Whereby, the radial part of the material movement of equal volumes is often repeated and amplified. In this sense, the above-mentioned results of the profile deviations depending on the feed rates can be seen. The material flows less high into the tooth gaps of the tools with increasing feed rate. The differences between the tooth height and the toothing variations over the axial length of the teeth, depending on the feed rate, will be discussed in the chapter "contour measurements" in detail.

Tooth geometry according to DIN in different axial heights

As stated previously, different tooth geometries result in the axial direction of the rolled parts. It is expected that these change in tip diameter also affects other changes in the toothing geometry. To investigate this issue, the toothed geometry was measured at different levels of its axial extension to DIN. (Chapter 5.3.3). The results of the determination of the deviations of the flank profile, the pitch and the concentricity are evaluated in different Z-heights of the teeth and documented. To recap, the Z-axis of the workpiece coordinate system is the central axis of the workpiece, the zero point in the Z-direction lies on the upper end face of the sample.

Tip circle diameter In figure 94 the different Z-heights of the profile measurements are shown. The comparison of the numerical values of the tip circle diameter shows the significant differences. The resulting axial course of the tip diameter of the toothing can be seen from the data.

For the two feed rates, $v = 100 \text{ mm / min}$ and 300 mm / min clear differences between the tip circle diameters result.

The graphs in figure 95 show profile lines measured in different Z-heights.

$Z = -25 \text{ mm}$ at the upper end of the toothing (tool inlet) which is characterized by axially strongly flowing material. In consequence result not well-formed teeth. $Z = -50 \text{ mm}$, approximately in the middle of the toothing area shows almost completely shaped teeth. $Z = -95 \text{ mm}$ at the lower end of the toothing is the area where the last tool contacts have taken place.

There, the toothing is not yet fully developed.

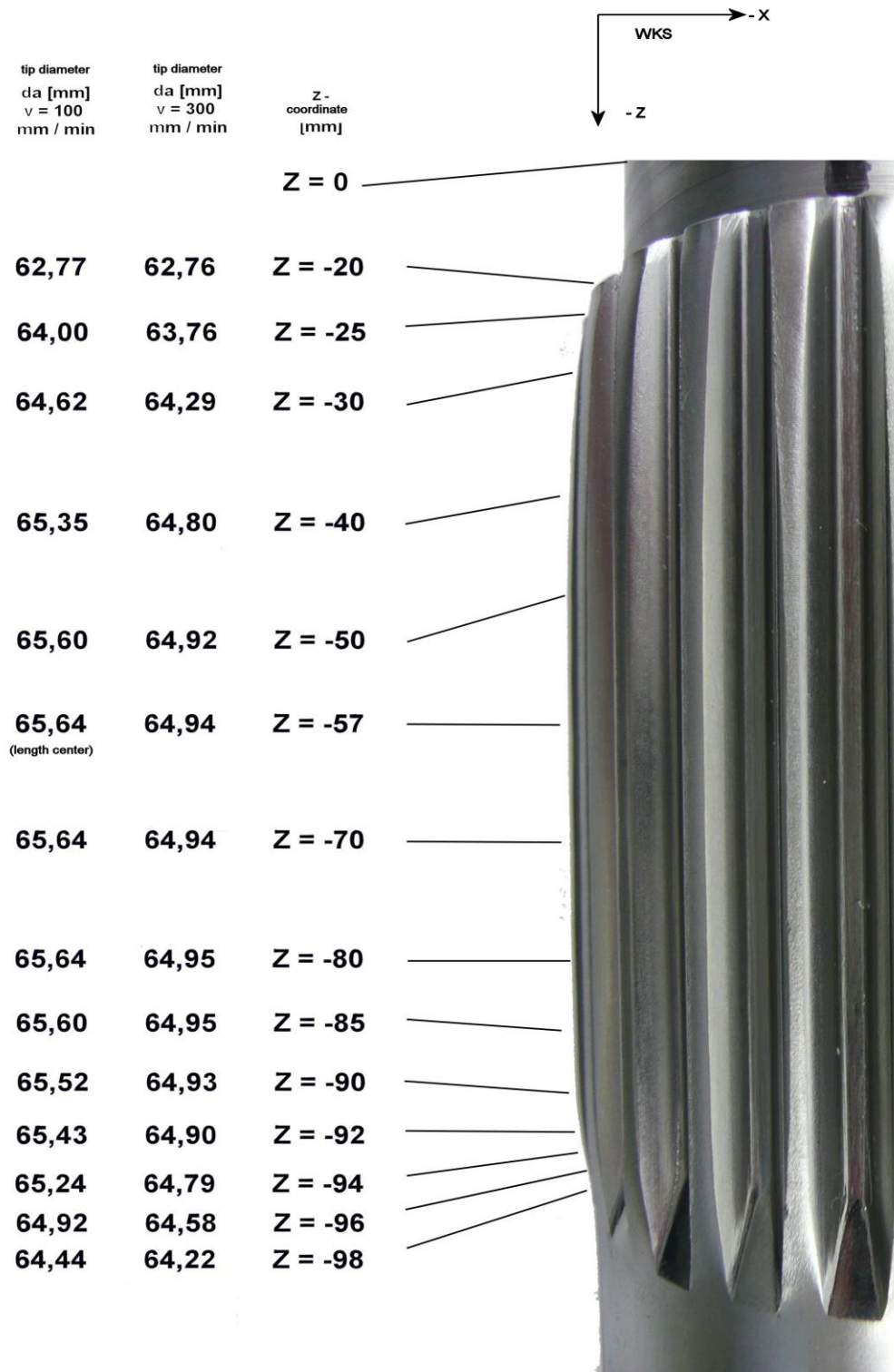


Figure 94 Axial Course of Tip Circle Diameter

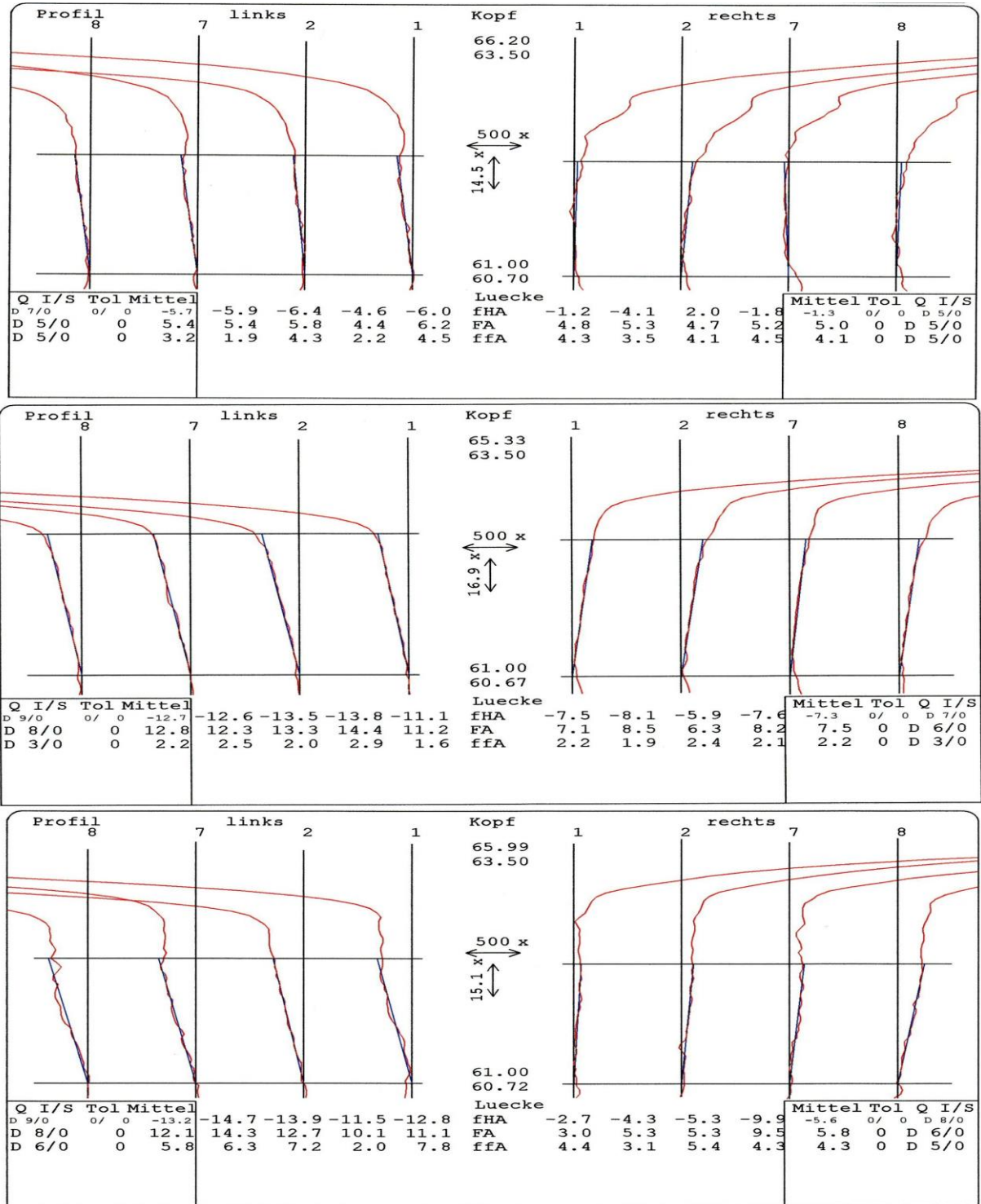


Figure 95 Profile Lines in different axial Heights

Profile In figure 95 above, the different configurations of profile of the teeth in the axial direction can be seen clearly. At $Z = - 25$ mm, the profile is not correctly shaped by the axially flowing material and the resulting material deficit. There, the material can flow axially into the free spaces of the tool geometry. In the central region the profile quality remains constant from about $Z = - 35$ mm up to $Z = - 90$ mm. In the area of the last tool engagement at about $Z = - 92$ mm, larger deviations result again, because the teeth are not yet fully formed. This is due to the conical inlet zone of the rolling tools. As figure 96 shows, applies this course of the deviation over the Z-height of the toothing for pitch and runout as well. The measurements and analyzes of the flank line in different diameters heights on the tooth flanks ($d = 61.3$ mm, $d = 62.3$ mm (middle profile), $d = 63.3$ mm) did not lead to meaningful results or recognizable trends.

Pitch / concentricity Figure 96 shows that, between the initial and end zone of the toothing results substantial differences. In this area, as noted above, the teeth are not fully formed. In the later shown countour sections, it is visible that the shapes of the teeth head are asymmetrical formed. Whereby, the major errors in pitch and concentricity can be explained.

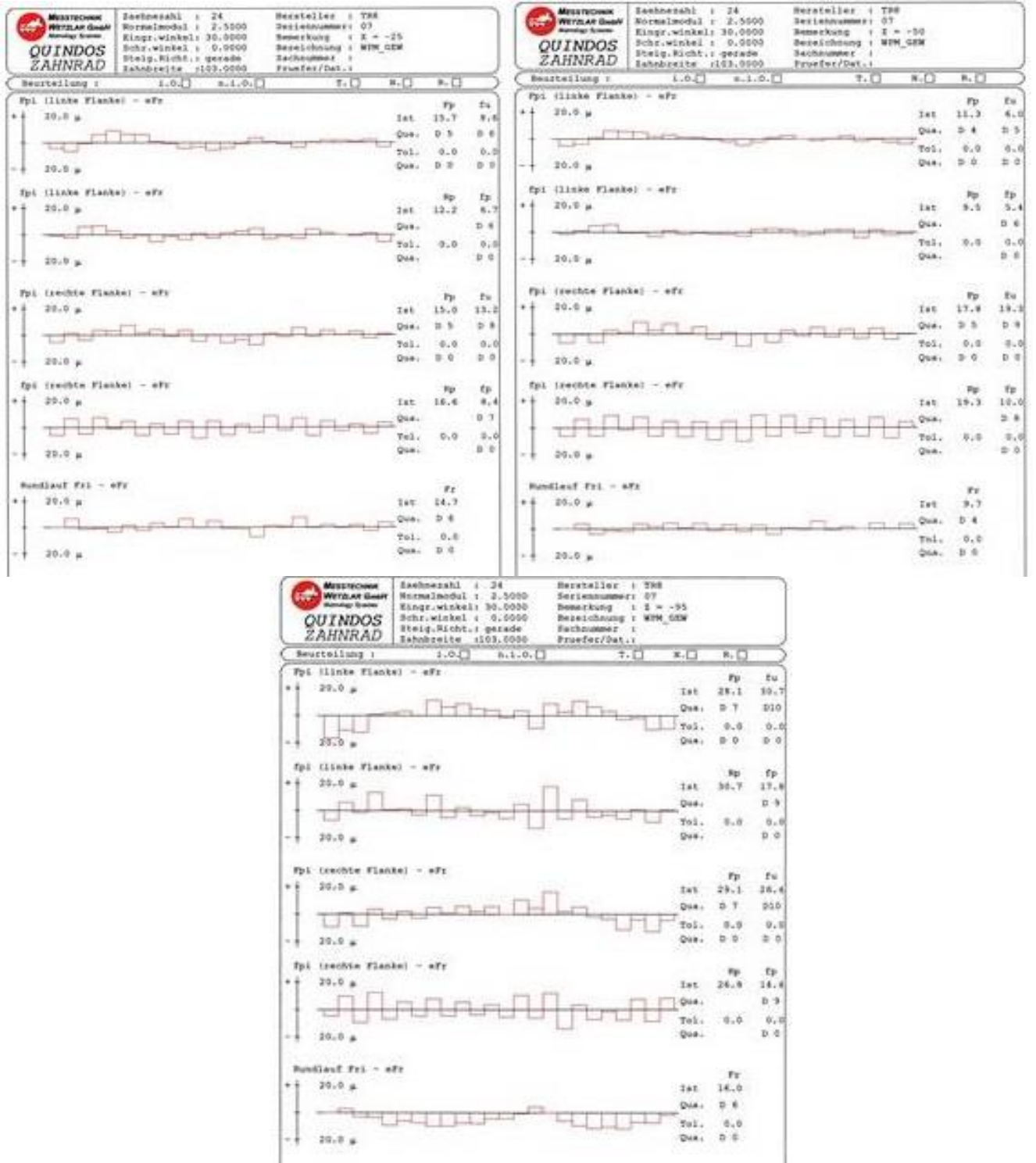


Figure 96 Pitch / Concentricity different Heights (Z=-25, -50.-95)

6.2 Evaluation / Discussion of Contour Measurements

In order to illustrate, the results of the contour measurements are exemplified by two test samples (07, 23), since in these two samples the explanatory facts are particularly pronounced.

Longitudinal sections The measurement and probing strategy, when capturing the longitudinal and cross-sections, has been explained in detail in section 5.5.1. Figure 97 shows a scanned longitudinal section (course of the tooth tip height) over the axial length of the rolled tothing. This course can be found - listed numerically - as the diameter of the tip circle in figure 94.

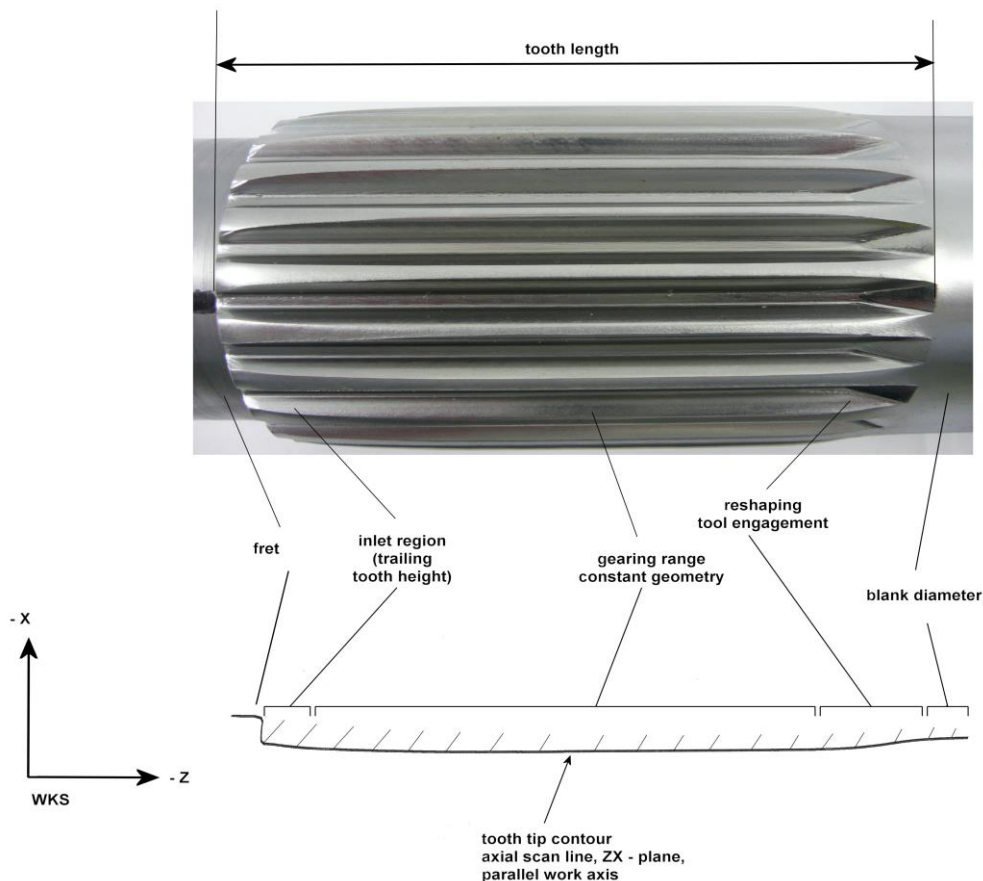


Figure 97 Axial Tooth Tip contour, Axial Scan Line in the ZX-Plane

Clearly the change of the head height contour is visible as a result of plastic flow of the workpiece material. The profile is essentially described geometrically by three zones. The towards the face side falling inlet zone at the roll

sample (left) is characterized by axially flowing material. The middle zone is nearly cylindrical, with slight variations. There, the teeth are fully formed. In the lower deformation zone (right), where the last tool contact has taken place, the head height decreases again because the teeth are not fully developed. This deformation area is impressively documented by the counterpart of the conical deformation zone of the rolling tools in the workpiece. A discussion about the changes in root diameter does not make sense, because a small change in the range of 1/10 mm is detectable only in the inlet area. The cause is probably axially flowing material as well. Except in the inlet region of the roll sample the root diameter remains constant within narrow limits.

Sections In figure 98, the tooth contours of the tooth 1 and 2 over the axial length of the teeth are shown. This tooth contours result from the scan lines of the cross sections in the XY plane. The measurement strategy has been described in Section 5.5.1. In figure 98 the tooth contours are shown for a feed rate $v = 100 \text{ mm / min}$ and $v = 300 \text{ mm / min}$.

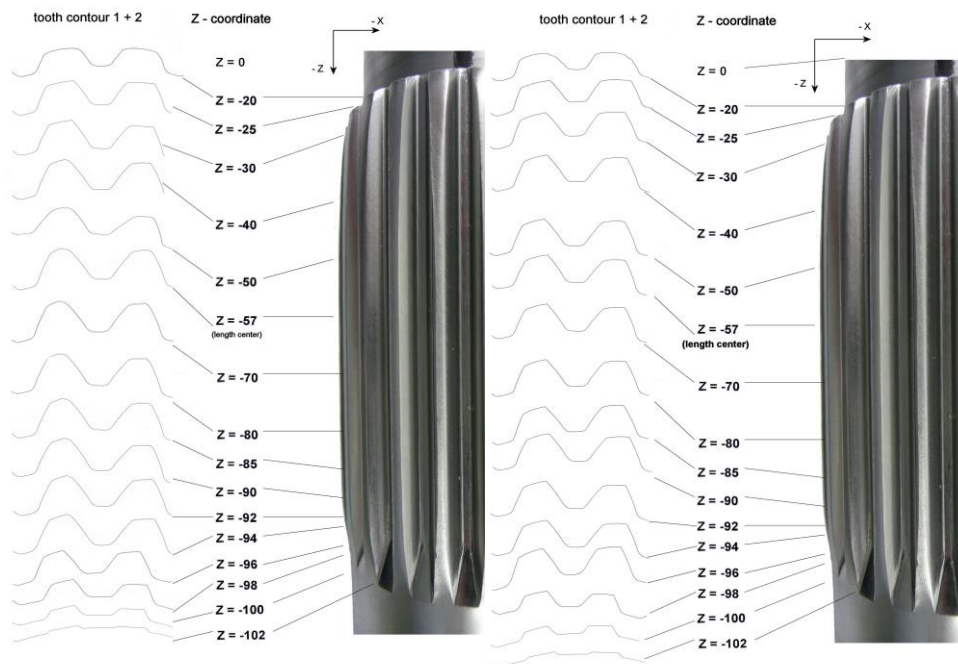


Figure 98 Cross-Sectional Contour of the Tooth

$v = 100 \text{ mm / min}$

$v = 300 \text{ mm / min}$

The analysis shows the following fact, which was also observed when looking at the tip-diameter circle on the axial length in the previous chapter.

In the upper part of the tothing results a non-fully-formed tooth contour caused by the material deficit by axially evasive material ($Z = -20$ to -40).

In the middle part the tothing is fully formed and almost cylindrical ($Z = -50$ to -90). In the lower part, the head height of the tothing falls again, because the forming zone starts (conical entrance zone of the tools), marked by the recent contacts of the rolling tools ($Z = -92$ to -102). In the region of the conical forming zone of the tools small volumes are to be displaced, thereby result less teeth head heights. The influence of the feed rate on the shape of the tooth contours is substantial. Upon closer examination of figure 99 can be seen that, when the feed rate of 100 mm / min significantly higher tooth heads result than when $v = 300 \text{ mm / min}$.

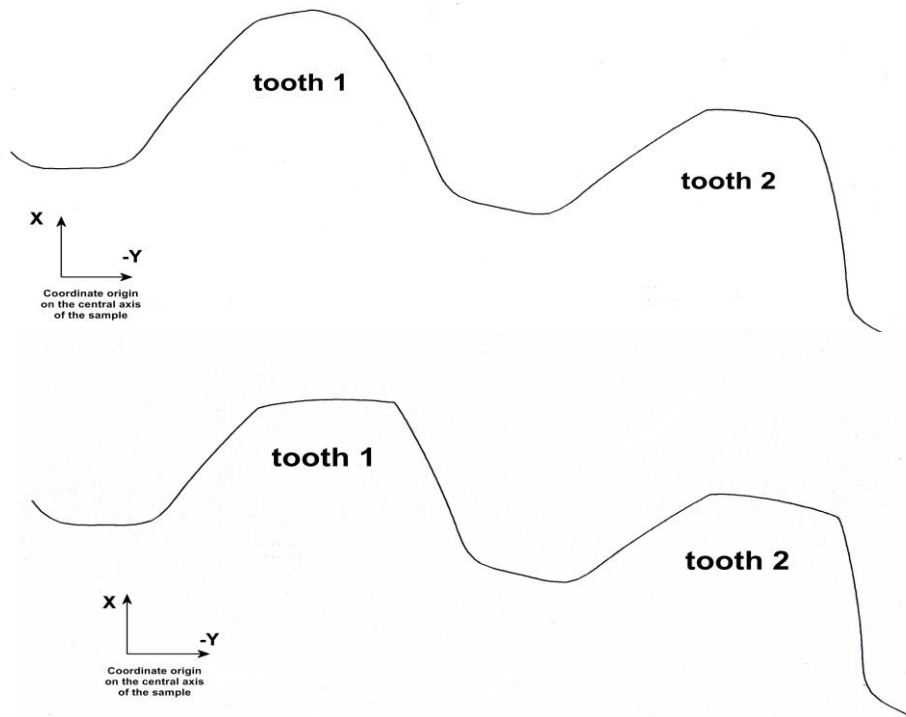


Figure 99 Forms of Teeth / Different Feed Rates
 $v=100 / 300 \text{ mm / min}$

This was already observed in the analysis of the tothing geometry according to DIN, mainly in profile and tip circle-diameter. When considering the shape of the head of the tooth contours the differences in the tooth heads are even more pronounced. Figure 99 shows the tooth contour of the tooth 1 + 2 at the middle of the tothing ($Z = - 50$) at the lowest and the highest feed rate ($v = 100$ and 300 mm / min). There, the difference in head shape is remarkably clearly visible. At the sample 07, ($v = 100$ mm / min), the tooth is higher, which means that the material flowed higher than in the sample 23, ($v = 300$ mm / min). Furthermore, a difference of the head shape can be observed at the tip circle. At the rolling sample 07 ($v = 100$ mm / min) the shape of every second tooth head is different and the tip circle is differently high. Tooth 1 shows at the tip a radius form, which suggests that the deformed material abuts the root-radius of the tool. The material at tooth 2 flows less high, but it forms an asymmetric flank height of the right and left flank. In figure 99, sample 23 ($v = 300$ mm / min), the differences in head shape in this distinct expression cannot be ascertained. But also, the asymmetry of the left and right flank can be recognized. The tooth heights (tip diameter) are different, the magnitude of these differences, however, is much smaller than at the lower feed rate. The differences between the contours of the head tooth 1 / tooth 2 were already detected in the analysis of the tip diameter in the preceding chapter, and explained in detail.

The above figures show in examples the results of the resulting contour measurements on the selected samples. It is noteworthy that these results are for all other rolling samples of all test series basically the same. The really important experimental parameter with clearly demonstrable influence on the resulting tothing geometry is the feed rate. This was detected reliably by the analysis of the measurement results according to DIN and is confirmed by the results of the contour measurements. The contour measurements illustrate these relationships in the sense that a detailed examination of the tooth forms in different tothing areas is possible now.

The determination of the geometric qualities of a tothing according to DIN allows a qualitative classification of the outputs.

For work pieces produced by metal forming, geometric characteristics occur that make an additional contour measurement necessary. This is significant, for example, for future developments of the tool geometry and for reviewing the technical functionality of the produced machine elements by metal forming.

Statistical Analysis In appendix 4 all results of the measured tothing qualities are shown. Basis for the statistical analysis are a batch of 10 samples per feed rate. At three speed rates, 30 samples were statistical analyzed and deviations were evaluated. The samples for the detailed analysis got selected randomly, even though all rolled samples have been measured completely (that means all teeth and flanks of the rolled samples have been measured). A separated analysis in evaluation is made in left and right flanks.

Statistical analysis of gear tooth quality of samples and flanks:

Total pitch deviation	FP	4.1 – 4.12
Individual pitch deviation	fp	4.13 – 4.24
Concentricity deviation	Fr	4.25 – 4.30
Total profile deviation	FA	4.31 – 4.36
Profile angle deviation	fHa	4.37 – 4.42
Profile form deviation	ffA	4.43 – 4.48
Tooth trace total deviation	FB	4.49 – 4.54
Tooth trace angle deviation	fHB	4.55 – 4.60
Tooth trace form deviation	ffB	4.61 – 4.66

7. In-Process Acquisition of the Geometrical Peculiarities

In the previous chapters 5 and 6, post-process geometry acquisition and valuation according DIN 3961 have been described. Hence, a validation of the formed work pieces from a quality point of view is possible. The profile measurements carried out, show the specific geometrical peculiarities which result from the forming process. These are not covered by the form deviations according to DIN 3961-3962 [ST 6, ST 7].

These geometrical peculiarities are of importance for the final technical functionality of the toothed components formed by the WPM process. Their change in dependence of feed velocity, for example, can be used to describe the forming process. Insofar the acquisition of the geometrical peculiarities in the machine could lead to early insights.

The advantage of such an action would enable an early assessment of manufacturing process. A subsequent just-in-time reaction would allow for cost reductions. On the base of the geometrical peculiarities detected by face profile measurement described above, it will be considered in the following part, which technical requirements have to be imposed on instrumentation and sensors in order to allow for future in-process monitoring of the WPM metal forming process [49, 50, 97, 98, 99].

Certain typical deviations of shape, position and orientation could detected in-process online and possibly even corrected in real-time by application of appropriate sensors / instrumentation devices. In the following, the geometrical peculiarities described in chapter 5 and 6, together with the resulting shape and orientation properties of the workpiece will be analysed and discussed regarding possible variables to be measured and significant process quantities which can be calculated thereof. From the results of this analysis, the requirements on the sensors, their range, accuracy and resolution will be derived [51, 52, 53, 56, 85, 86, 87, 90, 125, 127].

7.1 Acquisition of Geometrical Deviations

As mentioned, the geometrical peculiarities of the WPM process and the results of the tactile measurement of "Form, orientation, location and run-out" and the "Tolerances for Cylindrical Gear Teeth – Bases" will lead to the geometrical elements which shall be measured, calculated and monitored [ST 6, ST 16].

Among the geometrical deviations which influence the result of the WPM forming process mainly, the pre-dominant parameters are:

- Eccentricity
- Pitch
- Tooth trace
- Tooth Depth, Profile Form and Tip Form

The possibilities to acquire appropriate measuring quantities, which are able to describe these geometrical deviations and which will allow to perform real-time calculations of process quantities and are finally able to predict the further process. The properties of the WPM forming process prohibit the employment of tactile sensors, as the forming process is discontinuous, but yet the workpiece is subject to a continuously rotation. In principle, the use of tactile sensors coupled by means of friction could possibly be considered, but usually these devices feature higher measuring inaccuracy. Only for the purpose of additional tests before or after the process, a tactile sensor could brought in contact with the workpiece in a fixed measuring position; yet this would have the disadvantage of a complete change of the process and the a redesign of the power train and the feed drive train, in addition to an expansion and redesign of the axis control. Obviously, the recommended means for continuous acquisition of the surface geometry are non-tactile, non-contact distance sensors, which are able to capture the radial distance between their mounting position and the surface of the workpiece, as the primary measuring quantity [8, 83, 86, 100, 130, 131, 134]. From this distance quantity, the main quantities of the tooth profile geometry can be cal-

culated, which is root diameter and tip diameter on one hand, and some properties of tooth form on the other. By means of additional distance sensors which are to be mounted in a fixed offset from the first sensor, further information regarding tooth trace angle can be derived. A further measuring quantity which is necessary to be acquired, is the current value of the rotational angle of the workpiece. This quantity must be captured to enable an exact mapping of profile distance data to the appropriate location on the circumference of the workpiece surface. Besides the necessity of a distance sensor and a sensor for the rotational angle, the axial position of the workpiece during the forming process is required [10, 26, 29, 35, 36]. For this purpose, the measurement of the feed path versus time would be advantageous, as described in the previous chapters. This allows for tracking the progress of the forming process in axial direction, and, moreover, will allow for an exact mapping of the location of the measuring spot of the distance sensor. By means of this third measuring quantity, together with the first two, the geometrical properties Pitch, Tooth height and Tooth face thickness can be determined. Metrological, by choosing these three quantities, a workpiece co-ordinate system is created, which consists of two translator axes and one rotary axis. The configuration of the three axes is shown in Figure 100. The three workpiece-related axes are designated R , Z and φ , and are spanning a polar coordinate system [28].

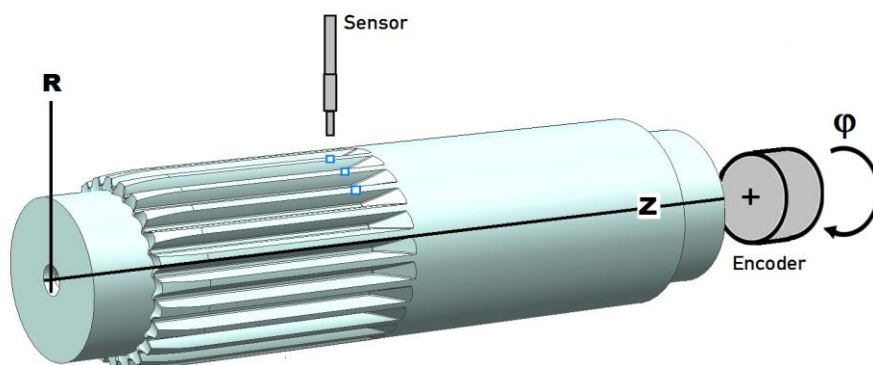


Figure 100 Config. sensors / workpiece coord. system R , Z , φ

7.1.1 Acquisition of Tooth Profile

For this purpose, a non-tactile distance sensor is required, which has to be mounted at a most rigid location in the machine frame. For the non-tactile measurement with direct-contact sensors, various sensor/instrumentation systems are available [23, 24, 34]. The sensor's physical principle of operation, range and achievable accuracy and sample rate are given in the following table briefly, only as a typical example, stating typical properties, without going into further details. The accuracy and sample rate achievable in a certain application depends on individual properties of the workpiece surface, measurement angle, lighting and other circumstances of the concrete case of application.

Displacement sensors / transducers

Table 9: Principle of Operation

Principle of Operation	Range	Accuracy	Sample Rate
Laserscanner, analog	0,5 - 100 mm	1 μm	40 - 100 kHz
Laser Triangulation	0,5 - 200 mm	1 μm	20 - 40 kHz
Laser Interferometer	1200 mm	0,02 μm	5 - 10 kHz
Stripe Projection	80 mm	?	?
Microwaves	12 mm	10 μm	?
Radar	100 mm	1 - 10 μm	?
Eddy Current, analog	0 - 8 mm	1 μm	?
Inductive LVDT	?	1 μm	?

7.1.2 Acquisition of Axial Position

The acquisition of the axial position of the workpiece can suitably be achieved by using a tactile digital linear position measuring system. CNC machines usually provide such measuring systems for the control of their feed axes, so no additional sensor is necessary. The actual position of the feed axis can be input over standard digital I/O interfaces from the CNC.

In the case of the existing WPM-120 Forming Machine, a direct measurement of the workpiece position seemed not to be necessary, as the workpiece is held axially between two tips.

So the feed position was measured symmetrically at the feed drive, using two high-accuracy incremental linear measuring systems, which are based on a magnetic 0.5 μm scale.

7.1.3 Acquisition of Angular Position

a) Direct measurement

Ideally, any non-tactile acquisition of the rotary angle position would be directly at the workpiece. As the surface and the edges of the workpiece are subject to inconsistencies and variations, measurement would only be possible with a reduced accuracy. There exist certain solutions which apply a flexible magnetic scale around the circumference of the workpiece, but then only a non-continuous measurement would be possible, which reduces the resolution considerably.

b) Indirect Measurement

Therefore, the only way remaining to achieve both, a high resolution and a high accuracy, is to take in account to measure indirectly at the rotary feed drive. Taking into account the particular conditions in the WPM, this has the disadvantage of having no rigid coupling of the workpiece to the feed drive, which means that the workpiece - being mounted between tips - may slip-rotate under certain conditions during the forming process cycle. In order to compensate for this disadvantage, additional marks around the circumference are used to sample the rotation of the workpiece every 15° , so it is possible to correct angular slips and to re-synchronise the angular position measured at the feed drive.

There are various rotatory sensor systems available, which are able to measure the angular position with high accuracy. Especially the systems used in CNC machines, measuring absolute or incremental angles, are well known. The practical conditions of the existing feed drive train only allow for measuring the workpiece rotary angle indirectly at the feed drive.

7.2 Application / Distance Sensors / WPM Work Cycles

First of all, the WPM work cycles can be divided in two phases, the forming phase (Figure 101) and the feed phase (Figure 102). During the feed phase, both the workpiece rotational drive and the axial feed drive are active at the same time; at the beginning of the forming phase, both tools get in contact with the workpiece and will block the axial feed against an overload function clutch.

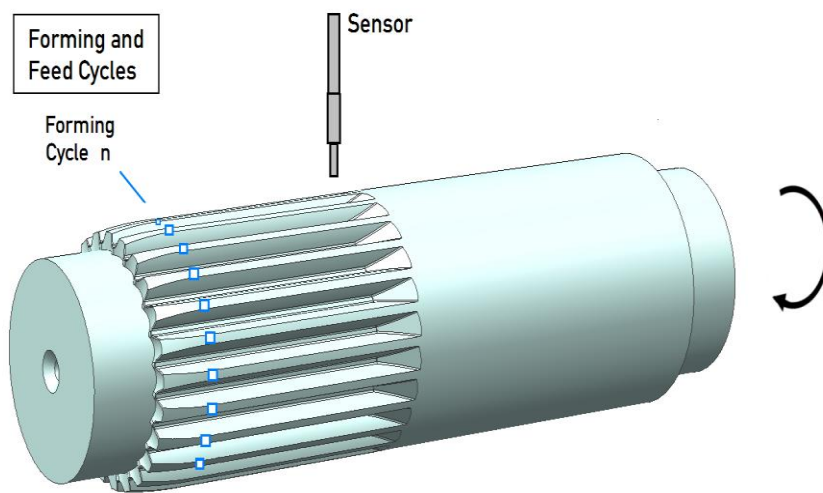


Figure 101 Principle sampling sequence / surface in forming phase n

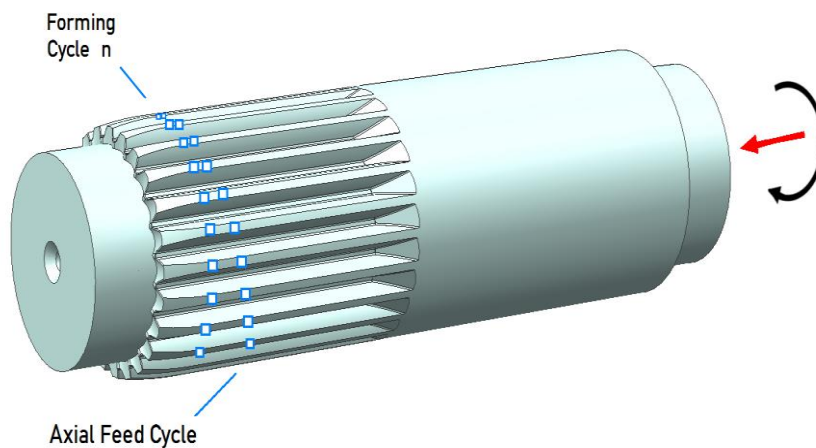


Figure 102 Principle sampling sequence / surface in axial feed phase

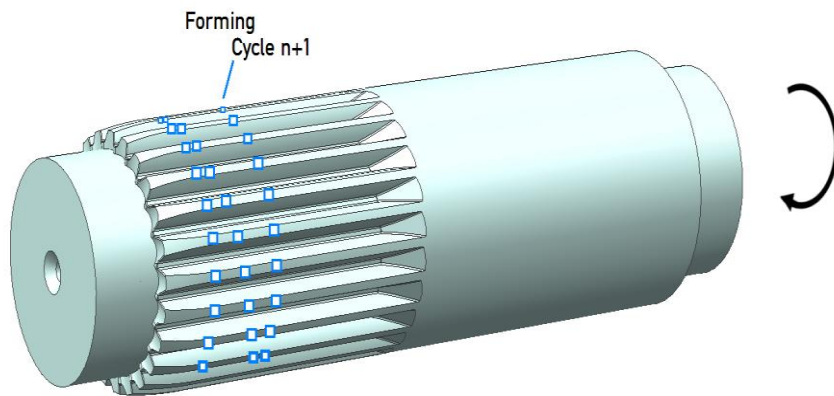


Figure 103 Principle sampling sequence / forming phase n+1

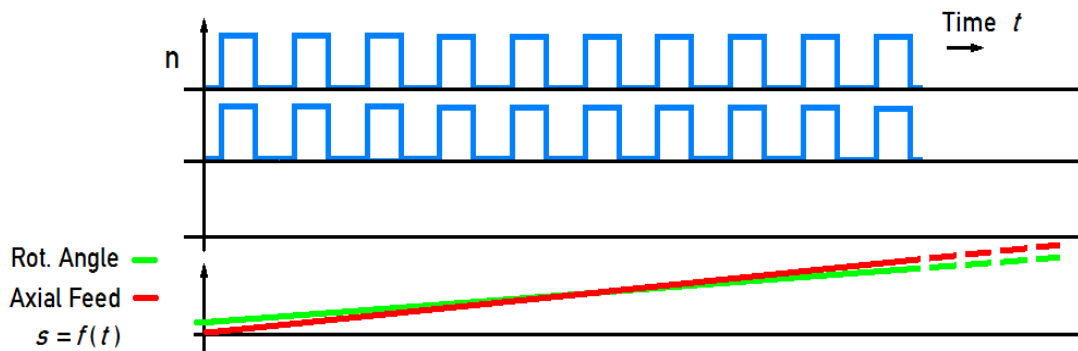


Figure 104 Sensor signals / forming / axial feed / rotational

It can be seen, that the sensor signals measured vs. time are not significantly different during the forming phase and the axial feed phase, as the workpiece rotation continues because of the auxiliary rotary drive even after the tools get out of contact. Angular velocity keeps nearly constant, only in the moment of the initial die-workpiece contact a short change of acceleration is to be expected, as a small difference in circumferential velocity can be observed. At the moment when the tools get out of contact, the blocked axial feed and the angular motion are resumed and at the same time, so that the sensor measuring spot moves along a helical path around the circumference of the cylindrical workpiece (Figure 103).

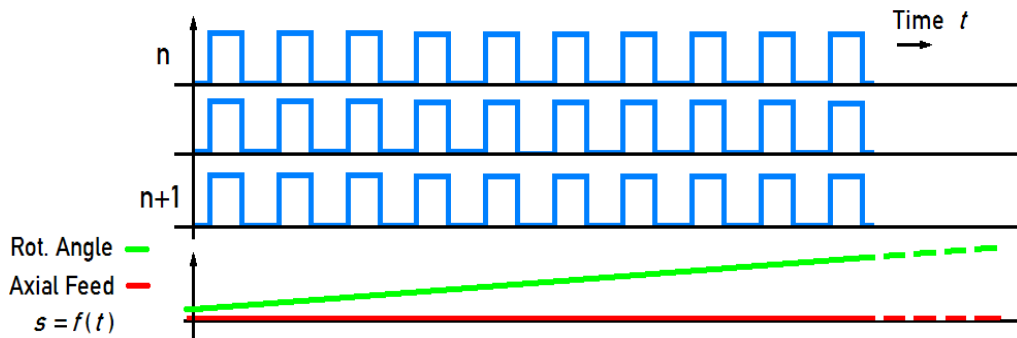


Figure 105 Signal curves for forming cycle $n+1$ (schematic)

In this way, an existing tooth profile will not be sampled on a circular path, but on a helical path. The geometrical information contained in the distance sensor's signal will relate one tooth after the other with an axial offset of the axial feed. Yet this fact cannot be detected in the sensor signal curve timing, as the rotational speed will be the same as during the forming cycle where no axial feed is superimposed. Forming cycle $n+1$ starts at the moment when the tools get in contact again. The signal curve forming cycle $n+1$ is shown schematically (after the curves of previous forming cycle n) in figures 104, 105. It can be seen from the diagram that axial feed (red curve) has stopped, and at the same time rotation (green curve) continues with constant slope.

7.3 Geometrical Deviations / Peculiarities

7.3.1 Eccentricity

The workpiece being held between two tips generally has certain concentricity (Figure 106). This concentricity deviation is composed of eccentricity plus roundness deviation, which both will be contained in any radial measurement. Roundness deviation of a cylindrical part can easily be measured before inserting a workpiece and by this measure it will become a priori known to the process, so that roundness deviation can be input to future process

control software and could be subtracted from the measured concentricity value, yielding pure eccentricity.

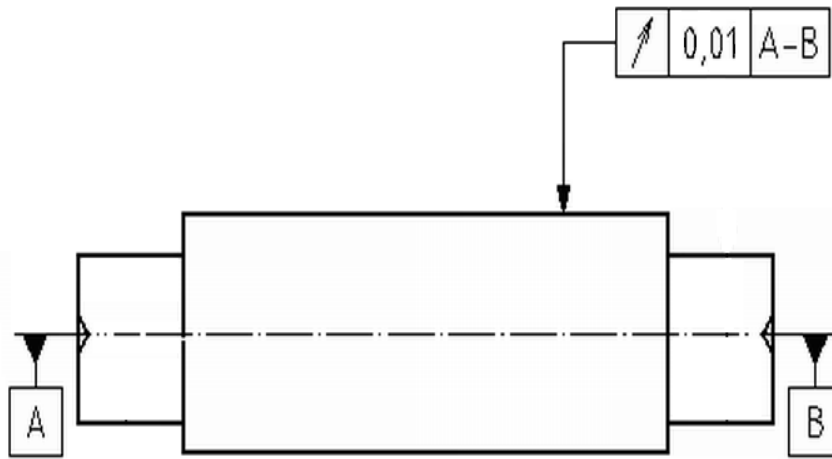


Figure 106 Specification Runout Tolerance / workpiece acc. ISO 1101

For the in-process measurement of eccentricity again a non-tactile distance sensor can be employed, which should be mounted in such a way, that it measures the radial distance to the surface of the workpiece during rotation (Sensor 1 in Figure 107). The changes of this radial values versus the rotational angle of the workpiece, reduced by the roundness deviation of the blank results in the process quantity eccentricity.

This measurement of eccentricity can be done during a forming cycles and during feed cycles as well. Fewer errors or interferences in the measurement signal can be expected, if the tools are not in contact, as this will eliminate most dynamic interferences caused by the forming process. Therefore, it is recommended to place the sensor in the zone outside the pre-forming and forming zone.

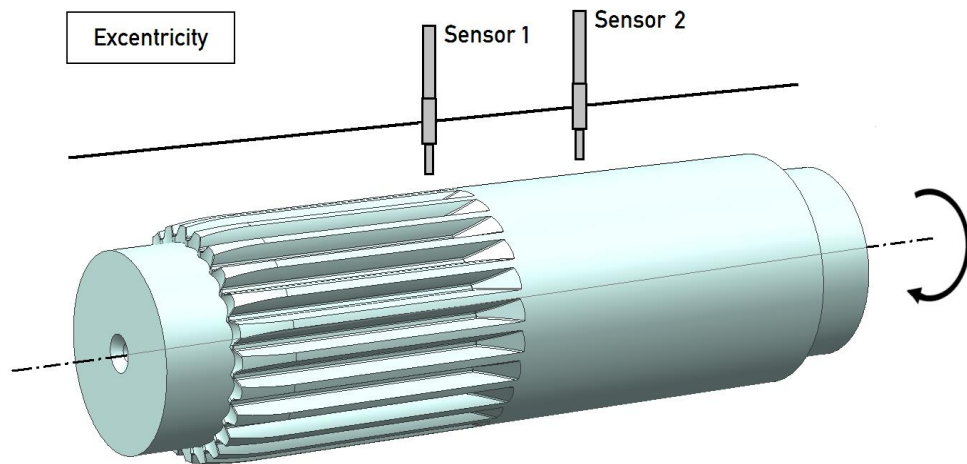


Figure 107 Sensor placement / determination eccentricity (Sensor 2)

It could also be an advantage to use two sensors, as depicted in Figure 107, which would allow monitoring the formed zone of the workpiece and the zone outside the forming zone as well. Sensor 1 was placed in the forming zone to measure the distance to the surface of the workpiece. The sensor signal vs. time which is measured during workpiece rotation exhibits a concentricity deviation, caused for example by a workpiece mounted eccentrically. Signal acquisition and signal processing for eccentricity monitoring is explained in detail, as shown in Figure 108 schematically.

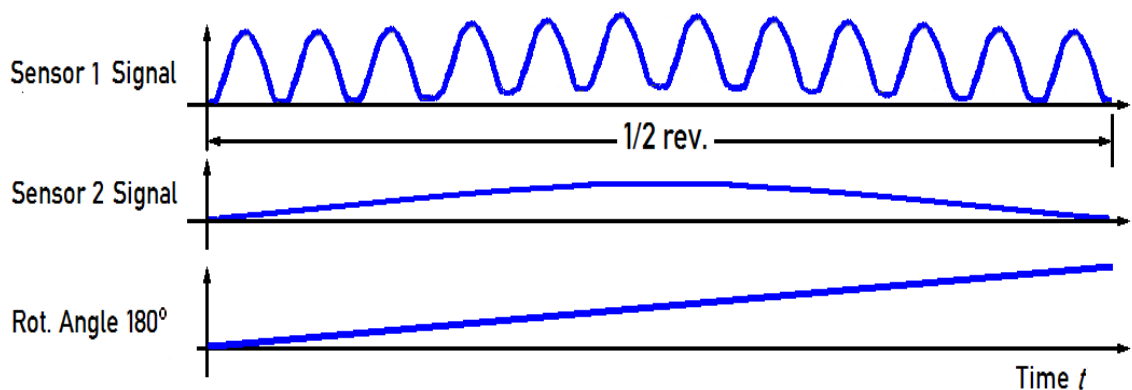


Figure 108 Principal sensor signal vs. time and calc. of eccentricity

First, the signal at the top of the diagram in Figure 108 represents the radial distance, as measured by sensor 1. The distance changes periodically between root and top of the teeth. Superimposed one finds a low-frequency periodical signal, which is synchronous with the workpiece revolution, which reflects concentricity. Further signal processing calculates the sequence of minima and maxima and subtracts the a priori roundness deviation of the workpiece, thereby determining its eccentricity. The minima (root) are better suited than the maxima (tip), as it could be shown in the tactile post-process measurement on the CMM, the base diameter is widely more invariant against process parameter changes than the tip diameter. Still better results will be found, when the sensor is placed in the yet non-formed zone of the workpiece (Sensor 2), because there all vibration and all signal components caused by the tooth-forming process will not be present, so eccentricity can be measured and calculated with less interferences. Figure 108 shows a typical sensor signal (Signal 1) vs. time. Where there exists a significant eccentricity rise within one half revolution superimposed on the periodical signal change from base to tip. The curve labeled Sensor 2 comes from a sensor placed outside the formed zone, so the pure periodical rise during 180° of a 1/2 revolution corresponds directly to the concentricity of the workpiece, as measured at the axial position of sensor 2, which again delivers eccentricity after subtraction of roundness deviation.

7.3.2 Pitch (Angular, Fluctuation) / Tooth Thickness

The tactile measurement of the work pieces manufactured in the WPM forming process (Chapter 5, 6) has shown that fluctuations of pitch and angular pitch have to be expected. Therefore, it is highly recommended to provide for an in-process detection and calculation of these parameters (Figure 109). Pitch p is defined as the arc length at the perimeter of the pitch or reference circle from one tooth to the next, or, the circumference of the pitch circle divided by the number of teeth.

$$p = 2\pi r / z = \pi d / z$$

$$\tau = 360^\circ / z$$

The Angular pitch τ is the appropriate angle (DIN 3960), with z = number of teeth, and pitch p , the arc length of the angular pitch. Applying this to the sample workpiece examined, which has $z = 24$ teeth, the angular pitch $\tau = 360 / 24 = 15^\circ$.

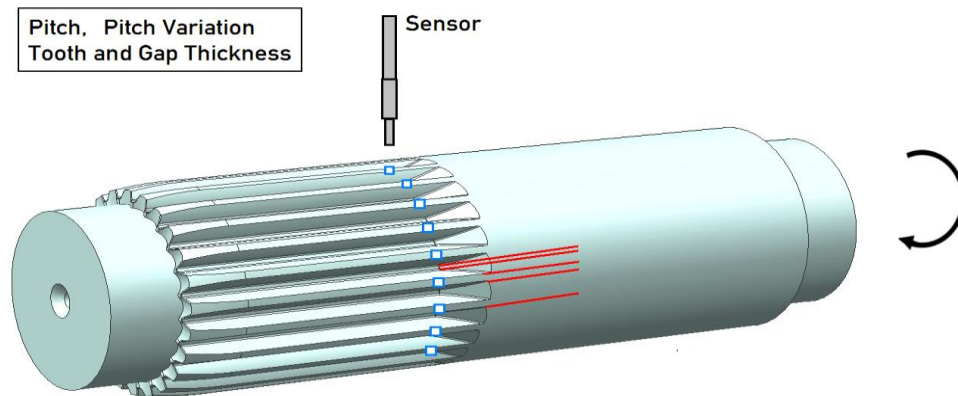


Figure 109 Path of the sensor spot pitch variation / gap thickness

Signal processing The sensor signal of a suitable distance sensor will deliver a raw signal vs. time, which reflects duration and height of the teeth sampled. By comparison with an adjustable trigger levels, pulses can be generated at the rising and at the falling edge of the raw signal. This can be done in both ways, by hardware or by software.

Fig. 110 shows an example, where by use of two different trigger levels, so that pulses just above the base circle and pulse just below the tooth will be generated. For each of the two trigger levels, this results in two rising edge pulses (S_r , blue line) and two falling edge pulses (S_f , red line).

Moreover, depending on individual requirements, also advanced methods of signal slope or edge detection could be applied. The next few steps of signal processing for the determination of pitch angular pitch and pitch fluctuation will be explained referring to Figure 110:

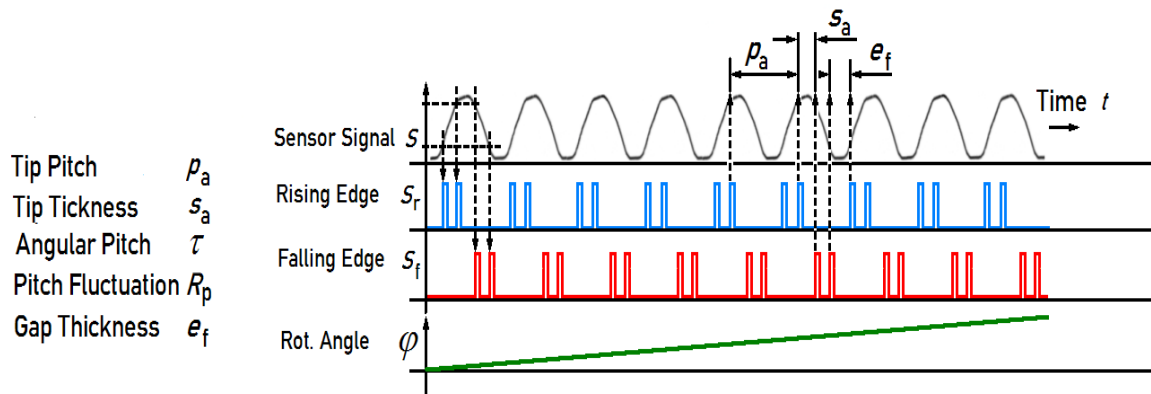


Figure 110 Signal process. pitch, pitch fluctuation, tooth, gap thickness

Angular Pitch and Pitch The points in time $t_1, t_2 \dots t_n$ can be derived from the first rising edge pulse $Sr_1, Sr_2 \dots, Sr_n$ and then be stored; time durations can easily be calculated from their difference. By registration of the rotation angles $\varphi(t) = \varphi_1, \varphi_2 \dots, \varphi_n$ at the same points in times $t_1, t_2 \dots t_n$, the calculation of angle differences directly yield values of *angular pitch* τ according equation:

$$\text{Angular Pitch } \tau(t) = \Delta\varphi(t) = (\varphi(t_1)) - \varphi(t_2))$$

Repeatedly calculating values of angular pitch can also be done for the rising edge and falling edge pulses separately, so there is another opportunity of detecting symmetry deviations of left and right flanks. It should be pointed out, that it is also possible to obtain the pitch at the tip diameter, or at the root diameter, by adjusting the trigger level accordingly. In this way special advanced analysis of various pitches becomes possible. The calculation uses the angular pitch and multiplies its values by the tip radius r_a or the bottom radius r_f . The equations are given as follows:

$$\text{Pitch: } p(t) = r \cdot \tau(t)$$

$$\text{Tip pitch: } p_a(t) = r_a \cdot \tau(t)$$

$$\text{Root pitch: } p_f(t) = r_f \cdot \tau(t)$$

If the adjustability of the Trigger level S_{TL} is used, it is possible to adjust to a medium height. This principle is capable of generating pulses at the pitch diameter, so one could immediately obtain pitch values $p(t)$. The achievable accuracy is unknown. Possibly that appropriate radii cannot be acquired and calculated with sufficient accuracy, so the pitch is not recommended as a process quantity.

Pitch fluctuation Having measured and calculated the individual pitch values p_i or angular pitch values τ_i , then these can be analysed regarding individual pitch fluctuation Δp_i and its Maximum Δp_{max} . It is advisable to further analyse the process data for systematic and random properties of the process. Therefore, the average (mean value, median) and the variance are calculated. The Median is not preferred in this case, because it drops the min and max values, whereas the gear quality criteria usually are oriented towards the concept of maximum deviation. In order to obtain the random characteristic of the process, the standard deviation σ , as well as Range R may be calculated, but the latter being preferable, as R represents the difference between maximum value and minimum value, which again corresponds to the maximum deviation quality criteria, used in coordinate metrology.

Pitch mean value:
$$\bar{p} = \frac{1}{n} \sum_1^n p_i$$

Pitch median:
$$\tilde{p} = \text{central value of sorted data}$$

Pitch variance:
$$\sigma_p^2 = \frac{\sum_1^n (p_i - \bar{p})^2}{n+1}$$

Pitch Range:
$$R_p = \max(p_i) - \min(p_i)$$

By use of these statistical quantities, systematic errors can be separated from random deviations, which promise to derive conclusions for process improvement. Offset of the mean value from the nominal value of a parameter allow for the conclusion of systematic errors, whereas a big value of

standard deviation σ or range R indicates process effects which are harder to find and to remove, as they are of random nature, like tolerances in guide rails or backlash in the drive chain. The use of the angular pitch τ as process quantity, instead of pitch p or p_a , has the advantage that angular pitch does not need a multiplication of the measured angle τ by a second measured and calculated parameter, the root radius r_f or tip radius r_a . By preferring angular pitch τ , fluctuations of the radii will have no influence, as can be seen from the following equations for the continuous calculation of the values of angular pitch, pitch and tip circle pitch:

Angular Pitch: $\tau_n = \Delta\varphi_n = \varphi(t_n) - \varphi(t_{n-1})$

Ref. Circle Pitch: $p_n = r_n \cdot \tau_n = r_n \cdot (\varphi(t_n) - \varphi(t_{n-1}))$

Tip circle pitch: $p_{an} = r_{an} \cdot \tau_n = r_{an} \cdot \Delta\varphi_n = r_a \cdot (\varphi(t_n) - \varphi(t_{n-1}))$,

Only the calculations of the process data for the angular pitch are based on the difference of measured values of the rotational angle at points in time of two tooth pulses in sequence, whereas the calculation of both pitch quantities need a radius, which is a second measured quantity depending on another calculation.

Tooth thickness s_a The raw signal of an distance sensor indirectly delivers the information of tool thickness at the tooth tip. Time duration of the radial tooth distance signal (Figure 111) is proportional to tooth thickness. It can be calculated from the angle difference of the rising edge to the falling edge of a tooth signal, and the difference between root and tip.

Tooth thickness at pitch diameter: $s = r(\varphi_f(t_n) - \varphi_r(t_{n-1}))$ with trigger level $S_{TL} = r$,

Tooth thickness at tip diameter: $s_a = r_a(\varphi_f(t_n) - \varphi_r(t_{n-1}))$

Tooth form The distance sensor signal (Figure 109) holds information about eccentricity, information about root geometry, involute flank geometry and the geometry of the tip. As described in chapter 5 and 6, the tip form shows specific deviations, this therefore should be considered.

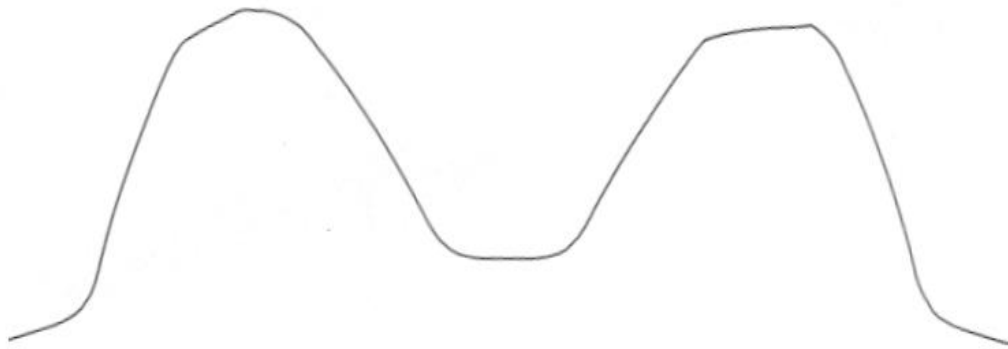


Figure 111 Tooth profile, (Chapter 5)

The result of a two-tooth profile measurement on a LEITZ CMM, as described in Chap. 5, is shown in Figure 111 for reference purposes. It shows the different tooth profiles of two adjacent teeth.

It can be seen clearly, that there is a big deviation in the form of the two tips even the two adjacent forms show a characteristic difference in tip-form. In particular, there is a left-right asymmetry, which in the case of the right tooth, where tool height rises from left to right in a straight line and continues with a sharp edge, to the right side of the tooth axis line of symmetry.

A possible strategy for analysis could be, to analyse the distance signal between the rising edge and the falling edge pulses in the tooth gap, near the bottom only, as this property has proved to be a stable and reproducible. Moreover, the influence of eccentricity could be removed by taking in account the signal of a second sensor mounted in the yet unformed zone of the workpiece, which delivers a pure eccentricity signal, not being influenced by the formed tooth profile.

Tip Form Deviation und Tip Symmetry The deviations of the tip form can also be determined from the signal of the radial distance sensor. They can be a sequence of signal processing steps, which will be explained as follows. In the first step the rising edge and falling edge pulse signals are gen-

erated by comparison with trigger levels, as described earlier. In this way, root, flank or tip pulses can be generated.

Assuming, that one trigger level at the end of the involute flank, at the start of the head rounding, which is used on both sides of the tooth. Here the maximum value and its angular position can be determined. Having the position of the maximum, it is possible to determine the degree of symmetry and hence symmetry deviation described as followed.

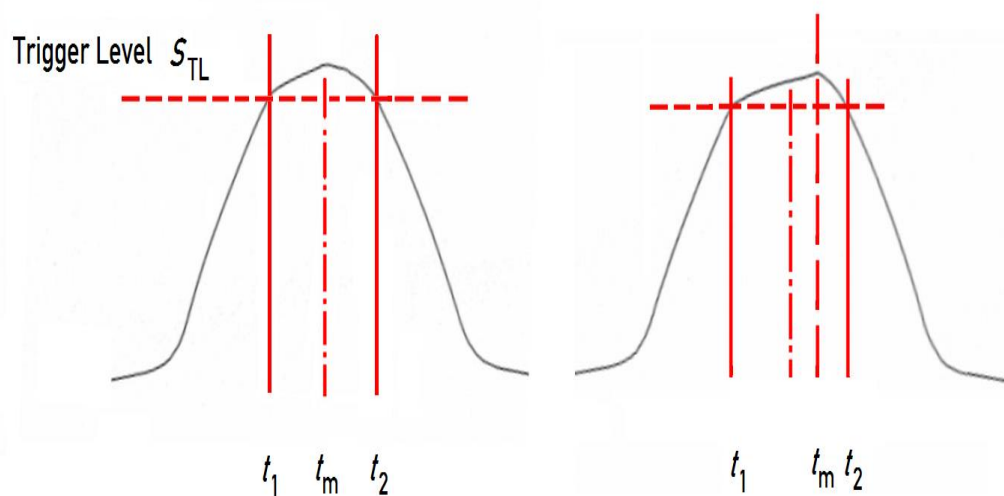


Figure 112 Analysis of form deviation / tip symmetry / asymmetric

Calculation of symmetry is done in such a way, that first of all the centre of the interval between time t_1 of the left pulse and time t_2 of the right pulse is calculated. Then a measure of symmetry is calculated, which is defined as the deviation of the time of the maximum point t_m from the time in the middle between t_1 and t_2 . The calculation of the position of the maximum point could simply be done by calculating the time differences, but as angular velocity cannot be assumed to be constant, it is more accurate to calculate it using the appropriate angles. In this way, a grade of symmetry will be calculated, which is related to the angles, which means also, that this calculation is similar to the calculation of the angular pitch.

Compared to the similar symmetry calculation based on the arc length, this alternative has the advantage of a lesser number calculations in real-time, so this angle-related "degree of symmetry" $\Delta\varphi$ is recommended.

The absolute angular deviation $\Delta\varphi$ of the maximum will be calculated as follows: From the measured pulse signals S_1 , S_2 and S_m follow the corresponding points in time t_1 , t_2 , t_m and the measured and registered angle data $\varphi_1(t_1)$, $\varphi_1(t_2)$ and $\varphi_m(t_m)$. The calculation of symmetry is now based on the offset of the maximum point to the centre point and will be calculated as follows:

a) Temporal:
$$\Delta t = t_m - \frac{t_2 - t_1}{2} \quad (\text{time offset})$$

b) Angular:
$$\Delta\varphi = \varphi_m - \frac{\varphi_2 - \varphi_1}{2} \quad (\text{angle offset})$$

c) Circumferential:
$$\Delta s = r_a \Delta\varphi \quad (\text{arc length offset}) \quad (r_a = \text{tip diameter})$$

The second alternative, the angular case (b) is preferred. Having available this angular offset, one can calculate a relative symmetry deviation in %.

7.3.3 Axial Position and Orientation

The axial position and orientation of the workpiece relative to guidance rails of the WPM machine can be acquired and monitored by the use of two distance sensors. Figure 113 shows the sensor configuration, where the two sensors mounted with a fixed axial offset. If a special axial measuring cycle is performed by the axial feed drive, there will result the signal curves of sensor 1 and sensor 2 in principle, as shown in Figure 113. The signal of sensor 1 shows a ramp starting from the root and extends to the tip over the pre-formed zone on the surface of the workpiece. As an example, there is also shown a case without any errors (curve horizontal; constant level, blue curve), whereas a slightly rising straight line (red curve) shows a misalignment. The signal of sensor 2 Signal, which is mounted outside the formed zone of the workpiece, shows the axial feed vs. time, in case of no error,

with constant height (corresponding to tip height), resp. in case of error, a slightly rising straight signal line.

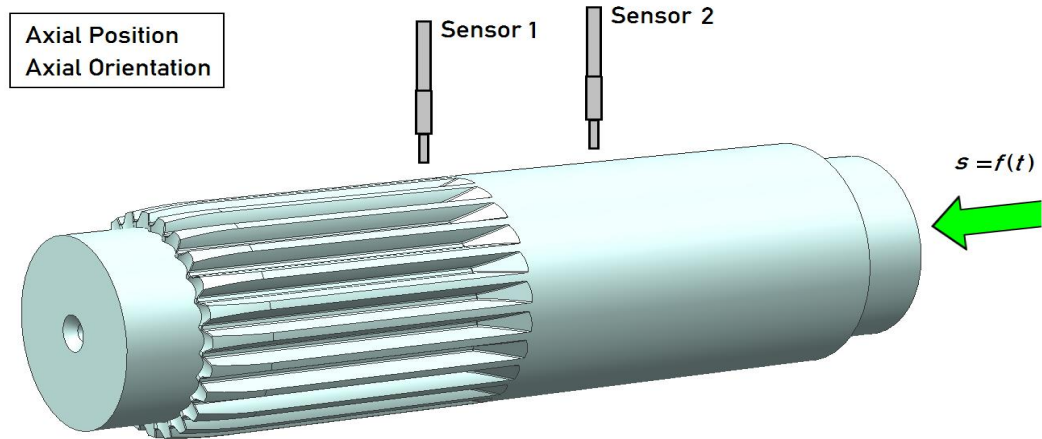


Figure 113 Measuring Axial Position Orientation

Two sensors, having been aligned parallel to the workpiece axis, and mounted with a fixed offset in axial direction, will produce a signal according to the axial movement, a radial distance signal, which is shown in Figure 114 in principle. Sensor 1 is measuring in this configuration the root in a tooth gap and moves along in axial direction, whereas Sensor 2 is measuring upon the cylindrical surface of the workpiece, which is not yet formed. The resulting signal curves are shown in Figure 114. In the case of workpiece without any alignment errors, which was mounted completely parallel to the guidance rails, we will see the signal curve in red. In case of a axial misalignment, the red curve („rejected.“) will be seen. In both cases one sees the linear rise (root to tip), which happens because of sensors passing the pre-form zone.

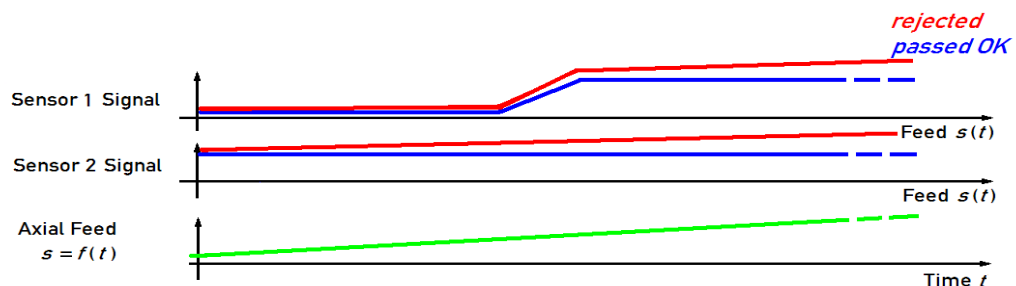


Figure 114 Sensor signals Axial- Position Orientation

7.3.4 Tooth Trace

One of the deviations of the work pieces formed by the WPM process is the tooth trace. In order to be able to acquire a process quantity, which can determine tooth trace ("lead"), a special two-sensor configuration has been found, which will allow measuring a proportional quantity. The two sensors have to mount with a known axial offset a (Figure 115). By this configuration it will be possible to determine any axial angular offset angular displacement of a tooth. The point at the surface which is to be used for the measurement should be unique and of good quality, with low diffusion, for example the flanks at the tooth tip. Another possible point would be at the root, as the good reproducibility of the root diameter is known from CMM measurement. Moreover, it is mandatory, that the sensors have been calibrated and aligned perfectly in parallel to the workpiece drive axis. In following it will be shown, by which signal processing steps tooth trace can be measured.

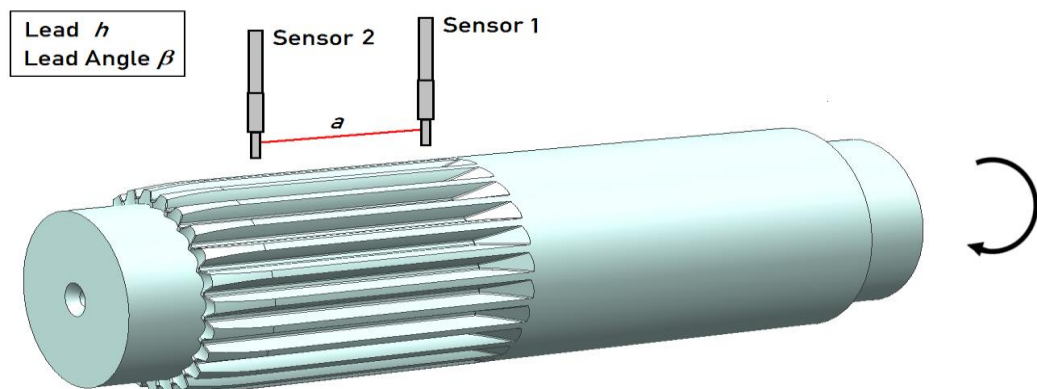


Figure 115 Axial Configuration 2 Sensors for the acquisition

Figure 116 shows the principle of signal acquisition and signal processing to determine tooth trace deviation. The distance proportional signals of the two Sensors will be sampled vs. time. The same goes for angular position of the workpiece resp. indirectly at the der workpiece drive unit.

At the points in time, when the rising edge pulse happen at both sensors, and the two corresponding angular position values will be registered. Immediately afterwards the difference will be calculated and stored as current $\Delta\varphi$ saved. The following figure 116 shows the principle of idealized square signals.

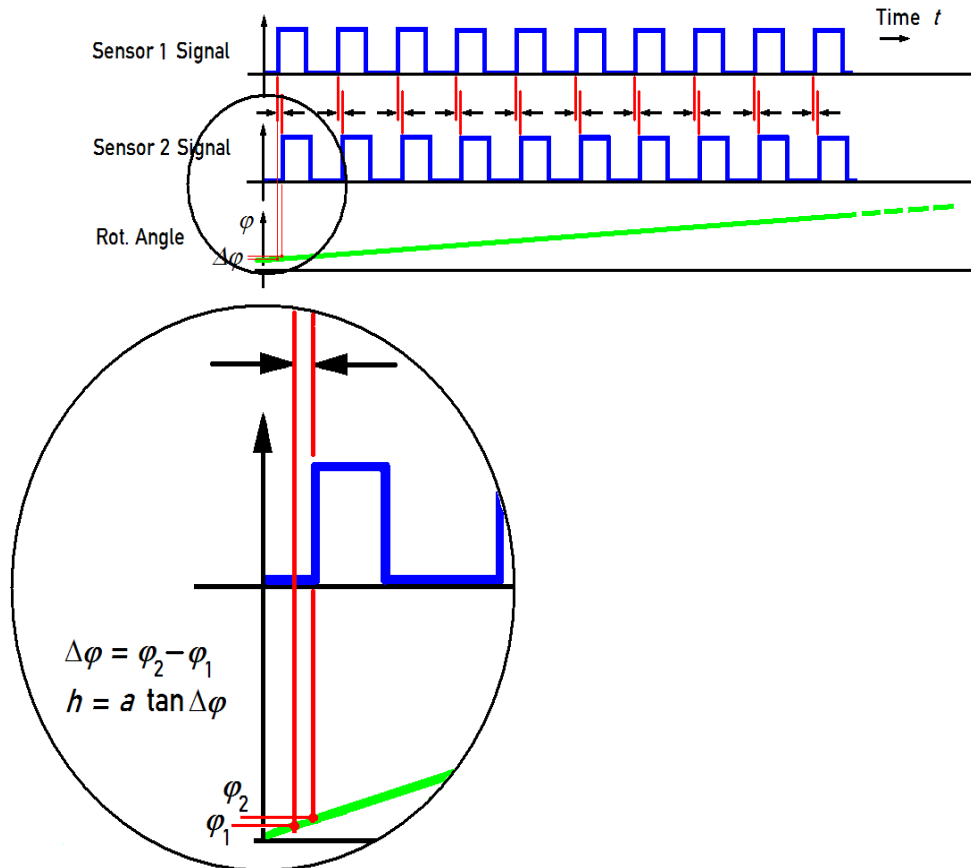


Figure 116 2 distance sensors / axial angle diff. / tooth trace deviation

The time offset of the rising edge signals of the two sensors determine the 2 points in time. In the next step, the corresponding angle difference $\Delta\varphi$ calculated. In the third step $\Delta\varphi$ is used to calculate the tooth trace deviation for the sensor distance, using the known geometrical conditions of the sensor configuration. Finally, the total tooth trace deviation (acc. to DIN 3961) can be estimated by extrapolation to the full length of tooth length. The calculation steps for the total tooth trace deviation from the axial angle offset are as follows:

Axial angular offset:	$\Delta\varphi = \varphi_2 - \varphi_1$
Geometry:	$\tan \Delta\varphi = \frac{h}{a}$
Lead between sensors:	$h(a) = a \tan \Delta\varphi$
Estimated total lead:	$h_{FB} \approx h(l) = l \tan \Delta\varphi$

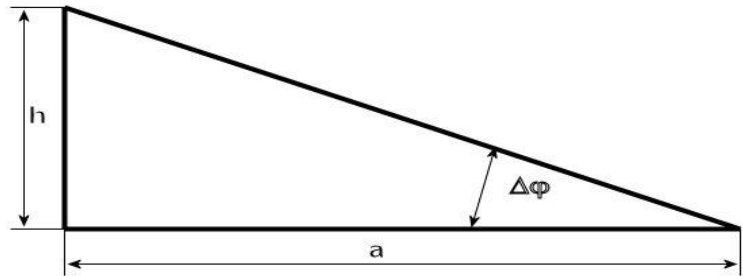


Figure 117 Calculation of tool trace deviation h_{FB}

7.4 Sensor Requirements

The measuring parameters described and the process parameters derived in the sections above, together with the current machine design and machine kinematics of the WPM, will be used to define the requirements on the sensors needed to allow for monitoring geometrical measuring quantities.

7.4.1 Instrumentation

The workpiece measuring quantities, the derived process parameters eccentricity, pitch, tooth trace as well as various parameters for monitoring tooth form, tip form, tip symmetry define the main requirements to sensors and instrumentation and their properties, such as range, accuracy and sample rate. It has been shown, that in order to monitor of geometric parameters of the workpiece during the forming process, a minimum of three measuring quantities are required. Among these a minimum of three workpiece quantities were found: radial distance R between a rigid point and the surface of the cylindrical workpiece, the axial workpiece position Z and the angular

workpiece position φ . This workpiece coordinate system will be sufficient to monitor the parameters described above.

From the measuring methods considered, certain consequences for the selection of sensors, their properties and accuracies can be derived.

Most of geometric properties of the workpiece during the gear forming process require sensors for measuring a combination of two geometric quantities: the *distance* between a fixed rigid point in the machine and the cylindrical workpiece to acquire the information of the tooth profile being formed.

As the workpiece is in a combined rotational and translational motion, which changes its characteristics periodically, it is essential to also provide for the acquisition of the rotation angle, which is mandatory for the interpretation of the raw sensor signals, which are basically acquired versus time, and which need a precise relation the momentary value of the rotation angle.

The requirements to the sensors regarding measurement range, measurement accuracy and the minimum sample rate will be considered for the suggested measurement quantities individually.

Quantity	Sensor type	Range
• Distance R	non-tactile	10 to 50 mm
• Position Z	directly coupled	0 to 500 mm
• Ang. Pos. φ	directly coupled	0 to 360 °

Distance R Measurement of distance between the sensors to the surface of the workpiece must be performed in a non-contact way. The relevant non-tactile method must be suitable for metallic surfaces, in this case turned parts. A special problem exists as a sensor mounted vertically above the workpiece will deliver an optimal signal in the range of the tip and the base, but a suboptimum signal when the sampling spot moves across the vertical section of the tooth, near the involute. The only solution will be to mount the sensor with inclined orientation. Sampling the surface with two sensors, one

mounted vertically and the other inclined, may be necessary, but this will increase the overhead and double the cost.

Circumferential resolution The resolution along the surface of the rotating cylindrical workpiece should at least be 50 to 100 sample points per tooth at the circumference. Assuming the present 24 teeth, the required sample point density at the perimeter and a minimum sample rate a measuring rate will be estimated. $\text{Res.} = 24 \text{ teeth} / 360^\circ \cdot (50 \dots 100) \text{ samples per tooth} = 1200 \dots 2400 \text{ samples}/360^\circ$

Assuming the current workpiece $n = 300 / \text{min}$ one can estimate the required sample rate t Sample rate at $n = 300 \text{ min}^{-1} = 5 \text{ s}^{-1}$: $f = n p = 5 (1200 \dots 2400) \text{ samples}/360^\circ = 6000 \dots 12000 \text{ samples} / \text{s}$

Rotational Angle φ Ideally, the angular position would be measured directly at the workpiece. This not possible continuously, so as a replacement solution, an indirect measurement of the rotational angle will be done at the workpiece drive unit, however an additional monitoring channel is required, which monitors the workpiece at certain points on its circumference, in order to detect any slip between the workpiece and the drive unit. In case of a rotational slip special measures to guarantee re-synchronisation have to be taken.

Axial Position Z The WPM machine has an axial feed drive mechanic which allows for indirectly measuring the axial position at the feed slide. Machine tools usually have feed measurement systems with a resolution of typically 0.5 to 1 μm , whereas the accuracy of machines without temperature control is worse, mostly 5 to 10 μm . The WPM-120 originally had no NC axes, but the feed axis has been equipped with a digital incremental position measurement system, using a magnetic scale with a nominal accuracy of 0.5 μm . The feed mechanics is not designed and constructed to guarantee a constant axial feed. The existing feed drive is fluctuating in the 0,1 mm range, so there is no requirement for a better axial feed position measurement system.

7.4.2 Conclusions of In-Process Measurement Requirements using Suitable Sensors

As the result of an analysis it could be shown that a minimum of three resp. four quantities have to be measured. The acquisition of measuring data from two non-tactile distance sensors, one linear position sensor and one rotational angle sensor for measuring the angular position of the workpiece, as well as the process quantities derived from these quantities by in-process real-time calculation was being discussed. The requirements regarding measuring range, accuracy and sample rate resulting from these considerations were determined resp. estimated. Which of the many sensors available on the market eventually could be selected according to these requirements, and the question if sensors having the required accuracy and sample rate do exist or have to be developed, is beyond the scope of this work.

8. Conclusion and Outlook

In the present work, the little-known rolling method WPM with internally toothed tools was used. This method was developed by Prof. Marciniak at the beginning of 70th in Poland. A corresponding experimental machine WPM 120 including rolling tools is located in Darmstadt and was used for the research.

First of all, roll samples were prepared, which were manufactured under controlled mechanical engineering conditions. Subsequently, these samples were geometrically measured on a coordinate measuring machine Leitz PMM 654. The geometry measurements were divided into the conventional gear measuring according to DIN and special contour measurements on the toothing. With the contour measurements, which are visible with the naked eye, geometrical characteristics of the teeth were examined. These geometrical features are typical for the metal forming by using internal toothed tools. It has been found that the resulting geometry of the examined samples is substantially dependent on the feed rate. In all other process parameters such as the blank material, no significant influence could be observed on the toothing geometry.

The aim of the presented study is to determine through tactile post process measurements, significant geometric features on the resulting component geometry. These should serve as a basis for a future in-process monitoring of the rolling process. The features of interest were found and described. Among other features, the different tooth heights and the tooth tip forms dominate the compiled results. Using the WPM method with internal toothed tools an asymmetrical distribution of the blank material results on the circumference.

The WPM-rolling is a metal forming method for chipless production of toothed machine elements. Methods of forming technology are generally used for the production of mass-produced parts. The mass production is

subject to specific criteria. These criteria basically relate to the profitability in consistency. This leads to the conflict to produce a maximum of toothed components in the shortest possible time. This is the main reason that the resulting tothing geometries can only be checked on a random basis.

This is today's industrial practice, because the required measurement quality leads to an expenditure of time. Therefore it cannot be checked each component. So it is now the target of the production technology to search for solutions which make it possible to monitor the production of any component already in the machine. This would save time and avoid that defective parts are produced in large quantities. To late noticed manufacturing errors cause costs. The efficiency of the entire production is adversely affected.

The own studies document the fact that during the metal forming with internally toothed tools typical errors at the tothing result. A timely detection of these geometrical features in-process is, in principle possible, since these geometrical deviations from the desired ideal shape of a tooth system are located on the surface of the cylindrical components.

Tactile probes for geometry detection are not suitable, because the work-piece rotates during the rolling process. Insofar measurement methods similar to the measuring structure in a coordinate measuring machine are unsuitable for this task. Constructive problem areas of the rolling machine would be affected and would lead to significant technical problems. The implementation of coordinate metrology within the rolling machine is therefore hardly possible for various reasons. Consequently, tactile measuring probes with respect to an in-process monitoring of the rolling process are unsuitable. Based on our own results, solutions to capture the geometric features of the process with non-tactile probes were developed. These suggestions are based on knowledge of the characteristics of head shapes and head heights. As a particularly stable feature of the WPM-rolling, was observed that the resulting root circle diameter results nearly identical for all examined parameter combinations. In this respect the features head height, head shape and foot circle are generally suitable for detecting the rolling process metrologi-

cal. It is presumed in this case that in addition to the detection of geometric features on the parts processed, also machine-technical data, such as drive power of the rolling tools and feed movement of the rolled part, would be measured and interpreted.

Changes of the special features in combination with machine-technical measurements in the single process or throughout the production time of many toothed components could be detected and interpreted. In this connection stands the monitoring of the uniformity of an ongoing mass production in the foreground. If nearly identical head and foot geometries result, it can be assumed that production takes place under the same conditions. When the corresponding measured values tend to change, then modified rolling conditions must have revealed. A timely response of the machine operator is therefore possible.

In terms of the previously mentioned proposals of a future in-process control of the WPM-rolling, non-tactile sensors would be used. This measures the geometric distance between the component surface and a mechanically stable point within the machine. The necessary number of sensors is dependent on the selected measurement and analysis strategy. Depending on the geometric issue are different combinations of sensors conceivable.

The question of an ideal in-process monitoring process cannot be conclusively answered today. This research does not explain in detail how the geometrical features emerge. It can be assumed that the contact under load between the tools and the blank lead to changes in the geometric center position of the rolled part. The knowledge of these relationships should be investigated in detail in the future. Furthermore, it is not sufficiently known in detail how the material is distributed on the circumference of the rolled part. It was found that on the circumference of the rolled sample asymmetries arise in the tooth tips. Whereby these geometric features are caused is not clear yet. If clarity would be gained, then different approaches can arise to define the strategy for the future geometric monitoring. In addition to the detection

of the resulting component geometry, capturing other features which characterize the forming process is also conceivable. The observed differences in tooth height and head shapes mean in consequence, that at the emergence of the tooth gaps different material movements must be preceded. Therefore, various material movements must have happened, relative to the individual teeth. These would lead to different work hardening gradients of the material. It would be ideal, if it would be possible to detect metrological different work hardening between the left flank and the right flank at every tooth. Measurements with an ultrasonic sensor could possibly be a reasonable approach in principle.

Another feature for the interpretation of the rolling process may be the condition of the rolled surface of the workpiece. This statement relates to the roughness and formation of cracks on the surfaces. In the preliminary experiments to the present work different rolling samples were examined under a microscope. Surface variations were clearly recognizable down to small cracks. To what extent appropriate sensor is already available on the market today and with how much effort this would be to develop, cannot be conclusively determined. The rotational movement of the part would be certainly the main problem.

The acquisition of geometrical features with non-tactile sensors based on detailed evidence regarding the contact situation between the tools and the material could serve as a starting point for the development of in-process monitoring. In addition considering the geometric relationships on the resulting workpiece geometry, further analysis of the work hardening of the material and the surface characteristics may lead to a comprehensive in-process monitoring of rolling with the WPM method.

9. Abstract/ Streszczenie

The subject of the present work concerns the production of splined shafts. On an industrial scale, they are made in series production using a succession of different manufacturing processes. The increasing demand of high precision machine elements manufactured in mass production results in a target conflict with respect to quality control of the production lots, esp. if metal forming techniques are the production principles. Usually individual parts are measured post process in form of random checks. This type of quality assurance is highly patchy and costly. The aim is thus to capture quality-related characteristics of the components in future integrated within the producing machine. In the case of the present work, the WPM-rolling was used in the final machining of the toothing. This method is a chipless process with internal gear rolling tools, which was developed in Poland by Prof. Marciniak in the 70s. The method is particularly suitable for the high speed production of splined shafts. The goal of the own investigations is to determine significant geometric feature characteristics of the toothed components that are suitable for future in-process measurement within the machine. For this purpose, different rolling series were performed on a rolling machine WPM 120. The technical process data of the WPM 120 were collected to ensure that all toothed components were produced under nearly identical conditions. By post-process measurements on a Leitz PMM 654 the geometric quality of all parts series was recorded and evaluated. It was found that the conventional definition of the gear quality is not sufficient to describe the resulting geometry after rolling. Through special section measurements on the splines in axial and radial directions, geometric characteristics of the gear components could be detected. The particular geometrical features of interest are the special head height and head shape of the rolled splines. These typical geometric features always arise during rolling with internally toothed tools. They are essentially dependent on the feed rate set on the machine. Using corresponding sensor systems provided inside the machine, these geometric features can serve as a reference base for a future in-process measurement framework. Further work on this topic should examine the problem of unbal-

anced volume distribution (tooth height and shape) of the deformed material at the circumference of the toothed sample.

Streszczenie

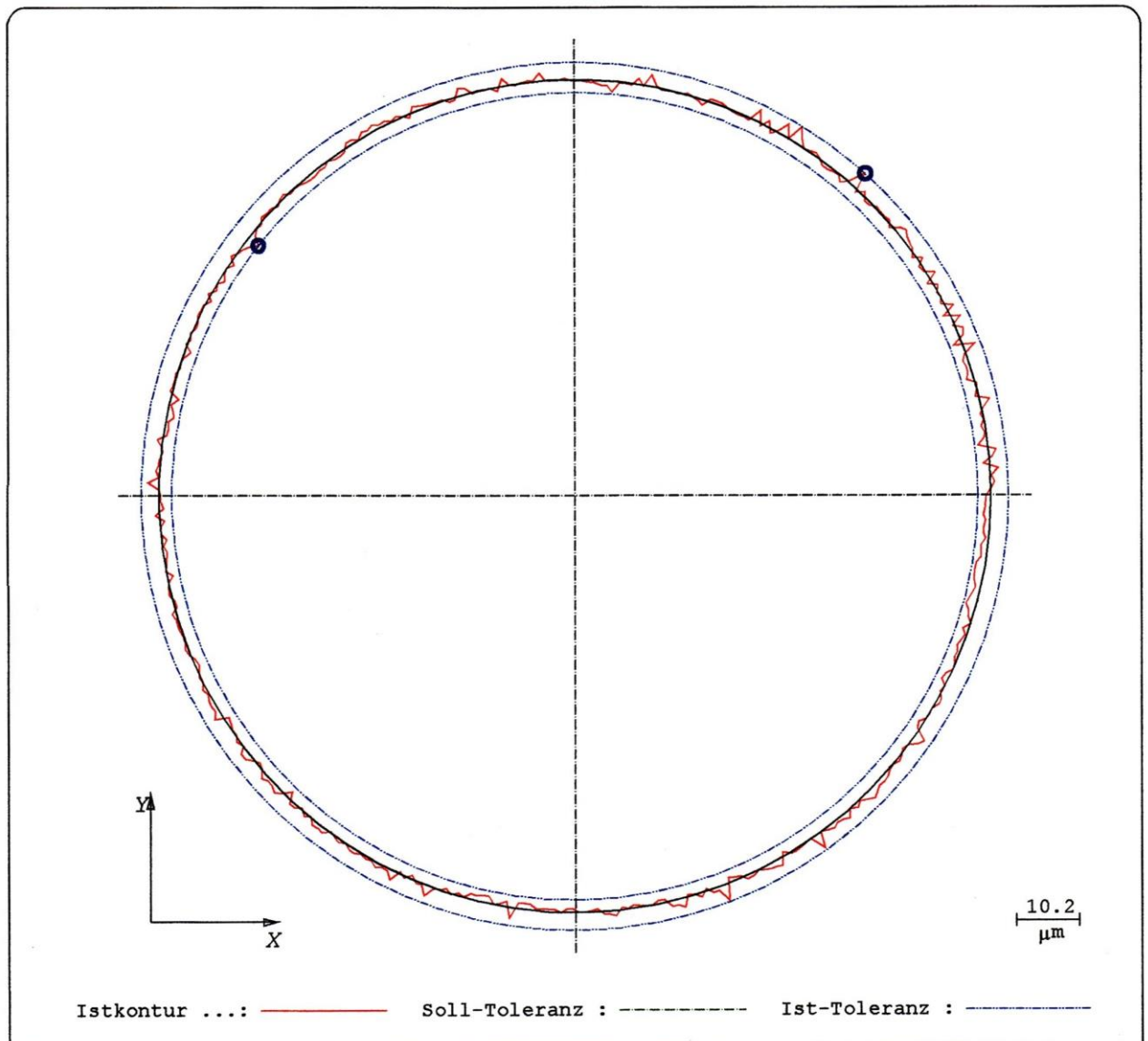
Tematyka rozprawy doktorskiej związana jest z produkcją wałków wielowypustowych. Na skalę przemysłową w produkcji seryjnej są one wytwarzane w ciągu różnych procesów obróbkowych. Rosnące wymagania dotyczące wykonywania części maszyn o wysokiej precyzji powodują konflikt pomiędzy koniecznością wytwarzania dużej liczby przedmiotów w produkcji masowej a koniecznością realizacji kontroli jakości partii, szczególnie jeśli wytwarzanie odbywa się przy zastosowaniu obróbki plastycznej. Zazwyczaj pojedyncze części mierzone są po zakończeniu procesu jako próbki losowe będące podstawą do oceny większej populacji. Ten sposób zapewnienia jakości przedmiotów jest bardzo wybiórczy i kosztowny.

W takim układzie celem rozprawy jest wyodrębnienie cech wykonywanych przedmiotów związanych z jakością w celu późniejszego integracji ich inspekcji w maszynie produkcyjnej. W pracy do wytwarzania gotowych elementów uzębionych zastosowano maszynę WPM opracowaną w Polsce przez profesora Marciniaka w latach 70-tych XX wieku. Pozwala ona realizować proces obróbkowy bezwiórowy, w którym narzędzia mają charakter elementów uzębionych o zębach wewnętrznych. Taka metoda wytwarzania jest szczególnie przydatna do bardzo szybkiej produkcji wałków wielowypustowych. Badania własne autora ukierunkowano na określenie istotnych cech geometrycznych charakteryzujących element uzębiony, które byłyby odpowiednie do kontroli w trakcie procesu. Do tego zadania wykonano serię przedmiotów badawczych na maszynie WPM 120. Dane procesu zostały zgromadzone i szczegółowo przebadane aby zapewnić, że wszystkie przedmioty wytworzono przy niemal identycznych warunkach obróbki. Zostały one następnie zmierzone po procesie wytwórczym na współrzędnościowej maszynie pomiarowej Leitz PMM 654, a wyniki poddano analizie. W jej trakcie okazało się, że konwencjonalna definicja jakości uz-

ębień jest niewystarczająca do opisu wynikowej geometrii po procesie walcowania. Poprzez odpowiednią selekcję sekwencji pomiarowych na wielowypustach w kierunku osiowym i promieniowym możliwe jest określenie cech geometrycznych elementów zębatych. Szczególnie interesującymi cechami są wysokość głowy zęba i jej kształt dla walcowanych wielowypustów. Te typowe cechy geometryczne są zawsze miarą jakości wykonania w czasie walcowania za pomocą narzędzi z zębami wewnętrznymi. Są one istotnie zależne od posuwu ustawionego na maszynie. Stosując odpowiedni system sensorów zainstalowanych wewnątrz maszyny produkcyjnej cechy te można wykorzystać jako bazę odniesienia dla przyszłego układu pomiarowego zrealizowanego w kontroli czynnej. Dalsze prace na ten temat będą dotyczyły badania problemu niezerównoważonego rozkładu objętości (wysokość i kształt zęba) deformowanego materiału na obwodzie przedmiotu uzębionego.

Appendix 1: Blank Geometry

Circles outer cylinder roundness	1.1 -1.3
Cylinder form deviation	1.4
List of measurement results	1.5 a -c



Bez.: Rohteil WPM

Herst. ...:

Zeich.-Nr.:

Ser.-Nr. : 32

Sachnr. ..:

Abteilung :

Berechn. : Gauss

Filter ...: Kein Wel./Umf.

Tast. Dur.: 5 mm

Element ..: CIR_U

Durchm. : 62.2825

Form: 0.0049

X-Koord. : -0.0009

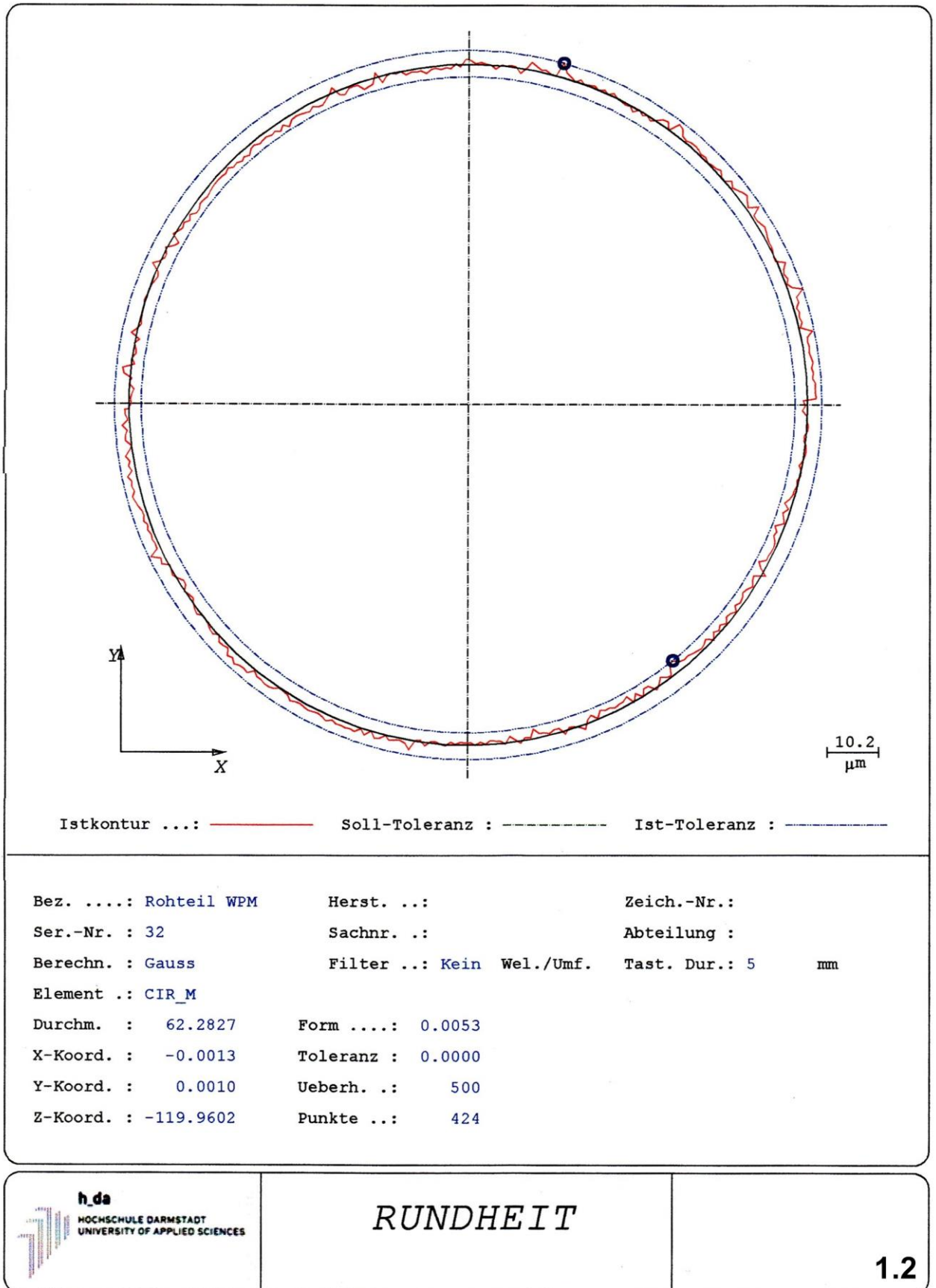
Toleranz : 0.0000

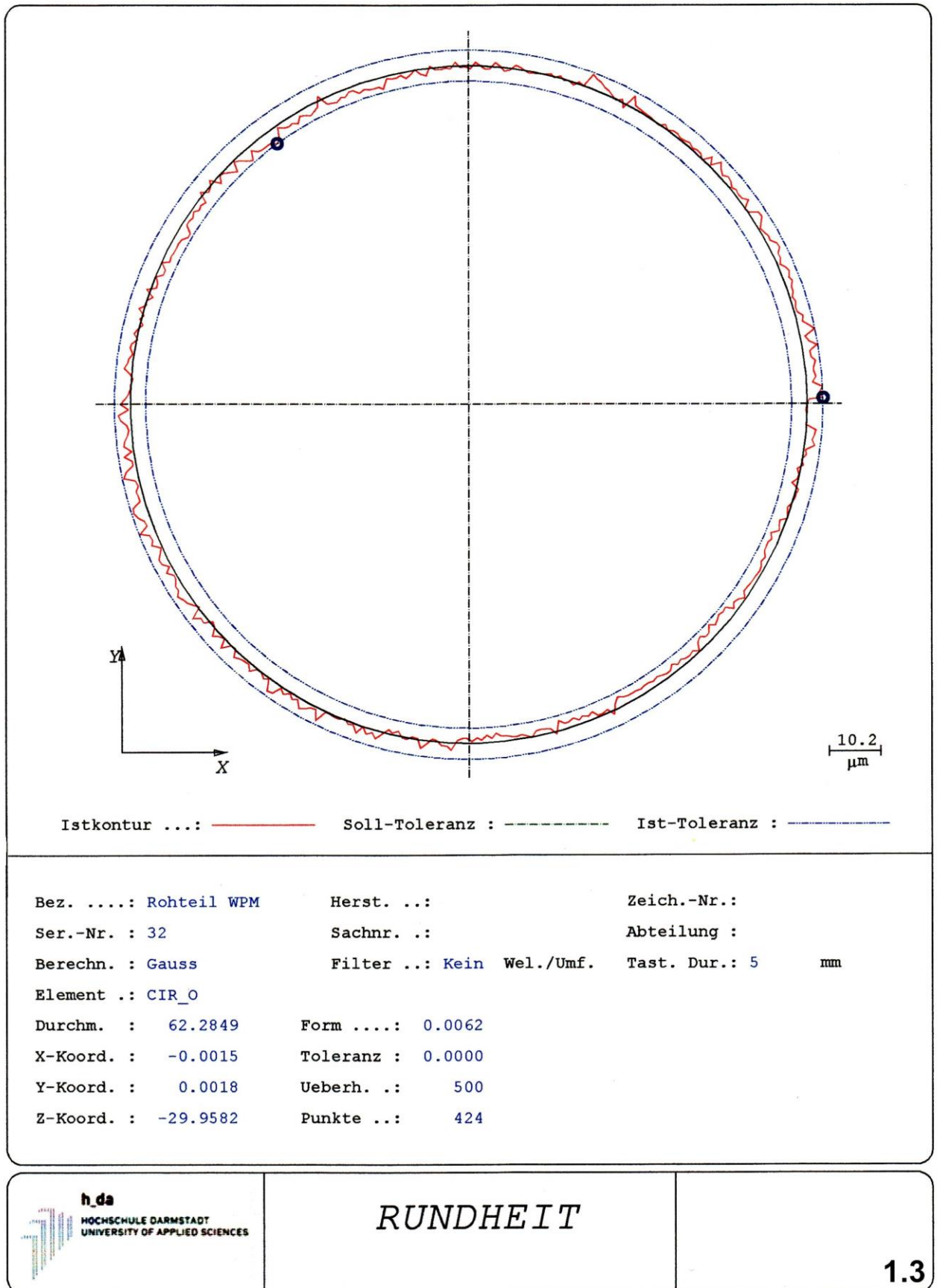
Y-Koord. : -0.0001

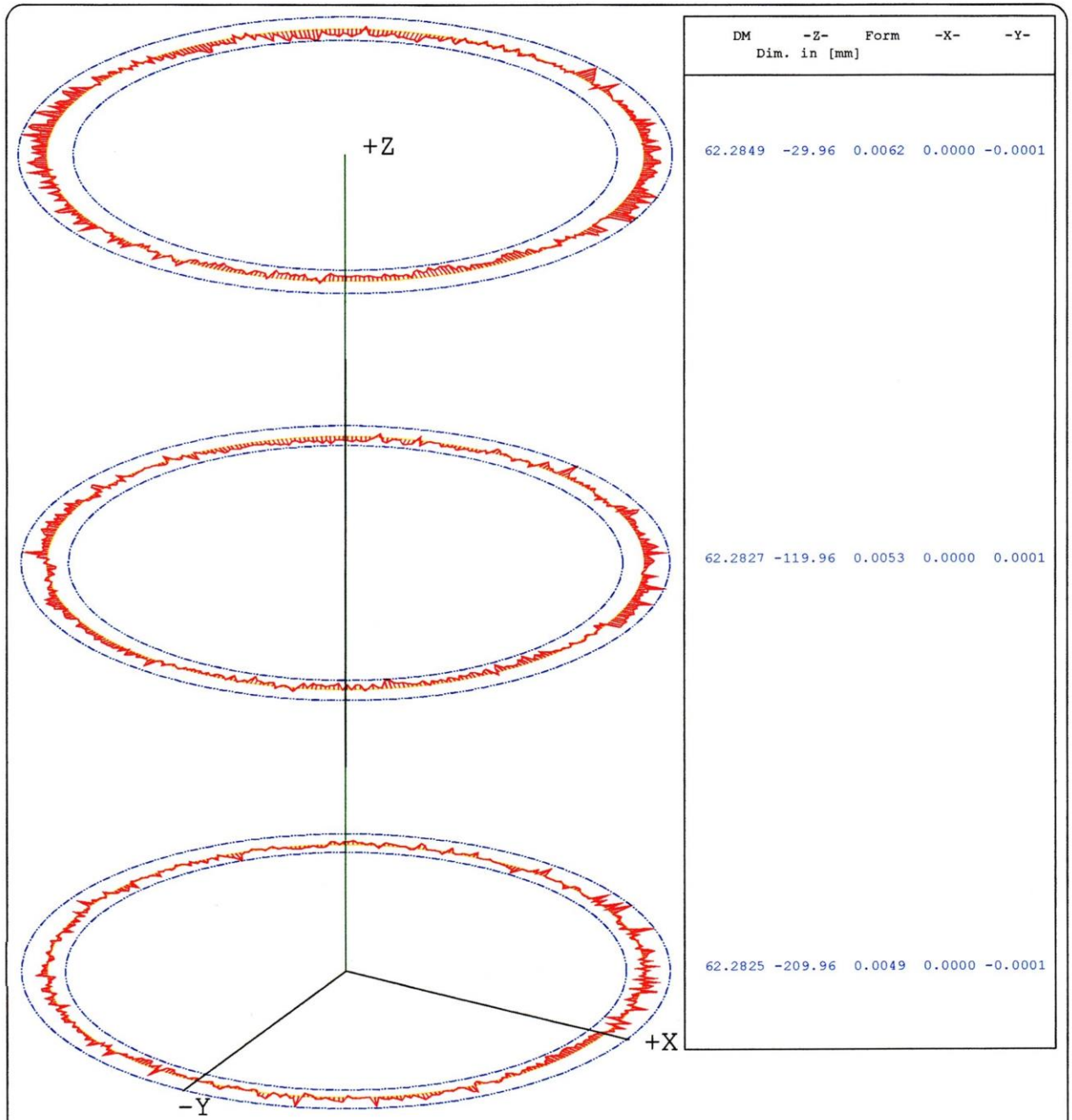
Ueberh. ..: 500

Z-Koord. : -209.9625

Punkte ...: 424



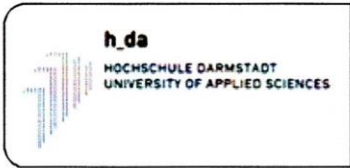




DM	-Z-	Form	-X-	-Y-
Dim. in [mm]				
62.2849	-29.96	0.0062	0.0000	-0.0001
62.2827	-119.96	0.0053	0.0000	0.0001
62.2825	-209.96	0.0049	0.0000	-0.0001

Istkontur: ————— Ist-Toleranz ..: - - - - -

Bez.: Rohteil WPM	Herst. ...:	Zeich.-Nr.:
Ser.-Nr. : 32	Sachnr. ..:	Abteilung :
Berechn. : Tschebyscheff	Filter ...: Kein Wel./Umf.	Tast. Dur.: 5 mm
Elemente : (CIR_U, CIR_M, CIR_O)		
Ueberhoehung Kreisform ...: 1000	Ueberhoehung Achse: 5000	
Toleranz Kreisform: 0.0000	Geradheit der Achse: 0.0002	
Zylinderform (Tscheby)...: 0.0065	Zylinderdurchmesser: 62.2846	



ZYLINDERFORM

ISO 1101

h_da HOCHSCHULE DARMSTADT UNIVERSITY OF APPLIED SCIENCES		Messprotokoll				Leitz	
Hochschule Darmstadt Haardtring 100				Maschinenbau & Kunststofftechnik D-64295 Darmstadt			
Bezeichnung	Rohteil WPM	Hersteller					
Zeichnungs-Nr.		Seriennummer		32			
Bemerkung		Sachnummer					
Laufende Nummer		Auftrag					
Prüfer		Abteilung					
Messgerät	PMM 6 5 4 #513	Prüfdatum					
Text	Ausw.	Istmaß	Nennmaß	O.Tol.	U.Tol.	Ist-Soll	Grafik
KREIS(1)		CIR					
	FORM	0.0023	0.0000	0.0500	0.0000	0.0023	
	DM	54.9967	0.0000	0.0500	-0.0500	54.9967	
	RA	27.4983	0.0000	0.0500	-0.0500	27.4983	
	X	361.5659	0.0000	0.0500	-0.0500	361.5659	
	Y	251.0563	0.0000	0.0500	-0.0500	251.0563	
	Z	-12.9937	0.0000	0.0500	-0.0500	12.9937	
KREIS(2)		CIR					
	FORM	0.0018	0.0000	0.0500	0.0000	0.0018	
	DM	55.0056	0.0000	0.0500	-0.0500	55.0056	
	RA	27.5028	0.0000	0.0500	-0.0500	27.5028	
	X	361.5081	0.0000	0.0500	-0.0500	361.5081	
	Y	251.0227	0.0000	0.0500	-0.0500	251.0227	
	Z	205.8265	0.0000	0.0500	-0.0500	205.8265	
AXI(1)		AXI					
	PA_PXPY	-149.8296	0.0000	0.0500	-0.0500	149.8296	
	PA_PXPZ	90.0151	0.0000	0.0500	-0.0500	90.0151	
	PA_PYPZ	90.0088	0.0000	0.0500	-0.0500	90.0088	
PNT(1)		POI					
	X	366.2157	0.0000	0.0500	-0.0500	366.2157	
	Y	233.4764	0.0000	0.0500	-0.0500	233.4764	
	Z	212.7089	0.0000	0.0500	-0.0500	212.7089	
EBENE(1)		PLA					
	FORM	0.0152	0.0000	0.0500	0.0000	0.0152	
	PA_PXPY	43.9510	0.0000	0.0500	-0.0500	43.9510	
	PA_PXPZ	89.9922	0.0000	0.0500	-0.0500	89.9922	
	PA_PYPZ	89.9925	0.0000	0.0500	-0.0500	89.9925	
	Z	-0.0238	0.0000	0.0500	-0.0500	0.0238	
FLAT(1)		PLA					
	FLATNS	0.0137	0.0000	0.0500	0.0000	0.0137	
	MIN	-0.0068					
	MAX	0.0068					
	SIGMA	0.0054					
Text	Ausw.	Istmaß	Nennmaß	O.Tol.	U.Tol.	Ist-Soll	Grafik
				WPMROH		Seite: 1 von 3	

Datum:			WPMROH				Seite: 2 von 3	
Text	Ausw.	Istmaß	Nennmaß	O.Tol.	U.Tol.	Ist-Soll	Grafik	
PLAN(1)			PLA					
	AXIRUN	0.0206	0.0000	0.0500	0.0000	0.0206		
RECHT(1)			PLA					
	SQRNES	0.0206	0.0000	0.0500	0.0000	0.0206		
ZENT(1)			POI					
	X	0.1047	0.0000	0.0500	-0.0500	0.1047		
	Y	-0.0149	0.0000	0.0500	-0.0500	0.0149		
	Z	-5.9537	0.0000	0.0500	-0.0500	5.9537		
	XY	0.1058	0.0000	0.0500	-0.0500	0.1058		
EXZENT(1)			AXI					
	DX	-0.1047	0.0000	0.0500	-0.0500	0.1047		
	DY	0.0149	0.0000	0.0500	-0.0500	0.0149		
	DZ	0.0000	0.0000	0.0500	-0.0500	0.0000		
	DXY	0.1058	0.0000	0.0500	-0.0500	0.1058		
CIR_U			CIR					
	FORM	0.0049	0.0000	0.0500	0.0000	0.0049		
	DM	62.2825	0.0000	0.0500	-0.0500	62.2825		
	RA	31.1412	0.0000	0.0500	-0.0500	31.1412		
	X	-0.0009	0.0000	0.0500	-0.0500	0.0009		
	Y	-0.0001	0.0000	0.0500	-0.0500	0.0001		
	Z	-209.9625	0.0000	0.0500	-0.0500	209.9625		
CIR_M			CIR					
	FORM	0.0053	0.0000	0.0500	0.0000	0.0053		
	DM	62.2827	0.0000	0.0500	-0.0500	62.2827		
	RA	31.1413	0.0000	0.0500	-0.0500	31.1413		
	X	-0.0013	0.0000	0.0500	-0.0500	0.0013		
	Y	0.0010	0.0000	0.0500	-0.0500	0.0010		
	Z	-119.9602	0.0000	0.0500	-0.0500	119.9602		
CIR_O			CIR					
	FORM	0.0062	0.0000	0.0500	0.0000	0.0062		
	DM	62.2849	0.0000	0.0500	-0.0500	62.2849		
	RA	31.1424	0.0000	0.0500	-0.0500	31.1424		
	X	-0.0015	0.0000	0.0500	-0.0500	0.0015		
	Y	0.0018	0.0000	0.0500	-0.0500	0.0018		
	Z	-29.9582	0.0000	0.0500	-0.0500	29.9582		
CYL(1)			CYL					
	DM	62.2833	0.0000	0.0500	-0.0500	62.2833		
	FORM	0.0068	0.0000	0.0500	0.0000	0.0068		
CYL_FM			CYL					
	CYLFRM	0.0065	0.0000	0.0500	0.0000	0.0065		
	MIN	-0.0033						
	MAX	0.0033						
	SIGMA	0.0013						
EX(2)			AXI					
	DX	-0.1064	0.0000	0.0500	-0.0500	0.1064		
	DY	0.0169	0.0000	0.0500	-0.0500	0.0169		
	DZ	0.0000	0.0000	0.0500	-0.0500	0.0000		
	DXY	0.1077	0.0000	0.0500	-0.0500	0.1077		
WINK(1)			ANG					
	ANG	0.0006	0.0000	0.0500	-0.0500	0.0006		
Text	Ausw.	Istmaß	Nennmaß	O.Tol.	U.Tol.	Ist-Soll	Grafik	
				WPMROH		Seite: 2 von 3		

			WPMROH			Seite: 3 von 3	
Text	Ausw.	Istmaß	Nennmaß	O.Tol.	U.Tol.	Ist-Soll	Grafik
WINK(1)			ANG				
	C_ANG180	179.9994	0.0000	0.0500	-0.0500	179.9994	
STIRN(1)			PLA				
	AXIRUN	0.0203	0.0000	0.0500	0.0000	0.0203	
RUND_CYL(1)			AXI				
	RADRUN	0.0091	0.0000	0.0500	0.0000	0.0091	
	RADMAX	0.0107	0.0000	0.0500	0.0000	0.0107	
RUND_KU			AXI				
	RADRUN	0.0052	0.0000	0.0500	0.0000	0.0052	
	RADMAX	0.0067	0.0000	0.0500	0.0000	0.0067	
RUND_KM			AXI				
	RADRUN	0.0075	0.0000	0.0500	0.0000	0.0075	
	RADMAX	0.0086	0.0000	0.0500	0.0000	0.0086	
RUND_KO			AXI				
	RADRUN	0.0087	0.0000	0.0500	0.0000	0.0087	
	RADMAX	0.0109	0.0000	0.0500	0.0000	0.0109	

Text	Ausw.	Istmaß	Nennmaß	O.Tol.	U.Tol.	Ist-Soll	Grafik
			WPMROH			Seite: 3 von 3	

Appendix 2: Gear tooth quality (DIN 3960 ff.)

Pitch and concentricity deviation	2.1 – 2.2
Root diameter, roundness	2.3
Tip diameter, roundness	2.4
Tooth trace deviation	2.5 – 2.10
Profile deviation	2.11 – 2.16

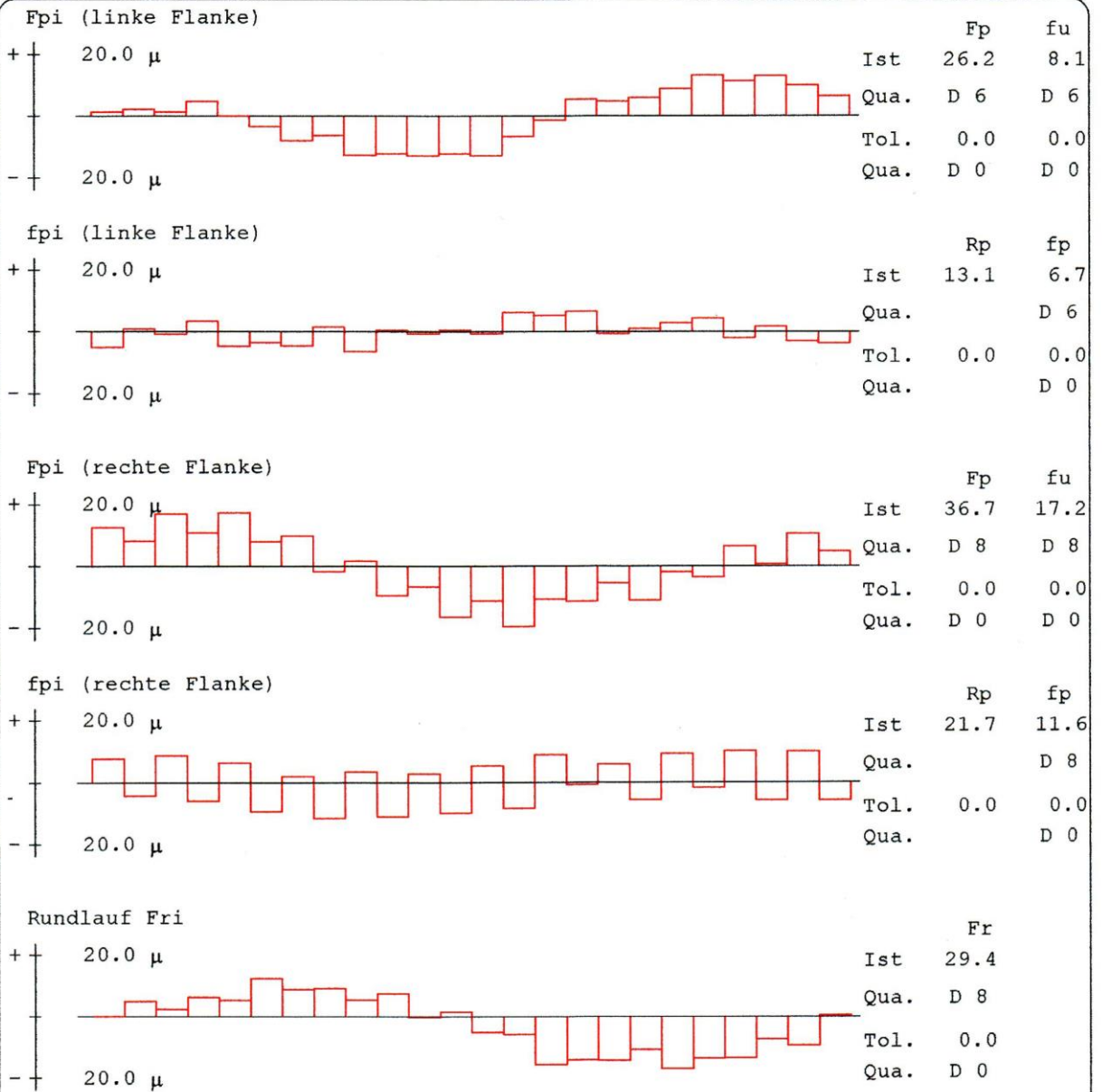


**QUINDOS
ZAHNRAD**


Zaehnezahl : 24
Normalmodul : 2.5000
Eingr.winkel: 30.0000
Schr.winkel : 0.0000
Steig.Richt.: gerade
Zahnbreite :103.0000

Hersteller :
Seriennummer: 07
Bemerkung : Z = -57
Bezeichnung : WPM_GEW
Sachnummer :
Pruefer/Dat.:


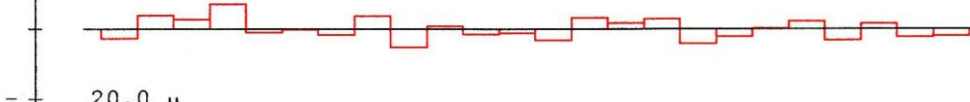
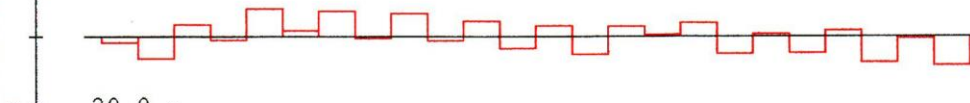
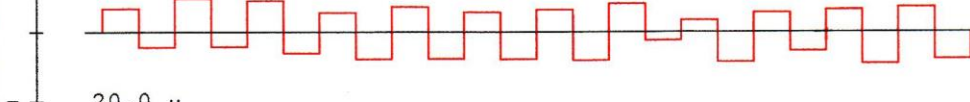
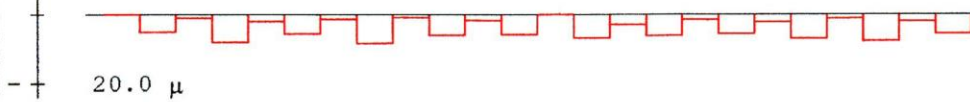
Beurteilung : i.O. n.i.O. T. N. R.

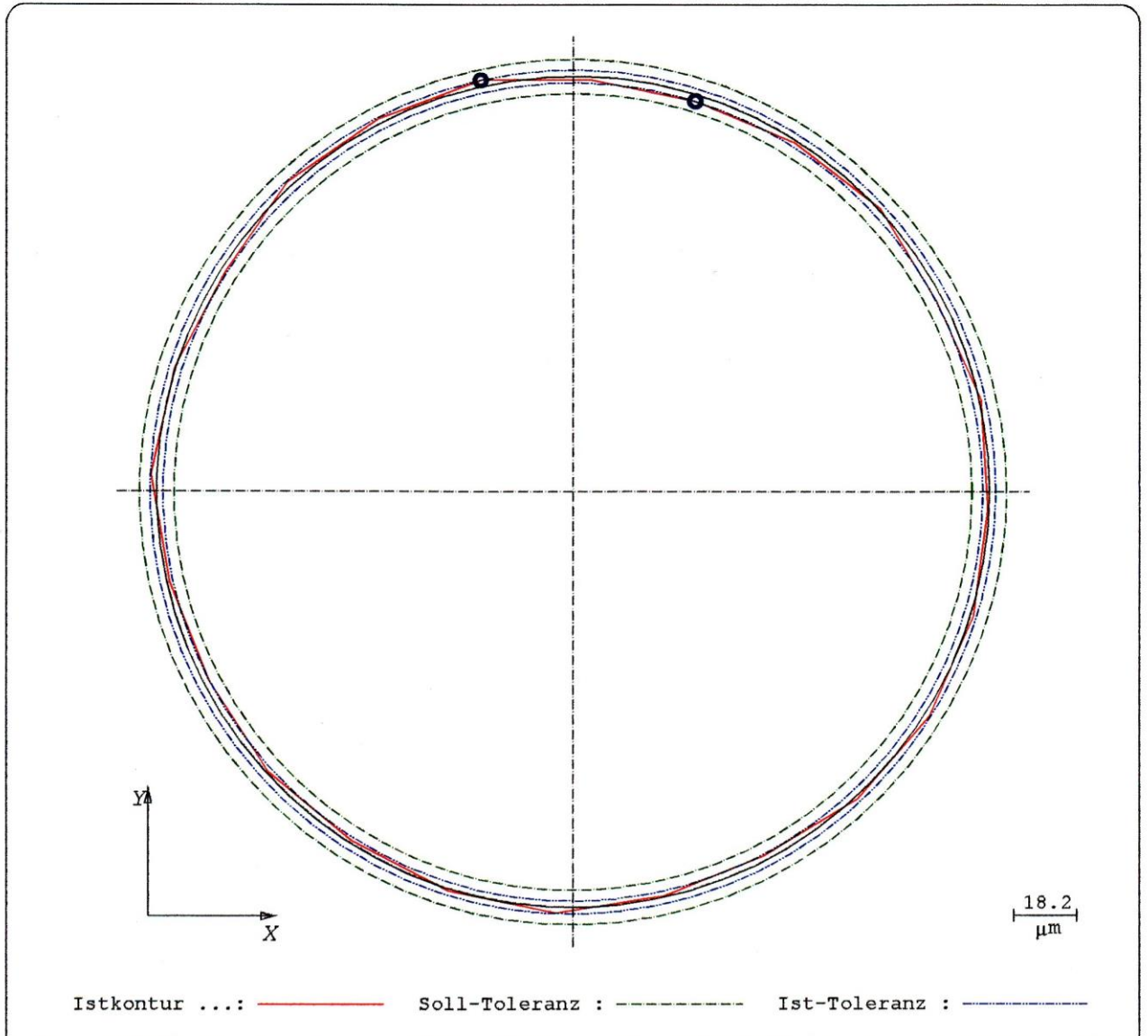


2.1

 <p>MESSTECHNIK WETZLAR GmbH Metrology Systems</p> <p>QUINDOS ZAHNRAD</p>	Zaehnezahl : 24	Hersteller :
	Normalmodul : 2.5000	Seriennummer: 07
	Eingr.winkel: 30.0000	Bemerkung : Z = -57
	Schr.winkel : 0.0000	Bezeichnung : WPM_GEW
	Steig.Richt.: gerade	Sachnummer :
Zahnbreite :103.0000	Pruefer/Dat.:	

Beurteilung : i.O. n.i.O. T. N. R.

Fpi (linke Flanke) - eFr		Fp	fu
+ 20.0 μ	Ist	14.8	9.0
	Qua.	D 5	D 6
- 20.0 μ	Tol.	0.0	0.0
	Qua.	D 0	D 0
fpi (linke Flanke) - eFr		Rp	fp
+ 20.0 μ	Ist	12.4	7.2
	Qua.		D 7
- 20.0 μ	Tol.	0.0	0.0
	Qua.		D 0
Fpi (rechte Flanke) - eFr		Fp	fu
+ 20.0 μ	Ist	16.3	16.3
	Qua.	D 5	D 8
- 20.0 μ	Tol.	0.0	0.0
	Qua.	D 0	D 0
fpi (rechte Flanke) - eFr		Rp	fp
+ 20.0 μ	Ist	18.8	9.6
	Qua.		D 7
- 20.0 μ	Tol.	0.0	0.0
	Qua.		D 0
Rundlauf Fri - eFr		Fr	
+ 20.0 μ	Ist	8.3	
	Qua.	D 4	
- 20.0 μ	Tol.	0.0	
	Qua.	D 0	
Exzentrizitaet 0.0125 X 0.0021 Y -0.0123			



Bez.: WPM_GEW

Herst. ...:

Zeich.-Nr.: 07

Ser.-Nr. : 07

Sachnr. ..:

Abteilung :

Berechn. : Gauss

Filter ...: Kein Wel./Umf.

Tast. Dur.: 1.5 mm

Element ..: Fk_M(1)

Durchm. : 58.7658

Form: 0.0037

X-Koord. : 0.0018

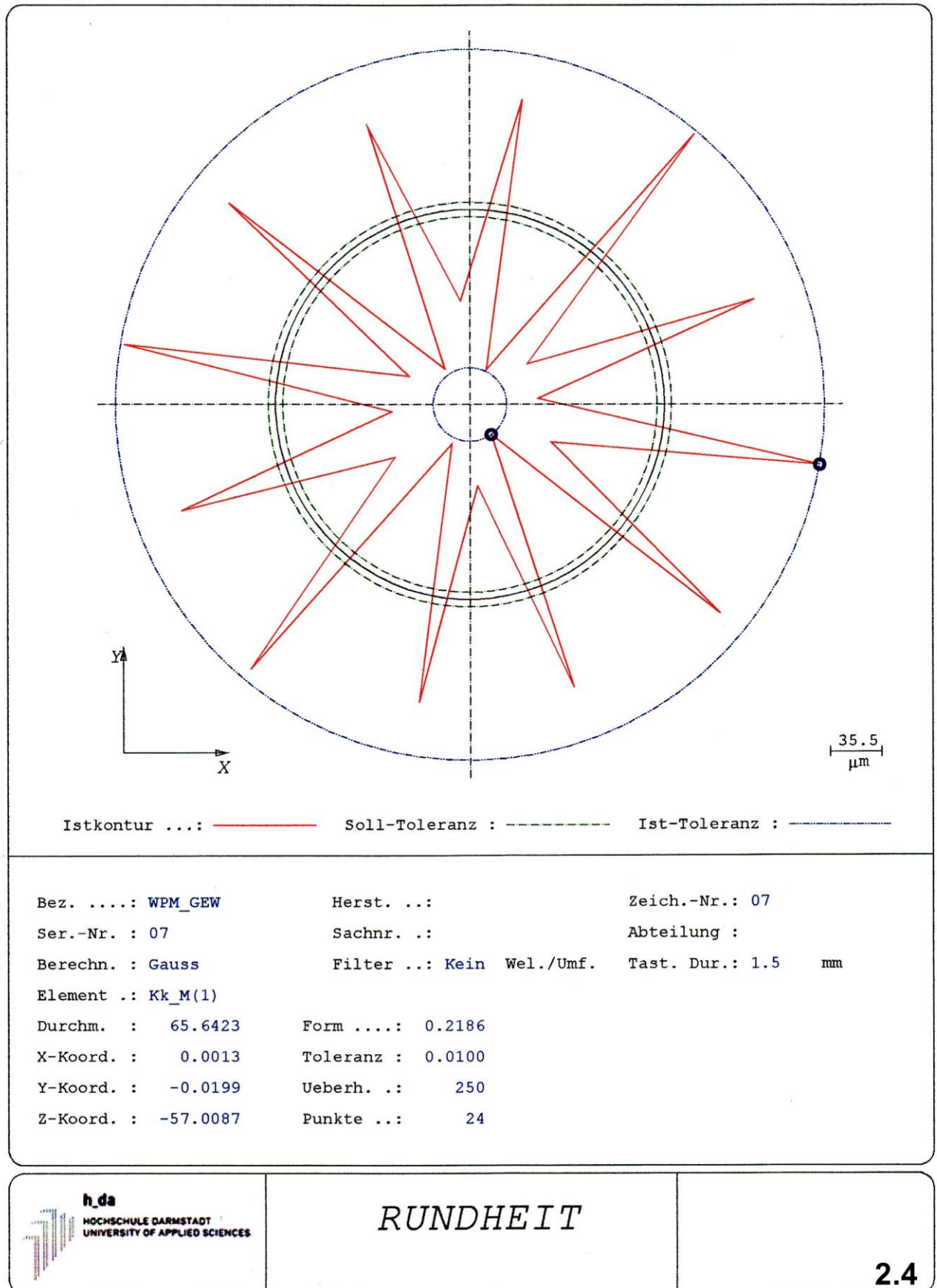
Toleranz : 0.0100


Y-Koord. : -0.0111

Ueberh. ..: 250

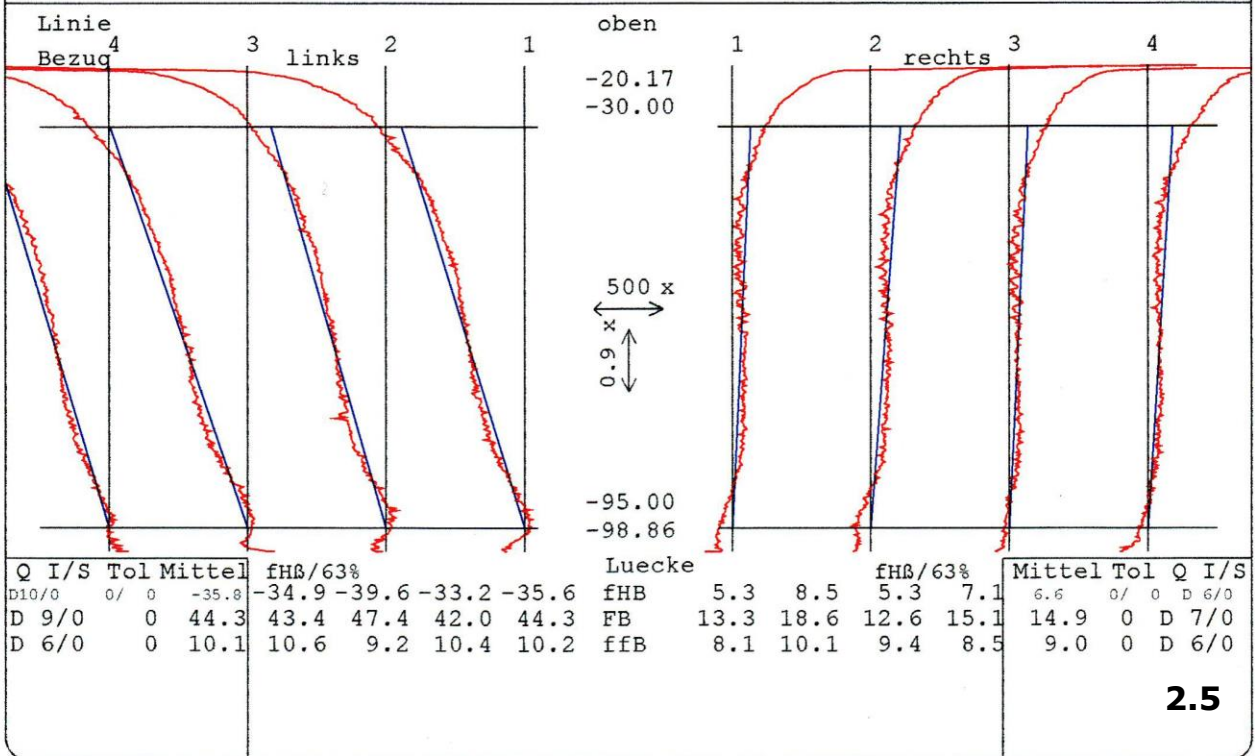
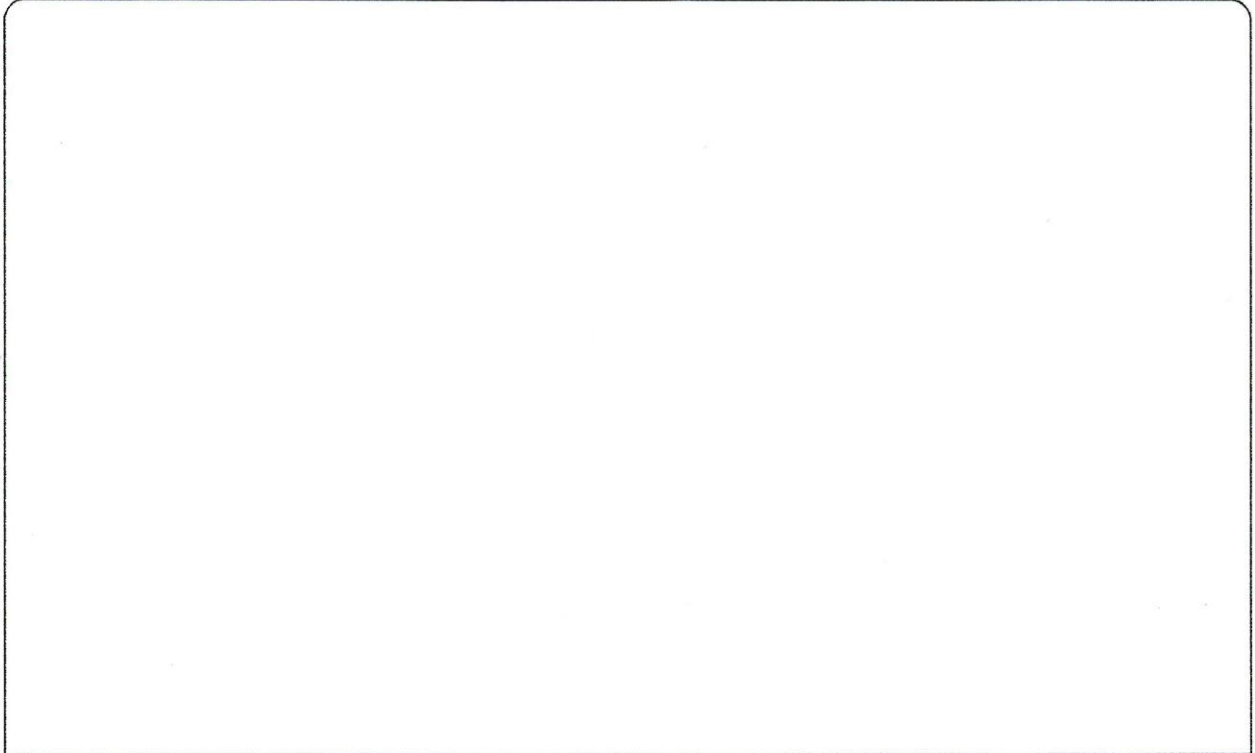
Z-Koord. : -57.0087


Punkte ...: 24



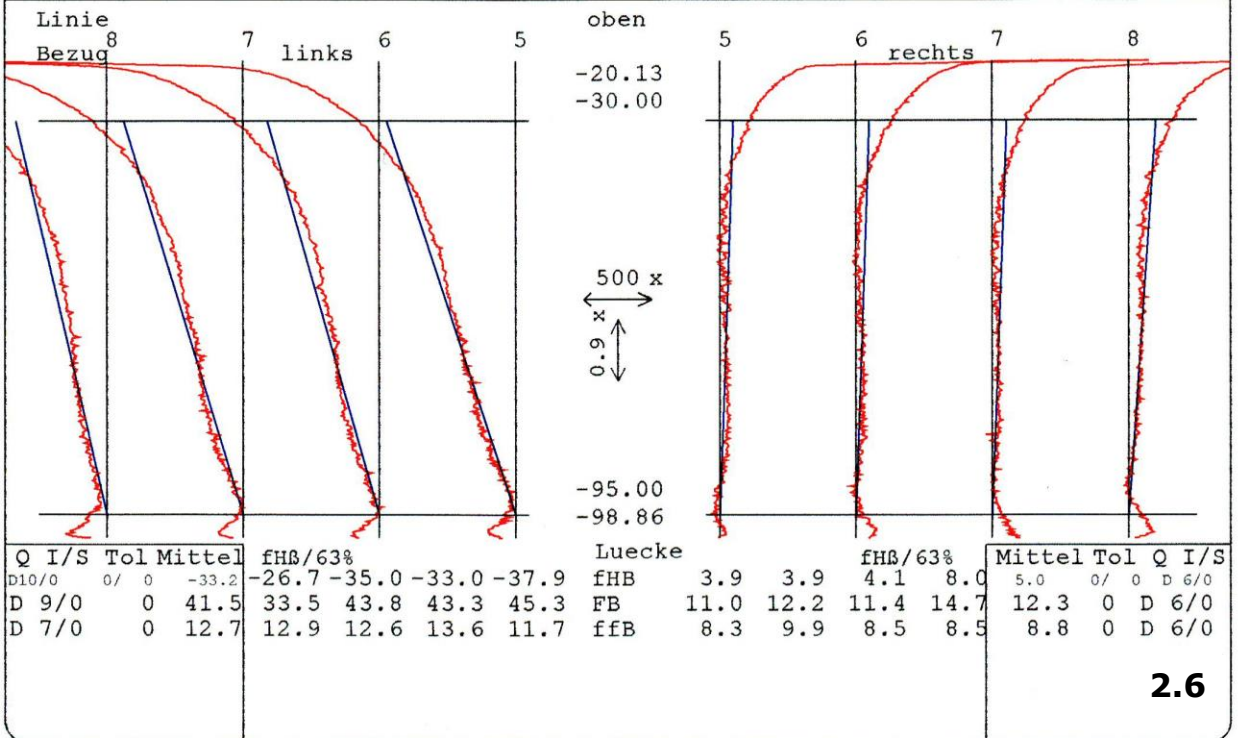
 MESSTECHNIK WETZLAR GmbH Metrology Systems QUINDOS ZAHNRAD	Zaehnezahl : 24	Hersteller :
	Normalmodul : 2.5000	Seriennummer: 07
	Eingr.winkel: 30.0000	Bemerkung : Z = -57
	Schr.winkel : 0.0000	Bezeichnung : WPM_GEW
	Steig.Richt.: gerade	Sachnummer :
Zahnbreite :103.0000	Pruefer/Dat.:	


Beurteilung : i.O. n.i.O. T. N. R.



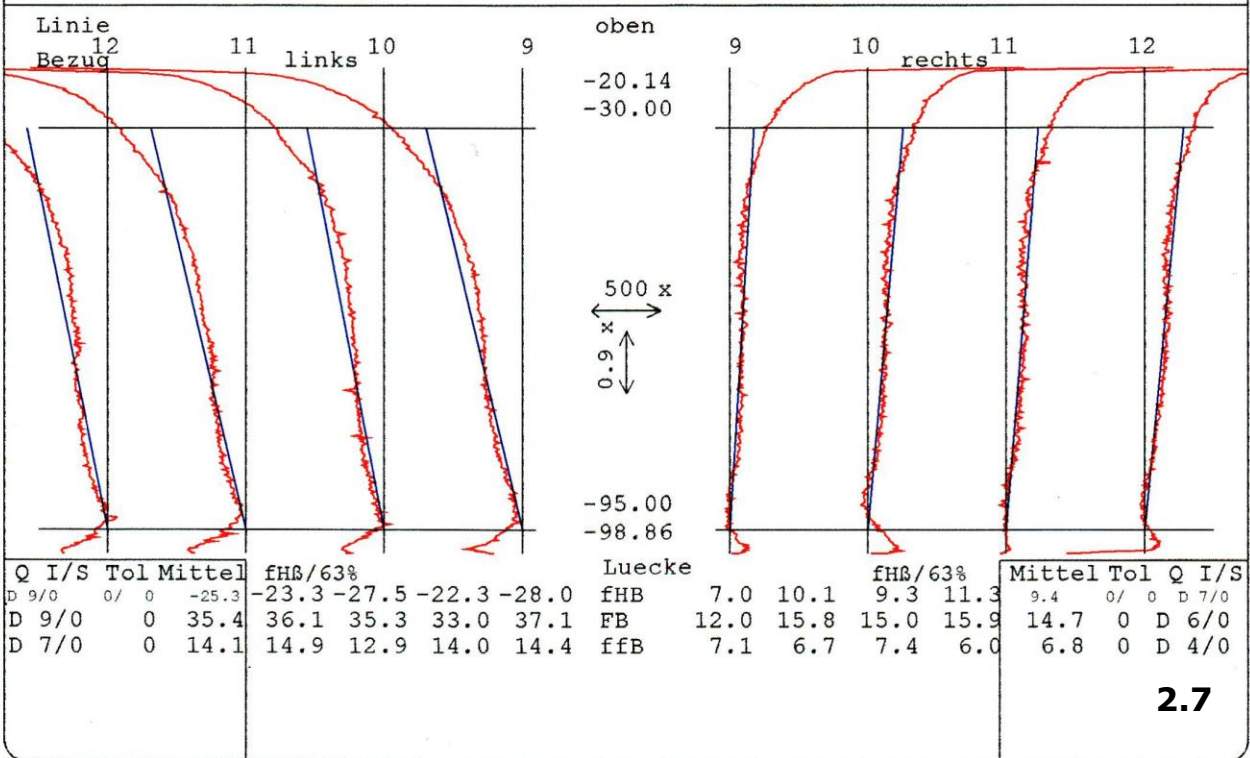
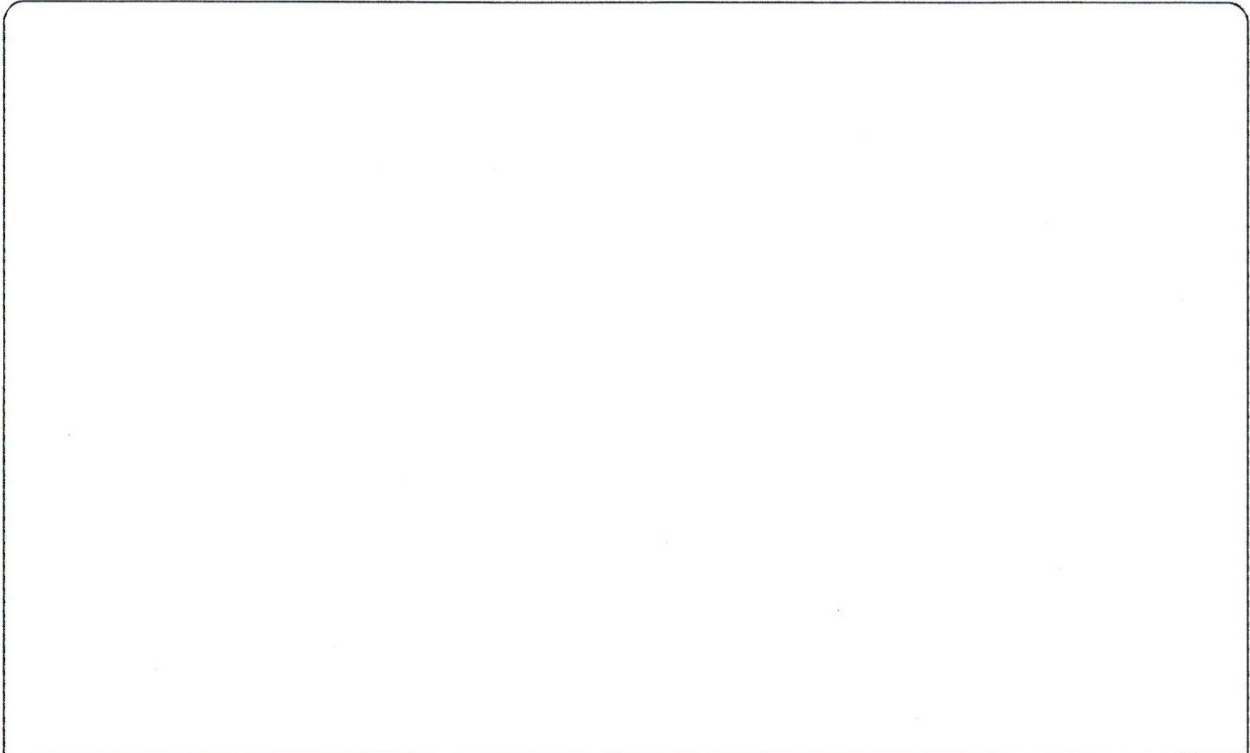
 <p>MESSTECHNIK WETZLAR GmbH Metrology Systems</p> <p>QUINDOS ZAHNRAD</p>	Zaehnezahl : 24	Hersteller :
	Normalmodul : 2.5000	Seriennummer: 07
	Eingr.winkel: 30.0000	Bemerkung : Z = -57
	Schr.winkel : 0.0000	Bezeichnung : WPM_GEW
	Steig.Richt.: gerade	Sachnummer :
Zahnbreite :103.0000	Pruefer/Dat.:	


Beurteilung : i.O. n.i.O. T. N. R.



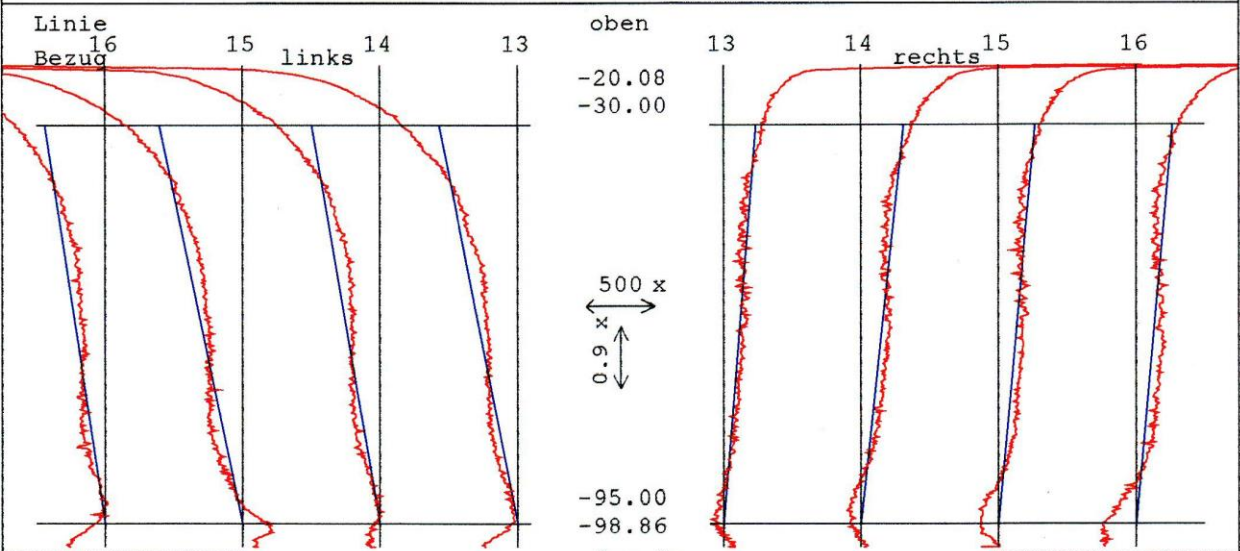
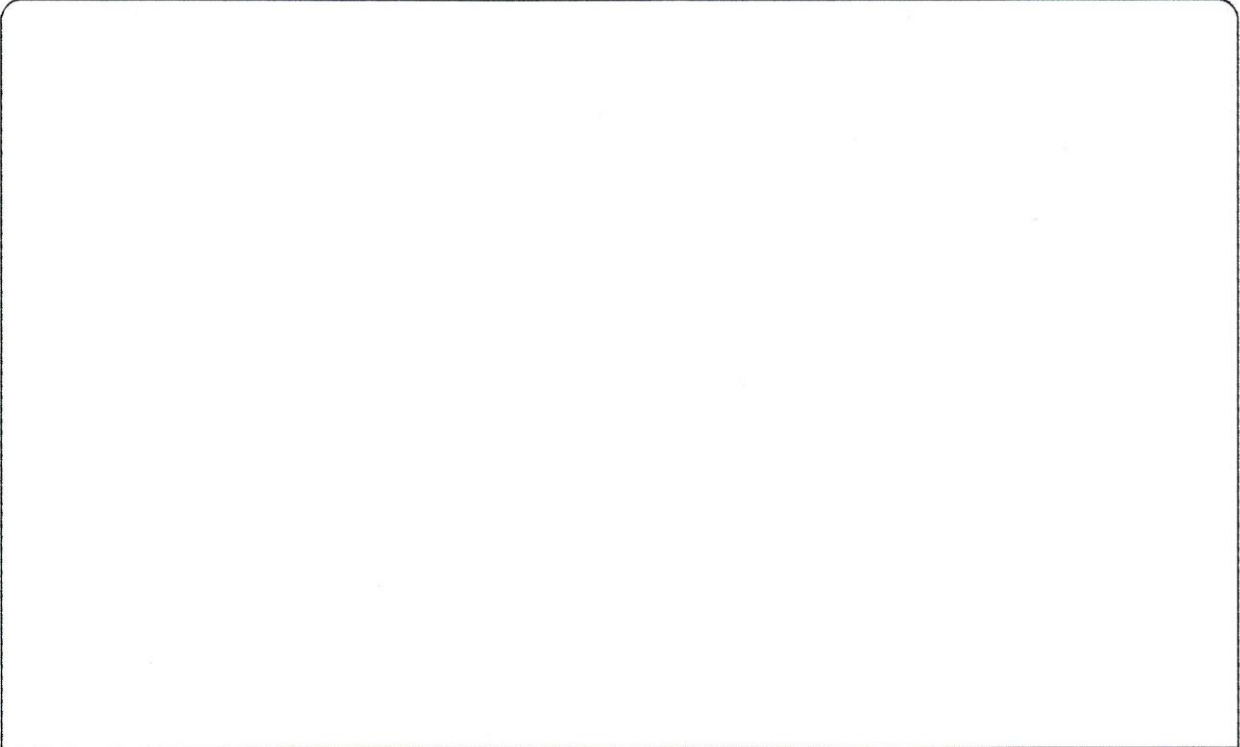
 MESSTECHNIK WETZLAR GmbH Metrology Systems QUINDOS ZAHNRAD	Zaehnezahl : 24	Hersteller :
	Normalmodul : 2.5000	Seriennummer: 07
	Eingr.winkel: 30.0000	Bemerkung : Z = -57
	Schr.winkel : 0.0000	Bezeichnung : WPM_GEW
	Steig.Richt.: gerade	Sachnummer :
Zahnbreite :103.0000	Pruefer/Dat.:	

Beurteilung : i.O. n.i.O. T. N. R.




 <p>MESSTECHNIK WETZLAR GmbH Metrology Systems</p> <p>QUINDOS ZAHNRAD</p>	Zaehnezahl : 24	Hersteller :
	Normalmodul : 2.5000	Seriennummer: 07
	Eingr.winkel: 30.0000	Bemerkung : Z = -57
	Schr.winkel : 0.0000	Bezeichnung : WPM_GEW
	Steig.Richt.: gerade	Sachnummer :
Zahnbreite :103.0000	Pruefer/Dat.: -	

Beurteilung : i.O. n.i.O. T. N. R.

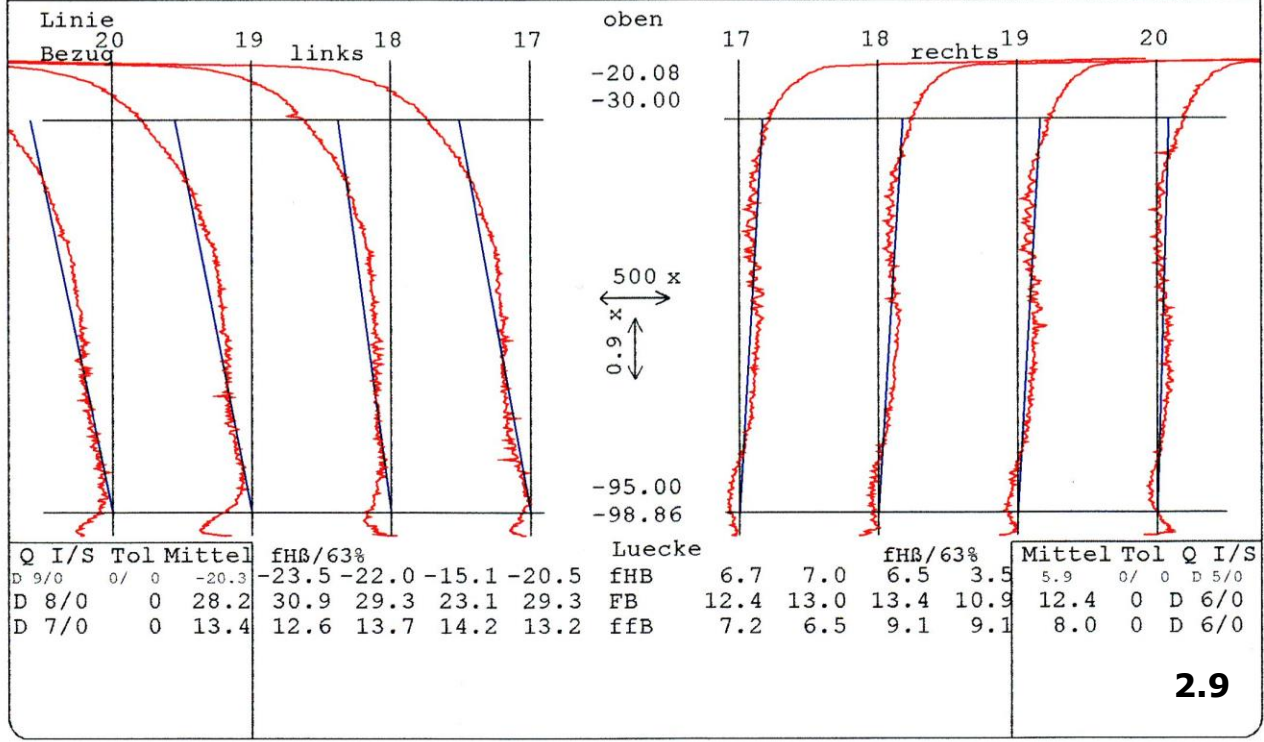
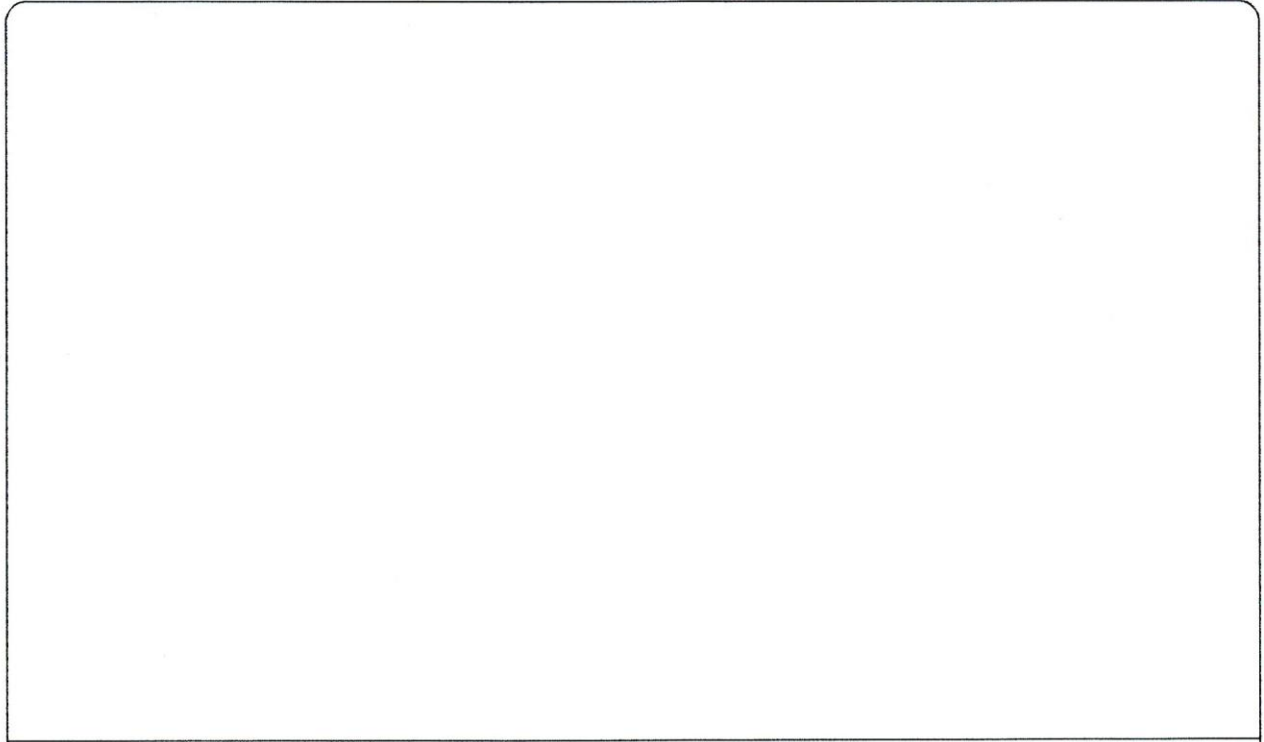



Q	I/S	Tol	Mittel	fH8/63%				Luecke	fH8/63%				Mittel	Tol	Q	I/S
D 9/0	0/ 0	0	-21.1	-17.5	-24.2	-19.9	-22.8	fHB	9.3	12.3	10.6	10.5	10.7	0/ 0	D 7/0	
D 9/0	0	0	32.7	27.0	40.4	30.6	32.8	FB	15.1	18.8	17.9	22.3	18.6	0	D 8/0	
D 8/0	0	0	15.2	13.7	16.5	14.8	15.8	ffb	6.0	7.4	9.2	13.6	9.1	0	D 7/0	

2.8

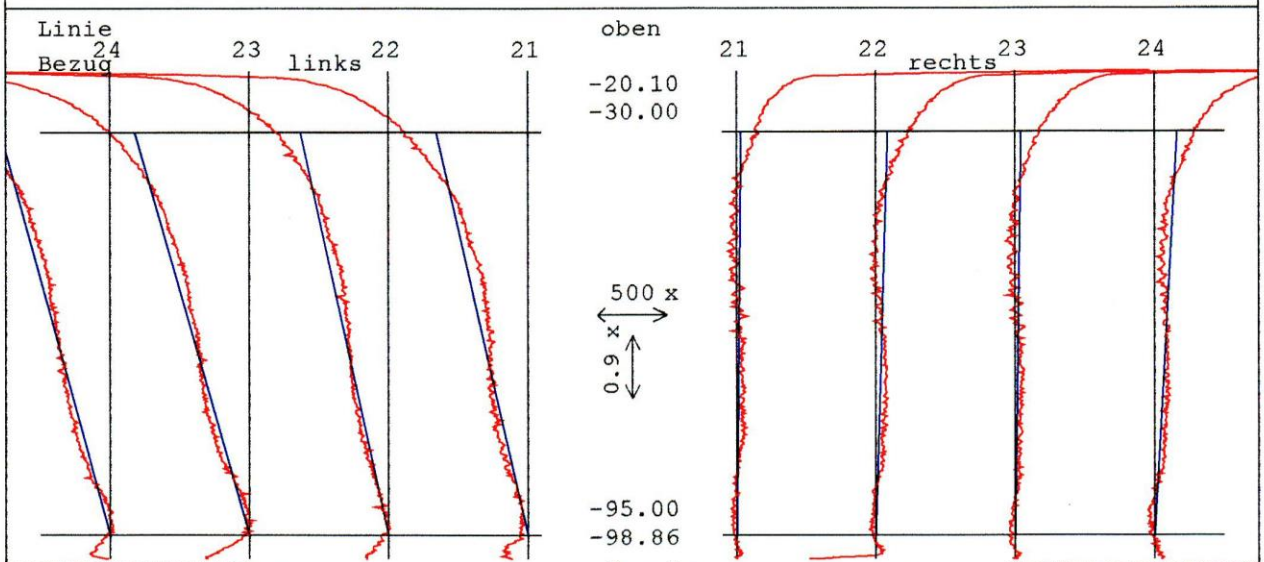
 MESSTECHNIK WETZLAR GmbH Metrology Systems QUINDOS ZAHNRAD	Zaehnezahl : 24	Hersteller :
	Normalmodul : 2.5000	Seriennummer: 07
	Eingr.winkel: 30.0000	Bemerkung : Z = -57
	Schr.winkel : 0.0000	Bezeichnung : WPM_GEW
	Steig.Richt.: gerade	Sachnummer :
Zahnbreite :103.0000	Pruefer/Dat.:	

Beurteilung : i.O. n.i.O. T. N. R.




 <p>MESSTECHNIK WETZLAR GmbH Metrology Systems</p> <p>QUINDOS ZAHNRAD</p>	Zaehnezahl : 24	Hersteller :
	Normalmodul : 2.5000	Seriennummer: 07
	Eingr.winkel: 30.0000	Bemerkung : Z = -57
	Schr.winkel : 0.0000	Bezeichnung : WPM_GEW
	Steig.Richt.: gerade	Sachnummer :
Zahnbreite :103.0000	Pruefer/Dat.:	

Beurteilung : i.O. n.i.O. T. N. R.

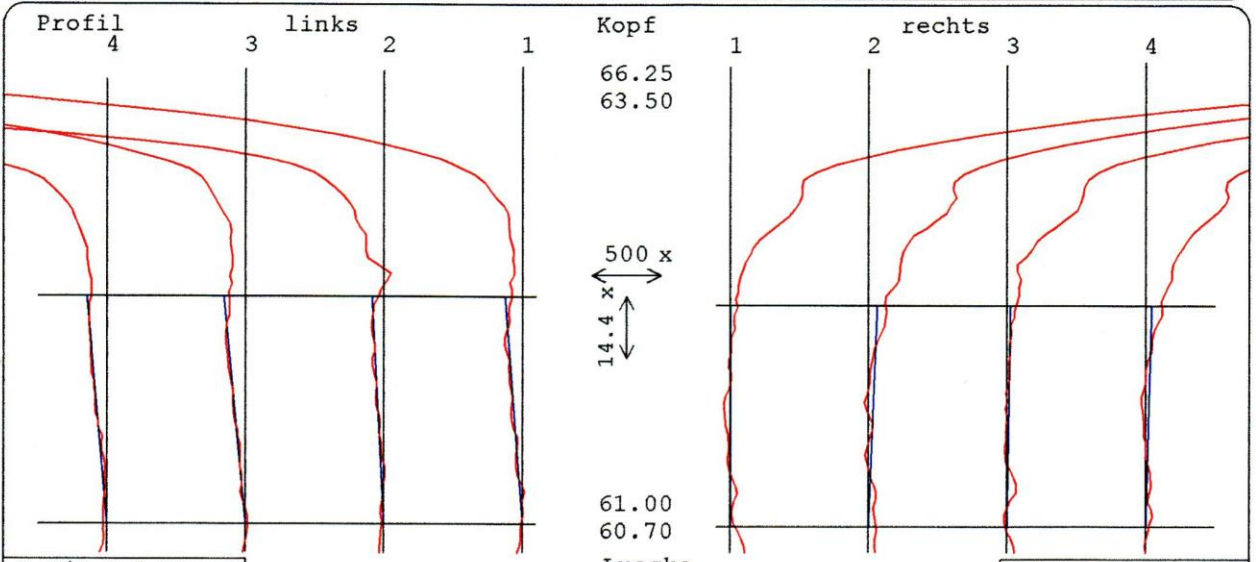


Q	I/S	Tol	Mittel	fHß/63%				Luecke	fHß/63%				Mittel	Tol	Q	I/S
D10/0	0/	0	-29.0	-31.5	-32.8	-25.3	-26.3	fHB	1.1	3.4	1.6	6.5	3.2	0/	0	D 5/0
D 9/0	0	0	36.4	38.5	40.5	31.9	34.4	FB	8.7	11.2	9.7	13.3	10.7	0	D 6/0	
D 7/0	0	0	10.8	9.5	10.2	9.8	13.7	ffB	8.4	9.8	9.2	8.7	9.0	0	D 6/0	

2.10


 <p>MESSTECHNIK WETZLAR GmbH Metrology Systems</p> <p>QUINDOS ZAHNRAD</p>	Zaehnezahl : 24	Hersteller :
	Normalmodul : 2.5000	Seriennummer: 07
	Eingr.winkel: 30.0000	Bemerkung : Z = -57
	Schr.winkel : 0.0000	Bezeichnung : WPM_GEW
	Steig.Richt.: gerade	Sachnummer :
Zahnbreite :103.0000	Pruefer/Dat.:	

Beurteilung : i.O. n.i.O. T. N. R.

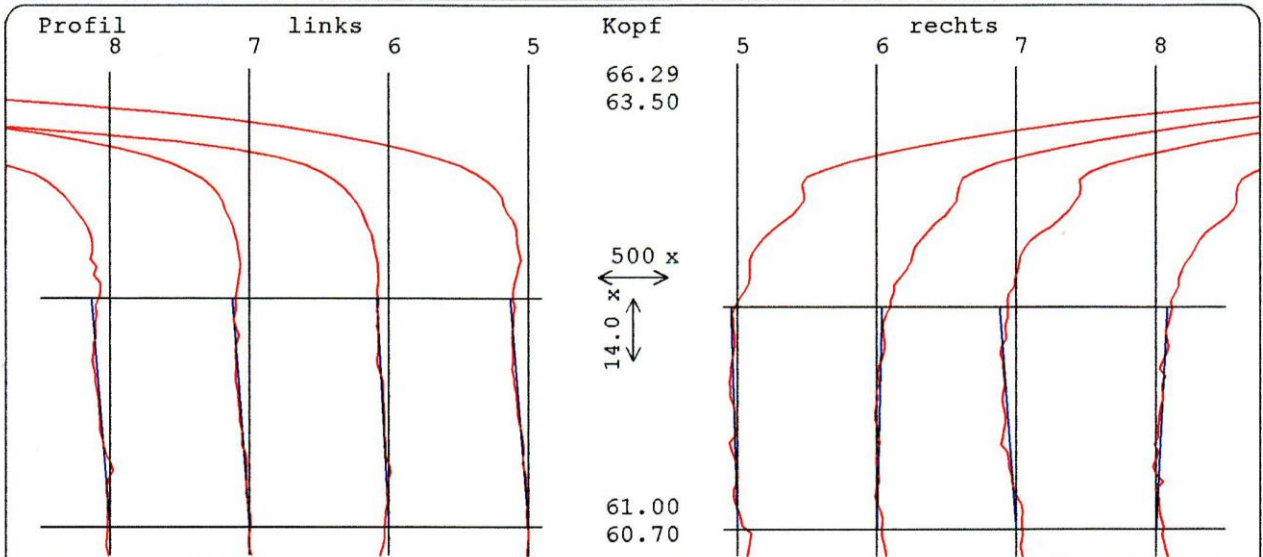


Q	I/S	Tol	Mittel					Luecke					Mittel	Tol	Q	I/S
D 7/0	0/ 0	-5.2		-6.0	-6.2	-3.5	-5.0	fHA	-0.1	-2.5	-1.0	-1.8	-1.3	0/ 0	D 4/0	
D 5/0	0	5.6		4.8	6.4	5.5	5.8	FA	4.1	6.4	3.5	6.0	5.0	0	D 5/0	
D 6/0	0	4.7		2.7	4.8	6.7	4.8	ffA	4.1	5.4	3.6	5.3	4.6	0	D 5/0	

2.11

 <p>MESSTECHNIK WETZLAR GmbH Metrology Systems</p> <p>QUINDOS ZAHNRAD</p>	Zaehnezahl : 24	Hersteller :
	Normalmodul : 2.5000	Seriennummer: 07
	Eingr.winkel: 30.0000	Bemerkung : Z = -57
	Schr.winkel : 0.0000	Bezeichnung : WPM_GEW
	Steig.Richt.: gerade	Sachnummer :
Zahnbreite : 103.0000	Pruefer/Dat.:	

Beurteilung : i.O. n.i.O. T. N. R.




Q	I/S	Tol	Mittel
D 6/0	0/ 0	-4.8	
D 5/0	0	4.9	
D 5/0	0	3.9	

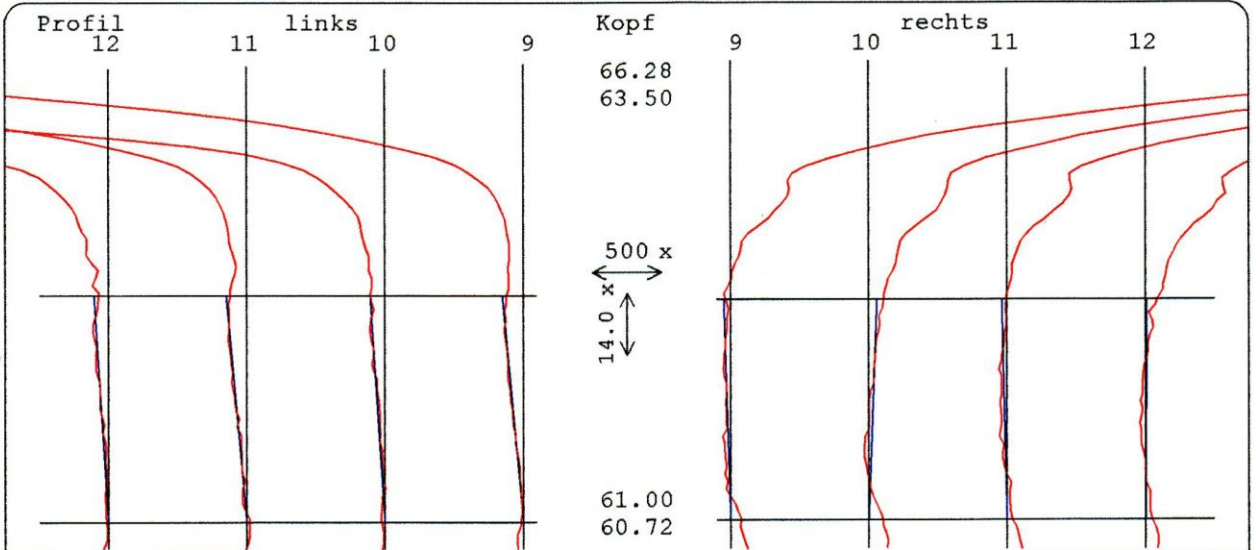
	5	6	7	8
fHA	1.9	-1.5	4.7	-3.3
FA	3.7	3.2	6.4	5.5
ffA	2.9	2.9	4.8	4.0

Mittel	Tol	Q	I/S
0.5	0/ 0	D 6/0	
4.7	0	D 5/0	
3.7	0	D 5/0	

2.12


 <p>MESSTECHNIK WETZLAR GmbH Metrology Systems</p> <p>QUINDOS ZÄHNRAD</p>	Zaehnezahl : 24	Hersteller :
	Normalmodul : 2.5000	Seriennummer: 07
	Eingr.winkel: 30.0000	Bemerkung : Z = -57
	Schr.winkel : 0.0000	Bezeichnung : WPM_GEW
	Steig.Richt.: gerade	Sachnummer :
Zahnbreite :103.0000	Pruefer/Dat.:	

Beurteilung : i.O. n.i.O. T. N. R.

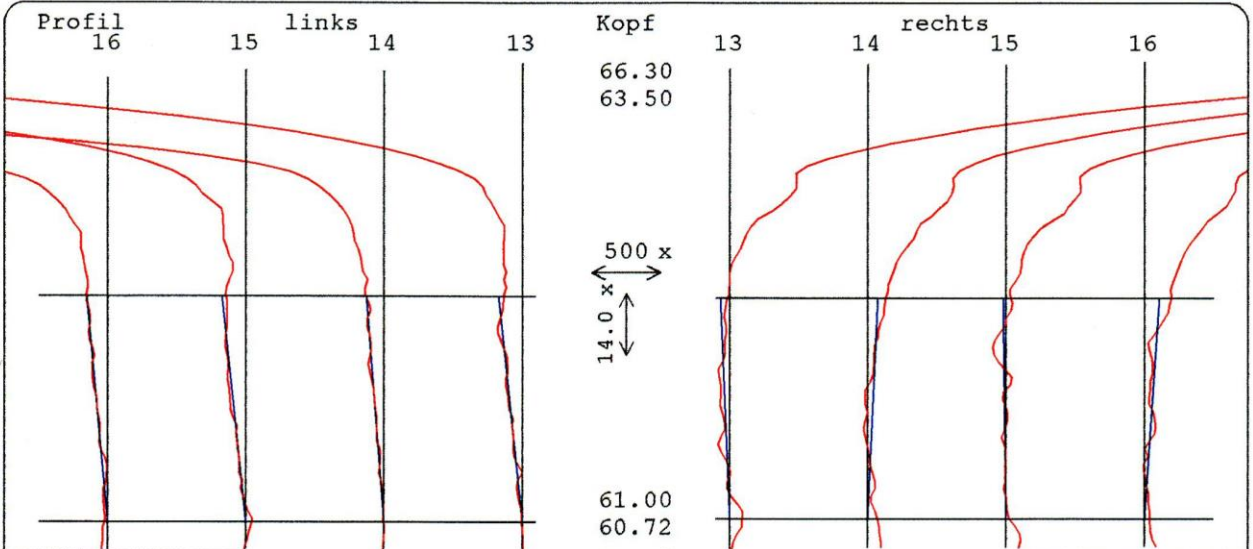


Q	I/S	Tol	Mittel					Luecke					Mittel	Tol	Q	I/S
D 7/0	0/ 0	-5.1	-4.3	-5.9	-4.2	-6.0	fHA	2.0	-2.4	1.7	-0.5	0.2	0/ 0	D 4/0		
D 5/0	0	5.0	4.1	6.3	4.5	5.1	FA	5.5	5.6	3.9	4.3	4.8	0	D 5/0		
D 5/0	0	3.2	2.7	4.4	2.0	3.9	ffa	4.7	6.1	3.1	4.0	4.5	0	D 6/0		

2.13


 <p>MESSTECHNIK WETZLAR GmbH Metrology Systems</p> <p>QUINDOS ZAHNRAD</p>	Zaehnezahl : 24	Hersteller :
	Normalmodul : 2.5000	Seriennummer: 07
	Eingr.winkel: 30.0000	Bemerkung : Z = -57
	Schr.winkel : 0.0000	Bezeichnung : WPM_GEW
	Steig.Richt.: gerade	Sachnummer :
Zahnbreite :103.0000	Pruefer/Dat.:	

Beurteilung : i.O. n.i.O. T. N. R.

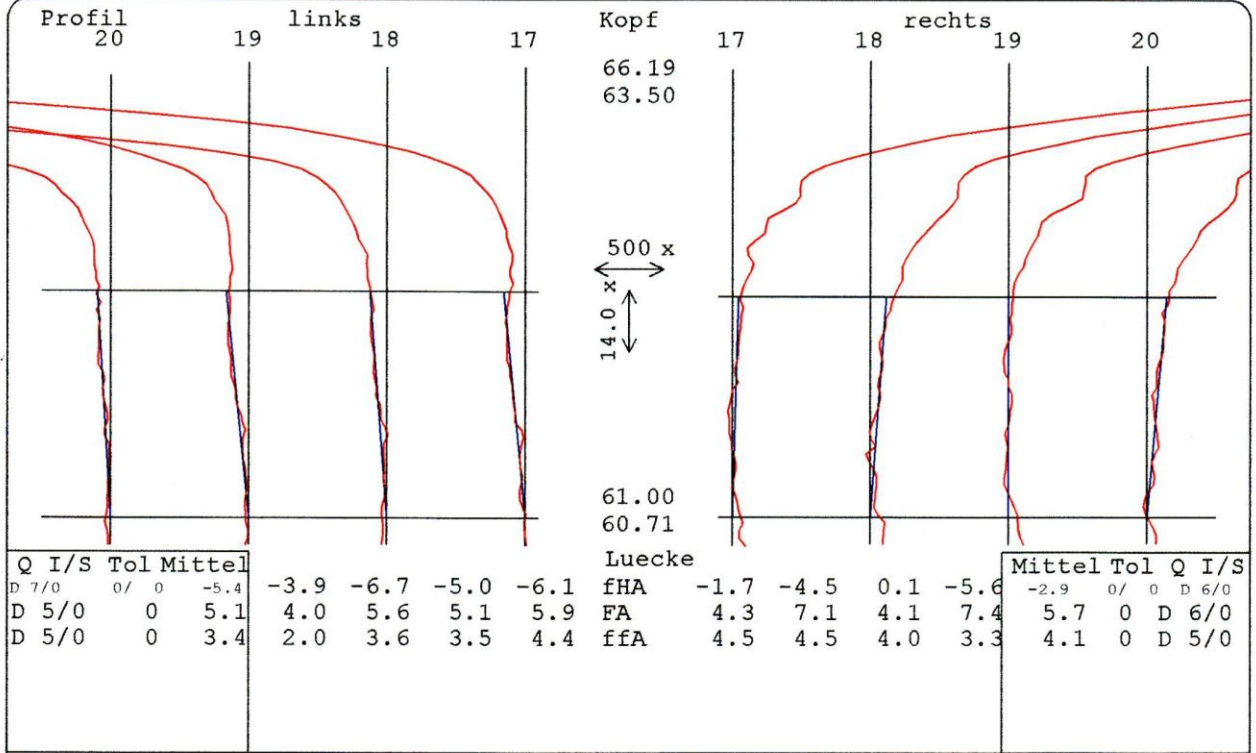


Q	I/S	Tol	Mittel					Luecke					Mittel	Tol	Q	I/S
D 7/0	0/ 0	-6.3	-6.0	-7.1	-5.2	-6.9	fHA	2.6	-2.8	0.9	-4.4	-0.9	0/ 0	D 5/0		
D 6/0	0	6.4	5.9	7.9	4.8	7.0	FA	7.1	6.2	5.8	7.5	6.7	0	D 6/0		
D 5/0	0	3.6	2.2	5.2	2.0	5.1	ffA	6.3	5.1	6.0	5.4	5.7	0	D 6/0		


2.14

 <p>MESSTECHNIK WETZLAR GmbH Metrology Systems</p> <p>QUINDOS ZAHNRAD</p>	Zahnezahl : 24	Hersteller :
	Normalmodul : 2.5000	Seriennummer: 07
	Eingr.winkel: 30.0000	Bemerkung : Z = -57
	Schr.winkel : 0.0000	Bezeichnung : WPM_GEW
	Steig.Richt.: gerade	Sachnummer :
Zahnbreite :103.0000	Pruefer/Dat.:	

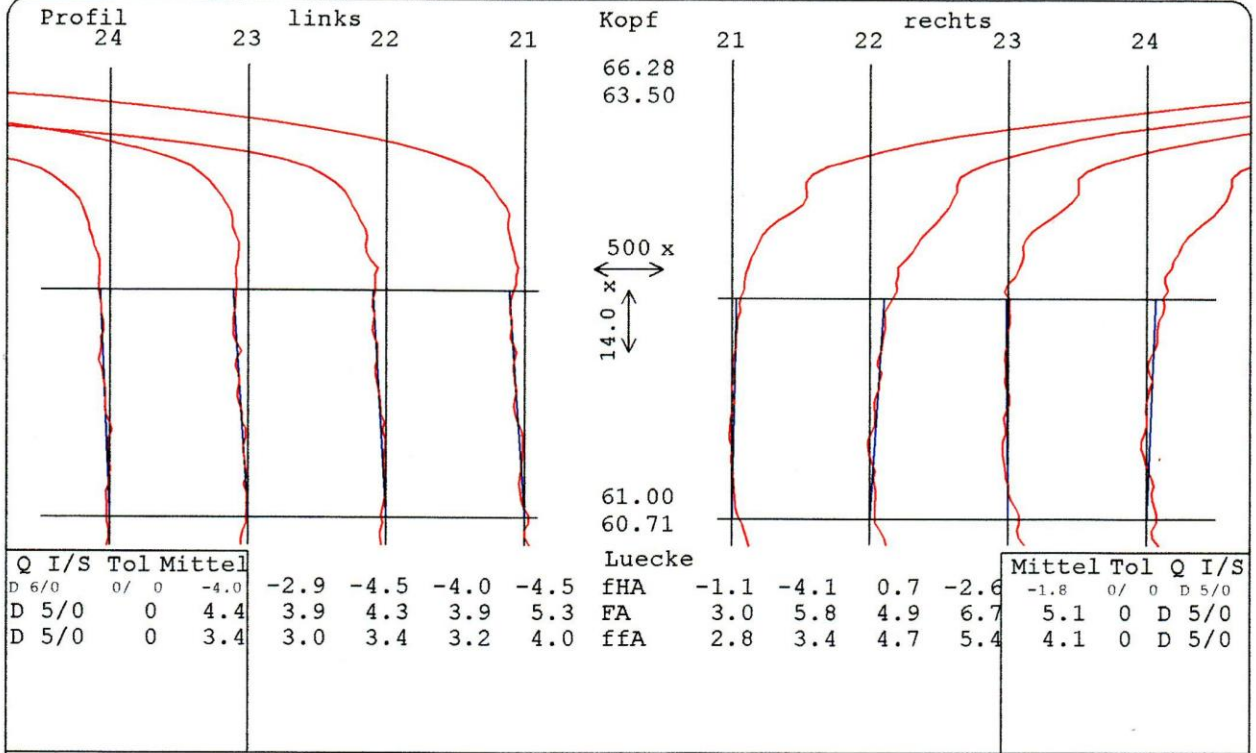
Beurteilung : i.O. n.i.O. T. N. R.



2.15

 <p>MESSTECHNIK WETZLAR GmbH Metrology Systems</p> <p>QUINDOS ZAHNRAD</p>	Zahnezahl : 24	Hersteller :
	Normalmodul : 2.5000	Seriennummer: 07
	Eingr.winkel: 30.0000	Bemerkung : Z = -57
	Schr.winkel : 0.0000	Bezeichnung : WPM_GEW
	Steig.Richt.: gerade	Sachnummer :
Zahnbreite :103.0000	Pruefer/Dat.:	

Beurteilung : i.O. n.i.O. T. N. R.



2.16

Appendix 3: Tool geometry (DIN 3960 ff)

Pitch and concentricity deviation	3.1 – 3.2
Root diameter, roundness	3.3
Tip diameter, roundness	3.4
Tooth trace deviation	3.5 – 3.7
Profile deviation	3.8 – 3.10
Outer cylinder, roundness	3.11 – 3.13



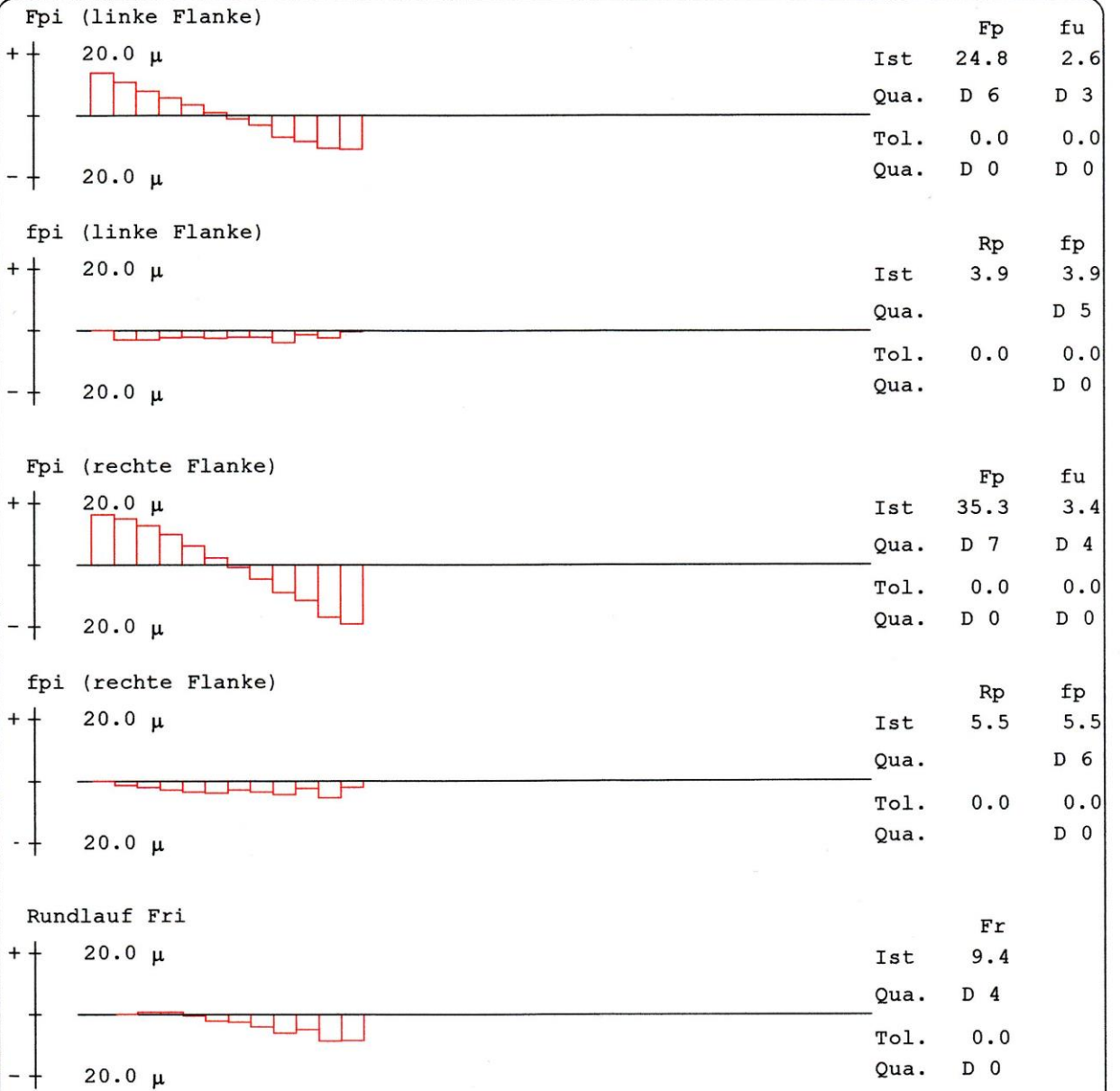
MESSTECHNIK
WETZLAR GmbH
Metrology Systems

QUINDOS
ZAHNRAD


Zahnezahl : 34
Normalmodul : 2.5000
Eingr.winkel: 30.0000
Schr.winkel : 0.0000
Steig.Richt.: gerade
Zahnbreite : 50.0000

Hersteller : SAND III DIAG
Seriennummer:
Bemerkung : Z = -17
Bezeichnung : WPM_WERKZ
Sachnummer :
Pruefer/Dat.:

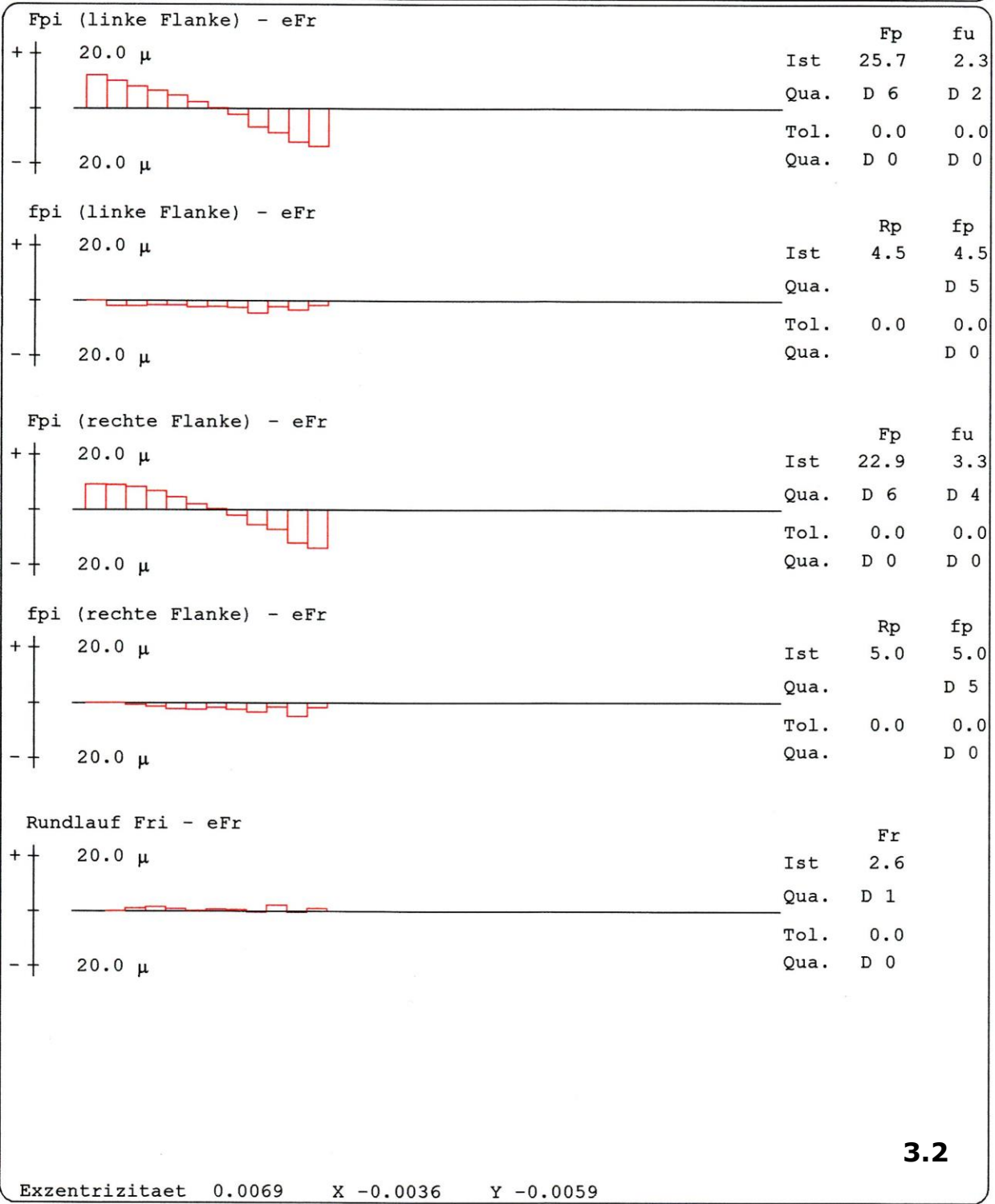
Beurteilung : i.O. n.i.O. T. N. R.

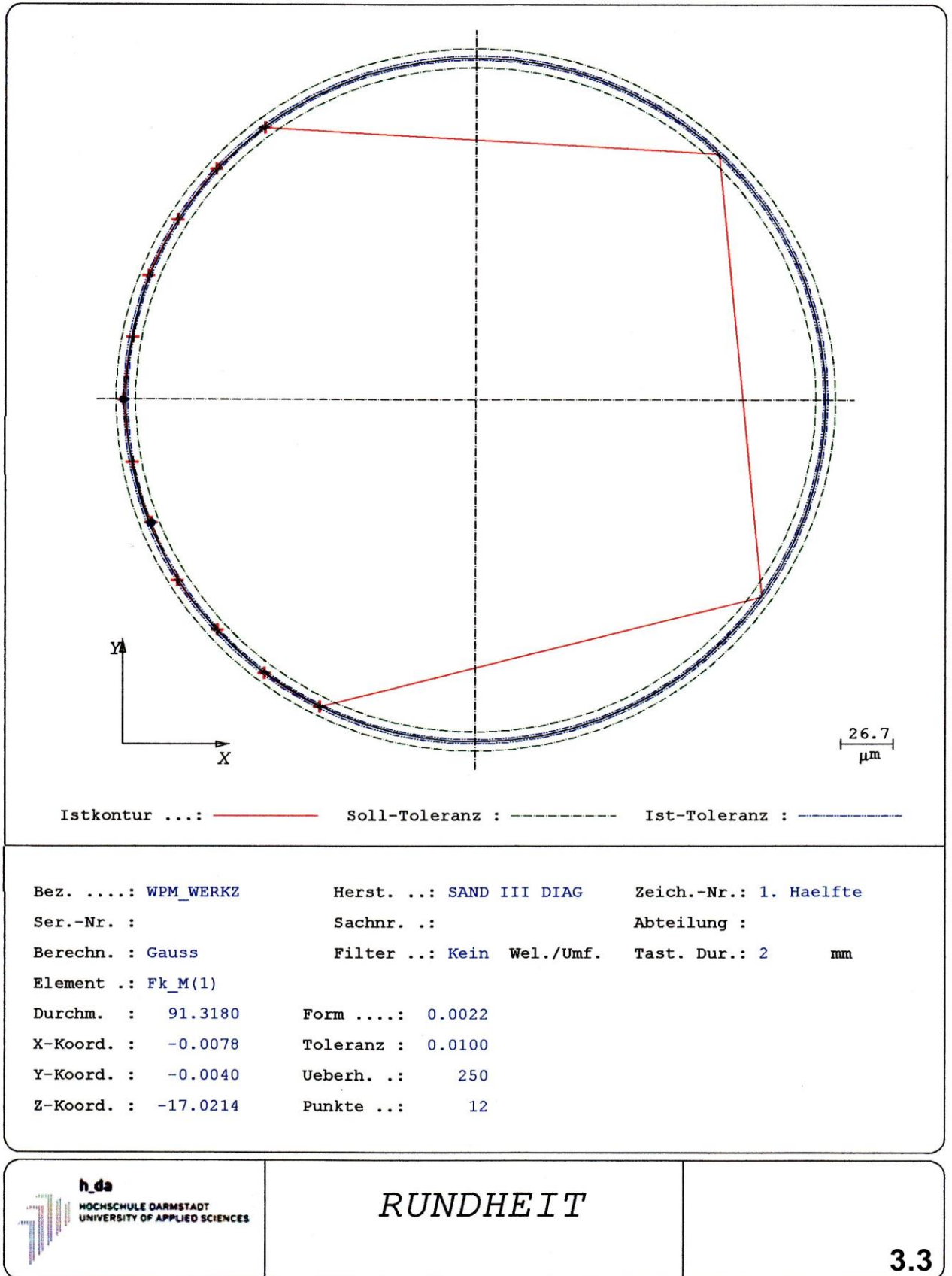


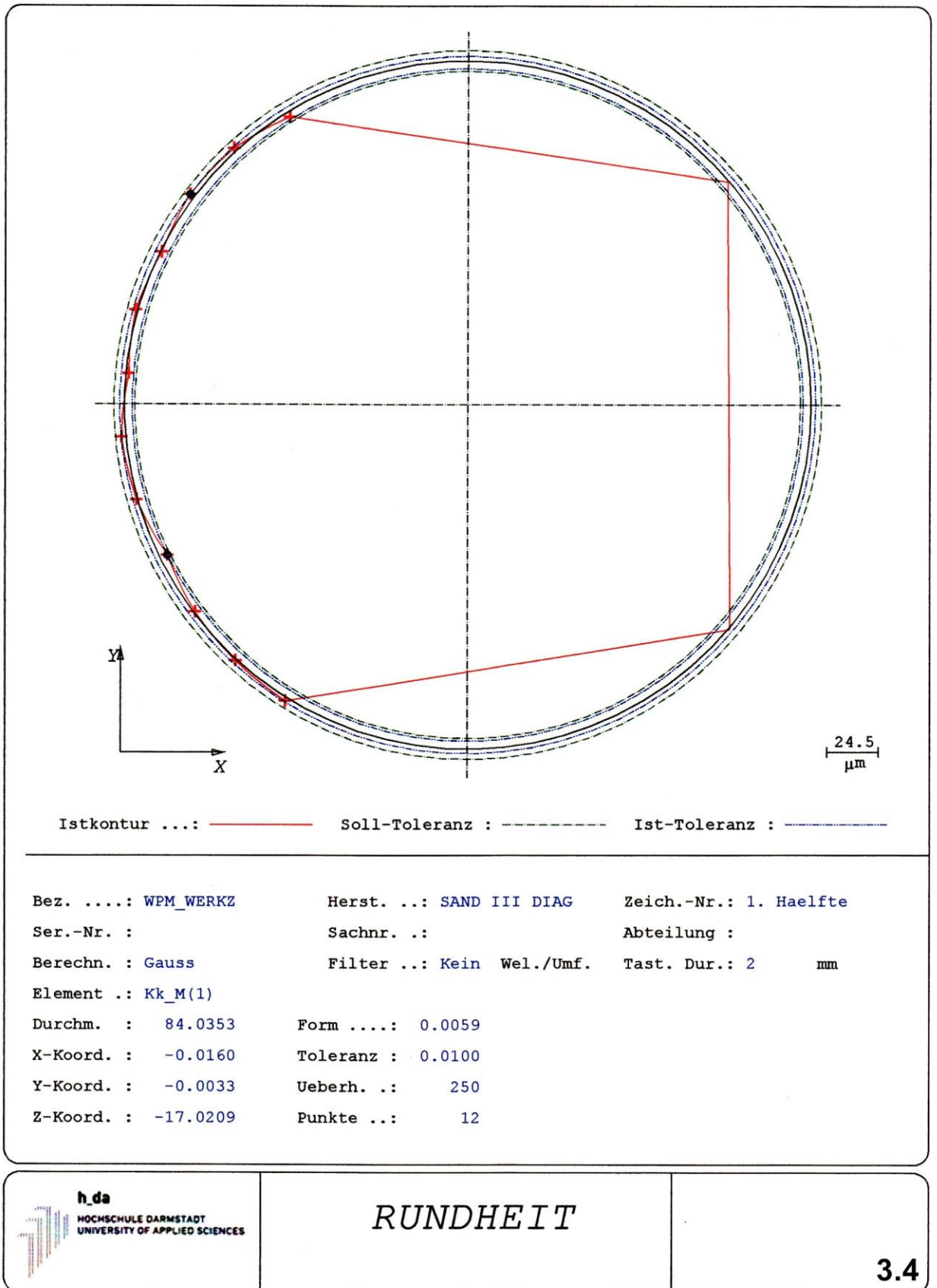
3.1

 <p>MESSTECHNIK WETZLAR GmbH Metrology Systems</p> <p>QUINDOS ZAHNRAD</p>	Zaehnezahl : 34 Normalmodul : 2.5000 Eingr.winkel: 30.0000 Schr.winkel : 0.0000 Steig.Richt.: gerade Zahnbreite : 50.0000	Hersteller : SAND III DIAG Seriennummer: Bemerkung : Z = -17 Bezeichnung : WPM_WERKZ Sachnummer : Pruefer/Dat.:
--	--	--

Beurteilung : i.O. n.i.O. T. N. R.









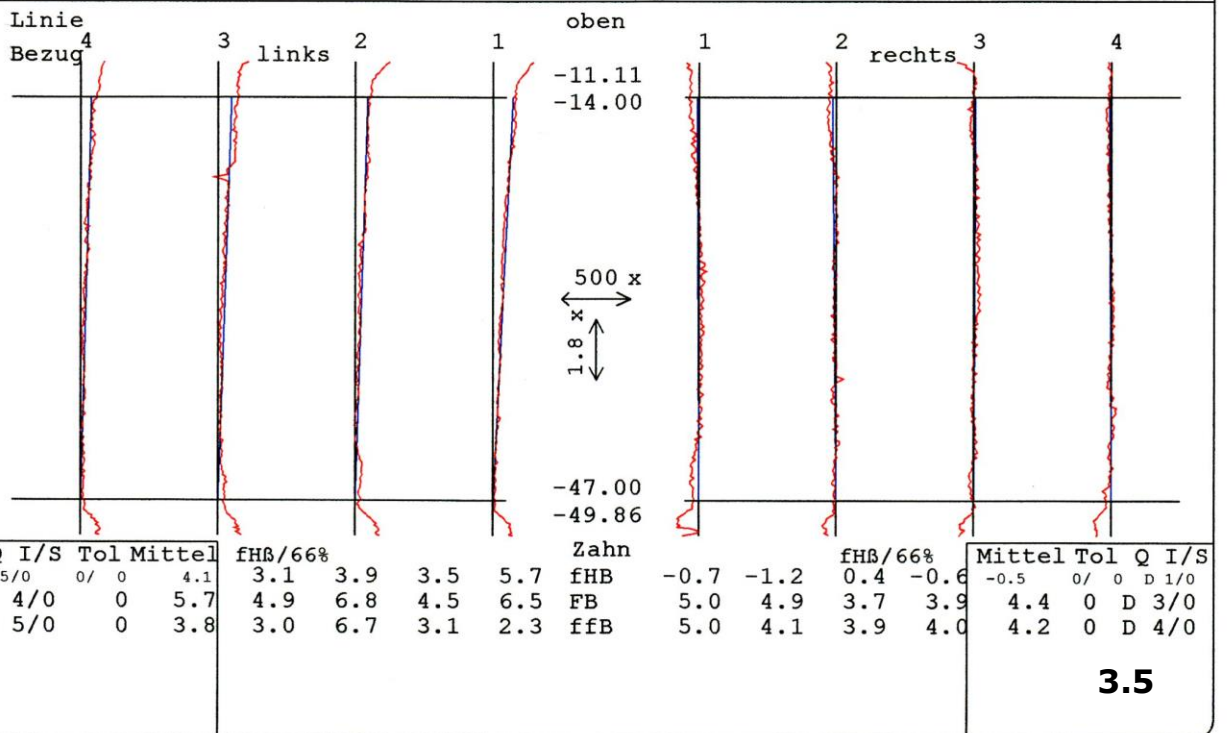
MESSTECHNIK
WETZLAR GmbH
Metrology Systems


QUINDOS
ZAHNRAD

Zaehnezahl : 34
Normalmodul : 2.5000
Eingr.winkel: 30.0000
Schr.winkel : 0.0000
Steig.Richt.: gerade
Zahnbreite : 50.0000

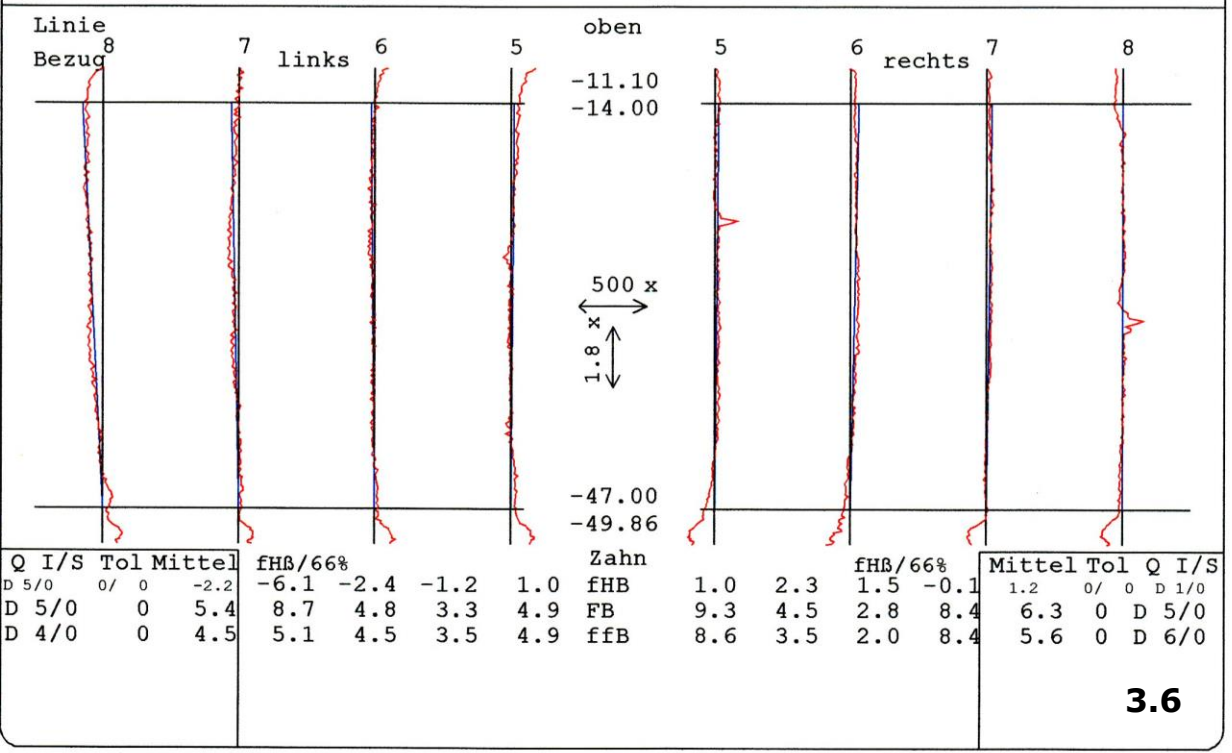
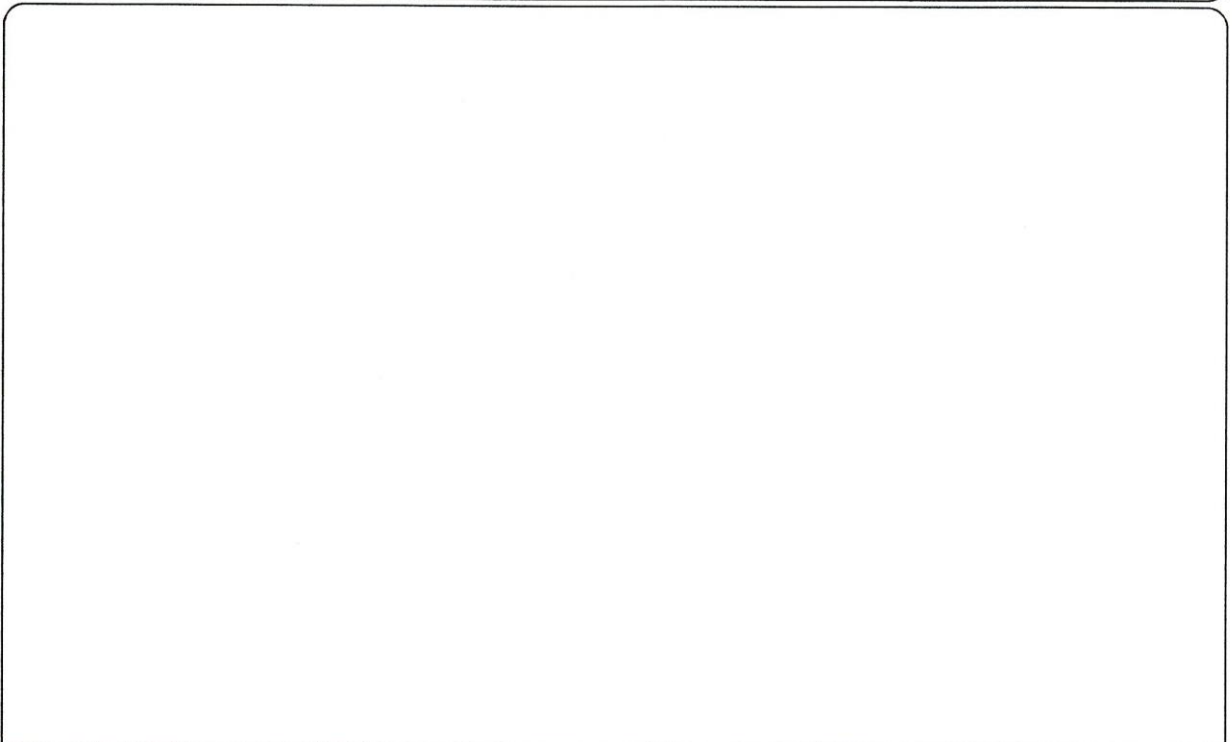
Hersteller : SAND III DIAG
Seriennummer:
Bemerkung : Z = -17
Bezeichnung : WPM_WERKZ
Sachnummer :
Pruefer/Dat.:


Beurteilung : i.O. n.i.O. T. N. R.



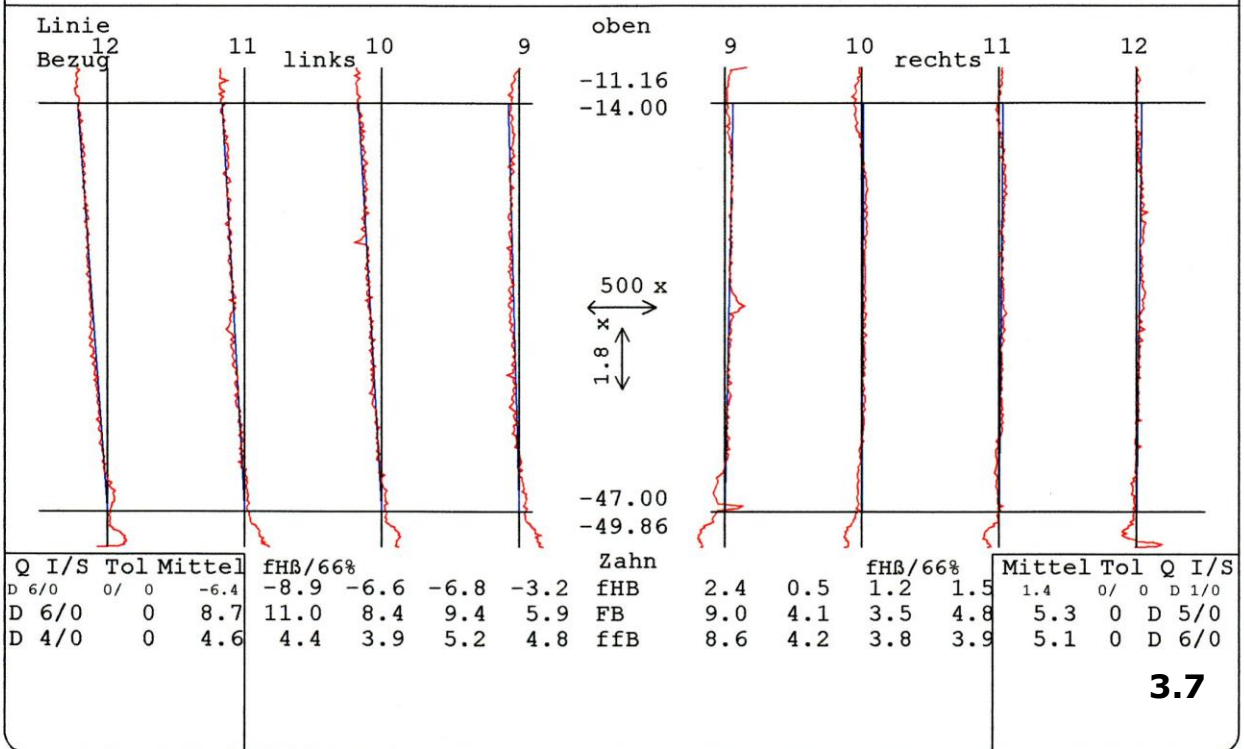
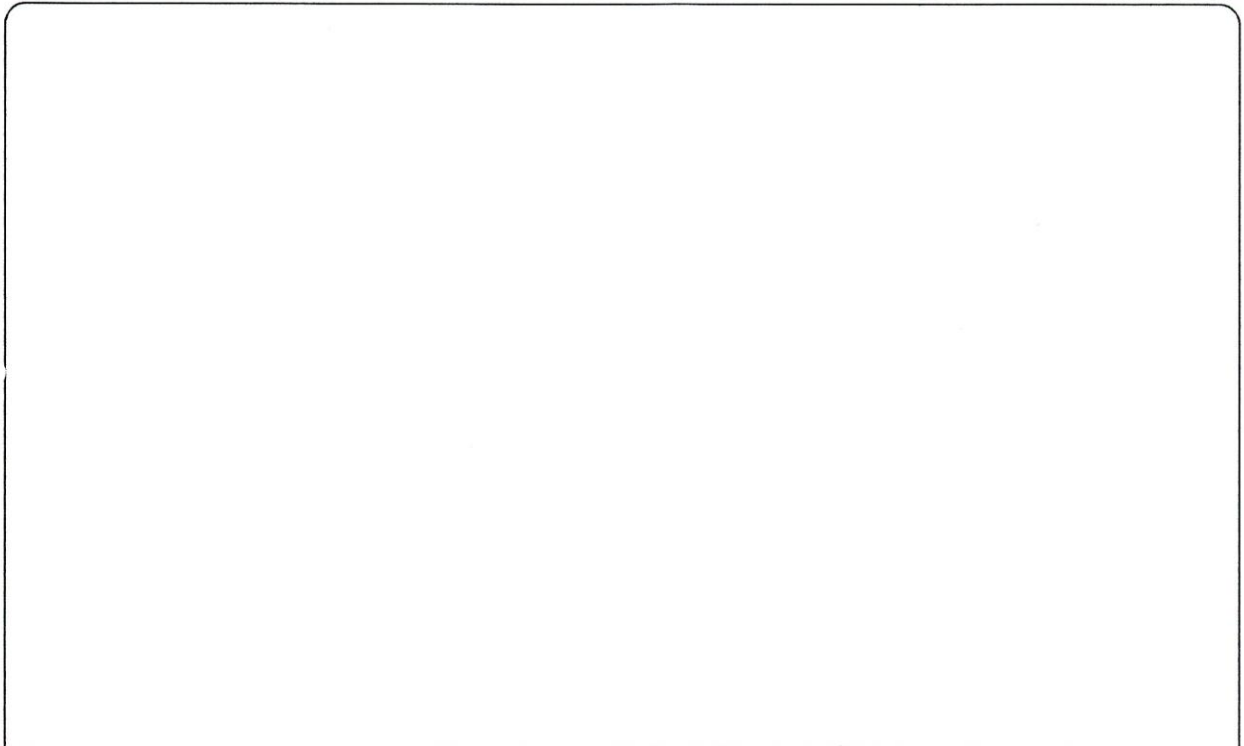
 MESSTECHNIK WETZLAR GmbH Metrology Systems QUINDOS ZAHNRAD	Zaehnezahl : 34	Hersteller : SAND III DIAG
	Normalmodul : 2.5000	Seriennummer:
	Eingr.winkel: 30.0000	Bemerkung : Z = -17
	Schr.winkel : 0.0000	Bezeichnung : WPM_WERKZ
Steig.Richt.: gerade	Sachnummer :	
Zahnbreite : 50.0000	Pruefer/Dat.:	


Beurteilung : i.O. n.i.O. T. N. R.



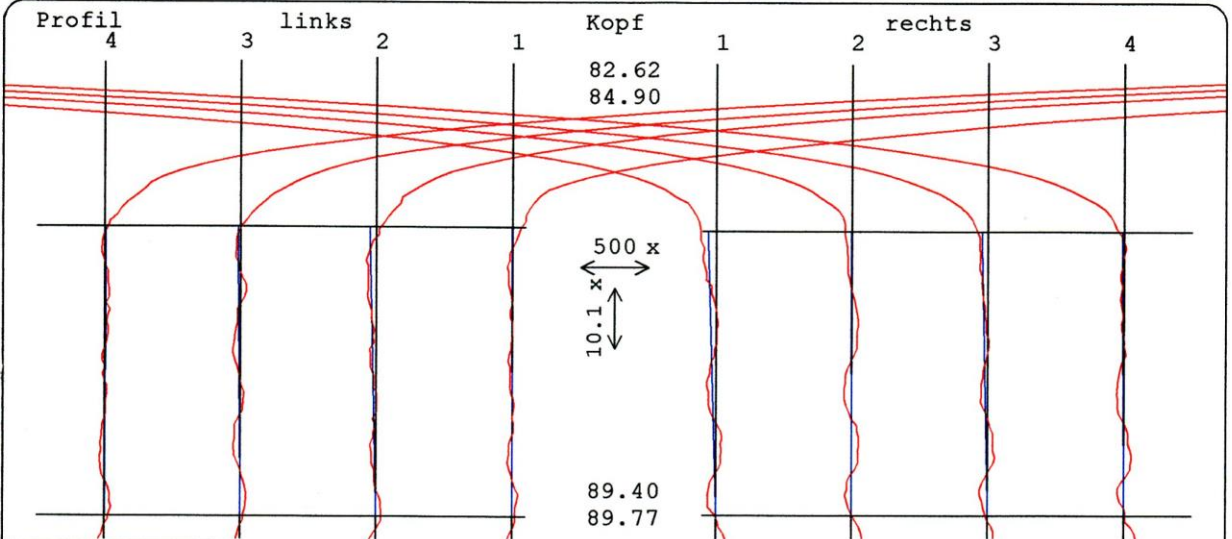
 <p>MESSTECHNIK WETZLAR GmbH Metrology Systems</p> <p>QUINDOS ZAHNRAD</p>	Zahnezahl : 34	Hersteller : SAND III DIAG
	Normalmodul : 2.5000	Seriennummer:
	Eingr.winkel: 30.0000	Bemerkung : Z = -17
	Schr.winkel : 0.0000	Bezeichnung : WPM_WERKZ
Steig.Richt.: gerade	Sachnummer :	Pruefer/Dat.:
Zahnbreite : 50.0000		

Beurteilung : i.O. n.i.O. T. N. R.




 MESSTECHNIK WETZLAR GmbH Metrology Systems QUINDOS ZAHNRAD	Zahnezahl : 34	Hersteller : SAND III DIAG
	Normalmodul : 2.5000	Seriennummer:
	Eingr.winkel: 30.0000	Bemerkung : Z = -17
	Schr.winkel : 0.0000	Bezeichnung : WPM_WERKZ
	Steig.Richt.: gerade	Sachnummer :
Zahnbreite : 50.0000	Pruefer/Dat.:	

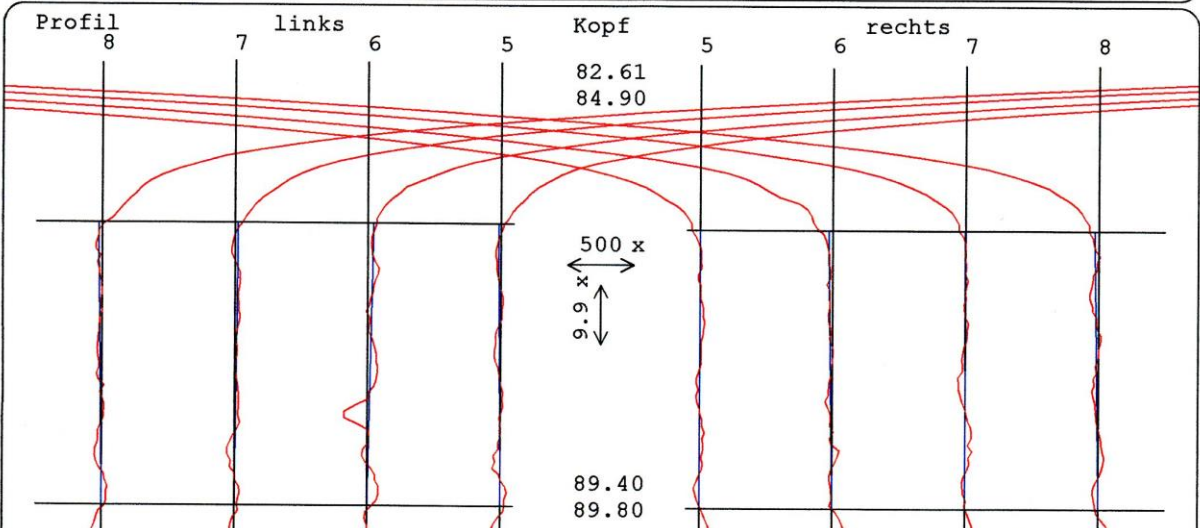
Beurteilung : i.O. n.i.O. T. N. R.



Q	I/S	Tol	Mittel					Zahn					Mittel	Tol	Q	I/S
D 4/0	0/ 0	0.8		-0.3	0.9	2.1	0.3	fHA	-2.5	-0.4	-2.0	-0.7	-1.4	0/ 0	D 4/0	
D 4/0	0	3.9		3.3	3.9	4.6	4.0	FA	6.4	4.3	5.1	4.3	5.0	0	D 5/0	
D 5/0	0	4.0		3.3	4.3	4.2	4.2	ffA	4.9	4.3	4.6	4.2	4.5	0	D 5/0	

 MESSTECHNIK WETZLAR GmbH Metrology Systems QUINDOS ZAHNRAD	Zaehnezahl : 34	Hersteller : SAND III DIAG
	Normalmodul : 2.5000	Seriennummer:
	Eingr.winkel: 30.0000	Bemerkung : Z = -17
	Schr.winkel : 0.0000	Bezeichnung : WPM_WERKZ
	Steig.Richt.: gerade	Sachnummer :
Zahnbreite : 50.0000	Pruefer/Dat.:	

Beurteilung : i.O. n.i.O. T. N. R.



Q	I/S	Tol	Mittel					Zahn					Mittel	Tol	Q	I/S
D 3/0	0/ 0	-0.1	1.1	-0.7	-1.6	0.7	fHA	0.0	-1.5	-0.3	-1.4	-0.8	0/ 0	D 2/0		
D 7/0	0	5.8	3.8	4.6	10.5	4.4	FA	3.9	4.8	4.4	4.4	4.4	0	D 4/0		
D 7/0	0	5.7	3.7	4.0	10.8	4.3	ffA	3.9	4.0	4.3	3.6	4.0	0	D 5/0		

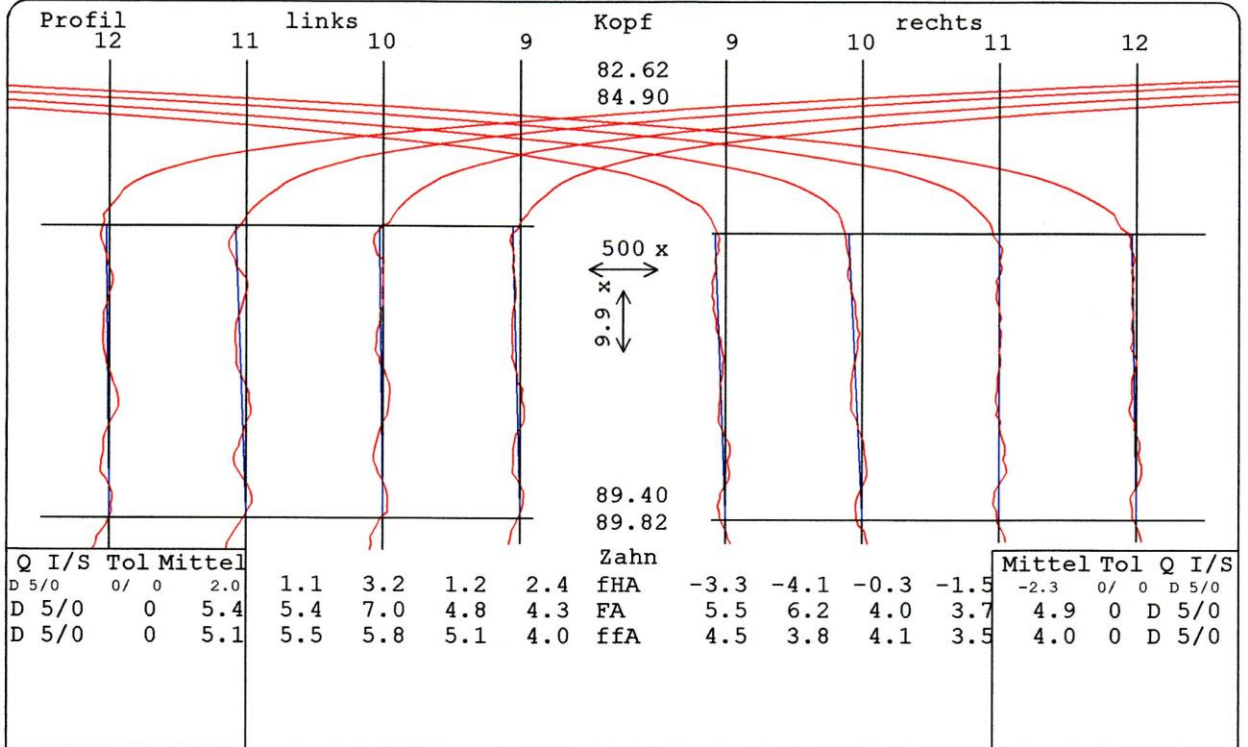


**QUINDOS
ZÄHNRAD**

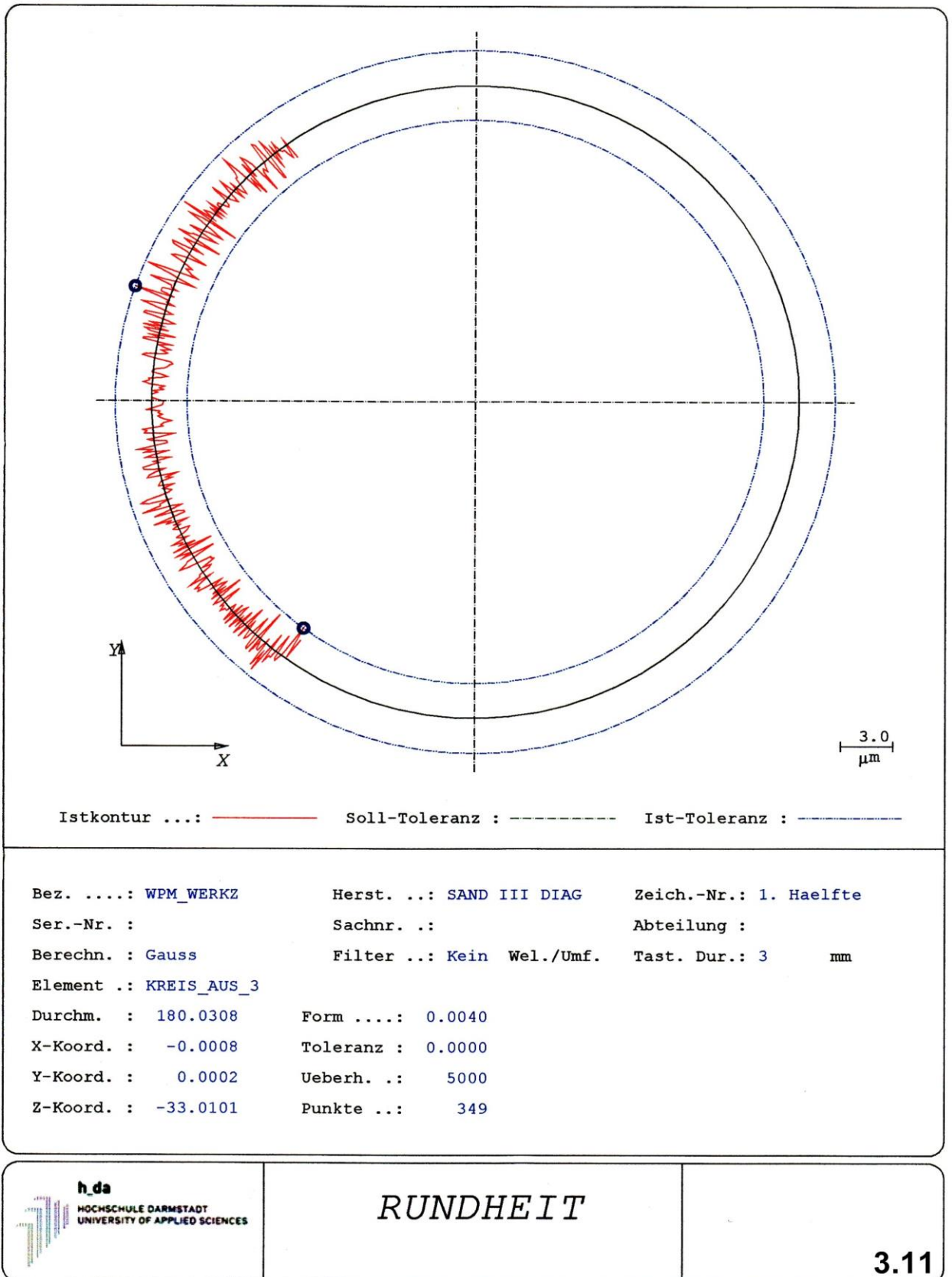
Zaehnezahl : 34
Normalmodul : 2.5000
Eingr.winkel: 30.0000
Schr.winkel : 0.0000
Steig.Richt.: gerade
Zahnbreite : 50.0000

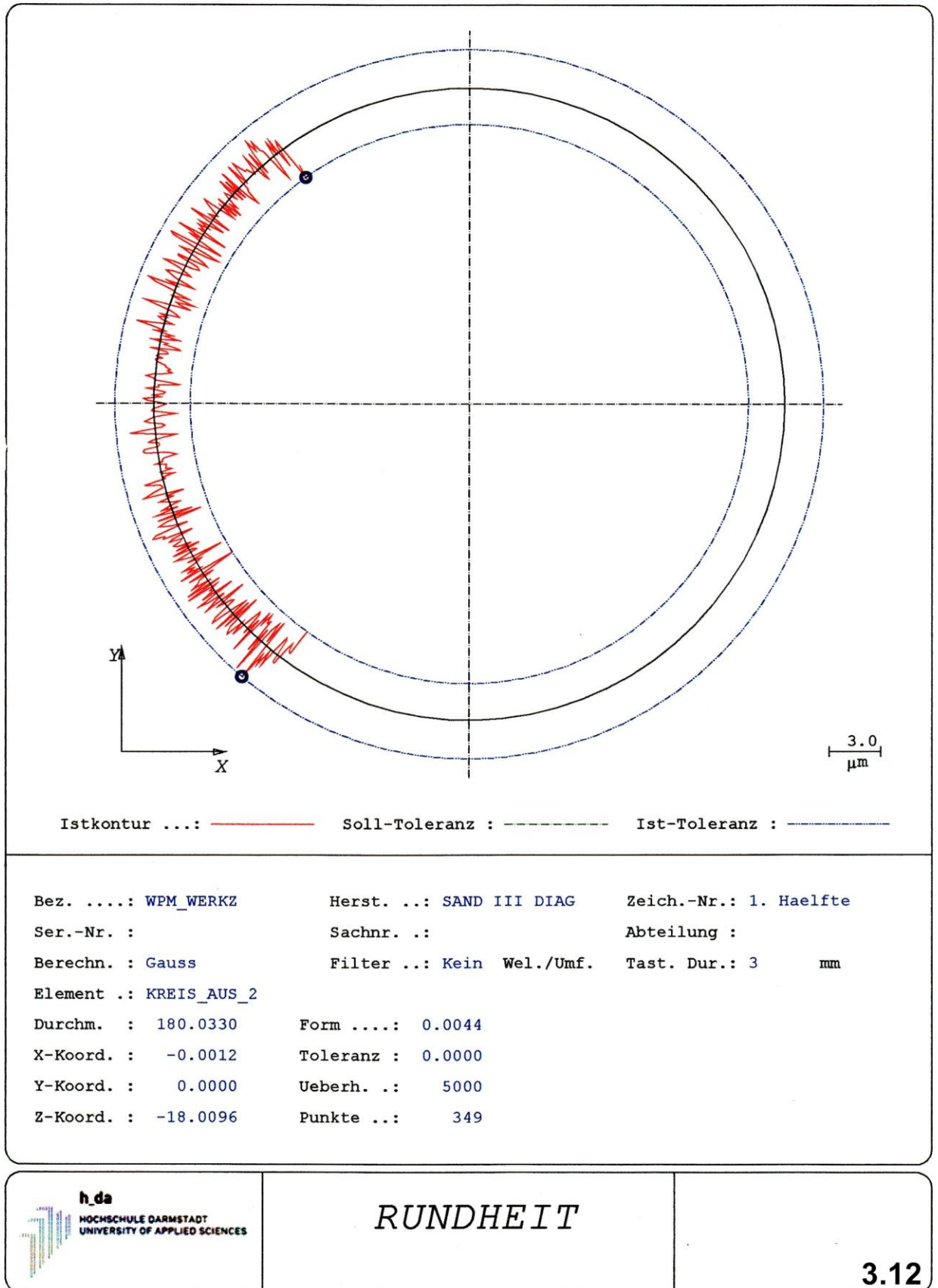
Hersteller : SAND III DIAG
Seriennummer:
Bemerkung : Z = -17
Bezeichnung : WPM_WERKZ
Sachnummer :
Pruefer/Dat.:

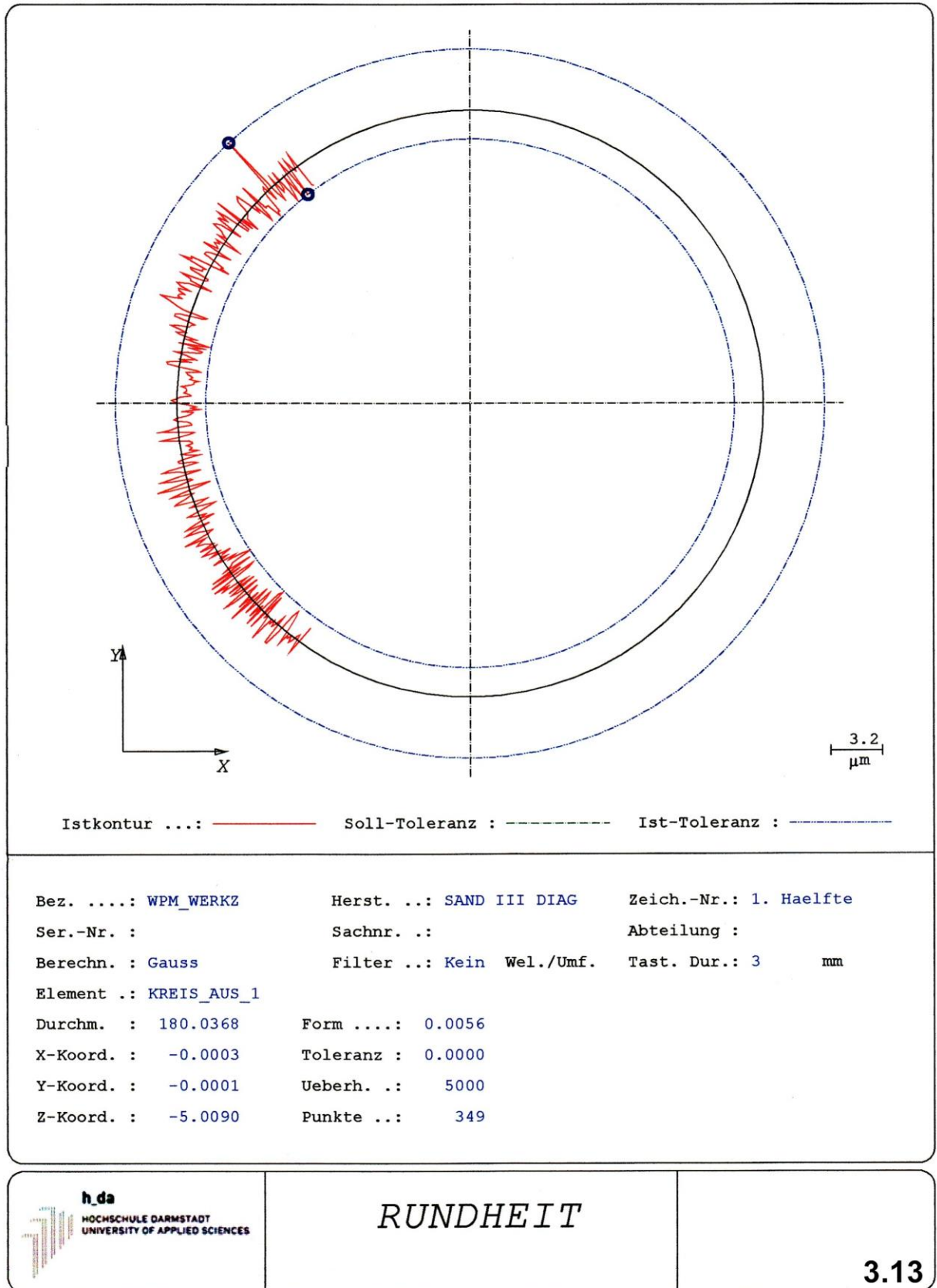
Beurteilung : i.O. n.i.O. T. N. R.



3.10



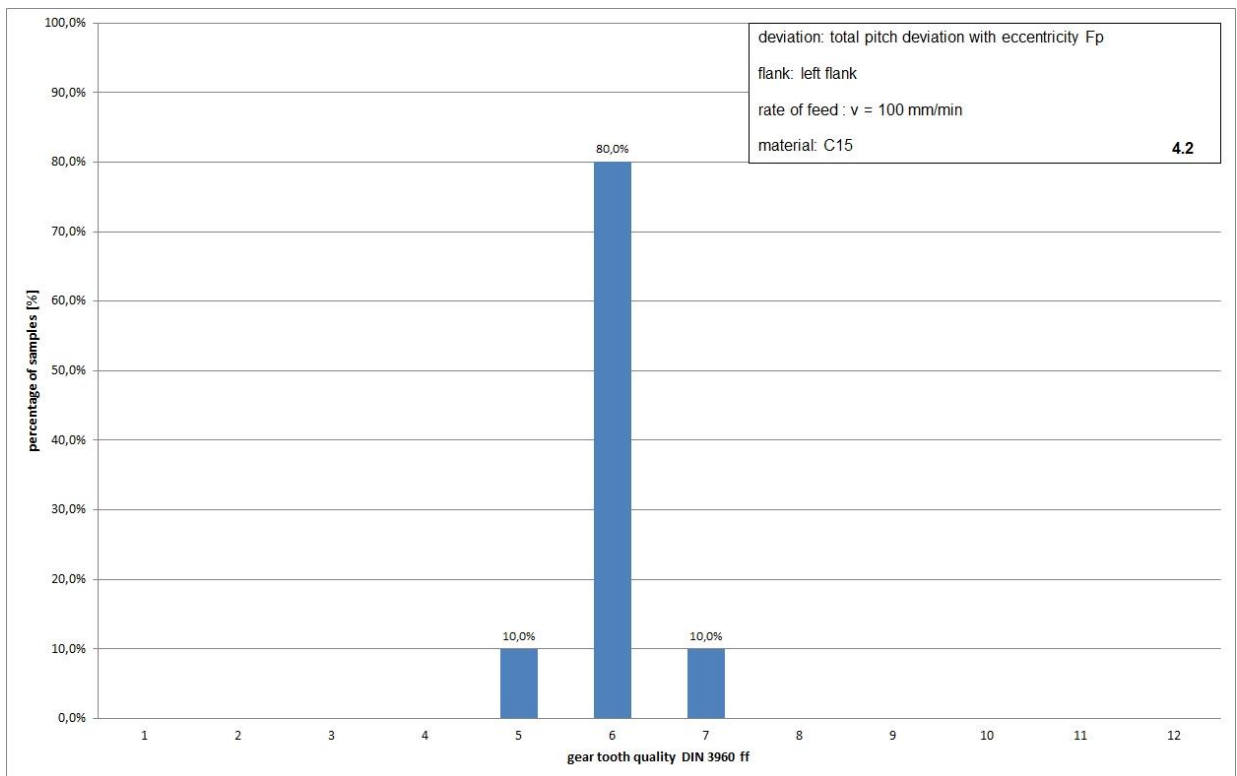
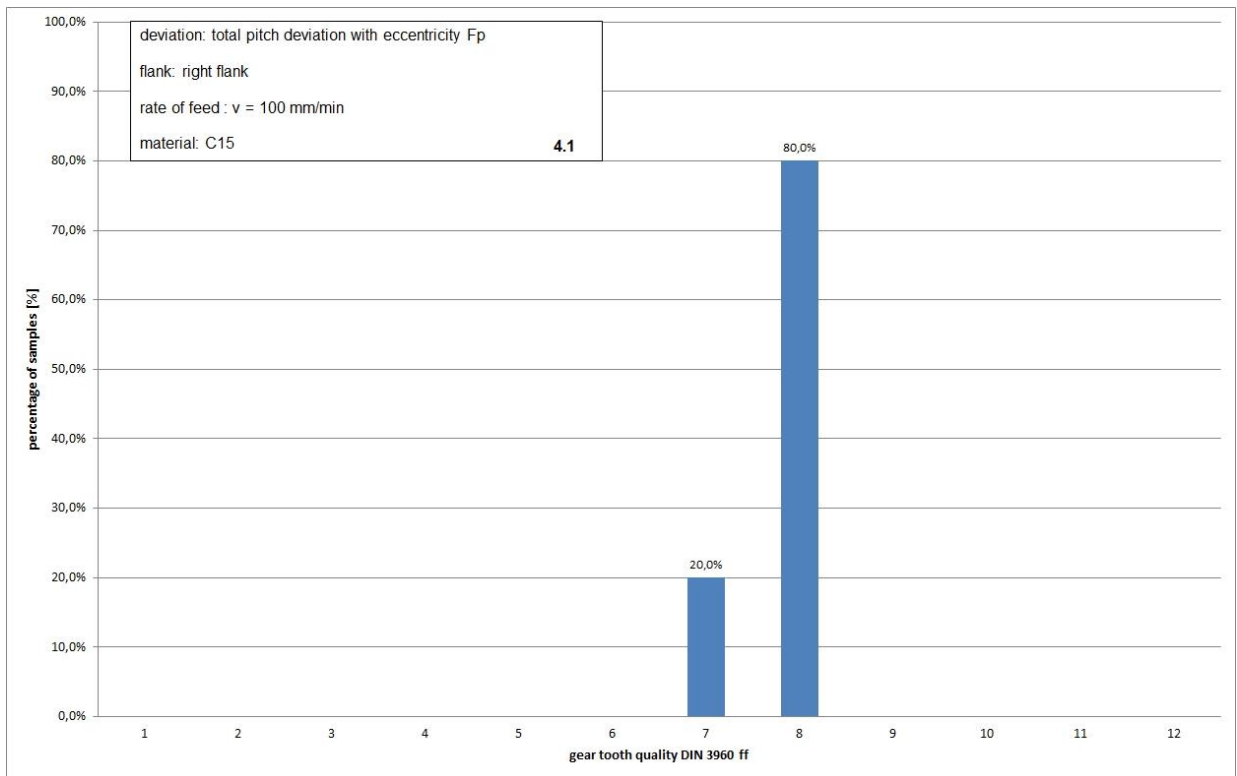


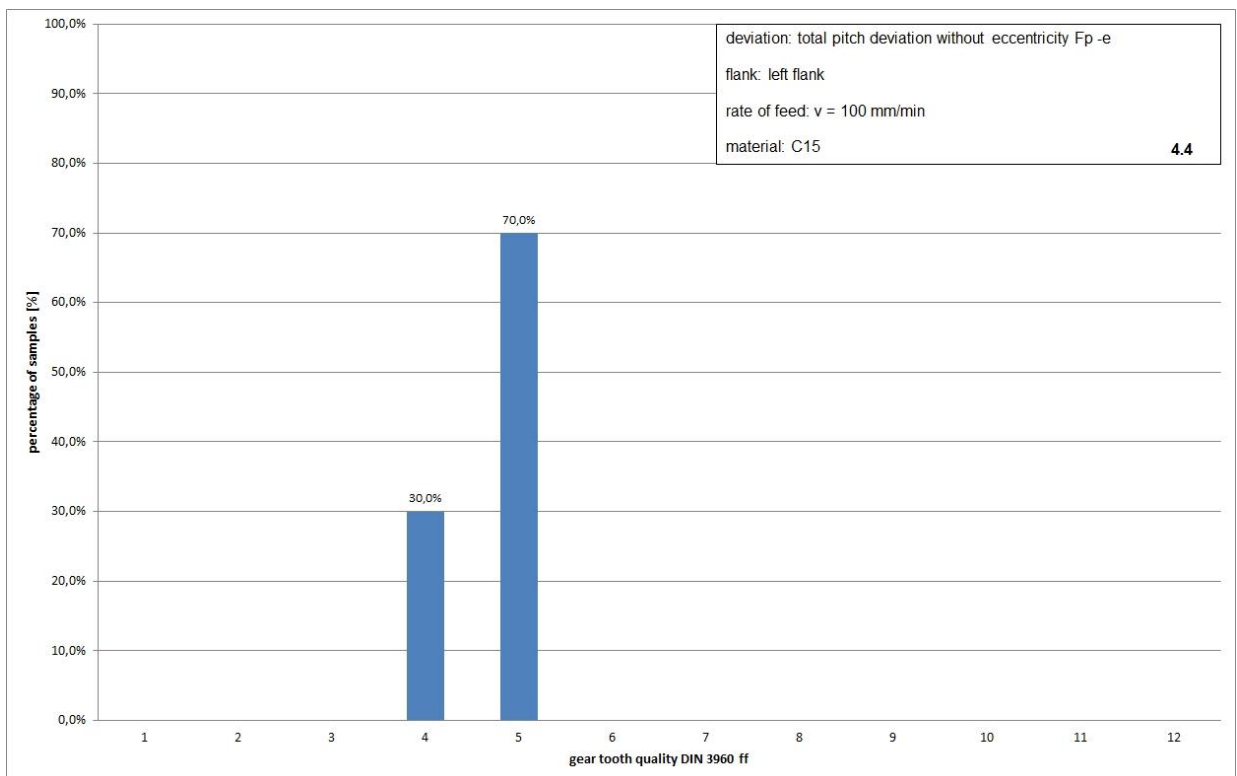
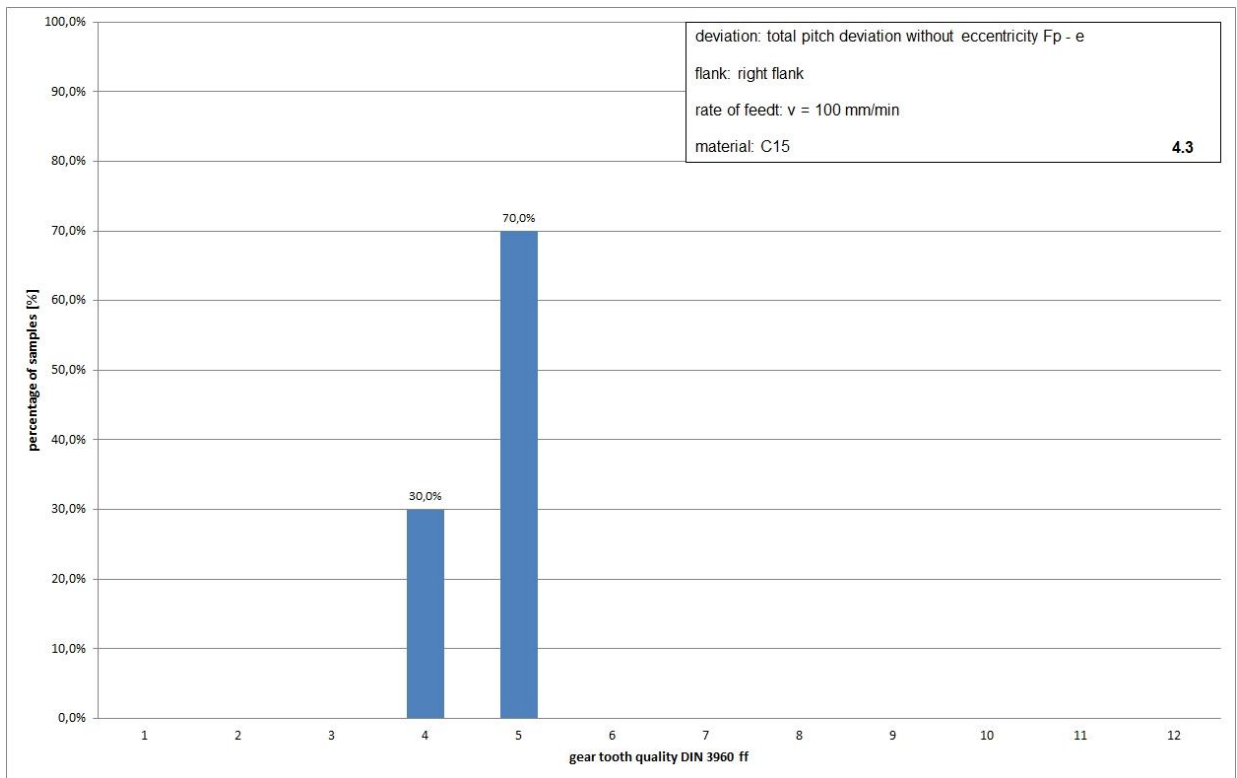


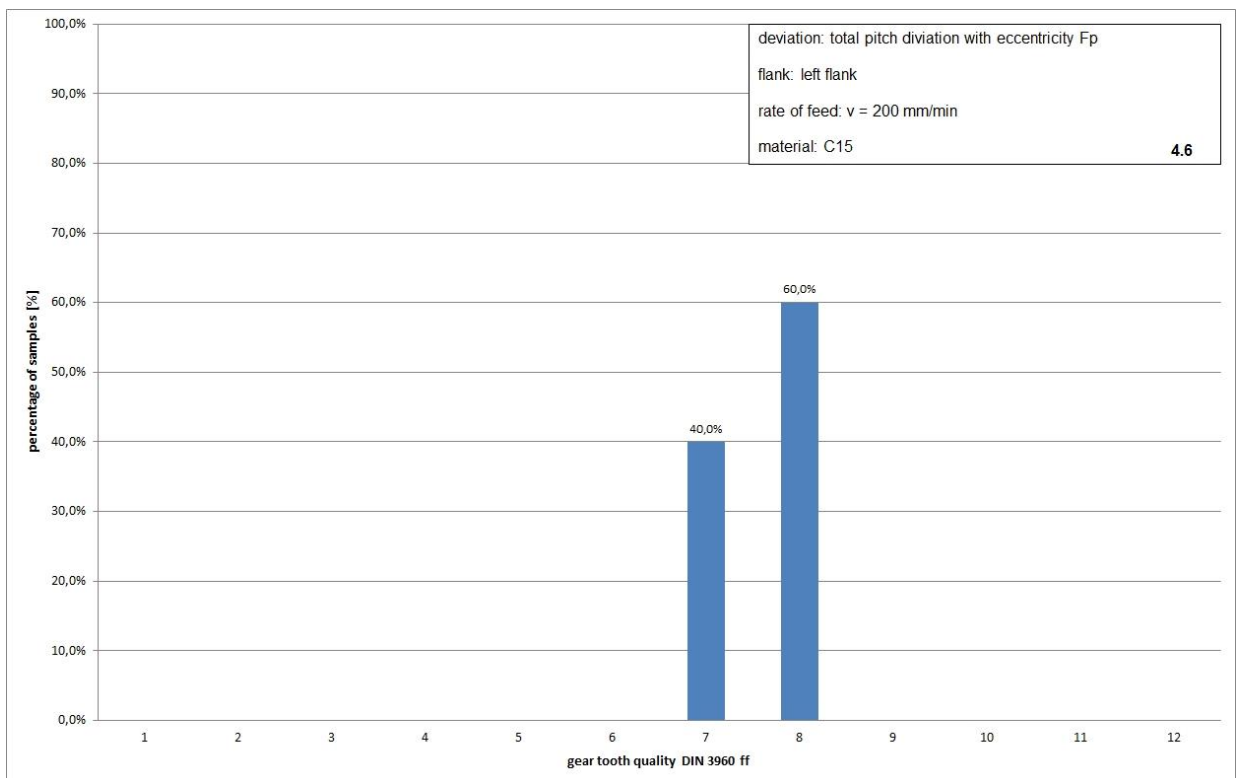
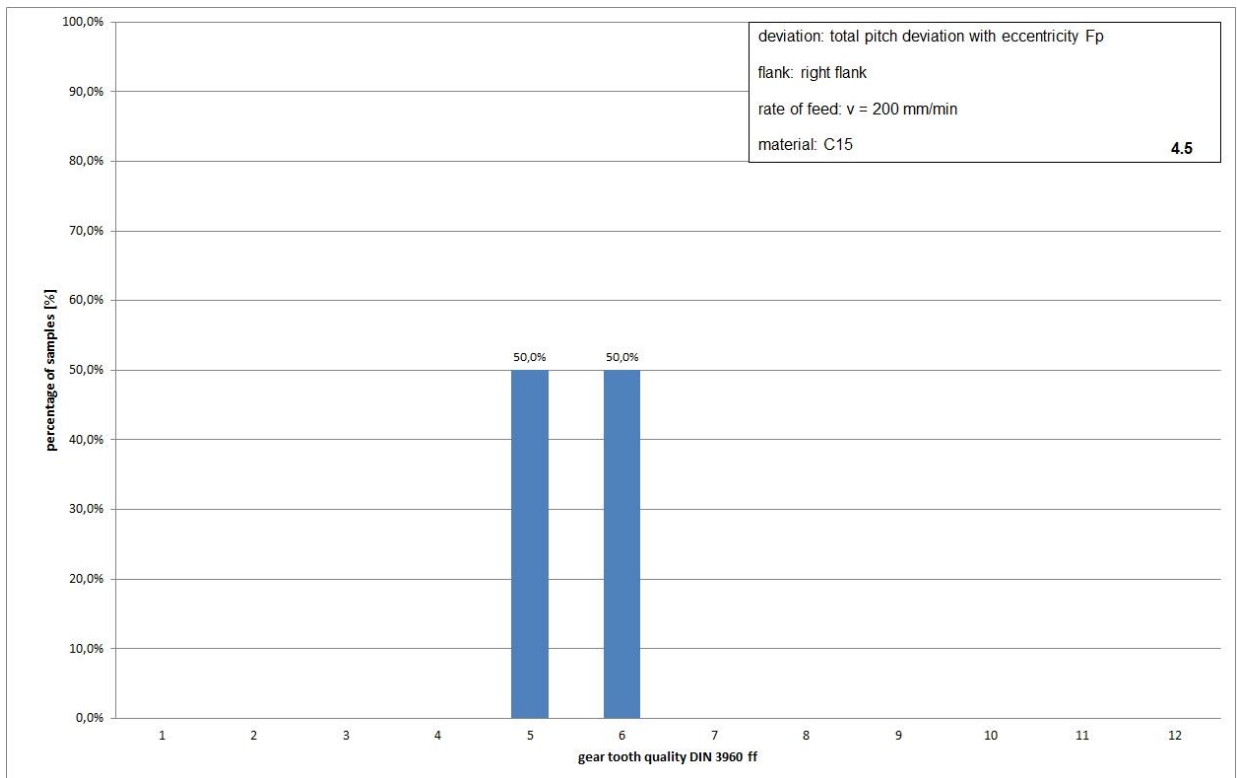
Appendix 4: Statistical analysis of gear tooth quality (DIN 3960 ff)
of samples and flanks

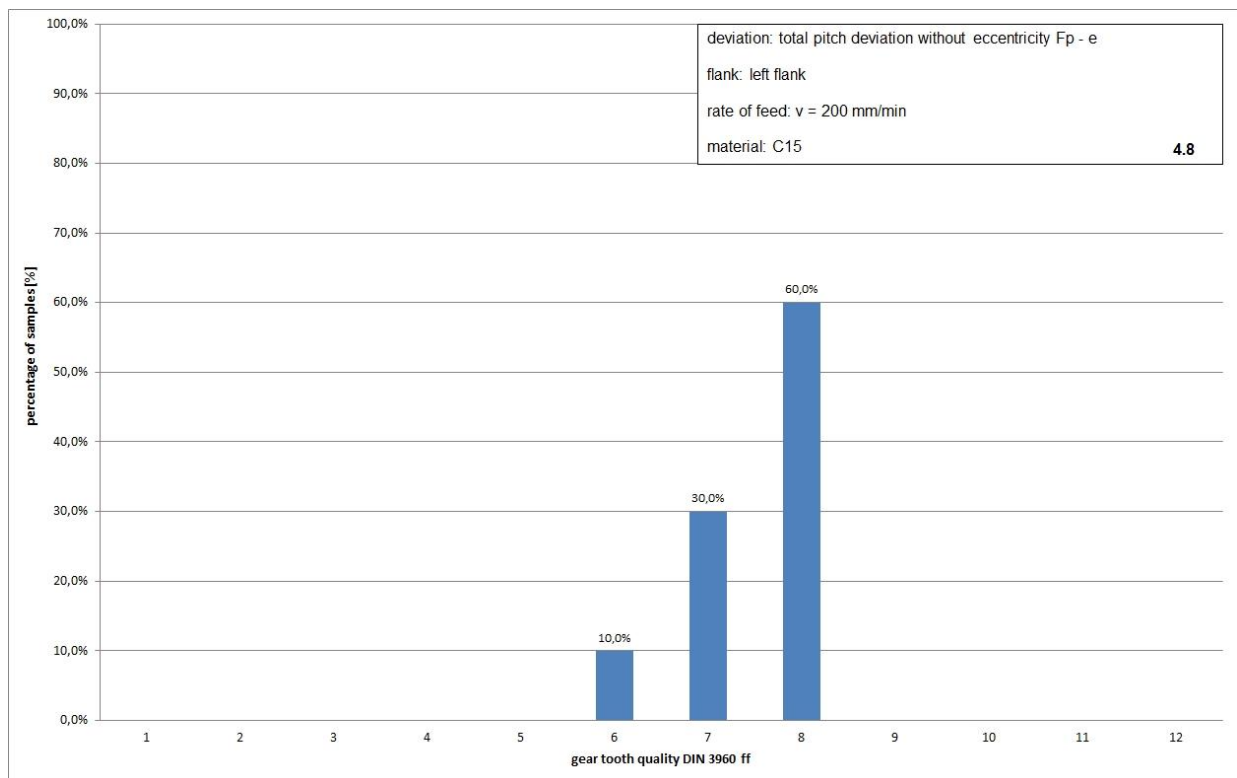
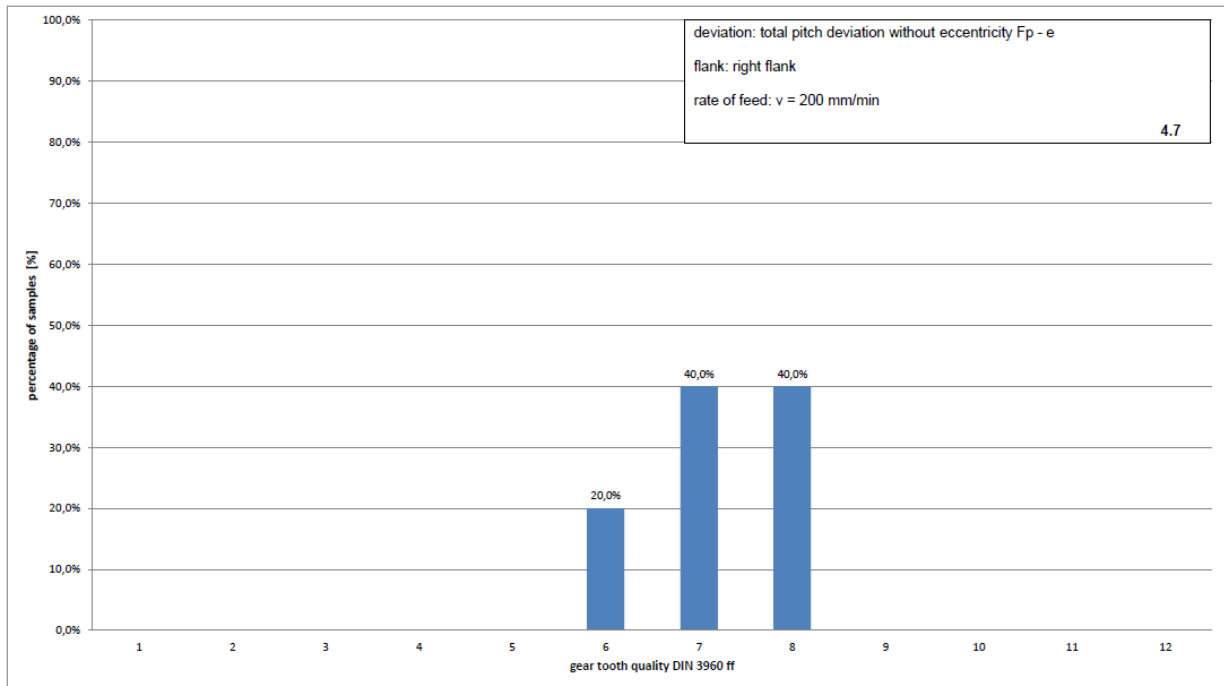
Total pitch deviation	FP	4.1 – 4.12
Individual pitch deviation	fp	4.13 – 4.24
Concentricity deviation	Fr	4.25 – 4.30
Total profile deviation	FA	4.31 – 4.36
Profile angle deviation	fHa	4.37 – 4.42
Profile form deviation	ffA	4.43 – 4.48
Tooth trace total deviation	FB	4.49 – 4.54
Tooth trace angle deviation	fHB	4.55 – 4.60
Tooth trace form deviation	ffB	4.61 – 4.66

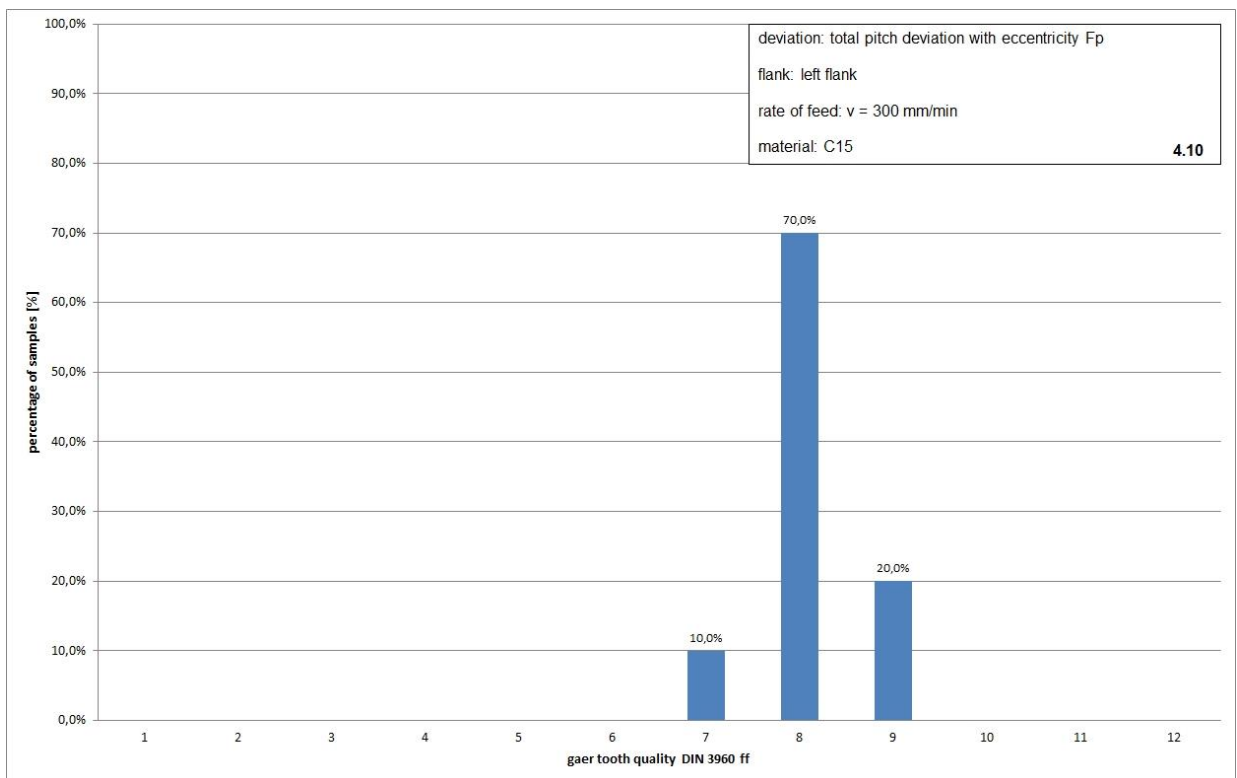
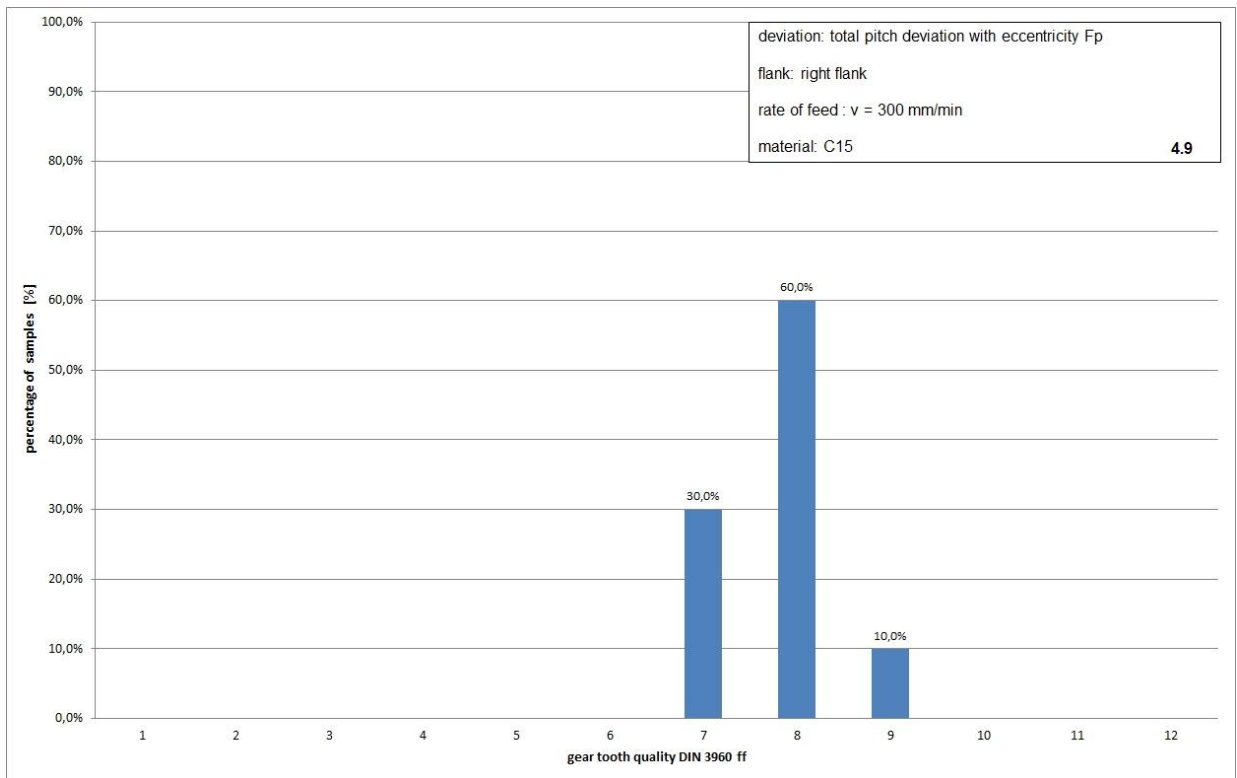
Basis for the statistical analysis are a batch of 10 samples per rate of feed. At three speed rates 30 samples were statistical analyzed and deviations were evaluated. The samples for the detailed analysis got selected randomly, even though all rolled samples have been measured completely (that means all teeth and flanks of the rolled samples have been measured). A separated analysis in evaluation is made in left and right flanks.

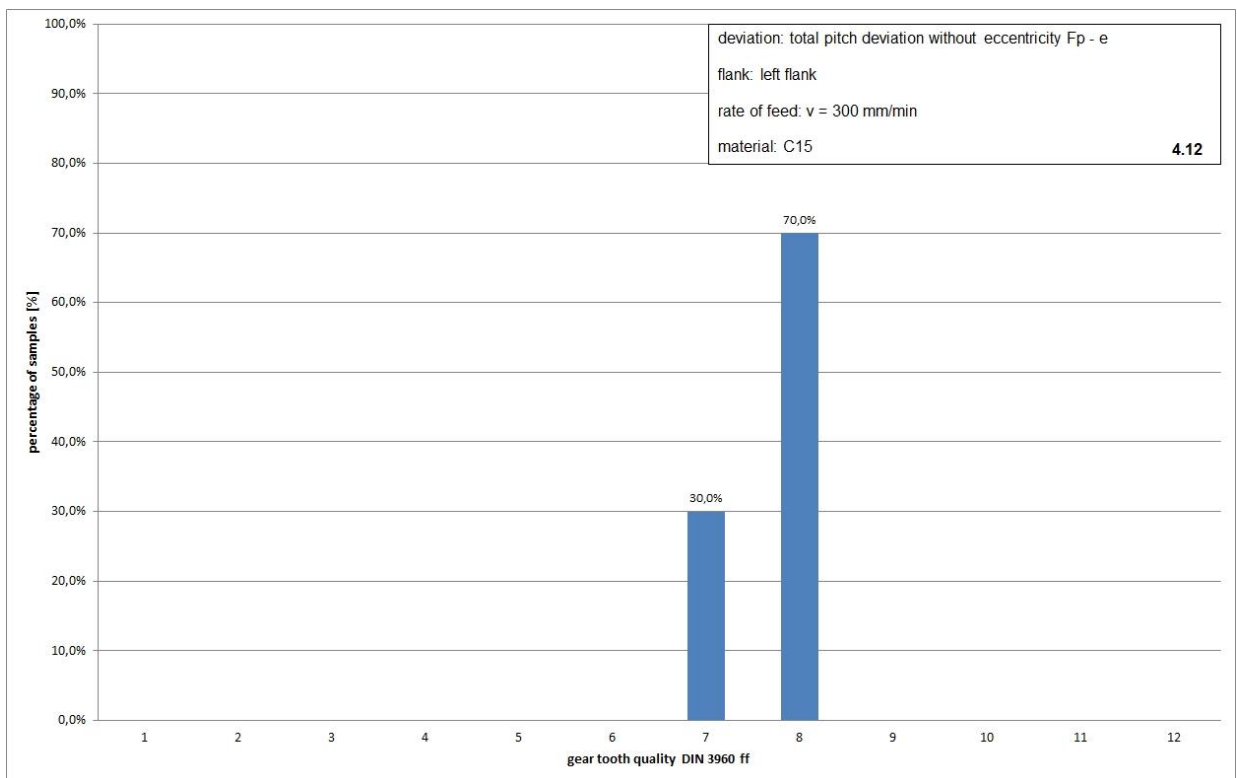
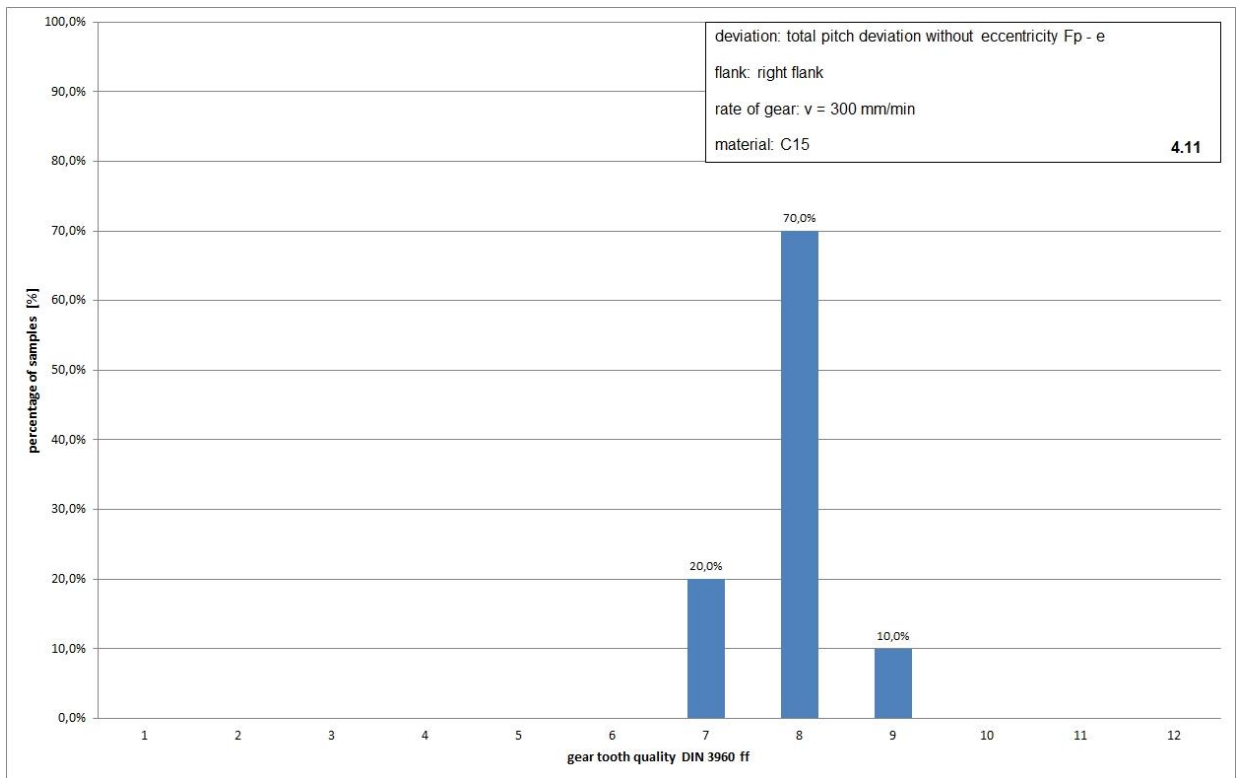


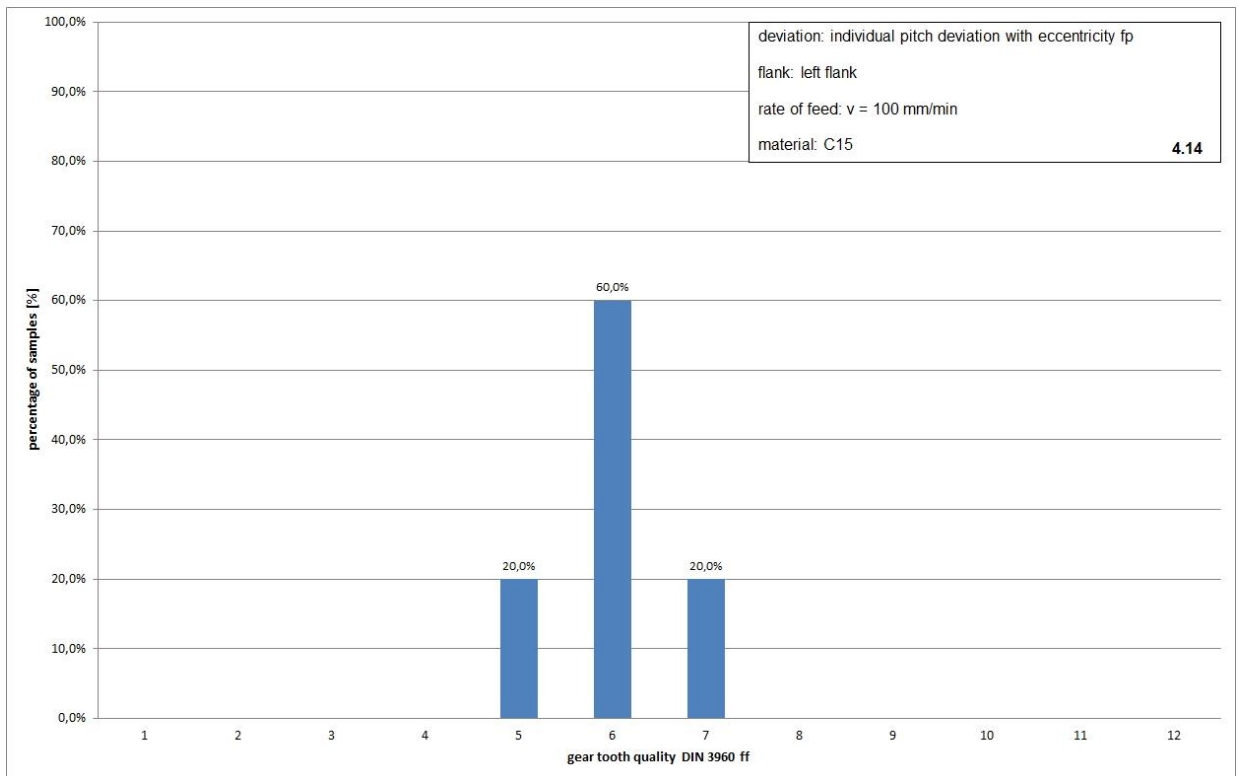
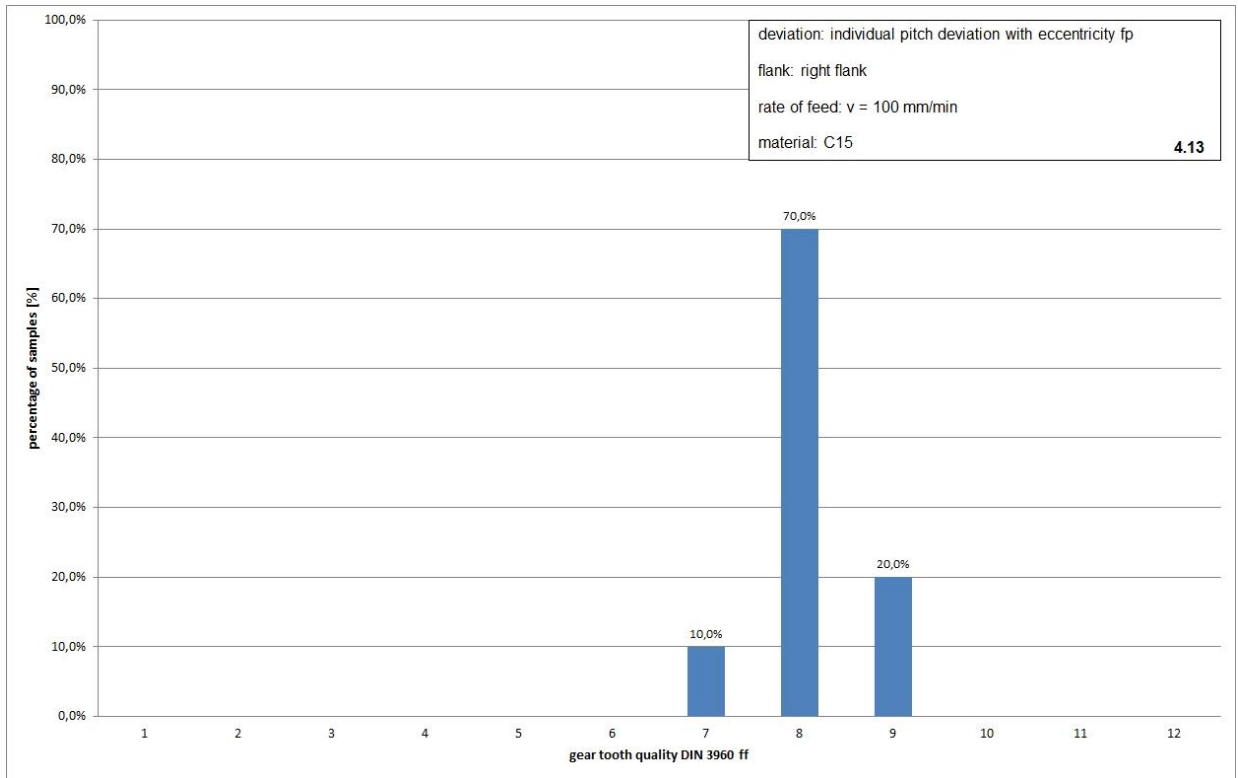


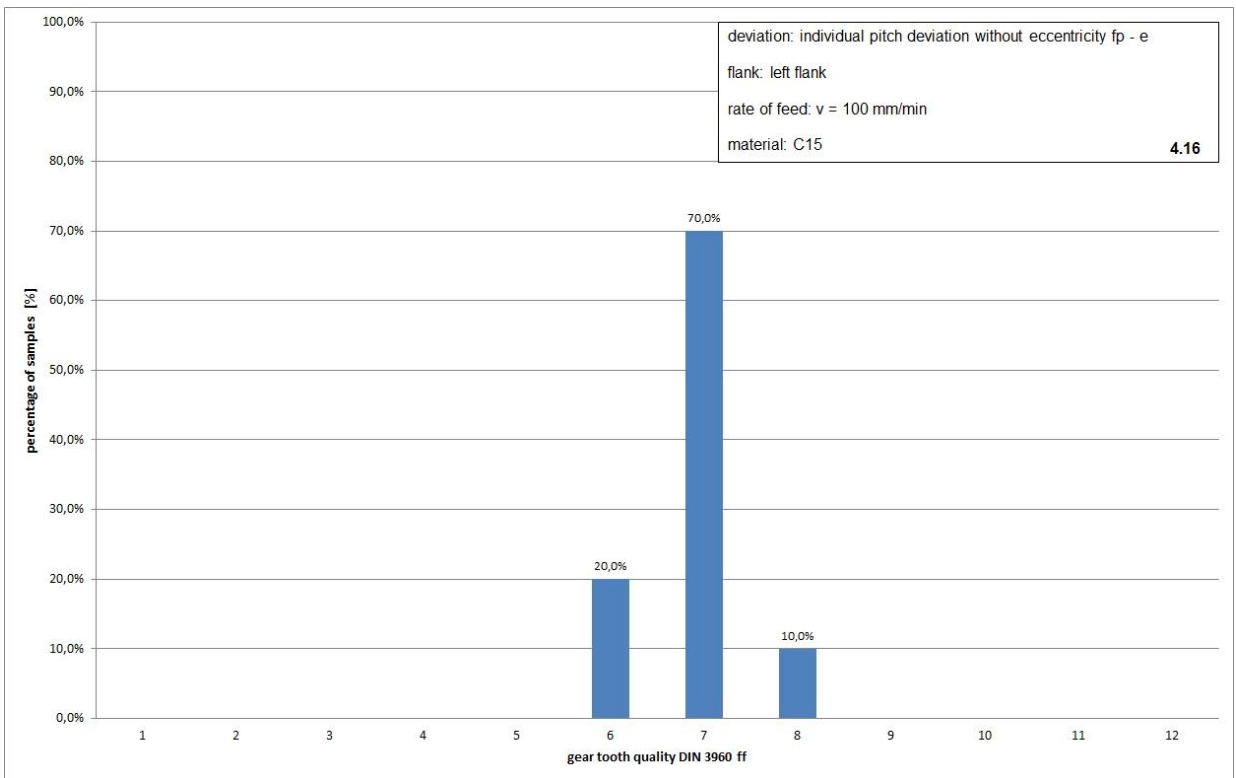
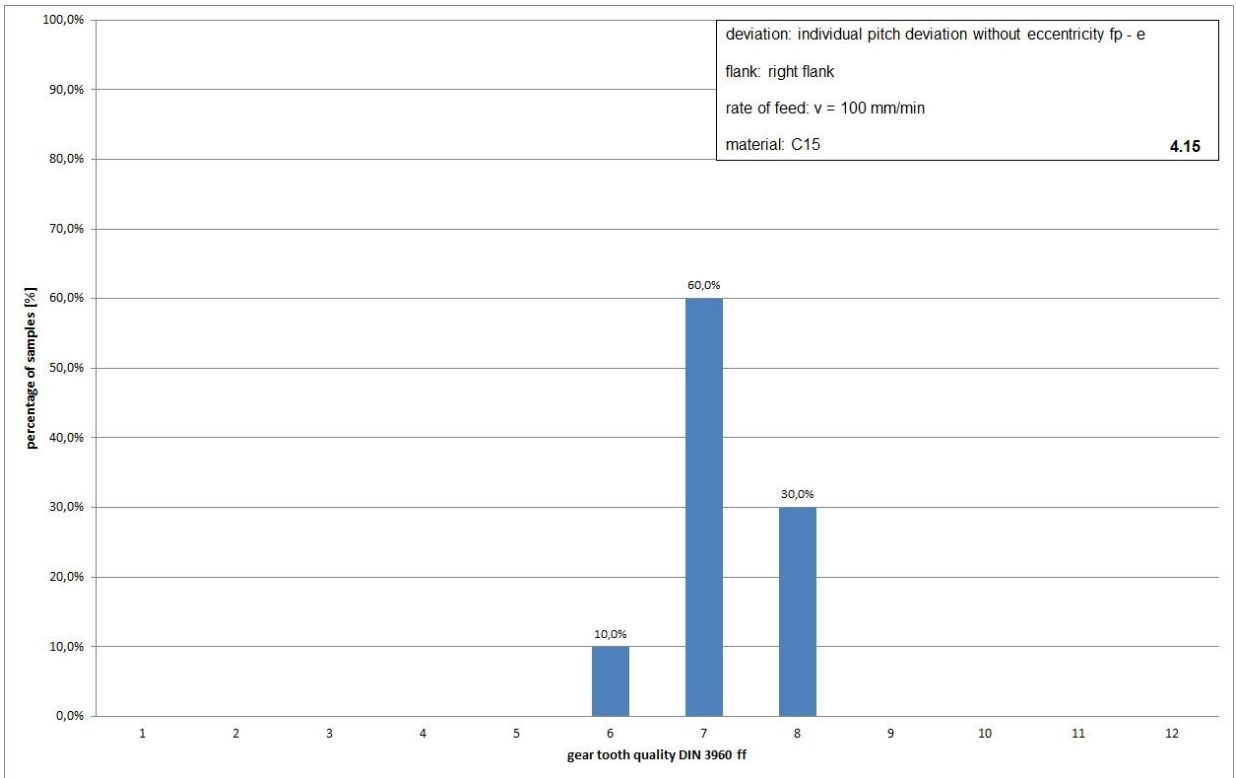


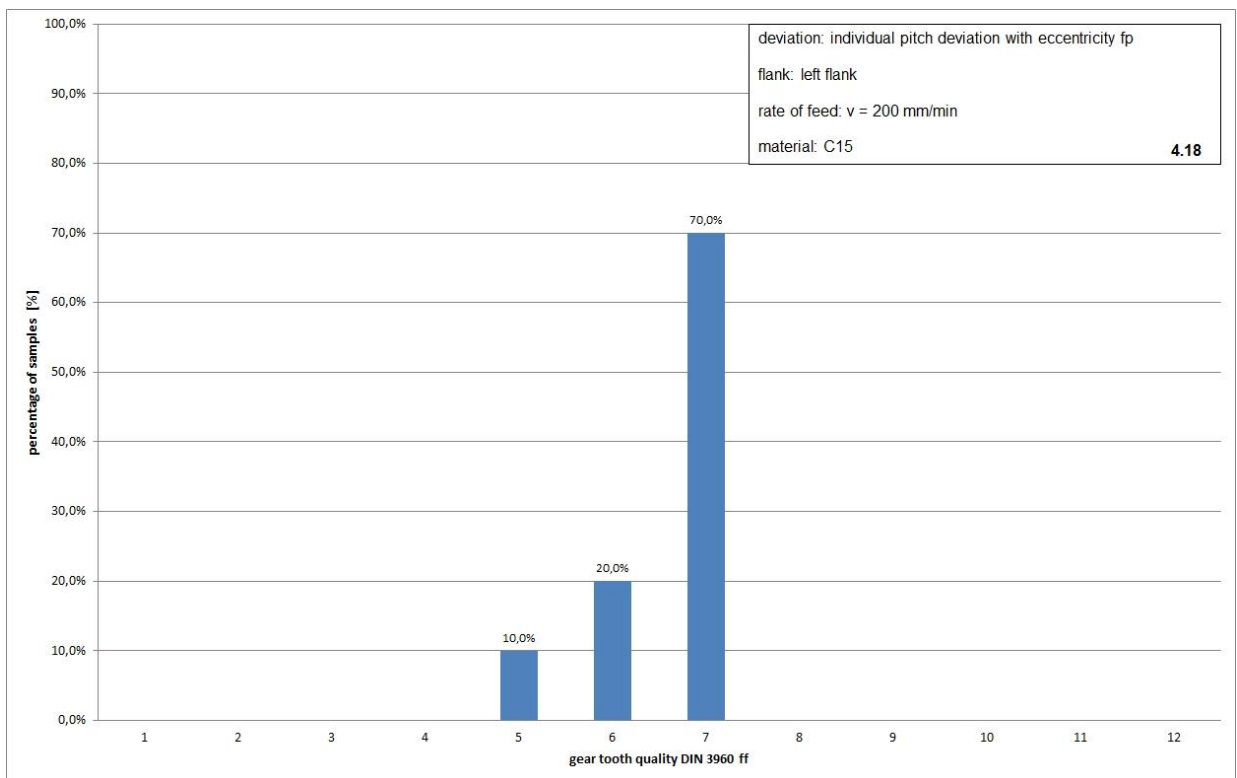
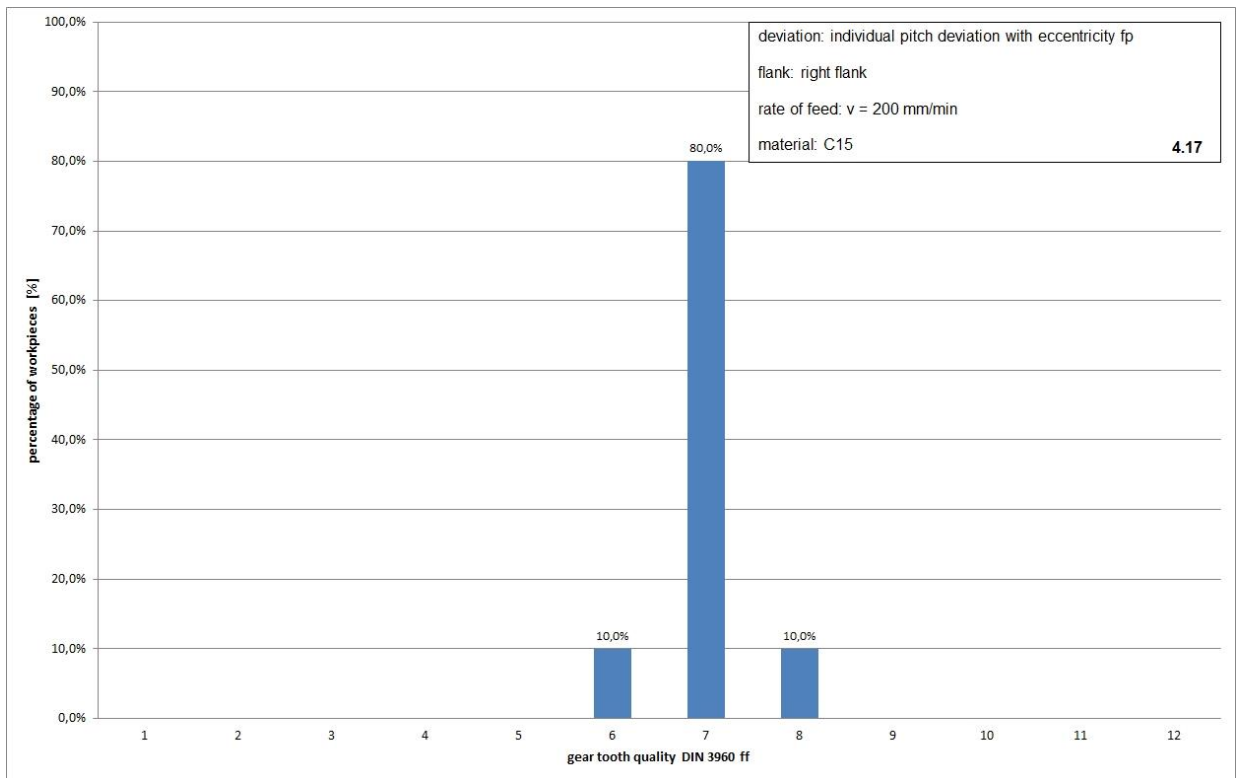


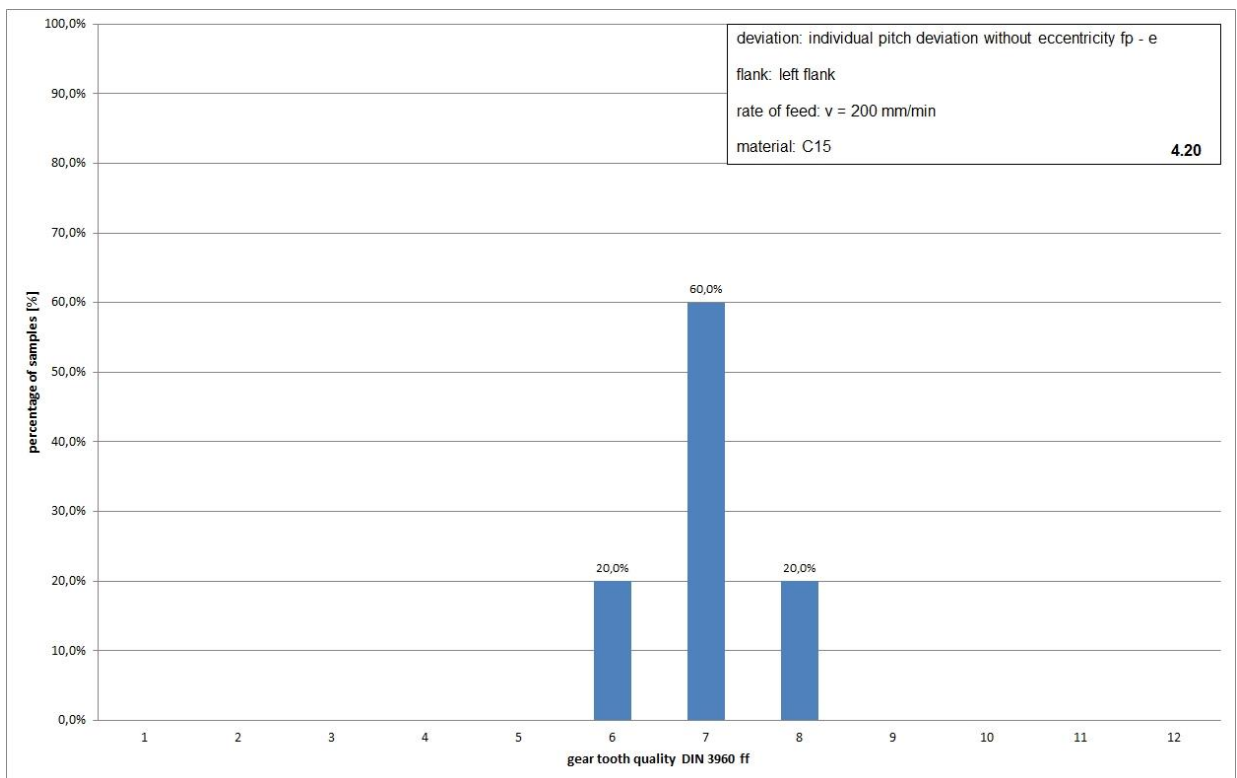
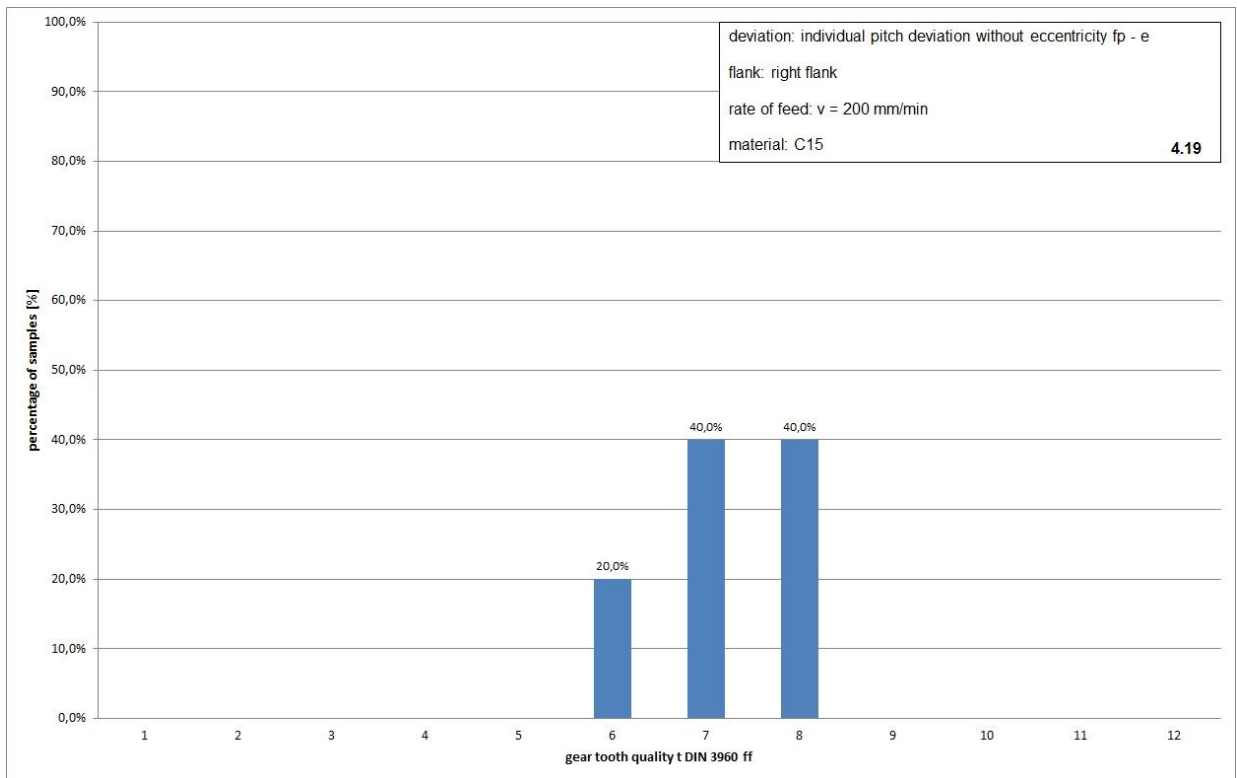


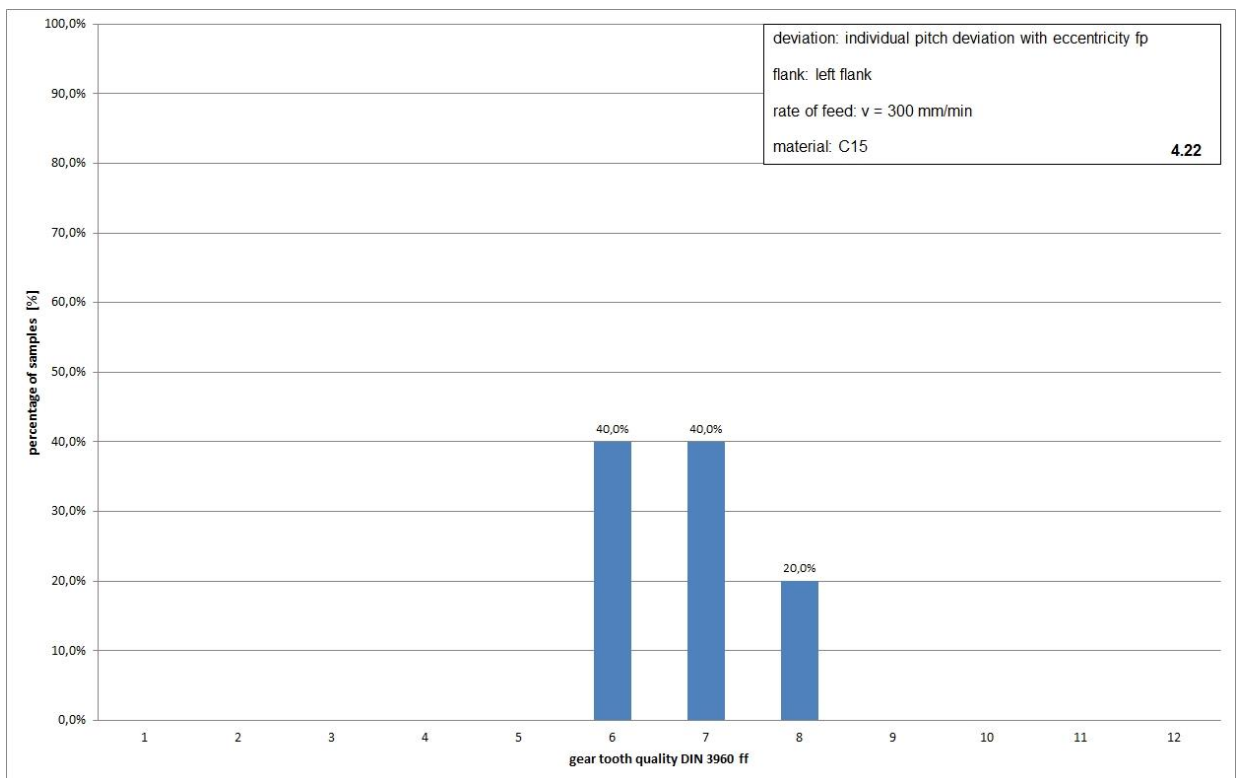
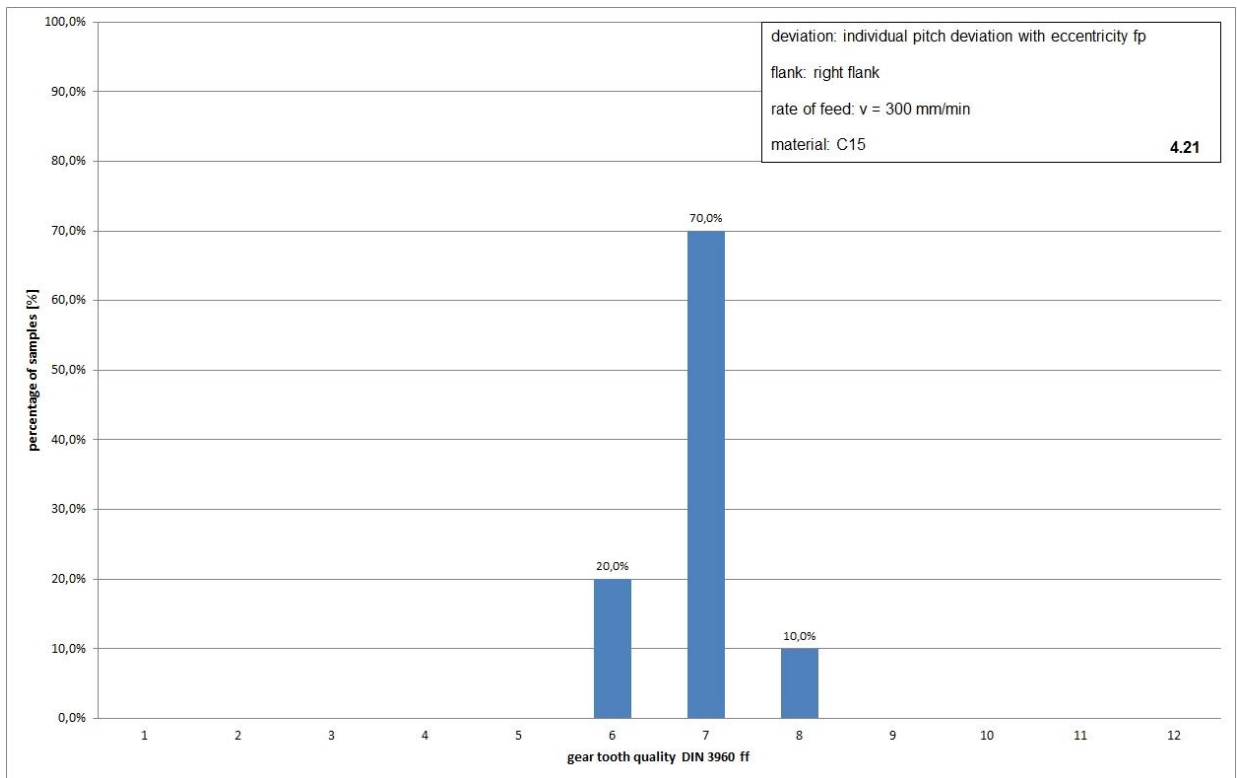


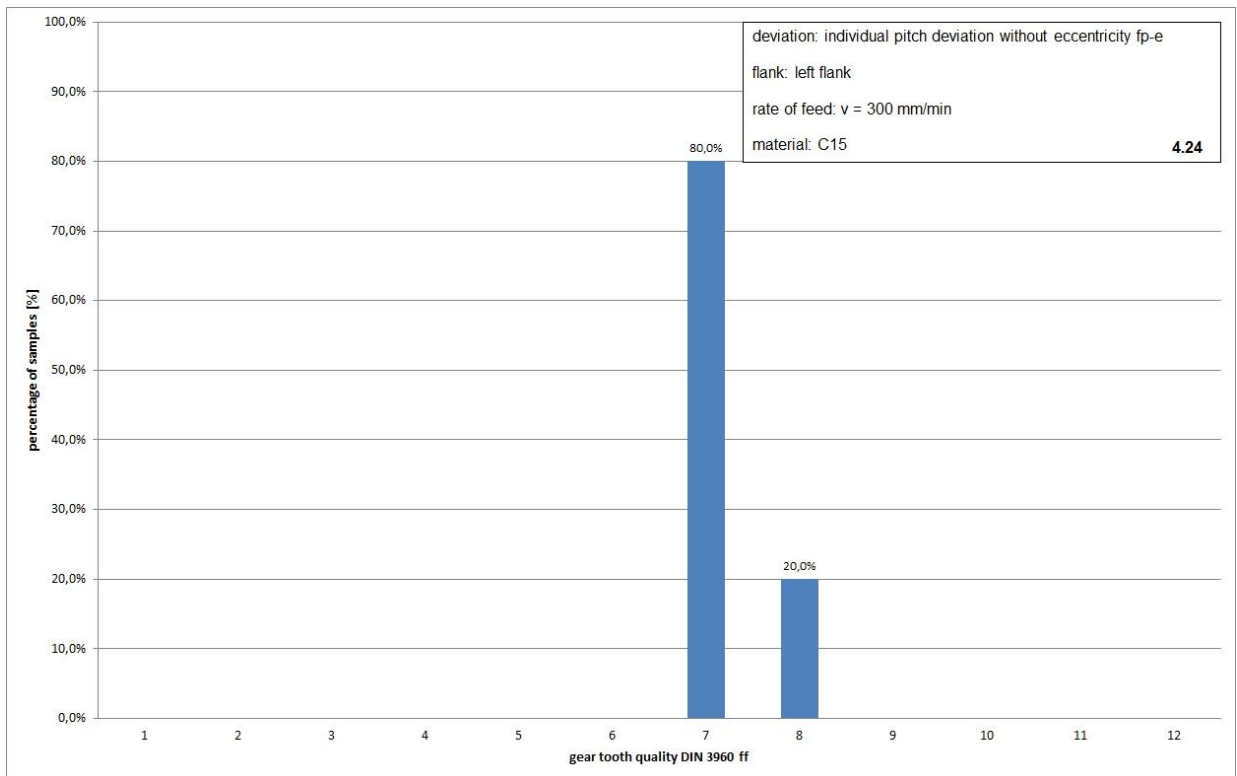
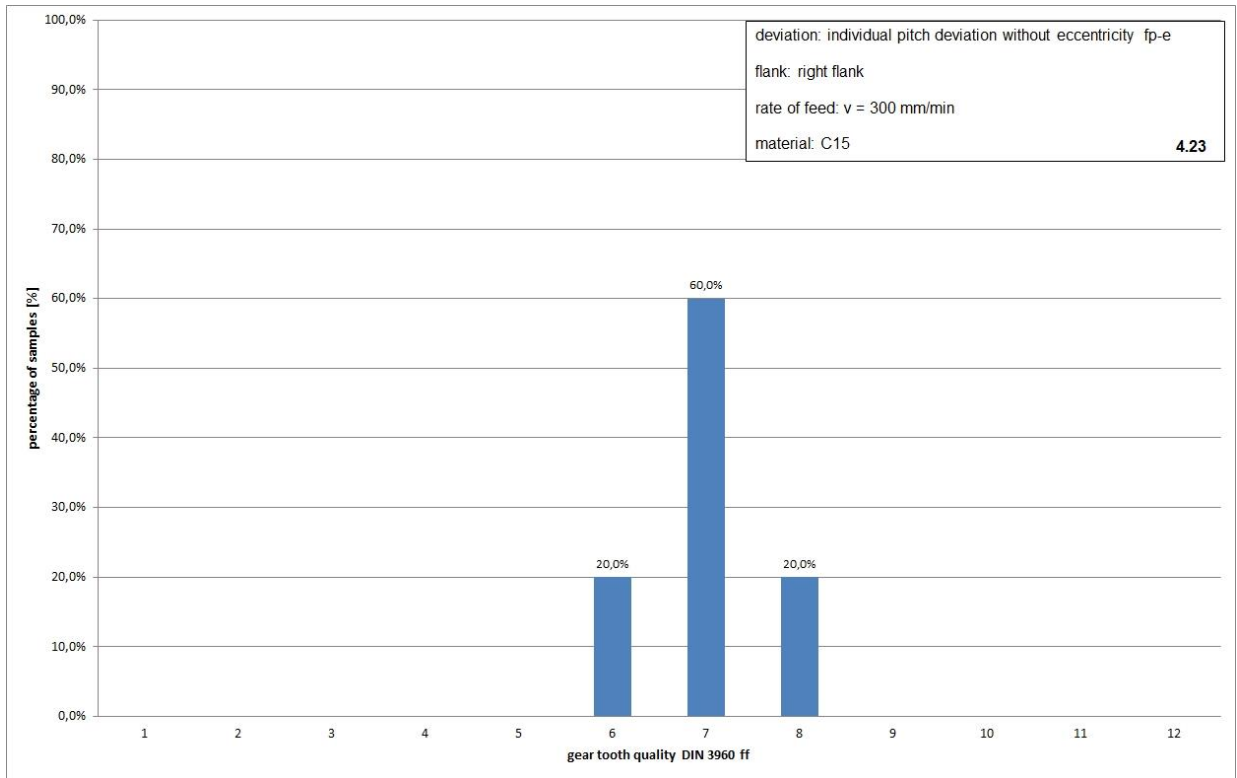


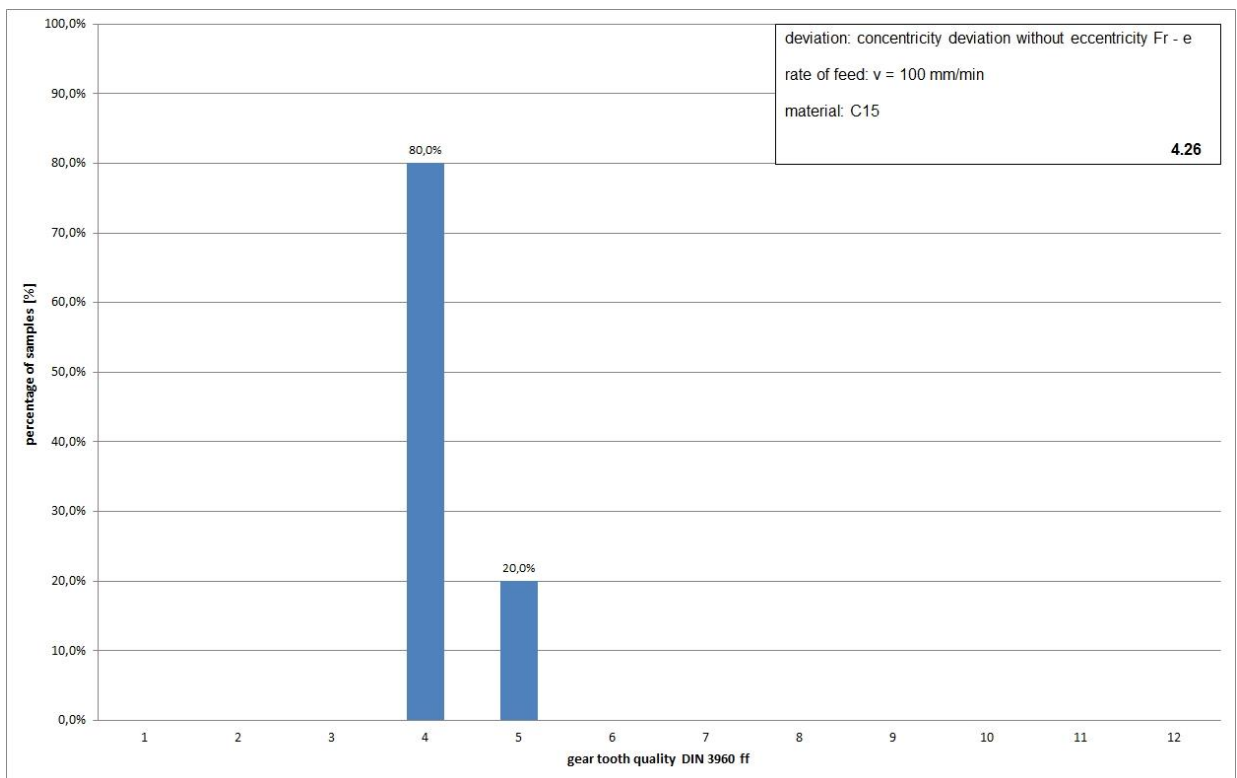
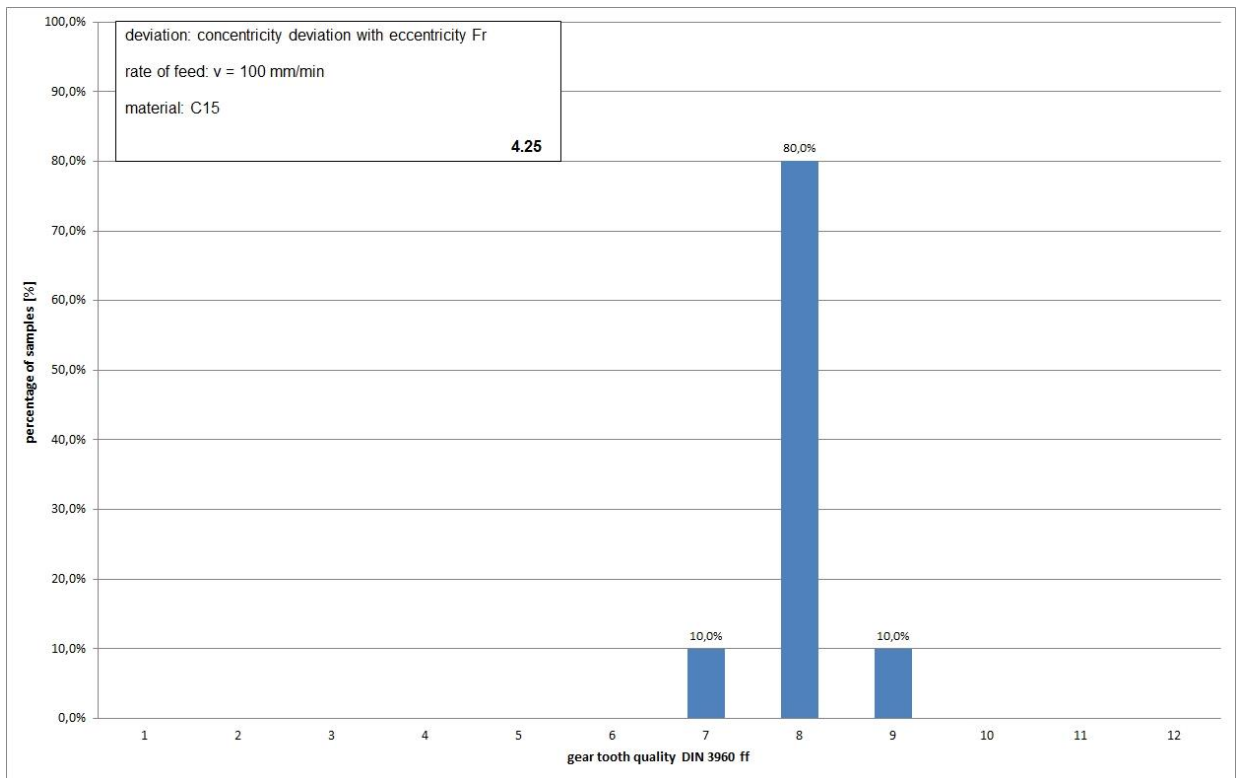


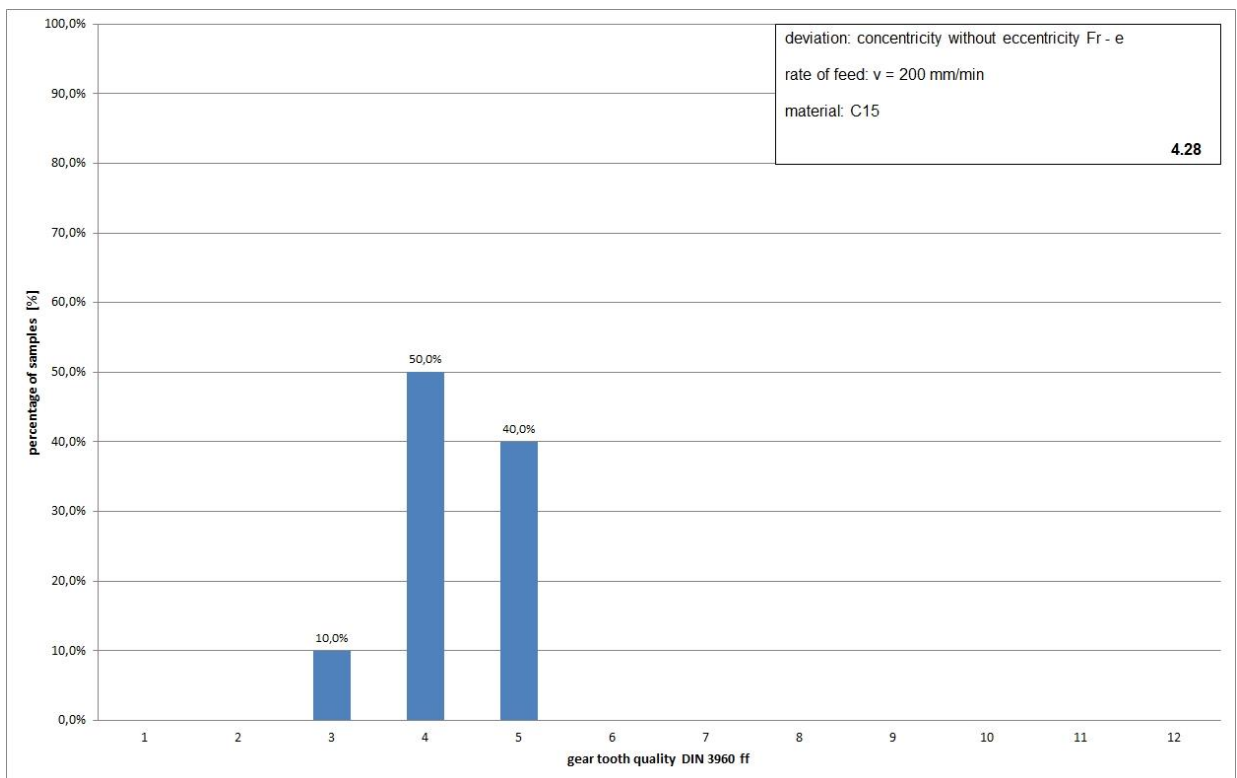
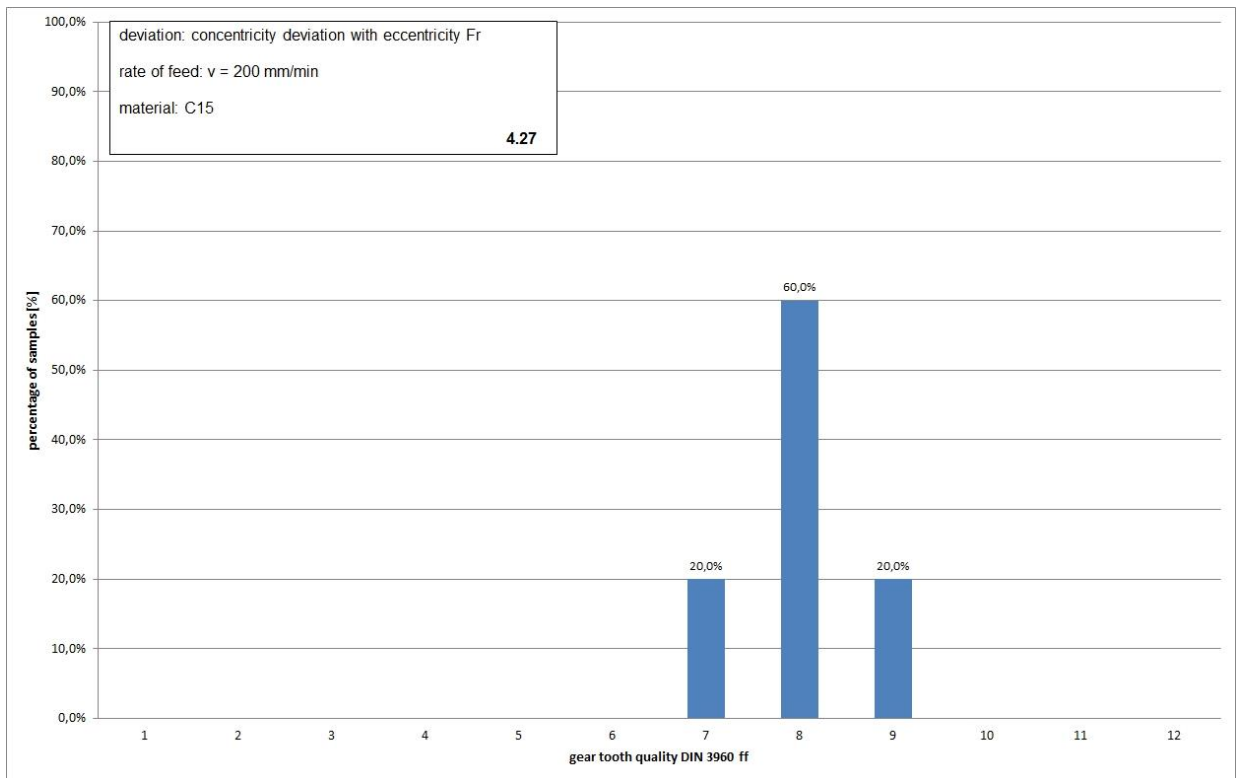


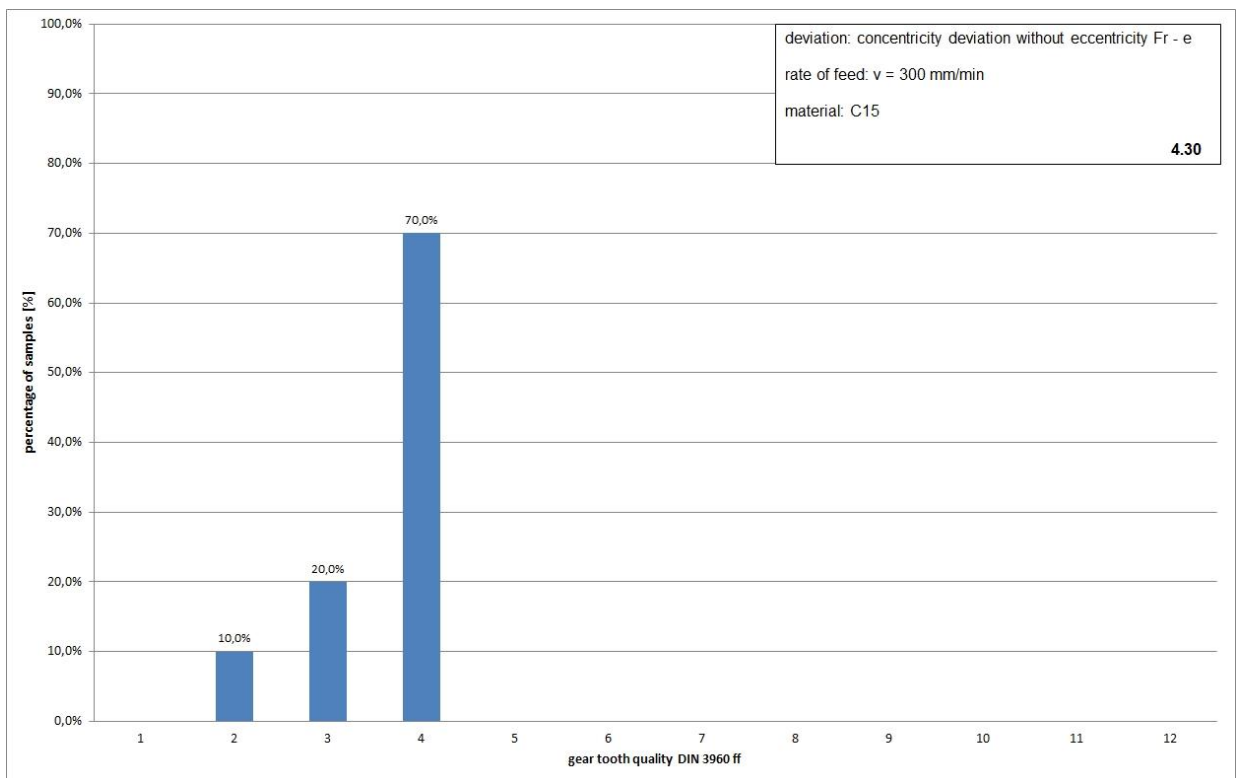
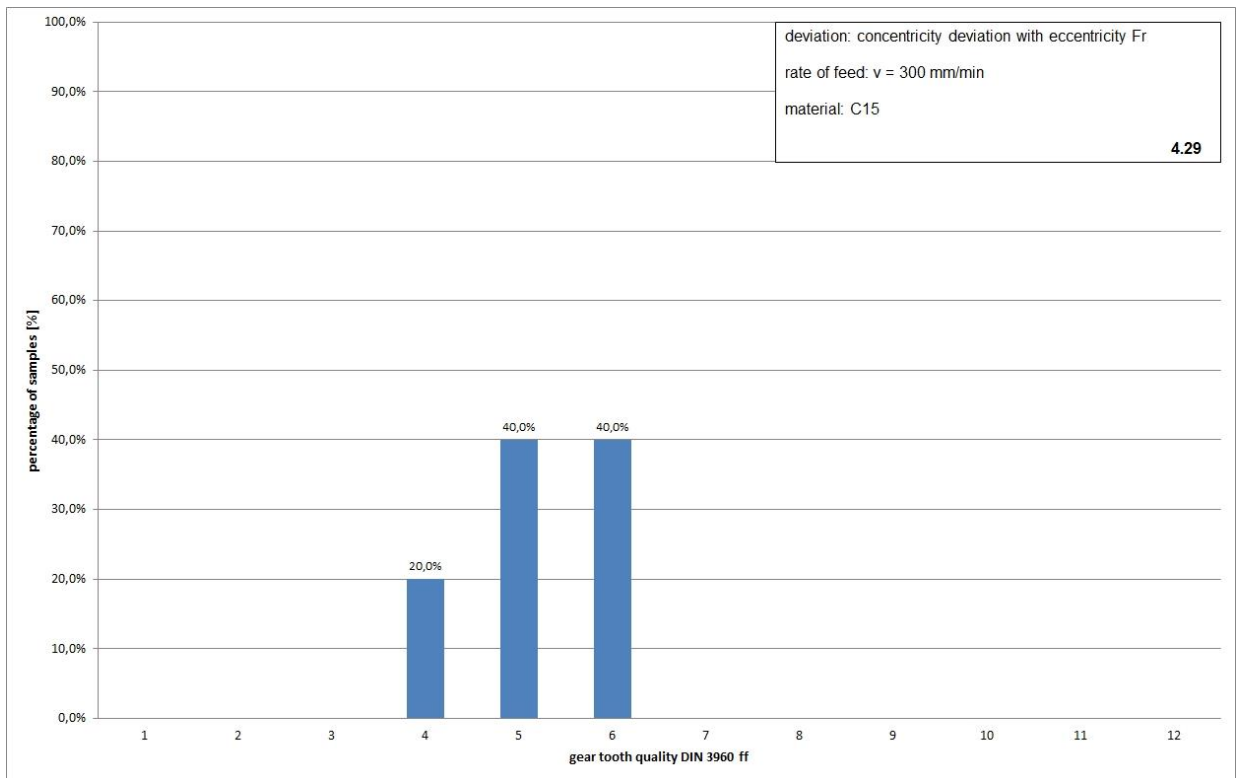


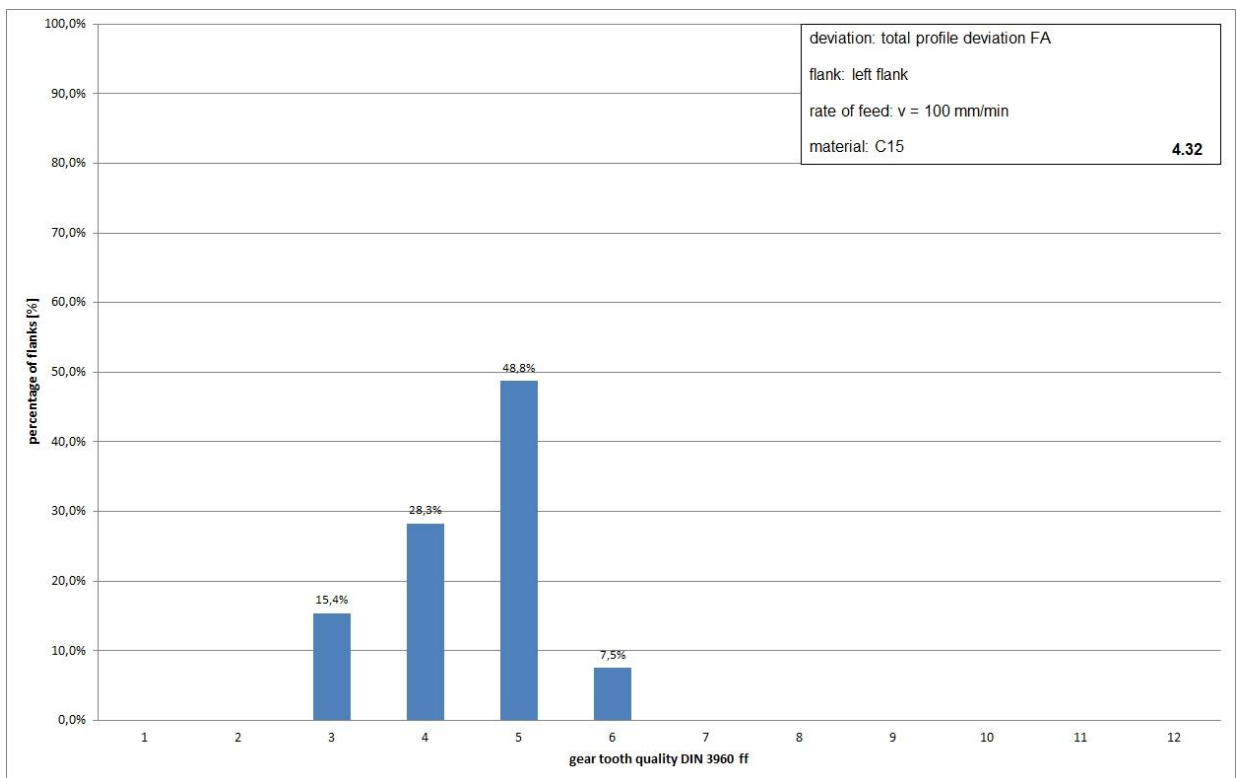
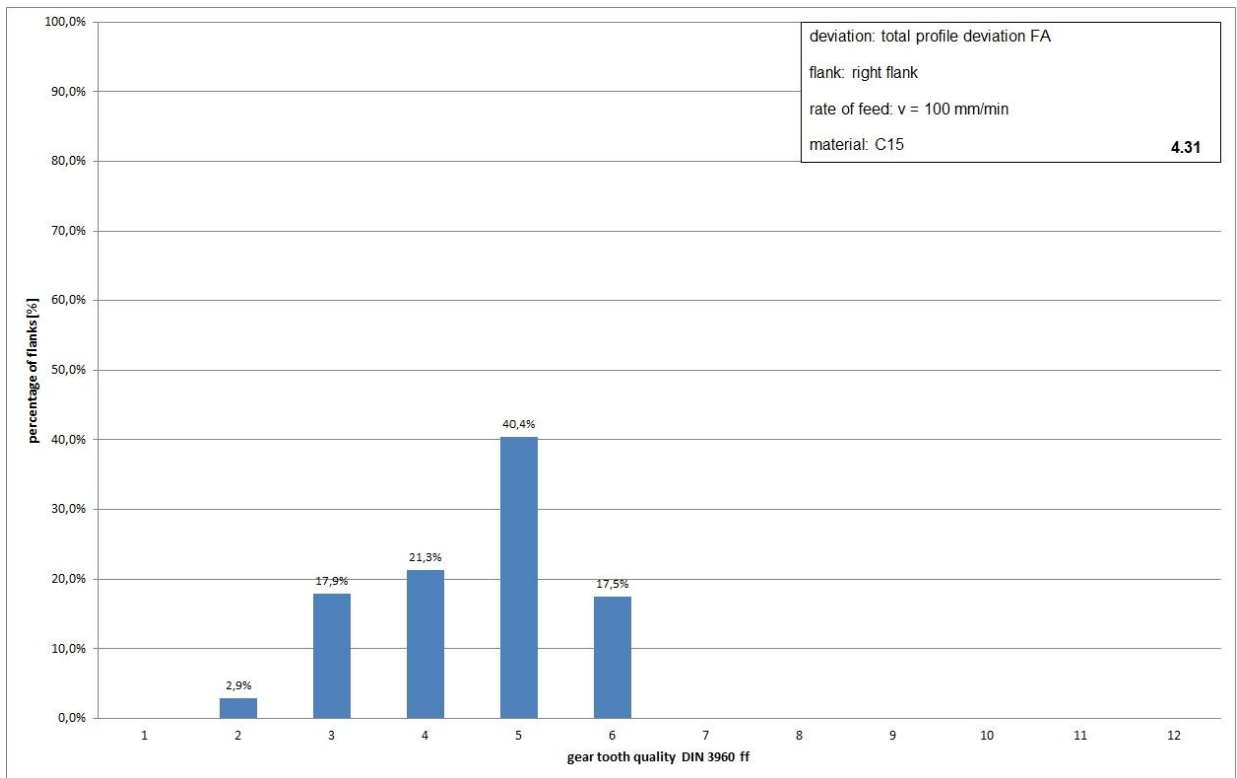


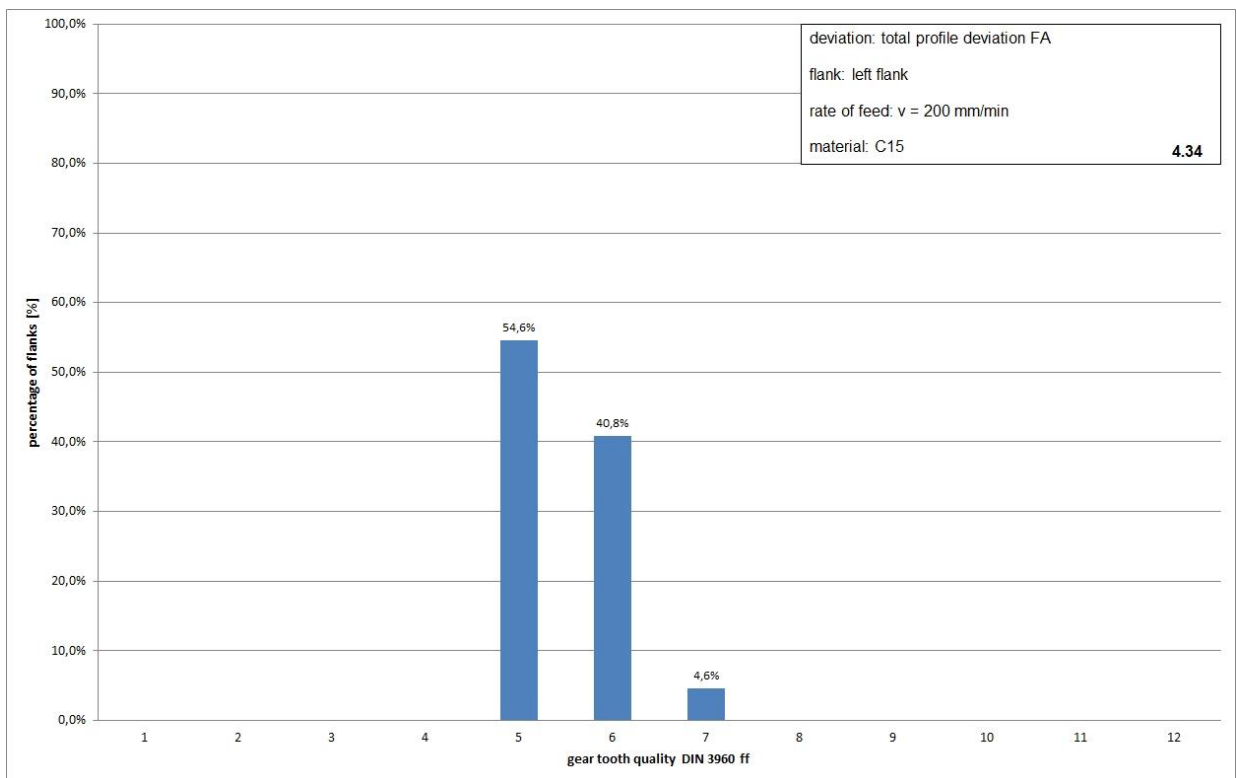
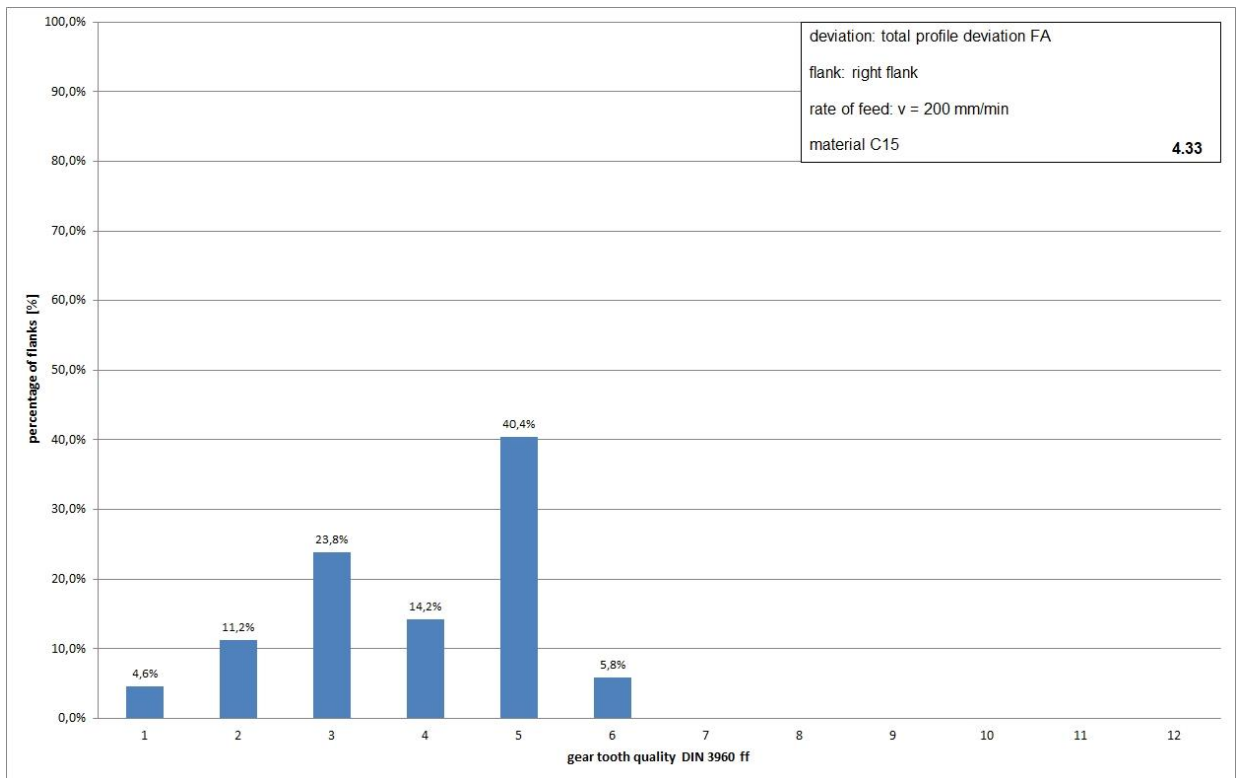


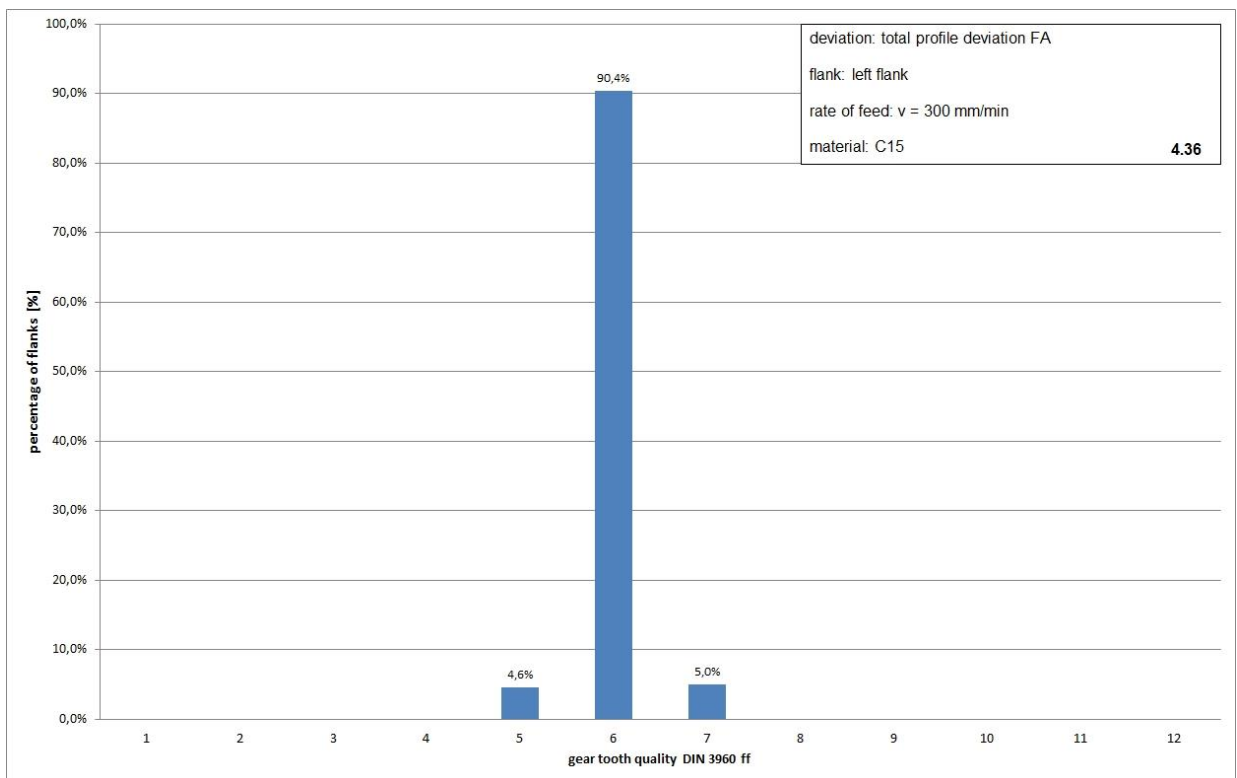
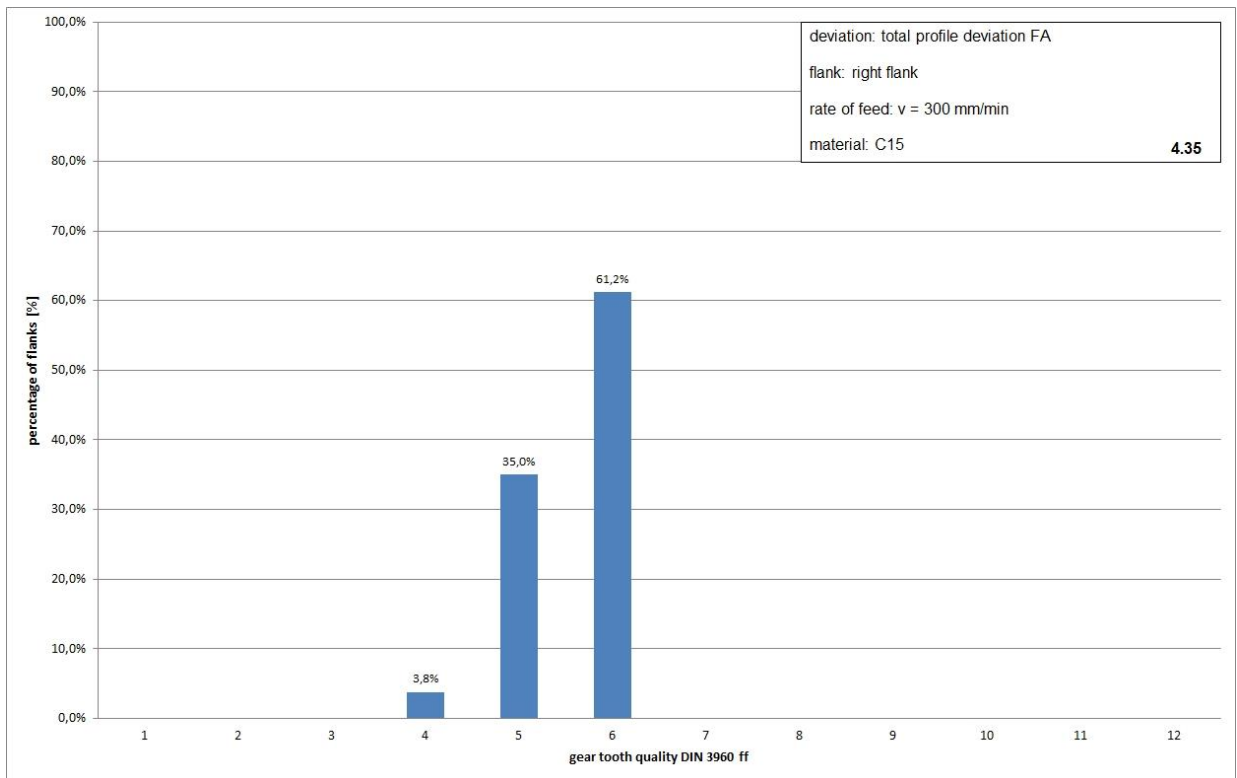


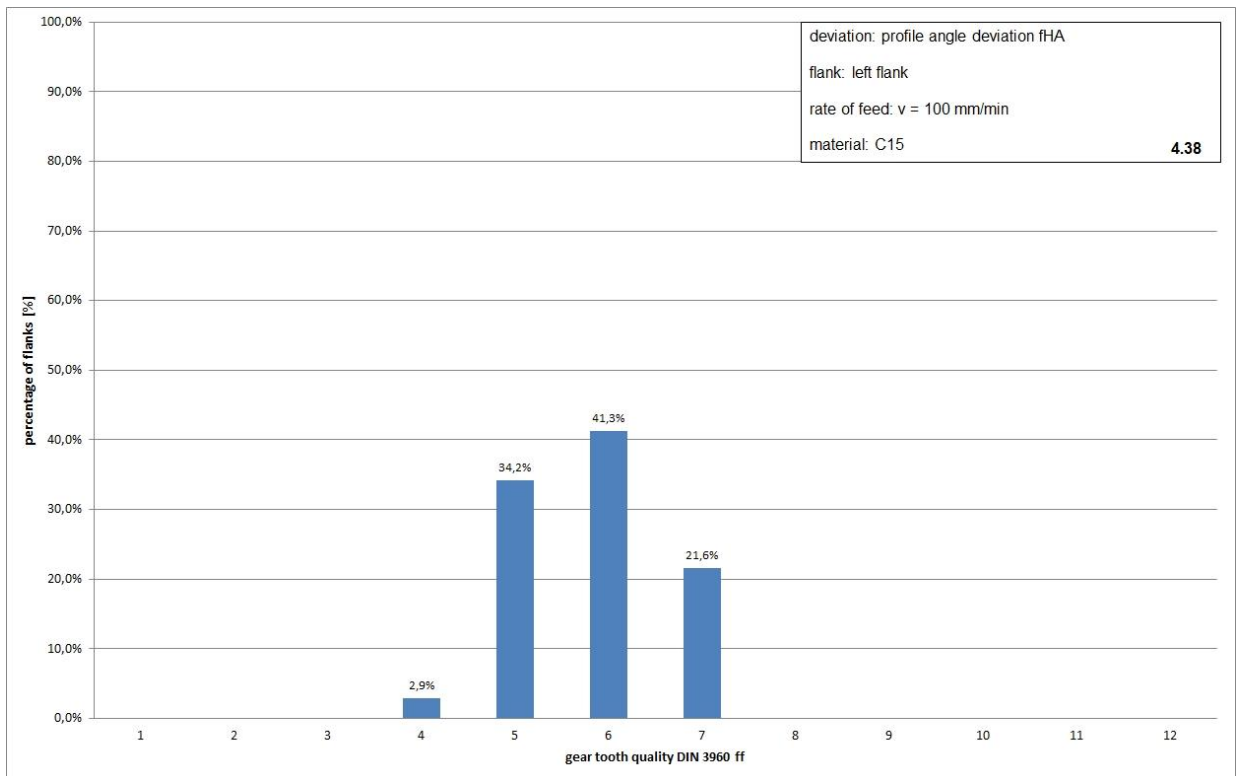
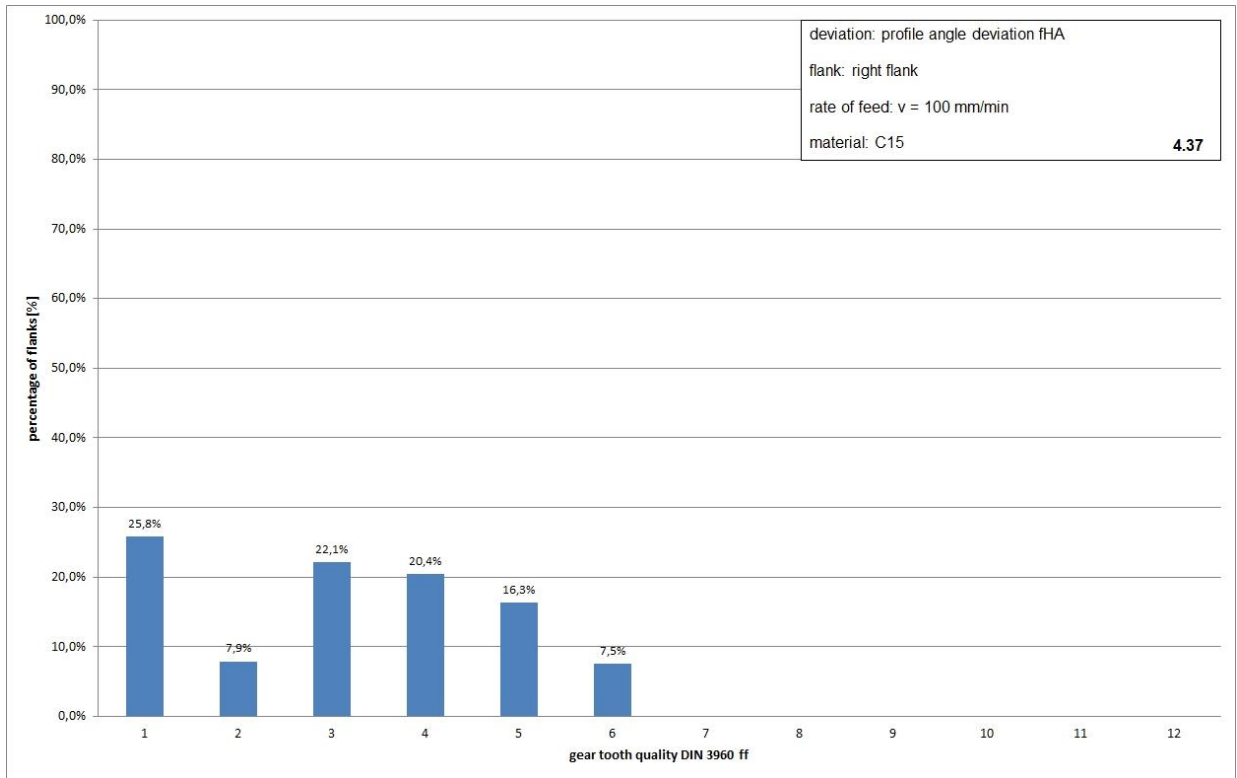


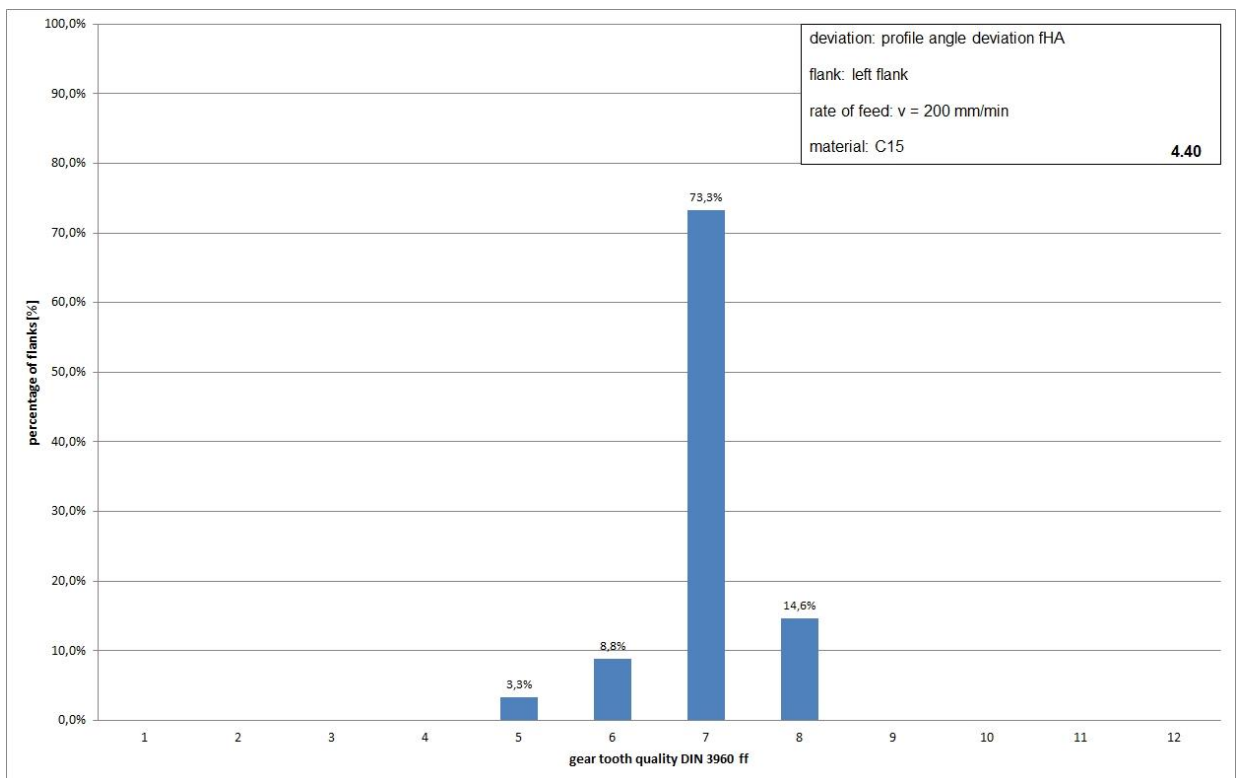
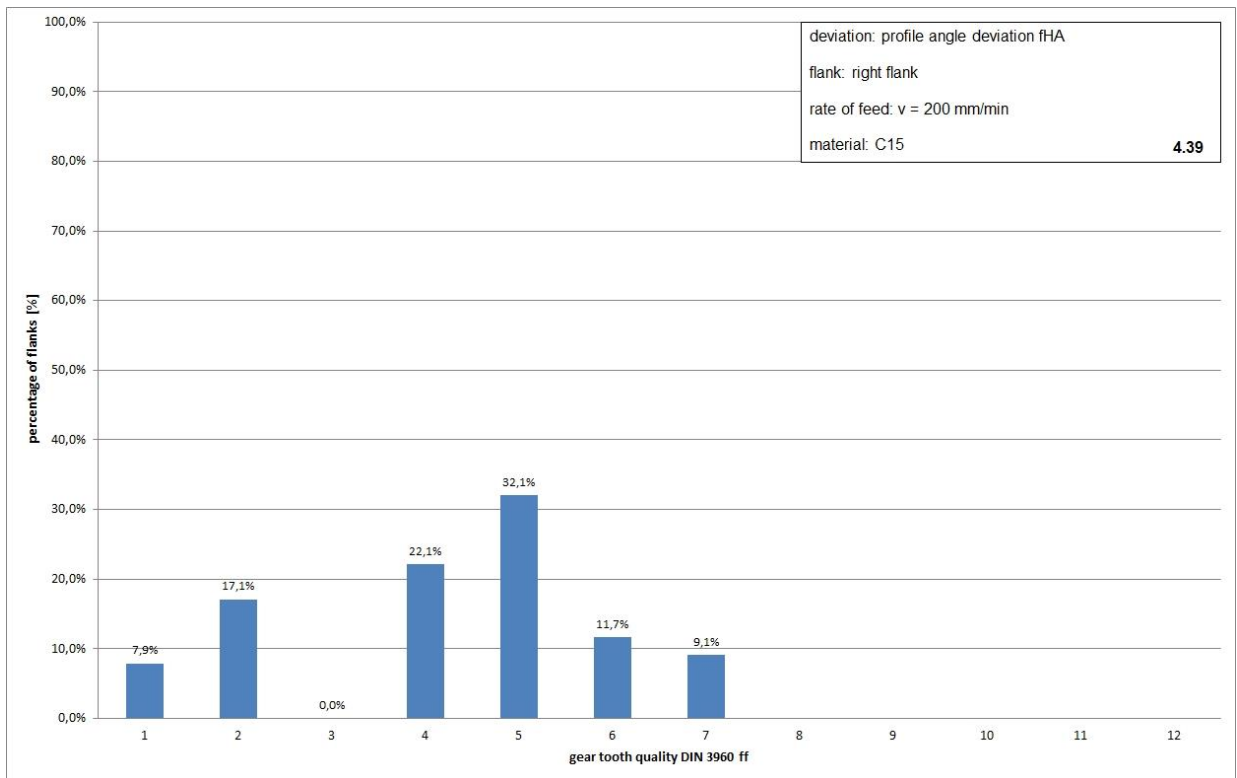


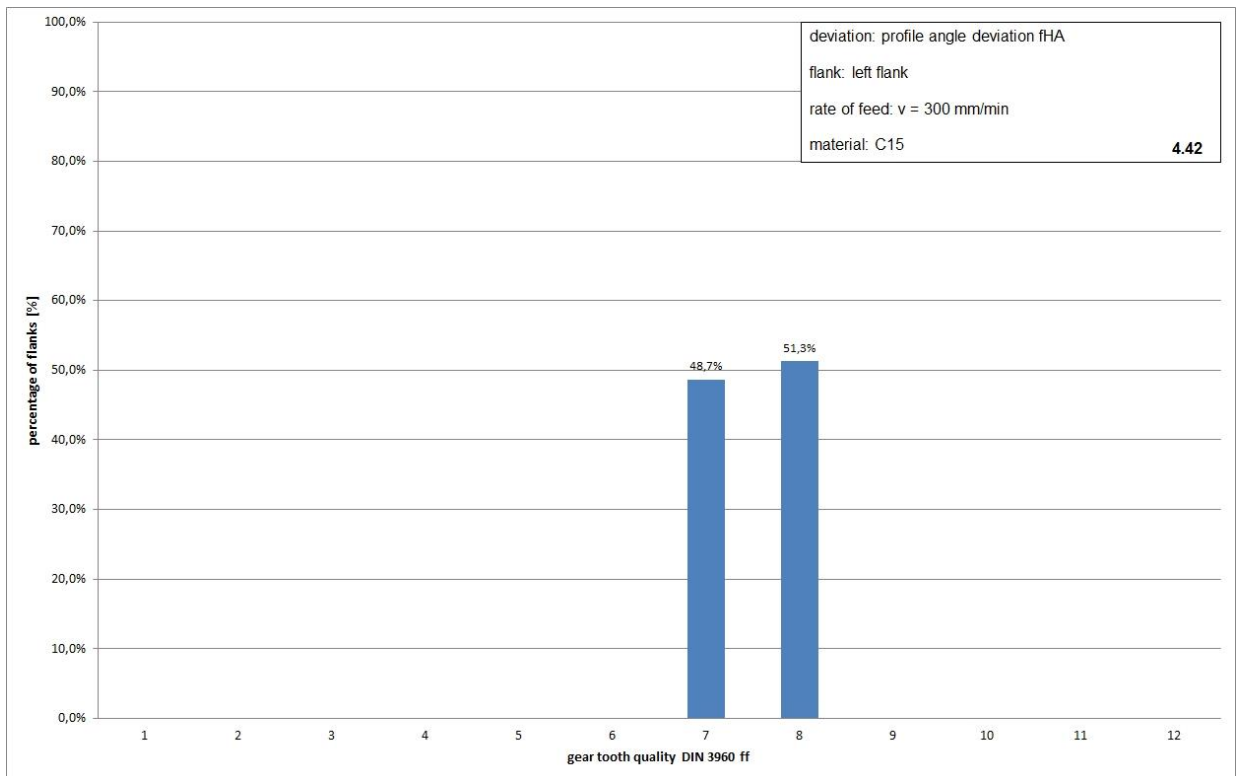
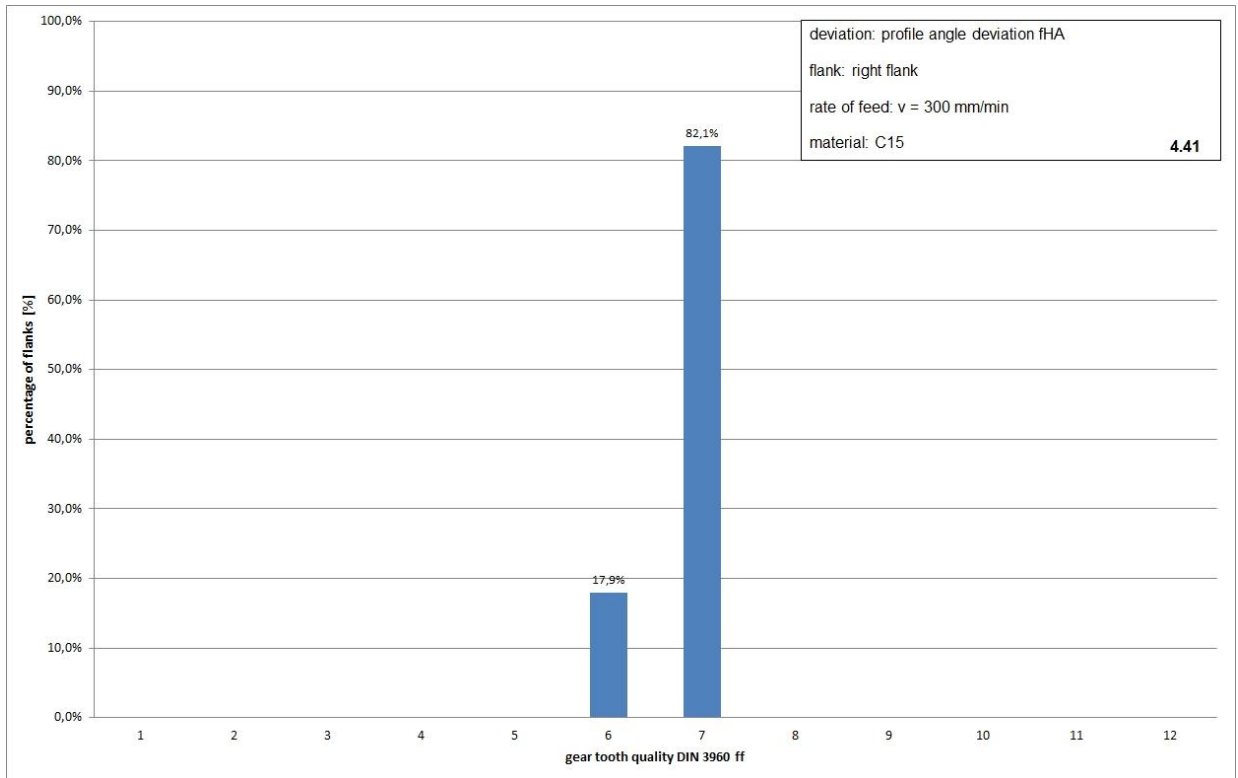


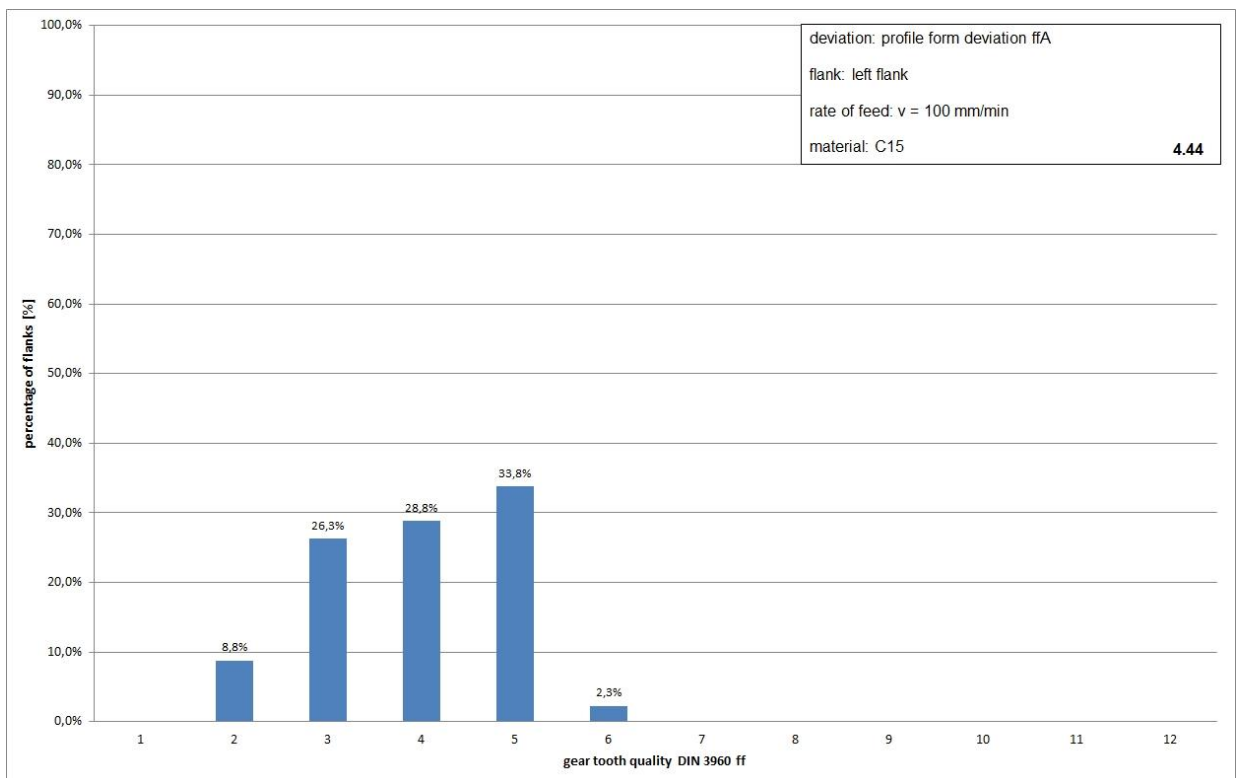
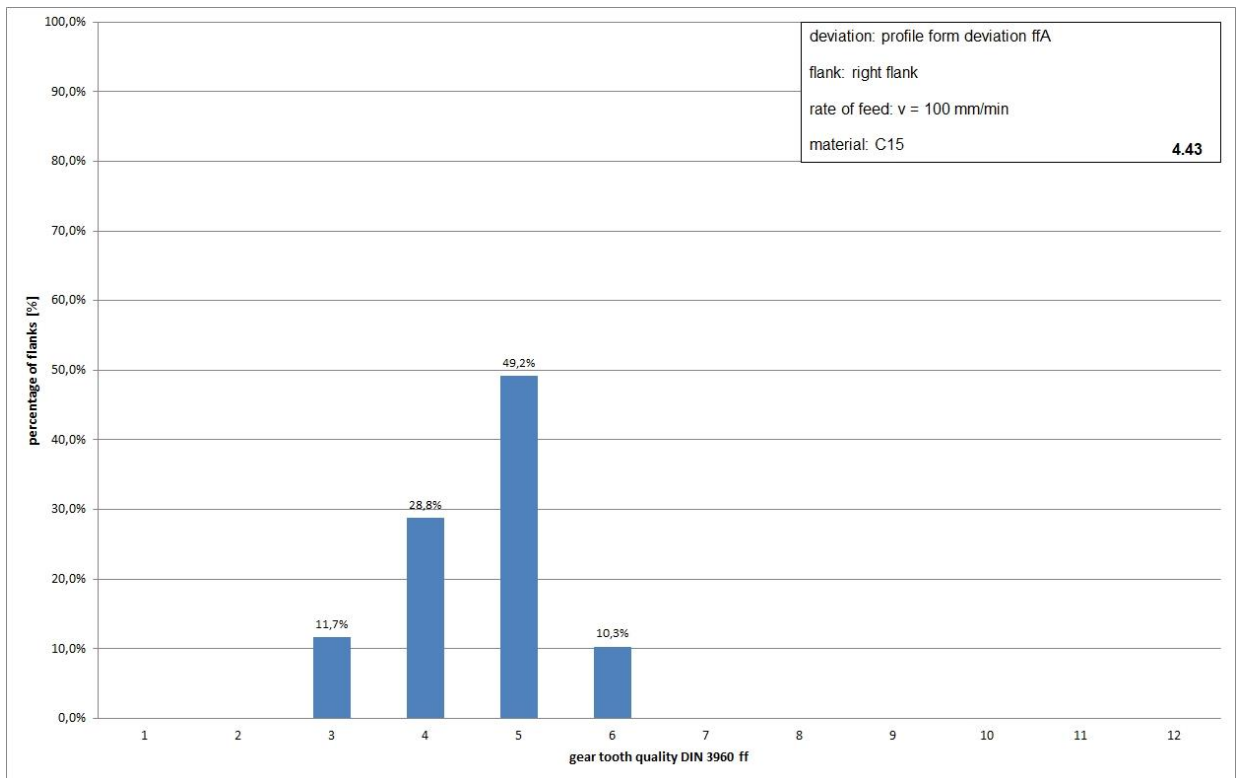


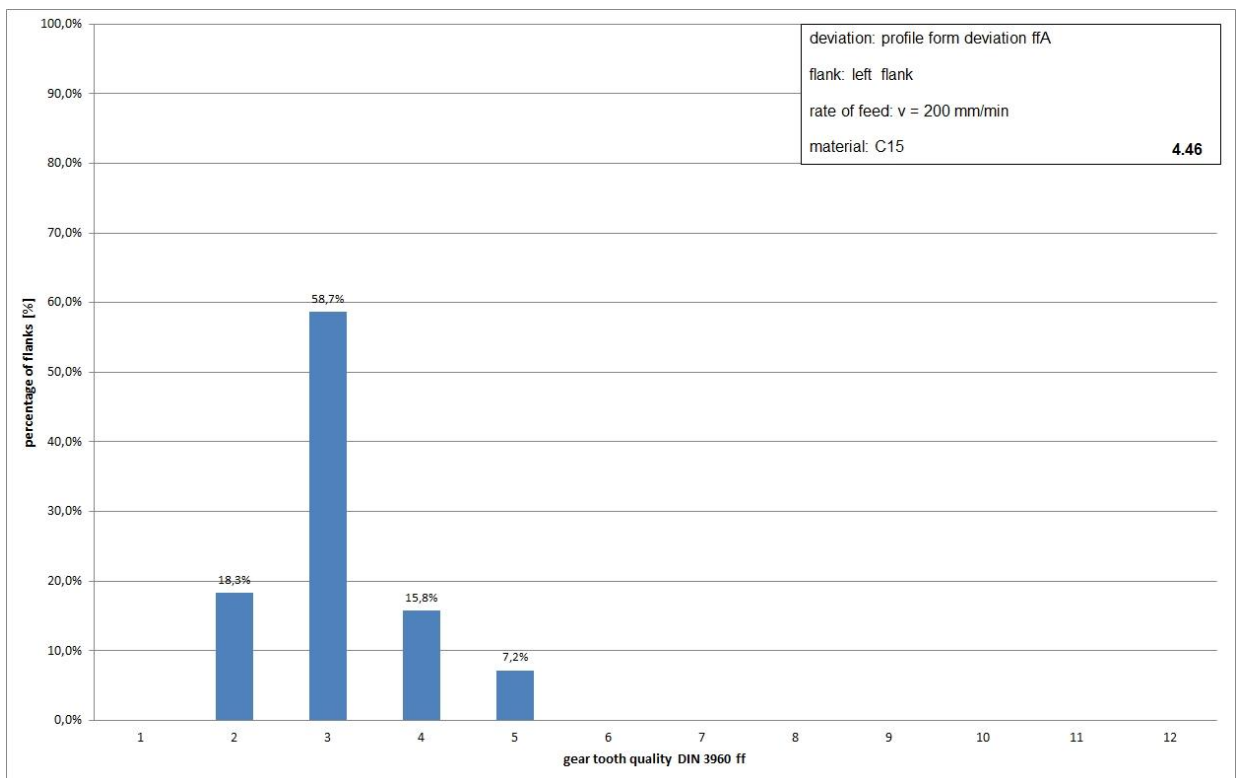
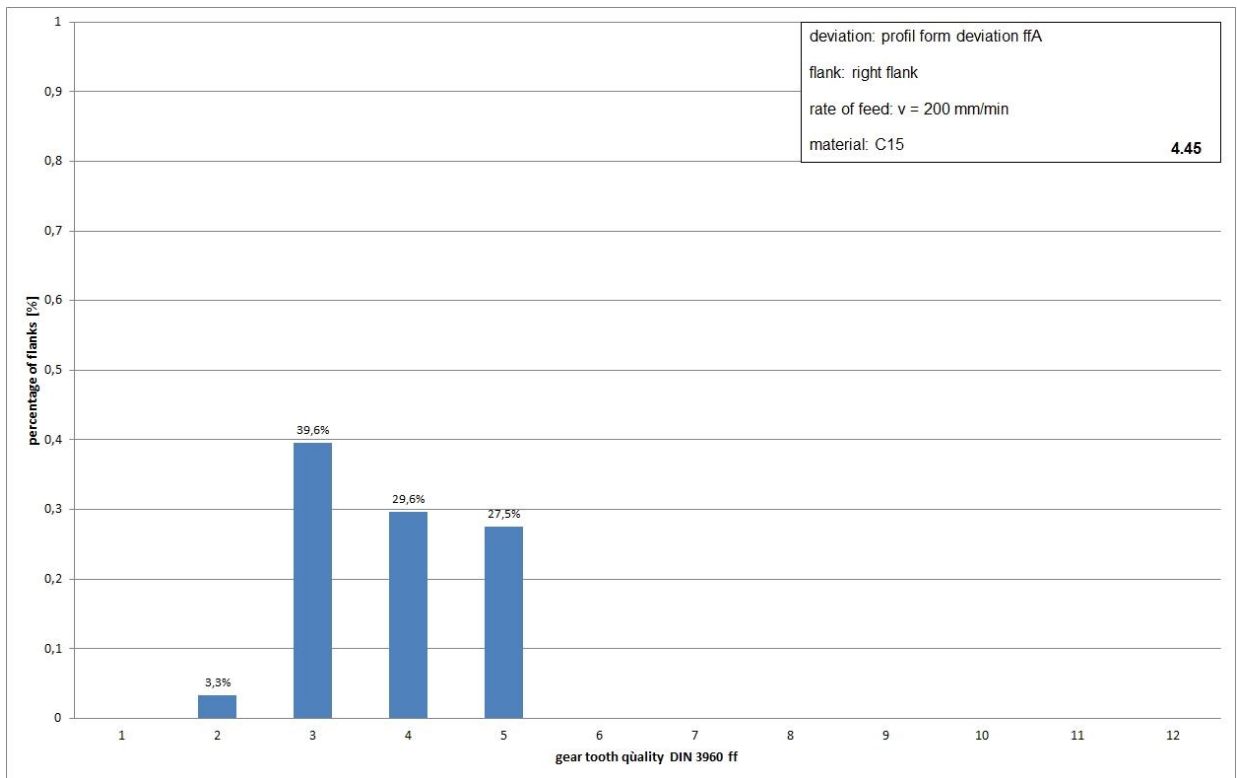


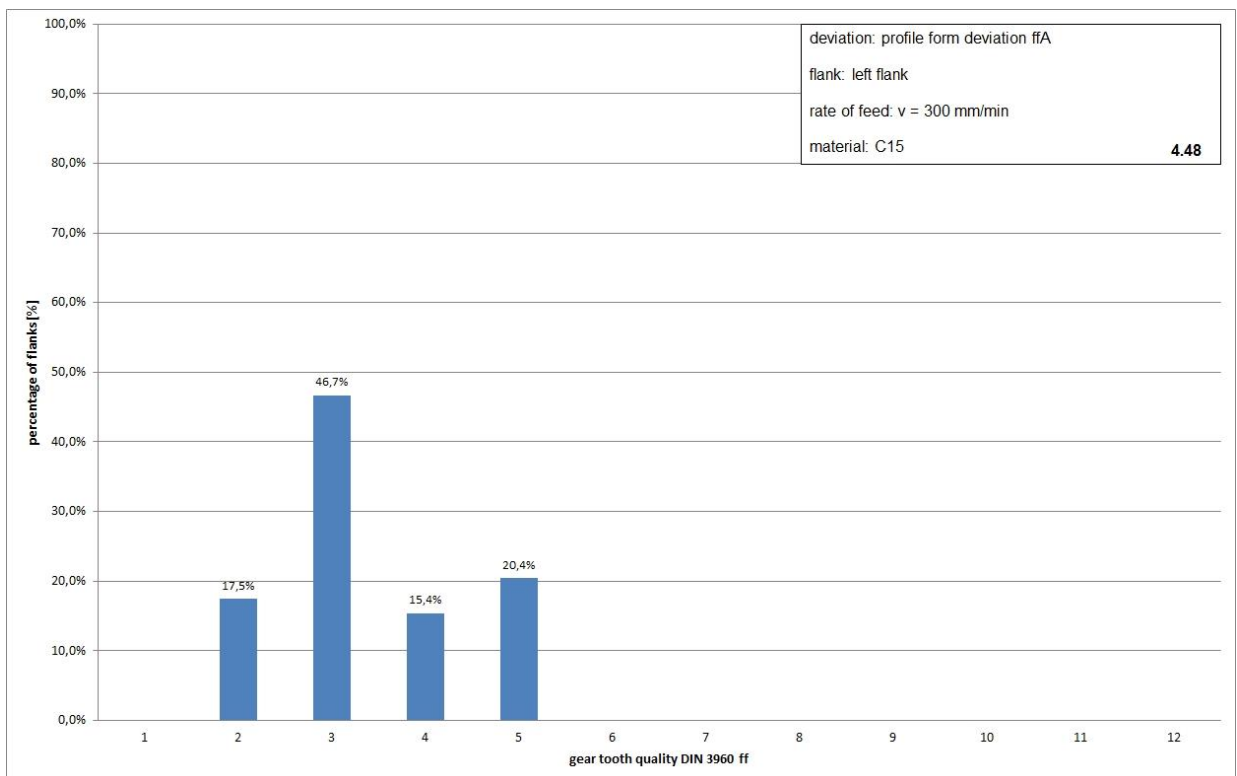
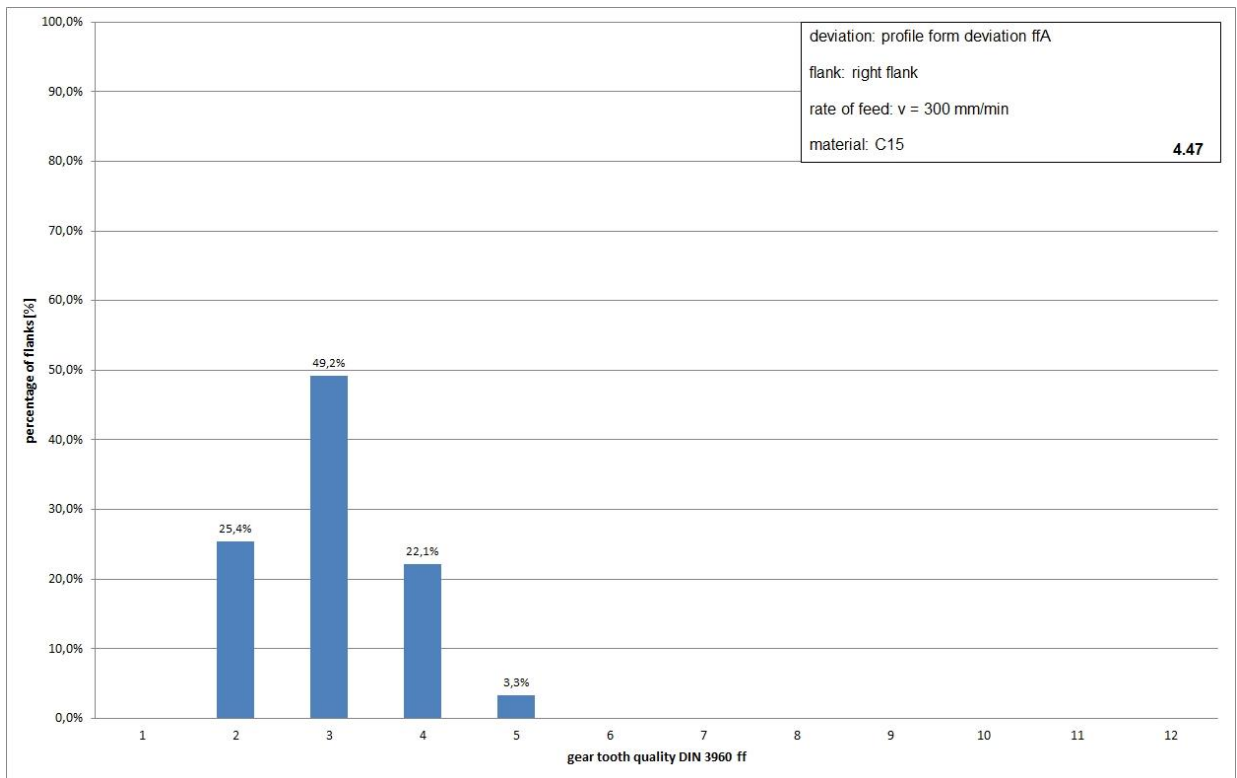


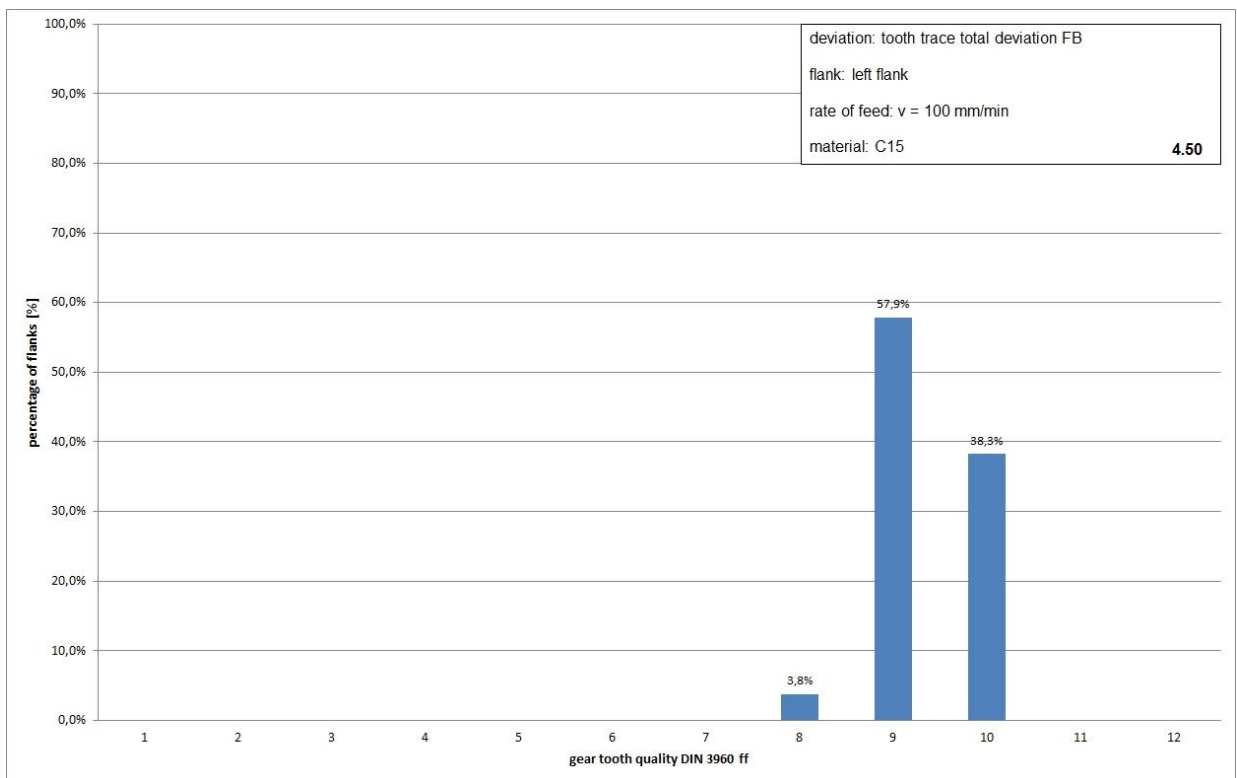
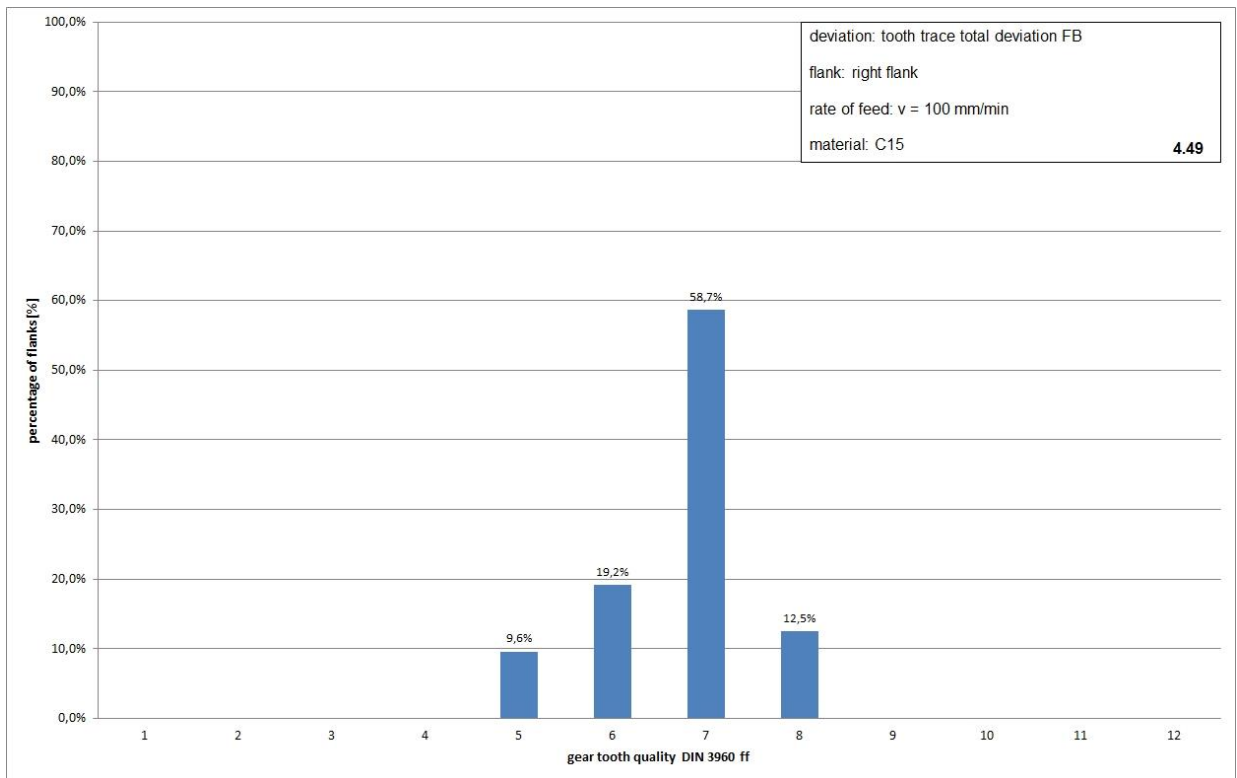


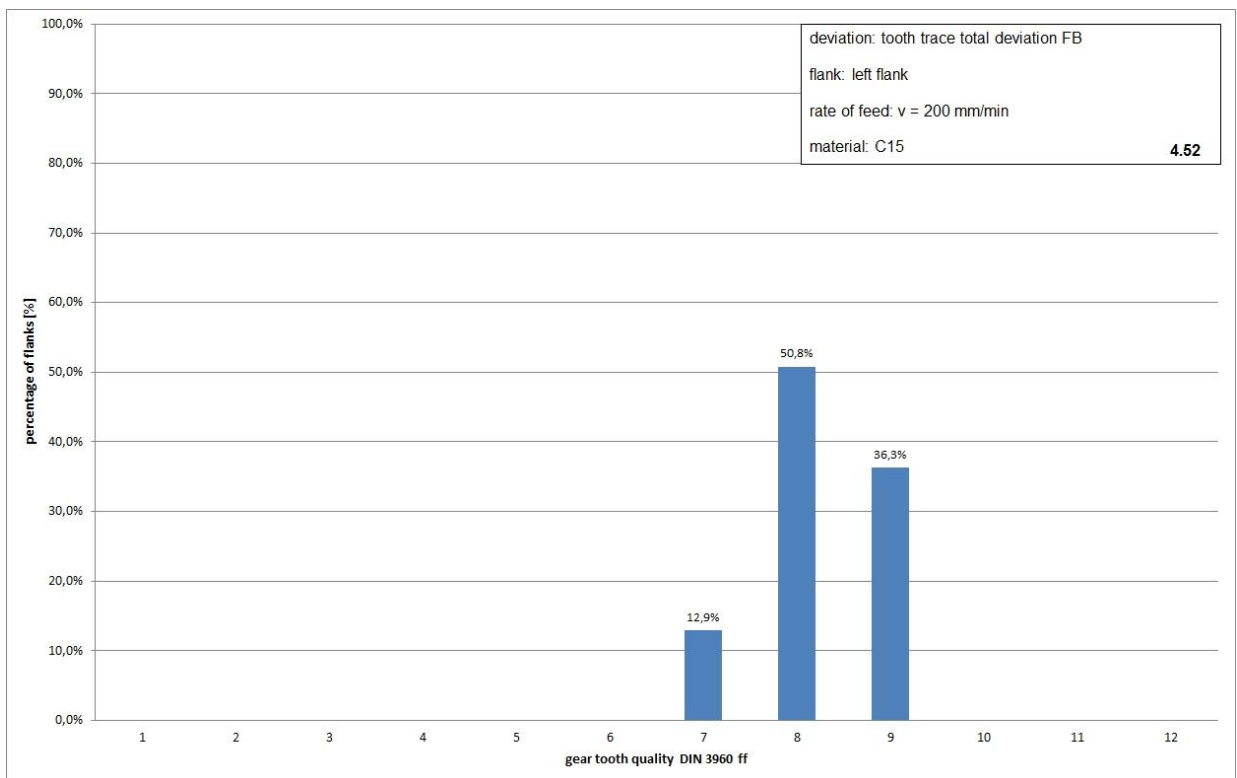
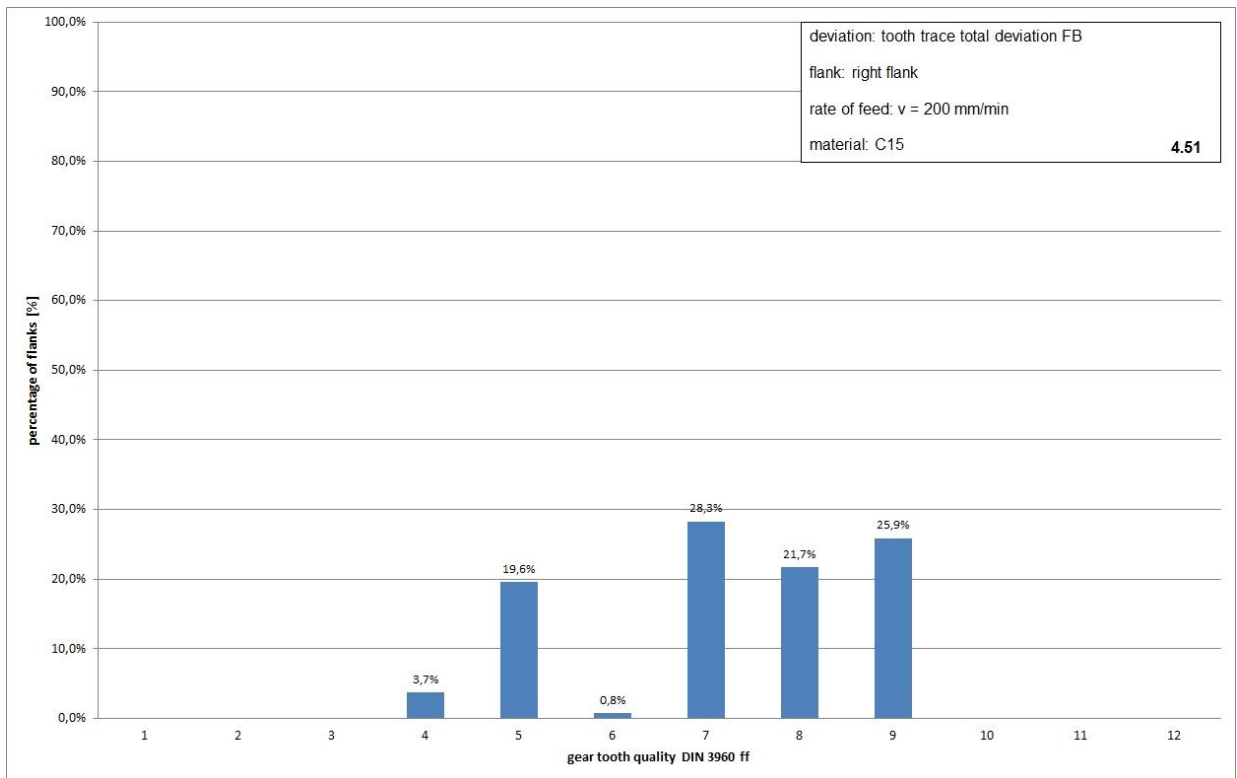


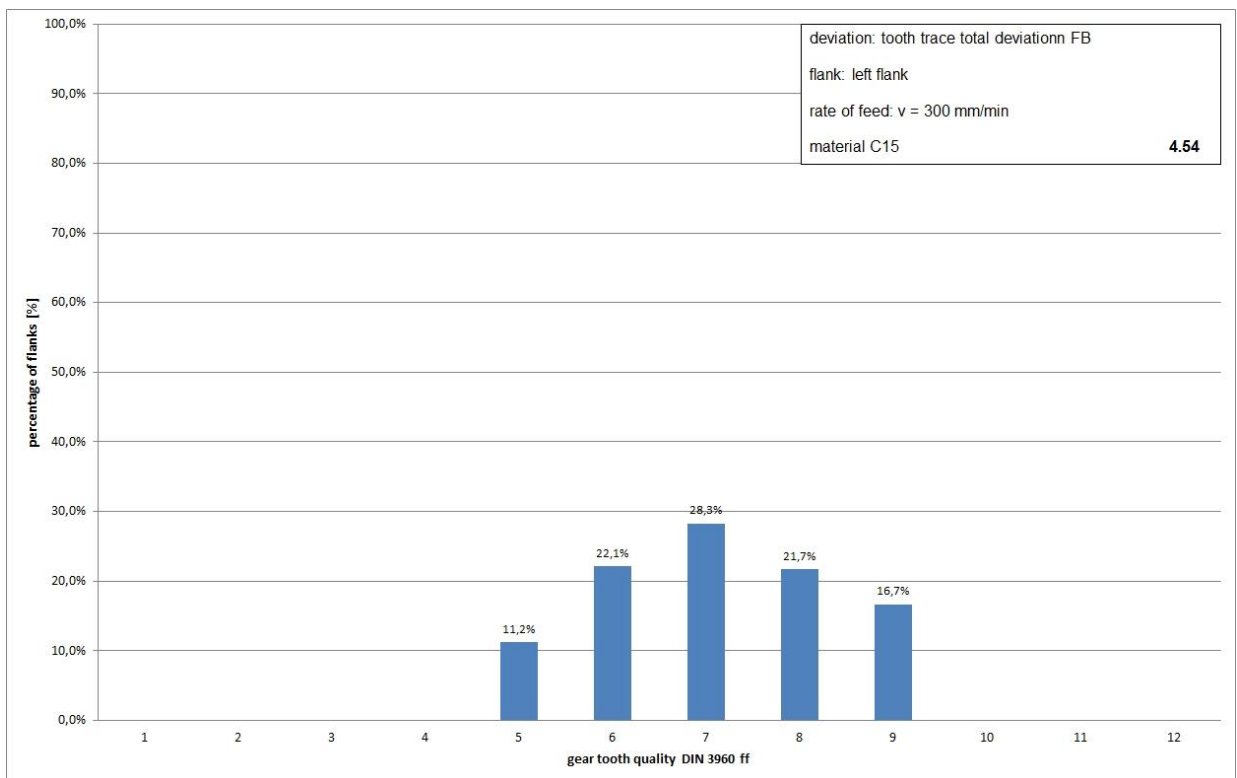
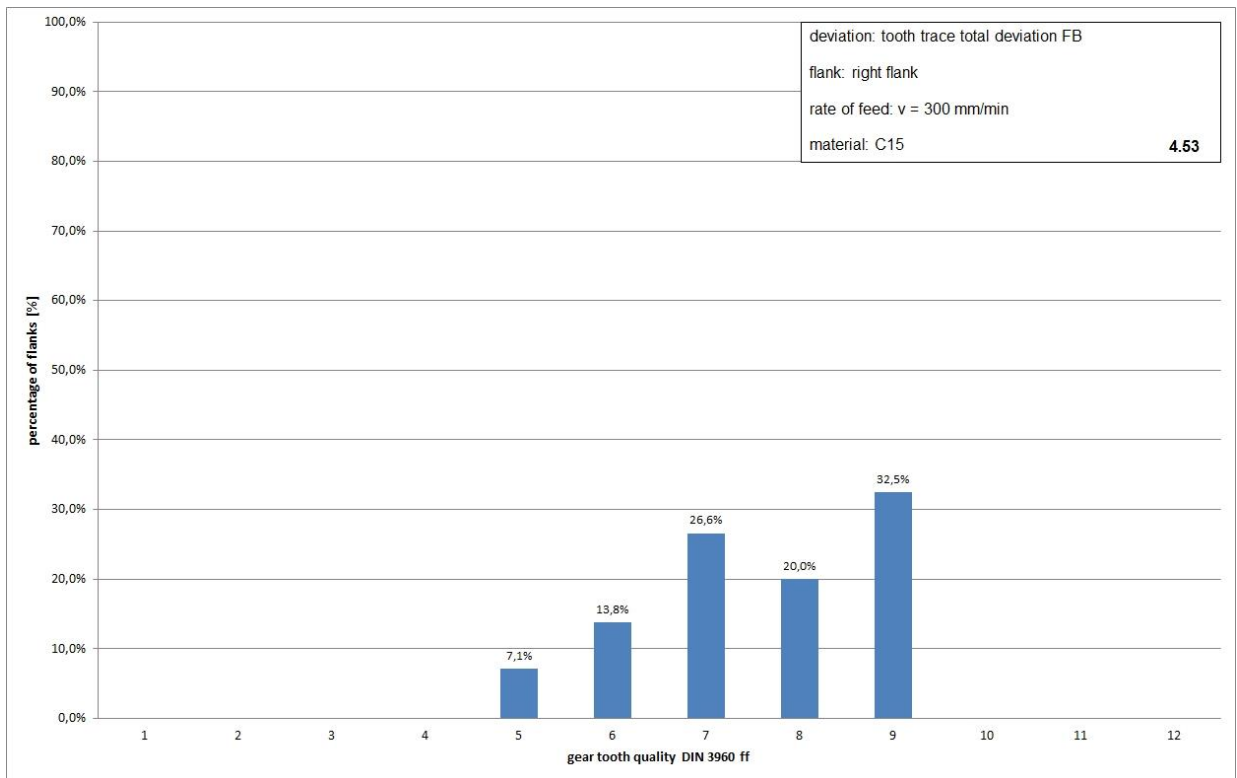


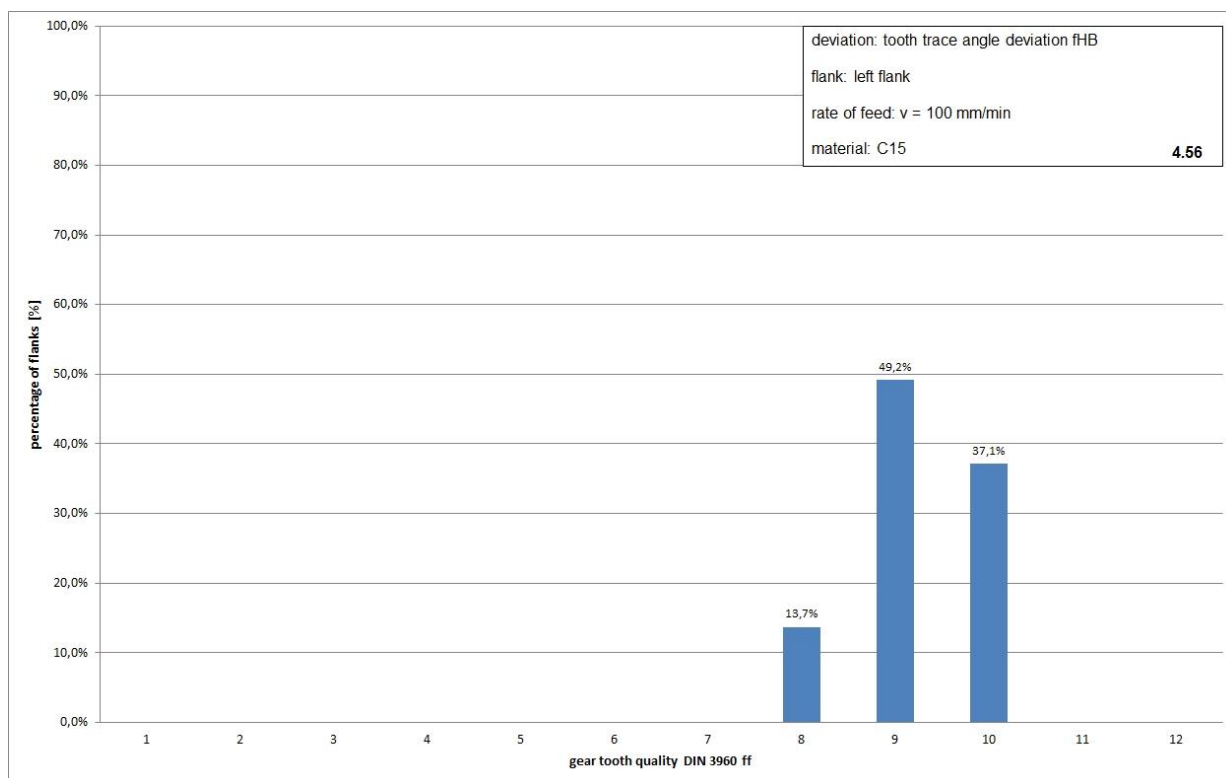
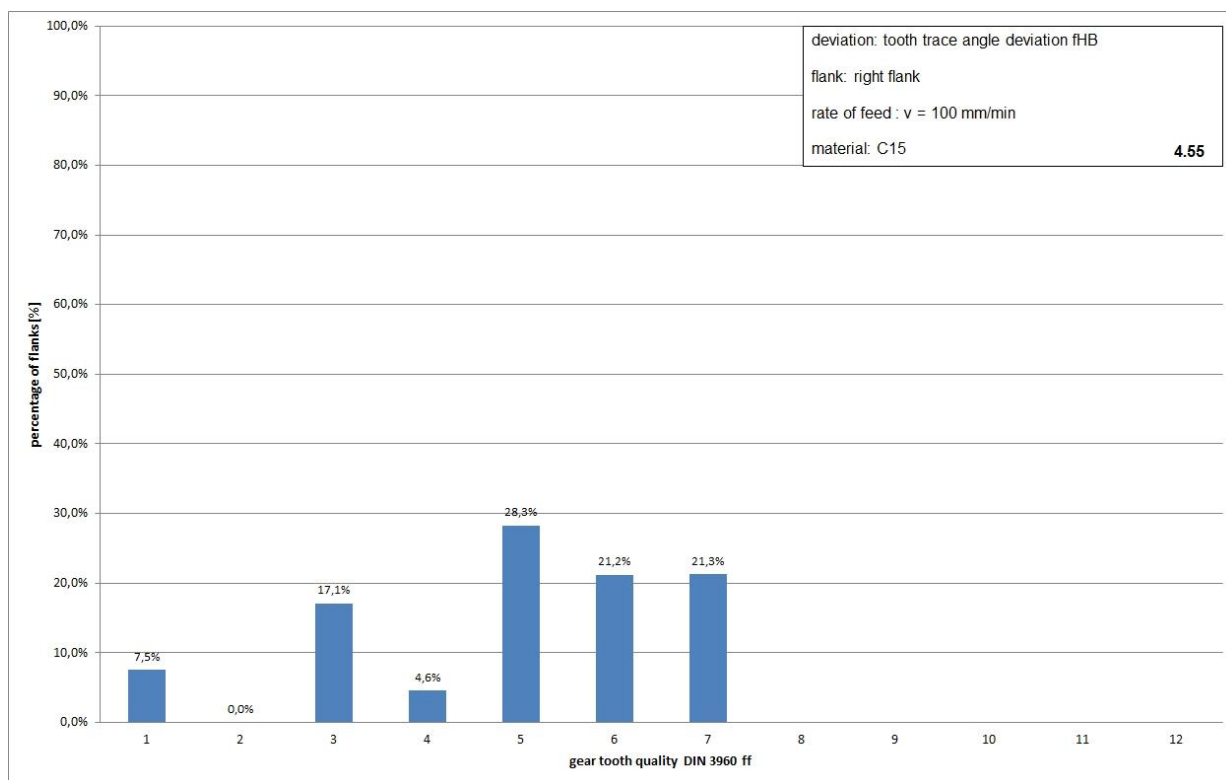


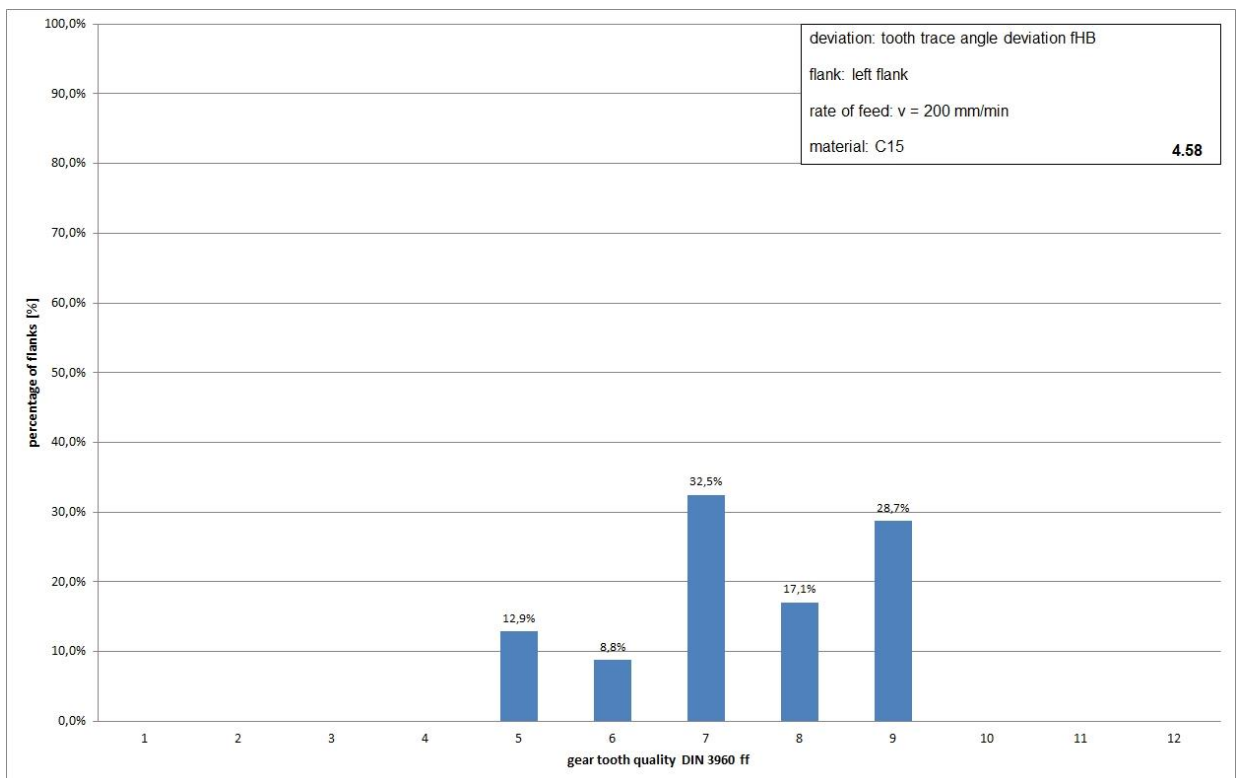
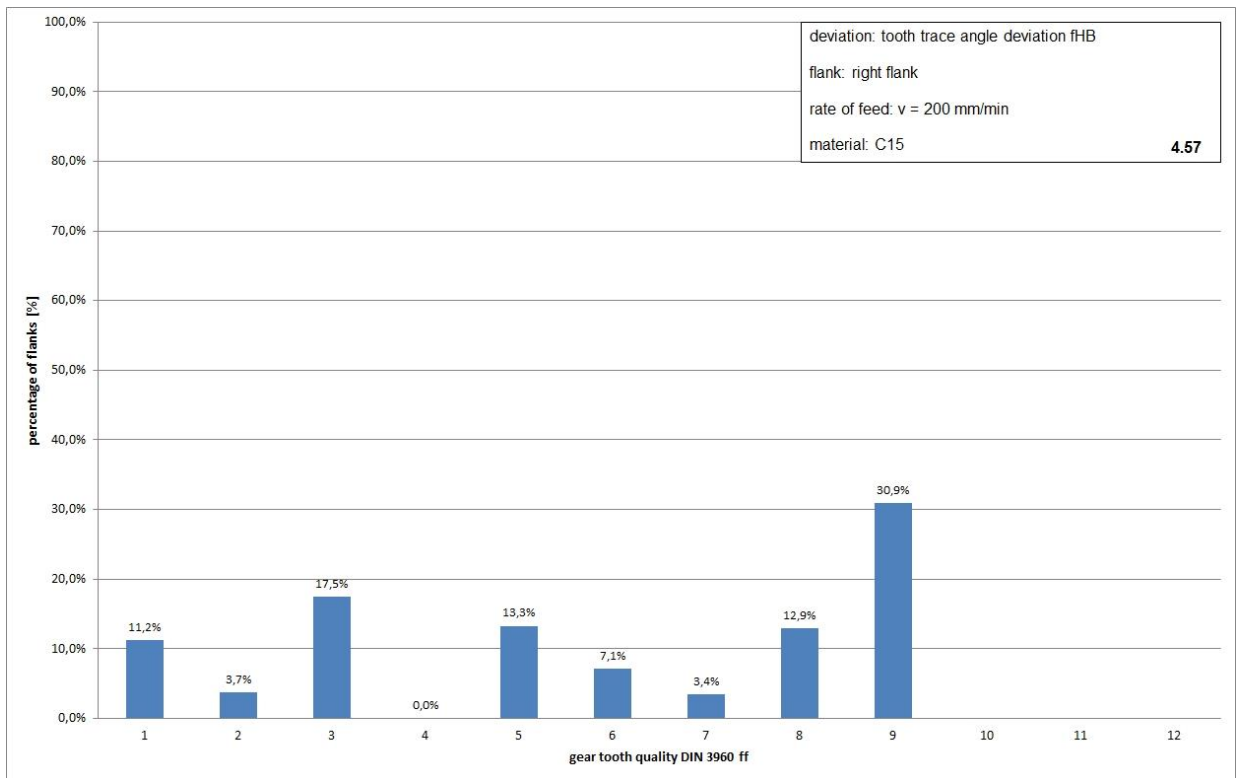


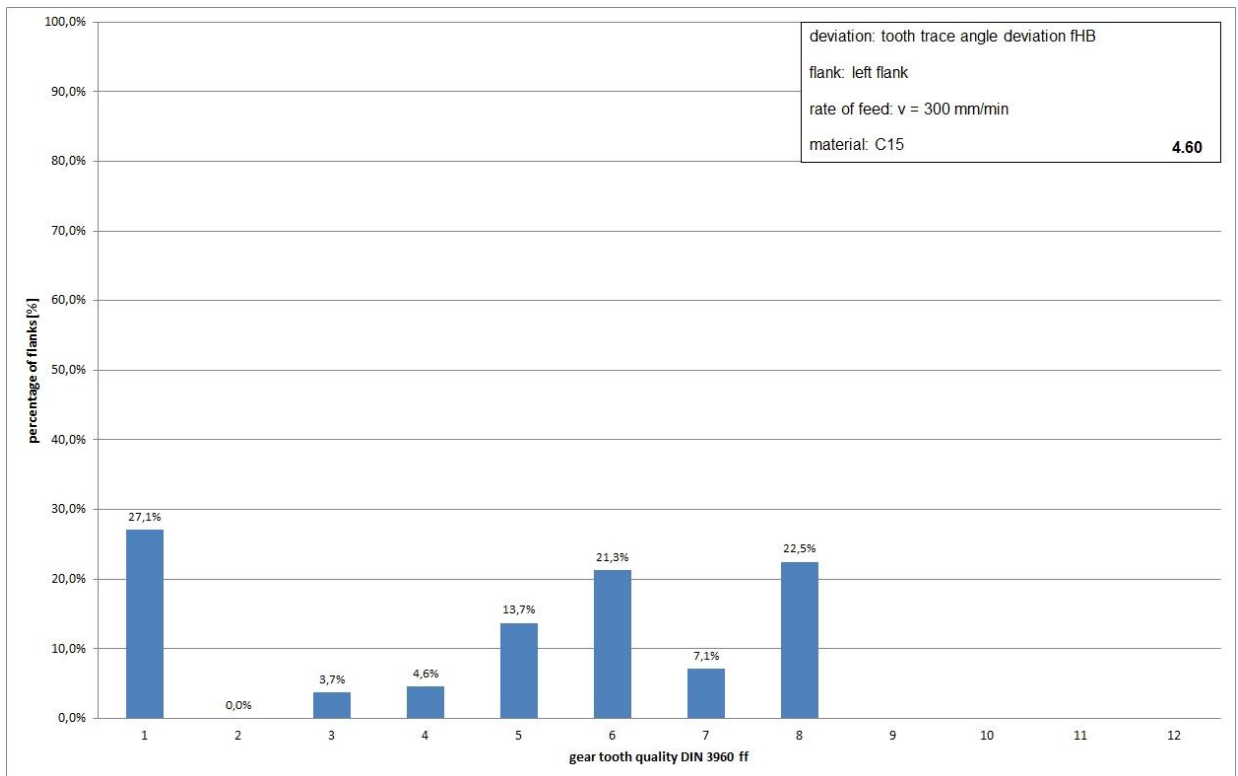
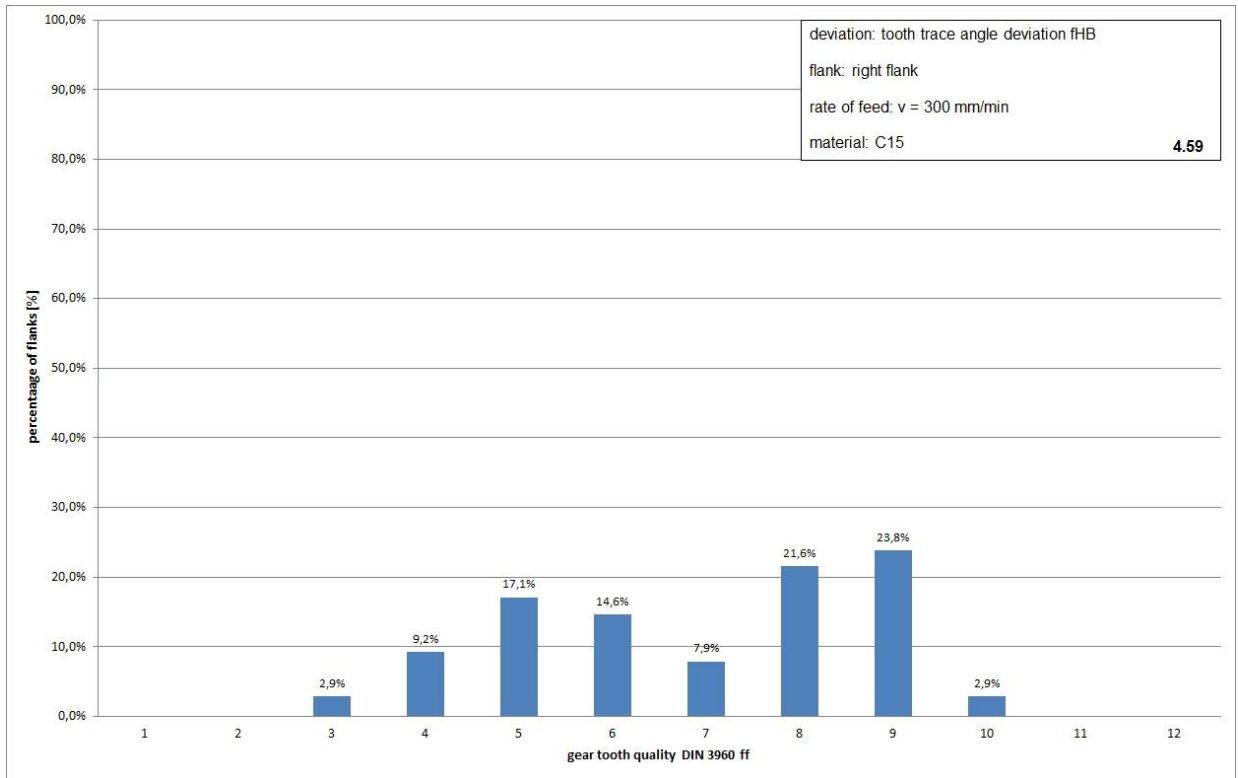


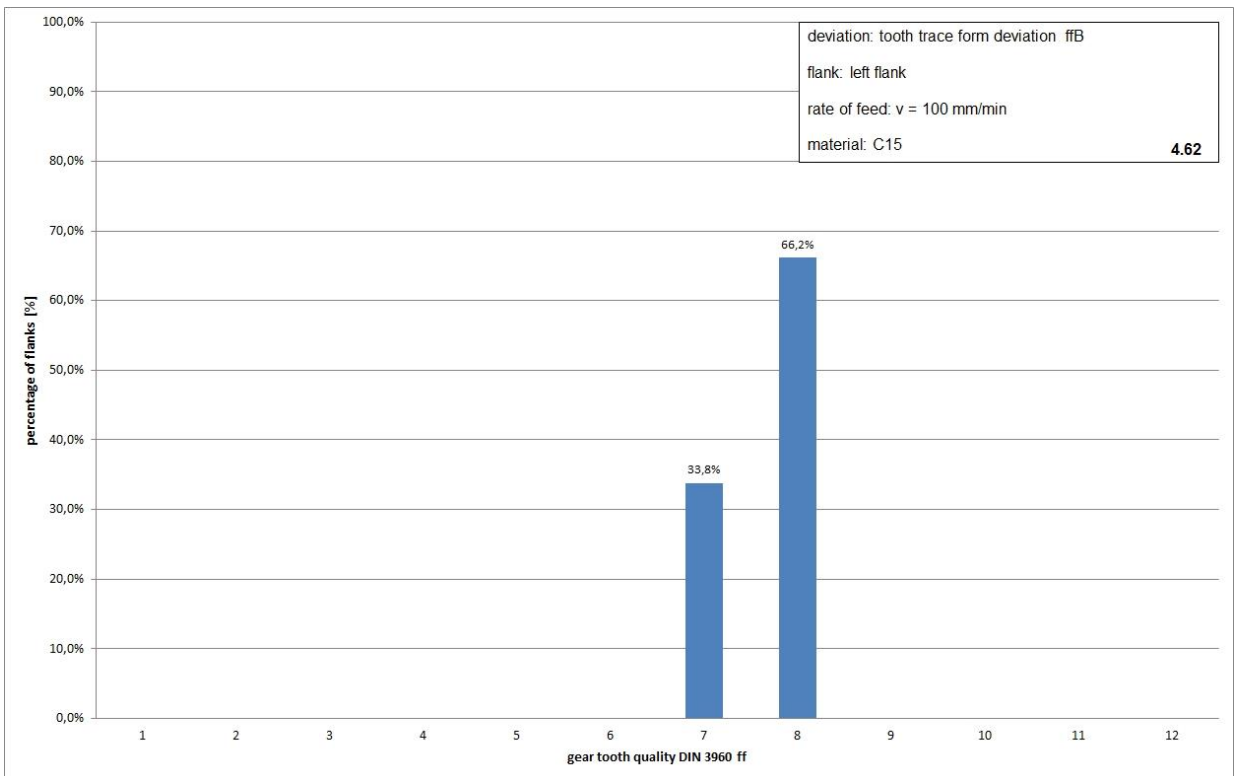
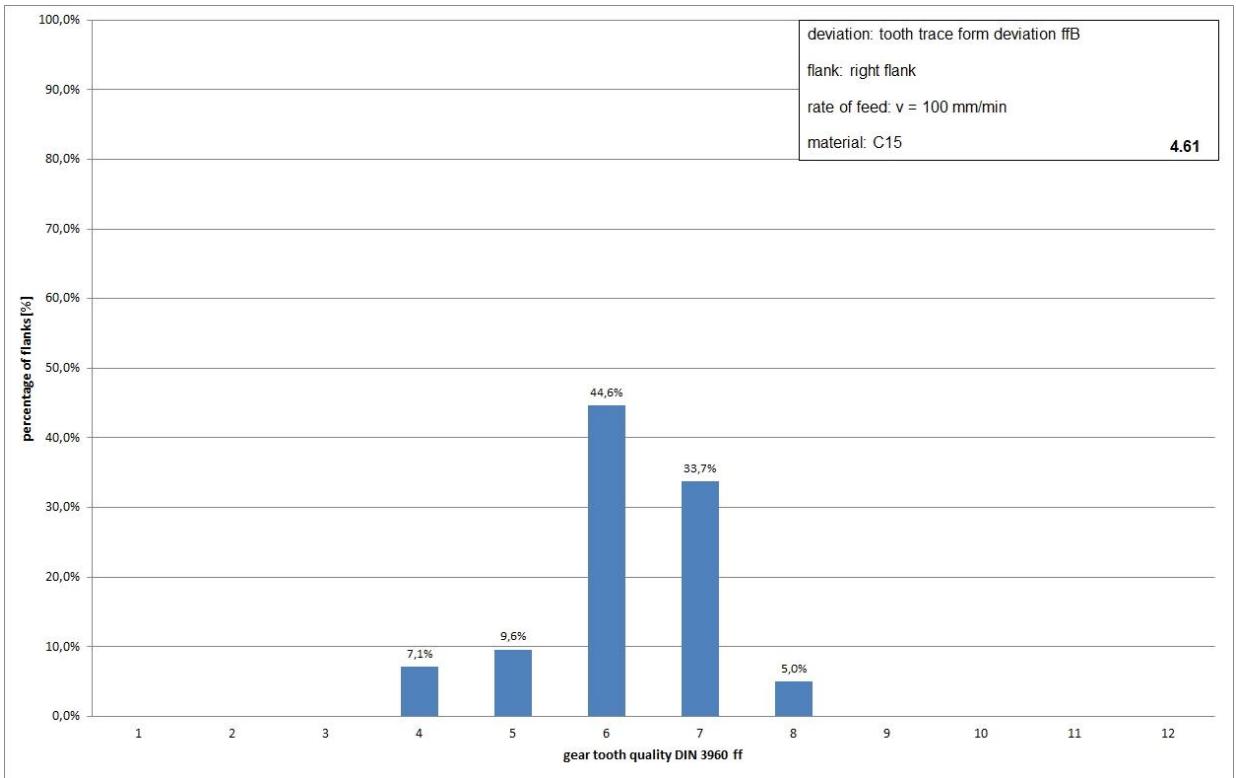


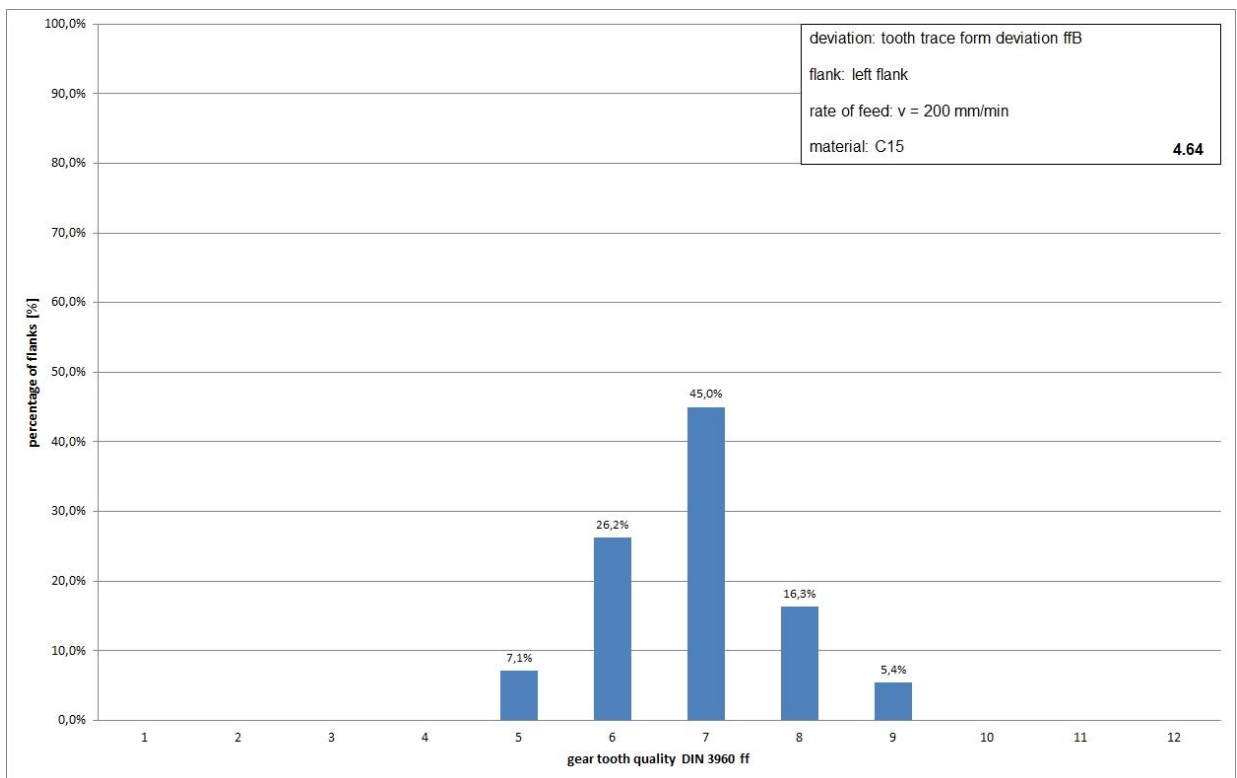
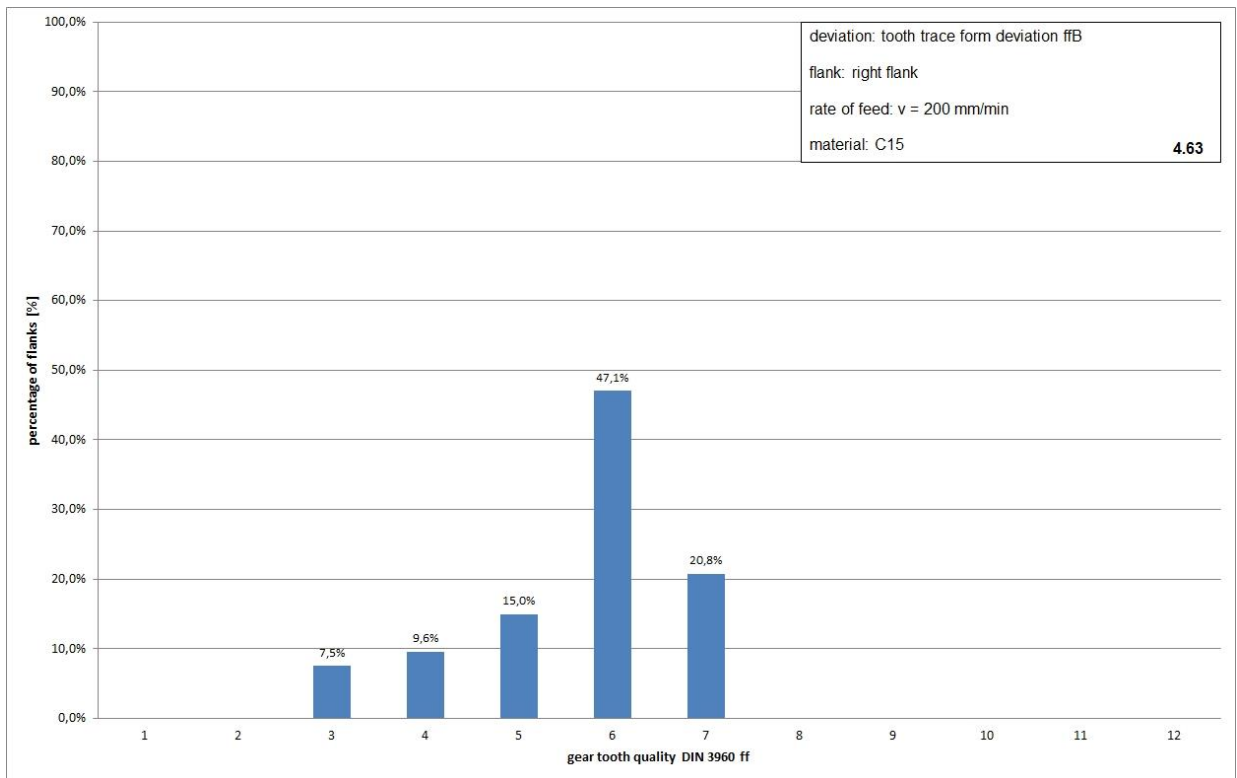


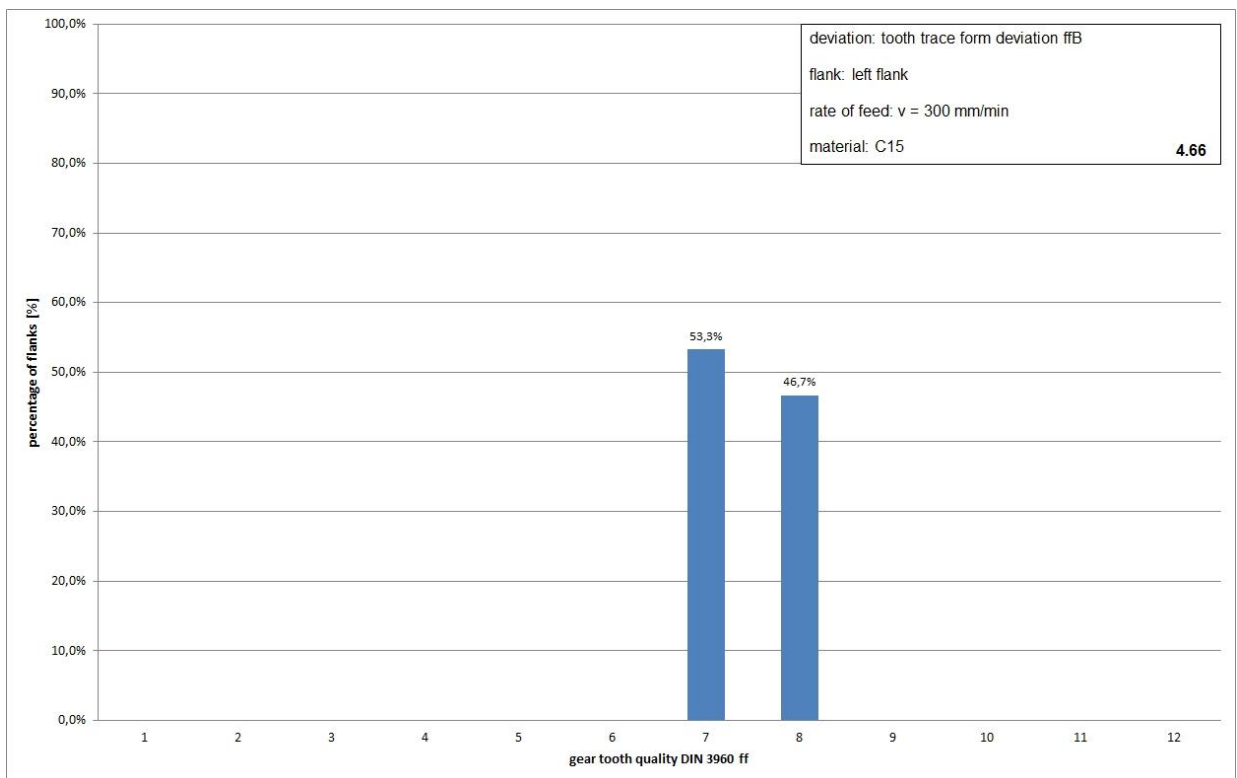
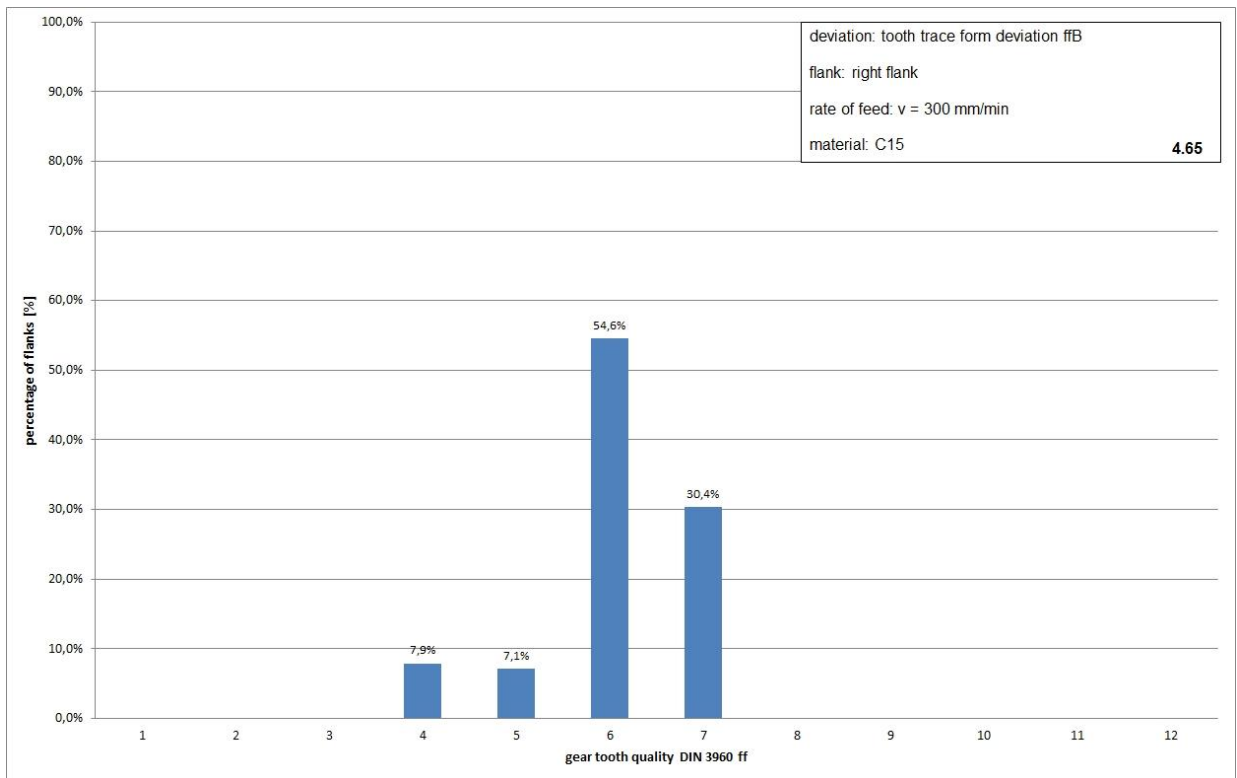












Appendix 5: List of Literature

Nr.	Author	Title	Date	Place	Publisher
1	Bach, F.W.; Doege, E.;	Auswirkungen einer Integration der Wärmebehandlung auf die Prozesskette zur Zahnradherstellung durch Präzisionsschmieden	2003	pp. 375-379	Berichte aus dem IWU
2	Basedow, G.,	Intermittierendes Kaltwalzen	1979	pp.1893-1895	Maschinenmarkt
3	Bausch	Moderne Zahnradfertigung	2011		expert-Verlag
4	Bausch, Thomas	Innovative Zahnradfertigung : Verfahren, Maschinen und Werkzeuge zur kostengünstigen Herstellung von Stirnrädern mit hoher Qualität	2011	pp. 777	Moderne Zahnradfertigung; pp., expert-Verl. , Renningen
5	Bogojavlenskij, K.N.	Kaltprofilwalzen von Schneckenwellen	1980	pp.30; 3	Fertigungstechnik und Betrieb
6	Bosch, M.; Rohmert, J.,	Verzahnen	1973	pp. 972-976	VDI-Zeitschrift
7	Dähndel, Helge	Beitrag zur Systematisierung der Prozessauslegung für das Präzisionsschmieden von Zahnradern	2011		Berichte aus dem IFUM. Universität Hannover
8	Dobosz, Marek,	Laser diode distance measuring interferometer - metrological properties	2012	pp. 553-564	Metrology and Measurement Systempp. Vol. XIX/3, pp
9	Doege, E.; Westerkamp, C.; Wiarda, M.; Nägele, H.	Präzisionsumformtechnik auf dem Weg zur Herstellung schrägverzahnter Zylinderräder	1994	pp. 24-25	MM-Maschinenmarkt, Würzburg
10	E. Schrüfer	Elektrische Meßtechnik, Studienbücher der techn. Wispp.	1992		Carl Hanser Verlag, München/Wien
11	Eichner, K.W.	Problembereich ist vielschichtig. Fuehrungseigenschaften eines Werkzeuges und Umformkraefte zum Verzahnen sind wichtige Beurteilungskriterien der Verfahren	1988	pp. 20-23	MM - Maschinenmarkt, Würzburg
12	Eichner, K.W.	Neuentwicklung gefordert. Verzahnungen fertigen mittels Walzen bei hoher Guete und Genauigkeit verlangt gezielte Stoffssteuering	1988	pp. 58-61	MM - Maschinenmarkt, Würzburg
13	Eichner, K.W.	Dimensionsanalytische Ueberlegungen zum Walzen	1981	pp. 37-38	Dissertation, TH-Darmstadt, Institut für Umformtechnik
14	Eichner, K.W.	Neuere Erkenntnisse beim Walzen von Profilen und Verzahnungen	1983	pp. 163-175	Deutsche Gesellschaft fuer Metallkunde e.V.
15	Eichner, K.W.	Herstellen von Zahnradern durch das Zwei-Walzen-Verfahren	1986	pp. 147-158	VDI-Gepp. Produktionstechnik
16	Eichner, K.W.	Ist umformende Verzahnungsherstellung ein Problem?	1988		Umformtechnisches Kolloquium
17	Eichner, K.W.	Problembereich ist vielschichtig. Fuehrungseigenschaften eines Werkzeuges	1988	pp. 20-23	MM - Maschinenmarkt
18	Eichner, K.W.	Neuentwicklung gefordert. Verzahnungen fertigen mittels Walzen	1988	pp. 58-61	MM - Maschinenmarkt
19	Eichner, K.W.	Ist umformende Verzahnungsherstellung ein Problem?	1988		Umformtechnisches Kolloquium Mar; 11-7 ; TH Darmstadt, 16.-17.3.1988
20	Eichner, K.W.; Heberer, C.	Kein Unterschied im Fließverhalten. Schrägverzahnungswalzen von Sinterwerkstoffen	1991	pp. 38-39	HGF-Bericht, 09/91
21	Feldmann, H.D.	Kaltmassivumformung	2003	pp. 42-46	VDI-Z Integrierte Produktion
22	Feldmann, H.D.	Kaltmassivumformung. Fachgebiete in Jahresübersichten	2003	pp. 145; 42-46	VDI-Z Integrierte Produktion
23	Francisco Javier Brosed, Juan José Aguilar, David Guillomía and Jorge Santolaria	3D Geometrical Inspection of Complex Geometry Parts Using a Novel Laser Triangulation Sensor and a Robot	2011	pp. 90-110	Sensors
24	Gan, Zhongxue, Tang, Qing	Visual Sensing and its application - Integration of Laser Sensors to Industrial Robots	2011		Series: Advanced Topics in Science and Technology in China, Springer & Zhejiang University Press
25	Giebecke, H.,	Anwendung und Gestaltung von Walzwerkzeugen fuer Profilwalzmaschinen	1983	pp. 17; 3	Umformtechnik
26	Goch, G.:	Gear Metrology	2001	pp. 659-695	Annals of the CIRP
27	Goch, G.:	Theorie und Prüfung gekrümmter Werkstückoberflächen in der Koordinatenmeßtechnik	1982		Universität der Bundeswehr
28	Goch, G.:	Efficient Multi-Purpose Algorithm for Approximation- and Alignment-Problems	1990	pp. 553-556	Annals of the CIRP Vol. 39/1
29	Goch, G.;	A Universal Algorithm for the Alignment of Sculptured Surfaces	1992	pp. 597-600	Annals Of the CIRP Vol. 41/1
30	Goch, G.; Günther, A	Future Gear Metrology	2003	pp.751-768	VDI-Berichte 1665

31	Goch, G.; Peters, R.-D	Beschreibung gekrümmter Werkstück-Oberflächenin der Mehrkoordinaten-Meßtechnik.	1980	pp. 85-91	VDI-Berichte Nr. 378
32	Günther, A.:	Flächenhafte Beschreibung und Ausrichtung von Zylinderrädern mit Evolventenprofil	1996	pp. 160-165	Diplomarbeit
33	Günther, A.; Peters, J.;	Flächenhafte numerische Beschreibung,	2001		VDI-Berichte Nr. 1880
34	H. Herold	Sensortechnik	1993		Hüthig-Verlag
35	H.R. Tränkle	Taschenbuch der Meßtechnik mit Schwerpunkt Sensortechnik (3. Auflage)	1992		R. Oldenburg-Verlag
36	H.R. Tränkle, E. Obermeier	"Sensortechnik" Handbuch für Praxis und Wissenschaft	1998		Springer Verlag
37	Hagener Symposium Pulvermetallurgie	Energie- und Ressourceneffizienz durch Pulvermetallurgie	2009	pp. 32-35	Heimdall Verlag
38	Hammerschmidt, E.	Innenprofilierter Verzahnungswerkzeuge erreichen großen großen Überdeckungsgrad	1998	pp. 22-26	HGF-Bericht, 06/98
39	Hammerschmidt, E.	Verbesserte Kinematik beim Profilieren führt Werkzeuge auch unter Last genau	1999	pp. 28-32	Maschinenmarkt, Würzburg
40	Hammerschmidt, E.	Verzahnungswalzen mit verschiedenen Maschinensystemen	1980		Umformtechnisches Kolloquium
41	Hammerschmidt, E.	Kaltwalzen von Profilverzahnungsfoermiger Geometrien	1985		Umformtechnisches Kolloquium, T H-Darmstadt, Institut für Umformtechnik
42	Hammerschmidt, E.	Geometrieuntersuchungen an gewalzten Oberflächenprofilen	1987		Instituts-Berichte über Fertigungsforschung
43	Hammerschmidt, E.	Geometrieuntersuchungen an gewalzten Oberflächenprofilen; Umformtechnik Darmstadt	1987	pp. 7	Berichte ueber Fertigungsforschung
44	Hammerschmidt, E.,	Verzahnungswalzen mit verschiedenen Maschinensystemen	1981	pp. 350-354	Draht
45	Hellfritsch, U.	Walzen statt spanen in der Stirnradfertigung	2002	pp. 54-56	WB Werkstatt und Betrieb
46	Hellfritsch, U.; Strehmel, P.	Walzen statt spanen in der Stirnradfertigung	2002	pp. 135; 3 ; 54-56	WB Werkstatt und Betrieb Aufsatz (Zeitschrift)
47	Höhn, B.R.	Gestaltung von Verzahnungsgeometrien für die Umformtechnik, Wege erkennen - Potentiale nutzen	2006	pp. 223-233	UKD, Umformtechnisches Kolloquium Darmstadt
48	Höhn, B.R.,	Gestaltung von Verzahnungsgeometrien für die Umformtechnik	1997	pp. 223-233	Umformtechnisches Kolloquium
49	J. Fraden	AIP Handbook of Modern Sensors: Physicpp. Designs and Application	1993		AIP American Institute of Physics Press, New York
50	J. Niebuhr, G. Lindner	Physikalische Meßtechnik mit Sensoren	1994		R. Oldenburg-Verlag
51	J.W. Gardner	Microsensors: Principles and Applications	1994		J. Wiley & Sons Ltd.. Chichester
52	James Clark, Emanuele Trucco, Lawrence B. Wolff	Using Light Polarization in Laser Scanning, Image and Vision Computing, Volume 15, Issue 2	1997	pp. 107-117	Elsevier Science
53	Jianxin Zhang, Alexandar Djordjevic	Study on laser stripe sensor	1999	pp. 224-228	Sensors and Actors, Elsevier Science
54	Jontschev, B.	Wirtschaftlichkeit durch höhere Genauigkeit. Kaltumformen genauer Zahnräder	1991	pp. 46-47	(Zeitschrift) Technische Rundschau, Bern
55	Jontschev, B.,	Wirtschaftlichkeit durch höhere Genauigkeit	1991	pp. 46-47	Technische Rundschau
56	K. B. Smith and Y. F. Zheng	Accuracy Analysis of Point Laser Triangulation Probes Using Simulation	1998	pp. 736-745	Journal of Manufact. Science & Eng., Vol. 120(4)
57	Kästner, M.; Meeß, K.; Seewig, J.; Reithmeier, E.,	Optische Geometrieerfassung von Zahnrädern. Flächenhafte Detektion von Verzahnungsabweichungen	2005	pp. 155-163	VDI-Berichte, VDI-Verlag , Düsseldorf
58	Kauffmann, Philipp	Impulse für Getriebebauer	2009	pp. 58-61	WB Werkstatt und Betrieb
59	Kauffmann, Philipp	Gear-rolling study	2009	pp. 58	PowderMet
60	Kauffmann, Philipp; Gorgels, Christof; Klocke, Fritz	Gear-rolling study, PowderMet	2009	pp. 6/47-6/58,	Metal Powder Industries Federation, Princeton
61	Kauffmann, Philipp; Gorgels, Christof; Klocke, Fritz	Impulse für Getriebebauer. Status quo und Trends der Stirnradfertigung	2009	pp. 142; 5 ; 58-61,	Aufsatz (Zeitschrift); WB Werkstatt und Betrieb
62	Klocke, Fritz;	Solutions in PM gear rolling	2010		Powder Metallurgy World Congress & Exhibition
63	Klocke, Fritz; Gorgels, Christof; Gräser, Eva; Kauffmann, Philipp; Strehmel, Peter; Hirsch, Michael,	Solutions in PM gear rolling, World PM,	2010	pp. 1-7	Powder Metallurgy World Congress & Exhibition
64	Klocke, Fritz; Kleinjans, Manfred; Klein, Alexander	Mikrometer für Millisekunden. Hartstoffsichten zur Leistungssteigerung beim Wälzfräsen	2004	pp. 67-69	VDI-Z Integrierte Produktion Aufsatz (Zeitschrift)

65	Koenig, W.,	Stand der Technik in der Zahnradfertigung	1985	pp. 173-182	VDI Berichte
66	Koenig, W.,	Stand der Technik in der Zahnradfertigung	1983	pp. 173-182	VDI Berichte
67	Koenig, W.; Gutmann, P.,	Aktuelle Technologien in der Fertigungsfolge Umformen	1986	pp. 114-127	VDI-Gepp. Produktionstechnik
68	Koenig, W.; Steffens, K.	Gear production by cold forming	1985	pp. 481-483	CIRP Annals
69	Koenig, W.;Bonzakis, K.	Wirtschaftliche Zahnradfertigung	1978	pp. 32; 19; 29	VDI-Nachrichten
70	Kohlhoff, T.; Prinz, C.; Rentsch, R.; Surm, H.	Influence of manufacturing parameters on gear distortion	2012	pp. 43; 1-2; 84-90	WILEY-VCH Verlag
71	Kotthoff, Gerd; Wattenberg, Frank	Hochfeste PM Zahnräder - Neue Werkstoffe und Verfahren	2006	pp. 113-138	Pulvermetallurgie in Wissenschaft und Praxis
72	Krapfenbauer, H.	Neue Einsatzmoeglichkeiten des Kaltwalzens dank CNC-Technik	1989	pp. 64-70	Zeitschrift für wirtschaftliche Fertigung und Automatisierung ZWF/CIM
73	Krapfenbauer, H.	Kaltwalzen eng tolerierter Verzahnungen	1978	pp. 657-661	Maschinenmark
74	Krapfenbauer, H.	Verzahnungswalzen mit verschiedenen Maschinensystemen nach dem Grob-Verfahren	1980		Umformtechnisches Kolloquium
75	Krapfenbauer, H.	Verzahnungswalzen mit verschiedenen Maschinensystemen nach dem Grob-Verfahren	1981	pp. 32; 7	Draht
76	Krapfenbauer, H.	Kaltwalzen von Innen- und Aussen-Verzahnungen an duennwandigen Hohlkoerpern	1981	pp. 161-164	Seminar
77	Krapfenbauer, H.,	Neue Gesichtspunkte fuer die Fertigung von Stirnzahnaedern durch Kaltwalzen	1984	pp. 40-47	Z. Wirtsch. Fertigung
78	Krapfenbauer, H.,	Neue Einsatzmoeglichkeiten des Kaltwalzens dank CNC-Technik	1989	pp. 64-570	Zeitschrift ZWF
79	Krapfenbauer, H.,	Kaltgewalzte Praezisionsverzahnungen	1979	pp. 107-112	VDI-Berichte
80	Lange, K.; Kling, E.	Stand und Entwicklung der Kaltmassivumformung	1981	pp. 76-1	Draht
81	Lange, Kurt; Liewald, Mathias	Umformtechnik	1988		Springer-Verlag
82	Latze, W.:	Neue Wege und Systeme für die wirtschaftliche 3D-Verzahnungsprüfung	1996	pp. 1021-1030	VDI Bericht Nr. 1230
83	Latze, W.; Härtig, F	Laser Metrology and Machine Performance	2002	pp. 333	Konferenz "Lambdamap"
84	Liebisch, A.	Durch Festwalzen induzierte Eigenspannungen in einsatzgehärteten Zahnrädern mit FEM bestimmen	1990	pp. 36-39	Aufsatz (Zeitschrift)
85	Lindsay Kleeman	Advanced Sonar Sensing	2003	pp. 485-498	Springer Tracts in Advanced Robotics, Vol. 6
86	Lindsay Kleeman, Roman Kuc	An Optimal Sonar Array for Target Localization and Classification	1994	pp. 3130-3135	IEEE International Conference on Robotics and Automation, San Diego
87	Lindsay Kleeman, Roman Kuc	Sonar Sensing	2008	pp. 491-519	Springer Handbook of Robotics, Part C
88	Linke, H.,	Stirnradverzahnung	1996	pp. 54. 547ff, 593 ff.	Carl Hanser Verlag, München/Wien
89	Loos, H.,	Zahnrad-rollen	1970	pp. 103; 7	Werkstatt und Betrieb
90	M. Cui , M.G. Zeitouny, N. Bhattacharya, pp.A. van den Berg, H.P. Urbach	New laser system for distance metrology - High Accuracy Long Distance Measurements with a Frequency Comb Laser	2010		Symposium Photonics and Opto-electronic (SOPO)
91	Mages,W.;	Vorteilhafte Anwendung neuzeitlicher Umformverfahren	1979		Dokumentation Kraftfahrtwesen e.V
92	Marciniak, Z.;Kopacz, Z.,	New rotary metalworking processes developed in Poland2. international conference on rotary metalworking processes	1982		Verlag IFS (Publications) Ltd. , Bedford (GB), 1982
93	Möller, Klaus; Ried, Jens	Komplettbearbeitung von Zahnradpaaren in den drei Arbeitsschritten Weichbearbeitung - Warmbehandlung - Hartfeinbearbeitung	2003	pp. 718	Forschungsvorhaben Nr. 443 "Komplettbearbeitung", Forschungsheft // Forschungsvereinigung Antriebstechnik e.V. FVA , Frankfurt
94	Neugebauer, R.; Putz, M.; Hellfritsch, U.	Improved process design and quality for gear manufacturing with flat and round rolling Manufacturing Technology - Annals of the International Institute for Production Engineering Research	2007	pp. 56; 1 ; 307-312	CIRP Annals, General Assembly of CIRP Elsevier , Amsterdam,
95	Neugebauer, R.;Putz, M.;	Improved process design and quality for gear manufacturing	2007	pp. 307-312	General Assembly of CIRP
96	Niemann, G., Winter, H.:	Maschinenelemente	1989		Springer-Verlag
97	Norbert Bauer (Pub.)	Handbuch zur industriellen Bildverarbeitung - Qualitätssicherung in der Praxis	2008		Springer Verlag

98	Oliver P. Lay, Serge Dubovitsky, Robert D. Peters, Johan Burger, William H. Steier, Seh-Won Ahn, Harold R. Fetterman	Jet Propulsion Laboratory	2004		California Institute of Technology, Pasadena CA
99	P. Hauptmann	"Sensoren: Prinzipien und Anwendungen"	1990		C. Hanser-Verlag. München/Wien
100	Pedrick, M., Tittmann, B.R.	Ultrasonic micrometer position indicator with temperature compensation	2004	pp. 1199 – 1202	Ultrasonics Symposium IEEE
101	Rentsch, H.,	blanksEinflussgrößen des Verzuges beim Schmieden von Zahnradrohlingen	2010	pp. 68-72	WILEY-VCH Verlag
102	Rohmert, J.	Verfahren und Maschinen zur spanenden Herstellung von Verzahnungen	1980		VDI Zeitschrift
103	Rohmert, J.,	Verzahnungen	1976	pp. 1085-1093	VDI-Zeitschrift
104	Rohmert, Jürgen	Verzahnungen	1997	pp. 36-43	VDI-Zeitschrift
105	Roth, K.:	Zahnradtechnik	1989		Springer-Verlag
106	Schmoeckel, D.,	Kaltwalzen von Verzahnungen durch Querwalzen	1983	pp. 75	Springer-Verl.
107	Schmoeckel, D.,	Kaltwalzen von Verzahnungen durch Querwalzen	1983	pp. 75	Springer-Verl.
108	Schmoeckel, D.; Hauk, pp.	Entwicklung eines kombinierten Drück-Walz-Verfahrens zur Herstellung von Zahnradvorformen	1996		VDI-Z Integrierte Produktion ; 138 , Special Blechbearbeitung ; 46-48, Aufsatz (Zeitschrift),
109	Schmoeckel, D.; Hammerschmidt, E.	Schmieden, Uebersicht der Verfahrenstechnologie	1980	pp. 1-10	Ingenieur Digest
110	Schmoeckel, D.; Hammerschmidt, E.	Uebersicht der Verfahrenstechnologie	1980	pp. 20	Ingenieur Digest
111	Schmoeckel, D.; Hammerschmidt, E.	Ermittlung des Einflusses der Maschinenkenngrossen	1983	pp. 43-48	Dt. Verb. f. Materialprüfung
112	Schmoeckel, D.; Kuebert, M.	Urformen und Umformen von Zahnradern	1982		Verein Deutscher Ingenieure
113	Schmoeckel, D.; Hauk, pp.,	Entwicklung eines kombinierten Drück-Walz-Verfahrens	1996		VDI-Z Integrierte Produktion
114	Schmoekel, D., Hammerschmidt	UKD'88. 3. Umformtechnisches Kolloquium	1988		UKD'88. 3. colloquium on metal forming
115	Schöck, J.; Kammerer, M.	Verzahnungsherstellung durch Kaltfließpressen	1999	pp. 36-42	Umformtechnik
116	Schuler GmbH	Handbuch der Umformtechnik	1996		Springer-Verlag
117	Sheljaskow, pp.	Kaltwalzen von Innenverzahnungen	1983		Forschungsgesellschaft
118	Sheljaskow, pp.	Kaltwalzen von Innenverzahnungen	1983		Forschungsgesellschaft
119	Siegert, K.; Geiger, R.	Neuere Entwicklungen in der Massivumformung	1991		DGM
120	Siegert, K.; Geiger, R.; Beuscher, K.; Zeller, R.; Keller, K.; Kopp, R.; Wiegels, W.; Lieb, A.; Nicoll, R.; Pöll, A. et al.	Neuere Entwicklungen in der Massivumformung	1991		Vorträge 13-23, DGM-Informationsgesellschaft, Oberursel,
121	Sladek J.	Errors Identification and Measurement Accuracy Assessment of Coordinate Measuring Machines (CMM)	1999	pp. 113-136	Postępy Technologii Maszyn i Urządzeń
122	Sladek J., Gawlik K.	Looking for uncertainty of measurement	2007		IV International Congress on
123	Spur u. Stöferle.	Handbuch der Fertigungstechnik	1983	pp. 200 ff.	Umformen Hanser-Verlag
124	Strehl, R.	Umformtechnische Herstellung von Zahnradern : Studie und Literaturrecherche; Forschungsvorhaben Nr. 219 "Umformverfahren"	1993		FVA-219(Vorhaben); FVA, Frankfurt a.M.
125	Swinkels, Bastiaan Lucas	High-accuracy absolute distance metrology	2006		Dissertation Technische Universiteit Delft
126	Symposium Praxis der Zahnradfertigung, Technische Akademie	Praxis der Zahnradfertigung : Symposium	2007		Tagungshandbuch 2007 TAE
127	Th. Eibel	Mikrosensorik	1996		Vieweg&Sohn Verlag
128	Uematsu, Seizo; Houser, Donald R.	A study on reducing gear tooth profile error	2005	pp. 34-39	Gear Technology
129	Volkov, M.; Korotkov, A	Thread-Rolling Worm Shafts	1970	pp. 90-92	W+B
130	W. Göbel, J. Hesse, J.N. Zernel	Sensors: A Comprehensive Survey	1995		VCH-Verlag Weinheim
131	W. Heiwang	"Sensorik". Reihe: Halbleiter-Elektronik Bd. 17	1993		Springer-Verlag
132	Weck, M.; Koenig, W.; Bartsch, B.	Production of involute-toothed gears by cold rolling	1981	pp. 125-132	Repp. Conf. Proc., SME

133	Weser, Gunther	Am Zahn der Zeit. Exakte Zahnform von Kegelrädern für alternative Herstellungsmethoden, Antriebstechnik	2010		Aufsatz (Zeitschrift)
134	Zhongxue Gan, Qing Tang	Laser Stripe Sensor Calibration, Visual Sensing and its Applications: Advanced Topics in Science and Technology in China, Vol. 0	2011	pp. 41-91	Springer Berlin

Appendix 6: List of Standards

Nr.	Standard	Description
ST 1	DIN ISO 14	Keilwellen-Verbindungen mit geraden Flanken und Innenzentrierung; Maße, Toleranzen, Prüfung; Identisch mit ISO 14
ST 2	DIN 0867	Bezugsprofile für Evolventenverzahnungen an Stirnrädern (Zylinderrädern) für den allgemeinen Maschinenbau und den Schwermaschinenbau
ST 3	DIN 0868	Allgemeine Begriffe und Bestimmungsgrößen für Zahnräder, Zahnradpaare und Zahnradgetriebe
ST 4	DIN 1319 -1	Grundlagen der Meßtechnik - Teil 1: Grundbegriffe
ST 5	DIN 3960	Begriffe und Bestimmungsgrößen für Stirnräder (Zylinderräder) und Stirnradpaare (Zylinderradpaare) mit Evolventenverzahnung; Zusammenstellung der Gleichungen
ST 6	DIN 3961	Toleranzen für Stirnradverzahnungen
ST 7	DIN 3962 - 1	Toleranzen für Stirnradverzahnungen; Toleranzen für Abweichungen einzelner Bestimmungsgrößen
ST 8	DIN 3963	Toleranzen für Stirnradverzahnungen; Toleranzen für Wälzabweichungen
ST 9	DIN 8580	Fertigungsverfahren - Begriffe, Einteilung
ST 10	DIN 5480 ff.	Keilwellenverbindungen
ST 11	DIN 8583	Umformverfahren
ST12	DIN 332	Zentrierbohrungen
ST 13	VDI 3200	Fließkurven metallischer Werkstoffe; Grundlagen
ST 14	VDI 2617	Messunsicherheit, Koordinatenmessen
ST15	VDI 2612	Anforderungen Messgeräte
ST 16	DIN 1101	Durchmesser und Rundheit